INFORMATION TO USERS

This manuscript has been reproduced from the microfilm master. UMI films the text directly from the original or copy submitted. Thus, some thesis and dissertation copies are in typewriter face, while others may be from any type of computer printer.

The quality of this reproduction is dependent upon the quality of the copy submitted. Broken or indistinct print, colored or poor quality illustrations and photographs, print bleedthrough, substandard margins, and improper alignment can adversely affect reproduction.

In the unlikely event that the author did not send UMI a complete manuscript and there are missing pages, these will be noted. Also, if unauthorized copyright material had to be removed, a note will indicate the deletion.

Oversize materials (e.g., maps, drawings, charts) are reproduced by sectioning the original, beginning at the upper left-hand corner and continuing from left to right in equal sections with small overlaps. Each original is also photographed in one exposure and is included in reduced form at the back of the book.

Photographs included in the original manuscript have been reproduced xerographically in this copy. Higher quality 6" x 9" black and white photographic prints are available for any photographs or illustrations appearing in this copy for an additional charge. Contact UMI directly to order.

UMI

A Bell & Howell Information Company
300 North Zeeb Road, Ann Arbor MI 48106-1346 USA
313/761-4700 800/521-0600

ORGANIC MATTER ACCUMULATION AND PRESERVATION IN ALASKAN CONTINENTAL MARGIN SEDIMENTS

A

THESIS

Presented to the Faculty

of the University of Alaska Fairbanks

in Partial Fulfillment of the Requirements

for the Degree of

DOCTOR OF PHILOSOPHY

By

Xiaoling Ding, B. S., M. S.

Fairbanks, Alaska

December 1998

ORGANIC MATTER ACCUMULATION AND PRESERVATION IN ALASKAN CONTINENTAL MARGIN SEDIMENTS

by

Xiaoling Ding

RECOMMENDED:

Advisory Committee Chair

Head, Graduate Program in Marine Sciences and Limnology

APPROVED:

Dean, School of Fisheries and Ocean Sciences

Dean of the Graduate School

11-16-98

Date

Abstract

Continental margin sediments provide a historical record of the sources and fate of organic matter (OM) originating both from the continents and from primary productivity in the overlying water column. However, since this record can be altered by microbial decomposition within the sediment, the history cannot be interpreted without understanding how decomposition can affect OM composition. Also, the margins accumulate much of the OM buried in ocean sediments; hence, knowledge of processes influencing preservation of OM in these sediments is essential to understanding the global carbon cycle.

OM preservation was examined using two approaches. First, I studied sediments in the northeastern Gulf of Alaska to determine sources of OM and temporal changes in carbon accumulation. A large amount of OM, 45 - 70 × 10^{4} tons/yr, accumulated in this region, about 50% from terrestrial sources. Most of the sediment cores showed little evidence of change in TOC, TN, or C and N stable isotope compositions due to decomposition within the sediment.

Second, I investigated the processes that control OM preservation, focusing on the role of the OM adsorption to mineral surfaces. Because proteins are major constituents of sedimentary OM, I examined factors controlling their adsorption, decomposition, and preservation. Three hydrophilic proteins were strongly adsorbed by two clay minerals, an iron oxide, sub-oxic sediments from Resurrection Bay (RB), Alaska, and anoxic sediments from Skan Bay (SB), Alaska. The partition coefficients were large enough to lead to their preservation provided that the proteins did not decompose while adsorbed. Generally, adsorption of proteins to solid phases decreased decomposition rates, suggesting that adsorption is important in protecting these compounds from microbial attack. Greater protein decomposition rates were found in SB than in RB sediments, indicating that anoxia did not inhibit protein biodegradation. Naturally-occurring adsorbed proteins were extracted from SB and RB sediments using a detergent solution. Most of these adsorbed proteins were small (< 12 kDa), indicating that only the proteins adsorbed within the micropores of particle surfaces are preserved long-term.

Table of Contents

List of Figures

List of Tables

Dedication

To my husband, Jianguo Wang

Acknowledgments

This dissertation represents my achievement, but it would never have been possible without the support, help and encouragement of many people. Most of all, I would like to thank Dr. Susan M. Henrichs, my research and academic advisor, for offering me a graduate assistantship through her National Science Foundation grants, for sharing with me her knowledge, experience and motivation. Her friendship over the years is greatly appreciated. I would also like to thank my committee members, Dr. Thomas Royer, Dr. Donald Schell, Dr. Richard Benner and Dr. Bruce Finney, for their help and encouragement of my work. Their insightful suggestions, valuable discussions and critical reviews of the manuscripts are greatly appreciated.

I give special thanks to Dr. Gerald Plumley for his help in protein synthesis and purification. I thank Drs. Gerald Plumley and John Keller for allowing me to work in their labs and to use their lab facilities.

There are also many other people who helped me in one way or another. I thank Dr. Susan Sugai for helping me to collect sediment samples and reviewing some chapters of this thesis; Drs. Charles Nittrouer and John Jaeger of the State University of New York, Stony Brook, for sharing their sediment accumulation rate and clay content data; Dr. Sathy Naidu for his kindly donating clays; and Bruce Barnett and Norma Haubenstock for determining organic matter isotopic composition. I also want to thank my friends, Stacy Smith, Grace Dugger and Deborah Haberkorn, for their help in improving my English.

There are no words I can use to thank my husband, Jianguo Wang. He has been my best advisor and friend over the years. I couldn't have gotten this far without his love, encouragement and support. Finally, I would like to thank my parents and my family for always being there when I needed them.

This research was supported by NSF grants OCE-9222503 and OCE-9530280 to Susan M. Henrichs and Susan Sugai.

Introduction

Sedimentary organic matter (OM) can provide rich biogeochemical information about sources and depositional environments of modern and past sediment accumulations (Hedges *et al.*, 1988a). In some coastal regions, sedimentary OM composition and distributions have been used to identify temporal variations in OM sources, overlying water column productivity, physical transport processes, geological events, and some of the processes that lead to long-term OM preservation (Ertel and Hedges, 1985; Hedges *et al.*, 1988b; Ishiwatari and Uzaki, 1987; Tyson, 1995a and b; Williams, 1995). However, on average, only 1/1000 of the organic material produced in the oceans or delivered to the oceans from continents is preserved in sediments (Hedges and Keil, 1995). This suggests that the preservation process could be highly selective, and that the sedimentary OM record should not be interpreted without knowledge of the preservation mechanism and its selectivity. While investigations of sedimentary OM have suggested that adsorption to mineral particles has an important role in the preservation of sedimentary OM (Mayer, 1994a and b), the mechanism by which adsorption preserves OM has not been determined. Other approaches are needed to further elucidate processes and conditions leading to preservation. Once these are understood, the record contained in the preserved OM will be more easily interpreted.

Indicators of OM Sources

The NE Gulf of Alaska is an interesting region for the study of OM sources and preservation. Due to both fluvial and glacial processes, the land is eroding rapidly, leading to a large Holocene sediment accumulation on the shelf and slope. Temporal changes in sediment accumulation and OM sources can be expected due to geological events, such as the retreat of several large glaciers during the past century and a major earthquake, associated with coastal uplift and subsidence, in 1964.

To investigate the fate of OM in marine sediments, it is necessary to distinguish OM from different sources, since different processes can be important during early diagenesis, depending on the chemical structure and physical environment of the OM. The stable

isotopes, ^{13}C and ^{15}N, are widely used for determining the source of OM, changes due to passage through the food web and decomposition by microorganisms, and paleoceanographic environment. The differences in $\delta^{15}N$ between marine and terrigenous materials are primarily controlled by their inorganic nitrogen sources. The nitrogen of terrigenous OM is isotopically lighter than that from marine sources (Ostrom and Macko, 1992). The variation of $\delta^{13}C$ in organic compounds reflects the isotopic composition of source carbon and the metabolic pathways by which the molecule originates. OM from C-3 land plants has a $\delta^{13}C$ averaging from -25.5 to -29.3‰, while the $\delta^{13}C$ of tropical and temperate marine phytoplankton ranges from -17.5 to -21.5‰ (O'Leary, 1988; Tyson, 1995b). The C/N ratio is another indicator of the origin of OM in marine systems. Typically, terrigenous OM has a higher C/N ratio, since terrestrial plants contain more carbon-rich carbohydrates and lignins, while phytoplankton have a lower C/N due to the greater abundance of nitrogen-rich proteins. However, during decomposition the difference tends to decrease, because nitrogen-poor organic matter gains nitrogen from bacteria and fungi, while nitrogen-rich OM tends to lose N due to preferential decomposition of N-rich compounds (Tyson, 1995a).

It is clear that very little of the OM produced by phytoplankton, or delivered to the oceans by rivers, survives in marine sediments. Globally, the ratio of preservation to supply is about 1 / 1000 (Hedges and Keil, 1995). Burial efficiency (OM burial rate / OM flux to the sediment-water interface) is greater in continental margin sediments, on the order of 1 - 10 %, than in deep-sea sediments, 0.01 - 1 %. But, even in continental margin sediments, the preservation process could be highly selective and the preserved OM might not represent what was originally supplied to the sediment. This is particularly true if, as proposed by Tegelaar *et al.* (1989), sedimentary OM consists predominantly of highly refractory biopolymers that are only minor constituents of living organisms. If adsorption plays a major role in preservation (Mayer, 1994b), the selectivity would likely be for the most strongly adsorbed molecules. If anoxia were a determining factor (Emerson and Hedges, 1988), then molecules such as lignin and hydrocarbons, which are clearly less rapidly metabolized under anoxic conditions, should be preferentially preserved.

Decomposition and Preservation of Organic Matter

The factors controlling OM preservation and the fates of many individual organic molecules in marine sediments have been investigated (e.g., Sugai and Henrichs, 1992; Wang and Lee, 1993, Mayer 1994 a and b). Although these studies have provided insight into the processes leading to OM preservation, the precise mechanisms of OM decomposition and preservation are still poorly understood.

One hypothesis is that adsorption of OM can change its availability to microbial degradation, and thus lead to preservation in marine sediments (Mayer, 1994b). Mayer (1994b) suggested that organic molecules adsorbed in the micropores of particle surfaces could be protected from biological attack, since enzymes could be excluded from these cavities due to their size being greater than the diameter of the pores (about 10 nm). However, such adsorption would need to be very strong (Henrichs, 1995) or "irreversible" (Lee, 1992) to lead to OM preservation. The adsorption of organic macromolecules onto a particle surface is a complicated process, which is affected by inorganic and organic constituents of adsorbent, as well as the structure of adsorbate (Andrade, 1985). Neither theoretical considerations nor previous experimental studies permit the estimation of adsorption partition coefficients for large molecules, such as proteins, on sedimentary particles.

Another hypothesis is that anoxic conditions lead to organic matter preservation, because microorganisms metabolize organic substances less efficiently in the absence of oxygen (Emerson and Hedges, 1988). Aerobic and anaerobic pathways of OM decomposition are quite different. In oxic sediments, oxygen is used as the electron acceptor, and monomers are oxidized directly by bacteria. Typically, the OM content of anoxic sediments is greater than that of oxic sediments (e.g., Reeburgh, 1993; Ahmed and Devol, 1995), although the rate of OM decomposition is often greater (Henrichs, 1993). However, simply comparing the OM content or decomposition rate in different sedimentary environments with differing conditions of oxygen availability can not demonstrate that aerobic mineralization is intrinsically more complete or faster. Other

factors besides oxygen availability, such as the quantity and quality of OM available for metabolism or the physical and chemical environments of the organic molecules, may also be different.

The remineralization of OM during early diagenesis in anoxic sediments has been extensively studied, with emphasis on the consumption of sulfate and the generation of CO_2 and CH_4 (Reeburgh, 1976, 1979 and 1980; Coleman *et al.*, 1993; Giordani *et al.*, 1996). It is thought that complete anaerobic decomposition requires the initial fermentation and hydrolysis of larger biopolymers to produce lower molecular weight compounds such as acetate, which are then utilized by bacteria to finally produce CO_2 and CH_4. Ferric iron (Fe(III)) reduction to ferrous iron (Fe(II)) is one of the most important geochemical reactions in anaerobic sediments (Lovley *et al.*, 1991). The study of sulfate and ferric iron reduction, coupled with the oxidation of important fermentation products such as acetate and hydrogen, has received increasing attention in recent years (Ehrlich, 1978; Lovley *et al.*, 1991).

Remineralization of amino acids in both oxic and anoxic coastal marine sediments has been investigated in detail (Burdige and Martens, 1988; Sugai and Henrichs, 1992; Wang and Lee, 1993). Amino acids, recoverable by acid hydrolysis, can account for about 30% of the carbon and 40 - 80 % of the nitrogen mineralized during OM decomposition (Henrichs and Farrington, 1987; Burdige and Martens, 1988). Generally, amino acids decompose rapidly, but their mineralization is slowed by adsorption to sediment particles (Sugai and Henrichs, 1992; Wang, 1993). Most amino acids are present as peptides, proteins, or another bound form. Studies of peptides (Luo, 1994) and aliphatic amines (Wang, 1993) indicated that adsorption and desorption also play an important role in their decomposition. There was no evidence that decomposition of amino acids, amines, or peptides was slower or less complete in anoxic sediments.

Proteins, the major biochemical component of the biomass in the oceans, make up about 50% - 75% and 35% - 55% of the total organic material in living bacteria and phytoplankton, respectively. Although there were some earlier studies of protein decomposition and adsorption, they were carried out using either pure minerals or artificial surfaces, rather than natural sediments (e.g., Grim, 1968b; Grinnel and Feld, 1982). Also,

most of these experiments were done under conditions (e.g., high concentrations, very low water/particle ratios) very different from those in marine sediments, although appropriate for soils. Previous studies of protein decomposition and preservation in marine sediments are few.

Why Study OM Preservation?

Study of the processes controlling OM accumulation and preservation will help us to better understand the global carbon cycle. Carbon is present in the atmosphere predominantly as CO_2. Oceanic carbon is present in four major forms: dissolved inorganic carbon (DIC), dissolved organic carbon (DOC), particulate organic carbon (POC) and the marine biota. Although the marine biota are a small carbon pool, they have a significant influence on the distribution of many elements in the oceans (Broecker and Peng, 1982). The major input of organic carbon to the oceans is fixation of DIC by phytoplankton (Mopper and Degens, 1979), estimated to be about 20×10^{12} ton/y (Murray, 1992). Most of this is decomposed within a few years and returned to DIC pool. However, about 0.1×10^{12} ton/yr of organic carbon are accumulated in marine sediments (Murray, 1992), mostly originating from phytoplankton, though some is terrigenous. Organic carbon burial represents a long-term removal of carbon dioxide from the ocean-atmosphere system. Hence, changes in the quantity buried can cause changes in global climate.

Fixed nitrogen has been classically viewed as the limiting nutrient in the oceans (Parsons *et al.*, 1984). While additional nutrients are now known to be important in regulating primary productivity (Coale, *et al.*, 1996), nitrogen availability is still considered to be an important factor in structuring the phytoplankton community (Welschmeyer *et al.*, 1993). Decomposition of OM in sediments is an especially important aspect of nutrient regeneration in shallow-water regions. The rate, pathway, and extent of OM decomposition influences the supply of nutrients to the euphotic zone, and thus affects coastal ocean productivity. Sedimentary denitrification (reduction of NO_3^- to any gaseous nitrogen species, generally N_2 or N_2O) results in the release of "greenhouse" gases to the atmosphere. Also, NO and N_2O play an important role in affecting the concentrations of tropospheric ozone (Bolin *et al.*, 1983).

For both scientific and economic reasons, an important goal of organic geochemistry is to understand the correlation between oil and its sources. Oil and gas are accumulations of fossil hydrocarbons originally generated from fine-grained, organic-rich rocks. Hydrocarbon generation in sediments involves the thermal decomposition of kerogen (macromolecular OM of biogenic origin, Rullkötter, 1993) over geological time. Study of the OM distribution and accumulation in Recent marine sediments, in comparison to that in ancient rocks, has provided information on the types of paleodepositional environments, tectonic history, stratigraphic succession and subsequent structural deformation affecting petroleum source rock composition (Curiale, 1993). The specific properties and distribution of organic compounds in fossil fuels, compared with that in source rocks, can be used to improve our understanding of how petroleum composition changes during expulsion, migration and entrapment after generation. The properties of the original OM, the extent of the maturation of the source rock, the extent and pathway of migration and the extent and cause of postmigrational alteration are the general factors controlling petroleum generation (Curiale, 1993).

The Purposes of This Study

Previous studies of sedimentary OM have left many unanswered questions: Is the preservation of OM selective for particular fractions of the OM supplied to sediments, and if so, which types of OM are preferentially preserved? Is the adsorption of common biochemicals, such as proteins, by sediments strong enough to lead to their preservation? Does adsorption protect proteins from decomposition, and if so, how? Is adsorption likely to be a selective preservation process? Here, I combine studies of the OM preserved in the sediments of the NE Gulf of Alaska with experimental studies of protein adsorption and decomposition to address these questions.

Chapter 1

Surface Sedimentary Organic Matter on the Shelf and Slope of the Northeastern Gulf of Alaska

Abstract

Total organic carbon (TOC), total nitrogen (TN), and carbon and nitrogen stable isotope composition were measured in 144 surface (0 - 2 cm) sediment samples at 72 locations in the NE Gulf of Alaska. Both TOC and TN were usually greater in areas with larger Holocene sediment accumulations, including the Kayak Trough (located immediately east of the Copper River Mouth), and the Hinchinbrook and Yakutat Sea Valleys. The major exceptions to this pattern were low-organic, rapidly accumulating upper Copper River Delta sediments, and glacially-derived sediments within and near the mouth of Icy Bay and within Yakutat Bay and central Prince William Sound.

Isotopically light carbon ($\delta^{13}C < -23.5‰$) was generally found in the areas of larger Holocene sediment accumulation, except in the Yakutat Valley and Prince William Sound. ^{15}N-depleted nitrogen ($\delta^{15}N < 4‰$) was usually associated with ^{13}C-depleted carbon, as were high C/N ratios, indicating a significant terrigenous contribution to sediment organic matter. Increased terrigenous organic matter and low organic content were found in surface sediments just off the Bering Glacier, associated with the Bering Glacier surge from 1993 to 1995.

Over the past century, the annual TOC accumulation on the shelf and upper slope in the studied region (excluding Icy and Yakutat Bays) was 45 - 70 $\times 10^4$ tons, and that of TN, 5 - 7 $\times 10^4$ tons. Copper River sediments contribute about 40%, and Bering and Malaspina Glacier-derived sediments about 30%, of the TOC accumulation. About 40% of the Copper River TOC was accumulated in the prodelta. Compared to those from other major rivers, shelf sediments delivered by the Copper River bury an unusually large amount of organic carbon, due to its large sediment load and small drainage basin.

§ 1.1 Introduction

The total organic carbon accumulation in marine sediments has been estimated at about 1.6×10^{22} g C, and its residence time is about 3.4×10^{8} yr (Summons, 1993). In most marine sediments, organic matter (OM) accounts for < 10% (w/w) of the material present (Mayer, 1993). Generally, OM content is greatest at the sediment-water interface and decreases with depth of burial, due to the rain of organic-rich particles from the overlying water column and decomposition within the sediment. OM decomposition rates are also greatest near the sediment-water interface and decrease to zero with depth, even though some OM remains.

Sedimentary OM can provide rich information about sources and depositional environments of modern and past sediment accumulations (Hedges *et al.*, 1988a). Elemental and isotopic compositions provide some information on OM sources and biogeochemical processes. At the molecular level, the structures and stereochemical variations of biomarkers are used to trace source organisms, diagenetic effects, and thermal history (Summons, 1993). In some coastal regions, OM composition and distribution have been used to identify temporal variations in OM sources, overlying water column productivity, physical transport processes, and geological events (Ertel and Hedges, 1985; Hedges *et al.*, 1988b; Ishiwatari and Uzaki, 1987; Tyson, 1995a and b; Williams, 1995). However, even in recent sediments, resuspension of sediments due to physical processes and bioturbation may result in the attenuation or loss of records of short-term variations. Also, because decomposition processes result in increases in the relative contributions of refractory components with time, the quantitative interpretation of biomarker data can be difficult (Meyer and Ishiwatari, 1993).

The successful identification of sources or end members using isotopic composition requires two basic premises. First, sources must have unambiguous characteristic isotopic and/or elemental compositions. Second, geochemical characteristics should not change during physical and biogeochemical processes (Ostrom and Macko, 1992). The stable isotopes, ^{13}C and ^{15}N, are widely used for determining the source of OM, changes due to

passage through the food web and decomposition by microorganisms, and paleo-oceanographic environments (Tyson, 1995b; Williams, *et al.*, 1992).

Equilibrium and kinetic isotope effects play important roles in controlling the isotopic fractionation during chemical reactions and biological processes. Organisms tend to discriminate against heavier isotopes because bonds of the lighter isotope generally react slightly faster (kinetic effect) and have a lower energy (equilibrium effect) than those of the heavier isotope (Bigeleisen and Wolfsberg, 1958). The considerable variation of $\delta^{13}C$ in organic compounds reflects the isotopic composition of source carbon and the metabolic pathways by which the molecule originates. If organic materials containing a mixture of organic substances are analyzed, then the chemical composition of the mixture will affect isotopic composition, since each component may have originated from a different source and pathway. Typically, the $\delta^{13}C$ of marine phytoplankton ranges from -17.5 to -21.5‰, and that of terrestrial C-3 plants from -25.5 to -29.3‰ (O'Leary, 1988; Tyson, 1995b).

The differences in $\delta^{15}N$ between marine and terrigenous materials are primarily controlled by their inorganic nitrogen sources (Ostrom and Macko, 1992). The main nitrogen source for land plants is the atmosphere, with $\delta^{15}N$ values near 0, since isotopic fractionation during nitrogen fixation is not significant (Hoering and Ford, 1960, Delwiche and Steyn, 1970). Marine algae use dissolved inorganic nitrogen, usually in the form of ammonium or nitrate, with typical $\delta^{15}N$ values from 6 to 10‰. Phytoplankton respond to nutrient variations quickly, and thus usually have isotopic compositions similar to their inorganic nitrogen sources (Miyake and Wada, 1967; Cline and Kaplan, 1975).

The C/N ratio is another indicator of the origin of OM in marine systems. Typically, terrigenous OM has a higher C/N ratio, since terrestrial plants contain more carbon-rich carbohydrates and lignins (Goodell, 1972), while phytoplankton have a lower C/N due to the greater abundance of nitrogen-rich proteins (Muller, 1977). However, during decomposition the difference tends to decrease, because nitrogen-rich OM tends to lose N due to preferential decomposition of N-rich compounds.

§ 1.2 Site Description

Sediments were sampled at 72 stations during two cruises, HX181 (August, 1994) and HX186 (July, 1995), in the northeastern Gulf of Alaska and Prince William Sound (138 °W - 148 °W and 59 °N - 61 °N). The locations of these stations are shown in Figure 1-1.

The land adjacent to the northeastern Gulf of Alaska is eroding rapidly, due to both fluvial and glacial processes, leading to substantial Holocene sediment accumulation on the shelf and slope. The continental shelf of the northeastern Gulf of Alaska, with an average gradient of about 0 °15 ', ranges from 80 km wide seaward of the Copper River to less than 30 km wide seaward of Kayak Island (Carlson *et al.*, 1982). The shelf is cut by several prominent valleys, which are separated by islands, banks, and ridges. The Bering and Kayak Troughs and Hinchinbrook Sea Valley are U-shaped longitudinal valleys approximately perpendicular to the shoreline. Yakutat Valley is a broad arc crossing the shelf. Egg Island Trough, a U-shaped channel, crosses the entire front of the Copper River Delta and is roughly parallel to the shoreline.

Sediments transported on the shelf and slope are subject to a variety of influences, including fresh water discharge, ice rafting, ocean currents, waves, and mass movements such as slides, slumps and flows (Hampton *et al.*, 1987). Alaskan rivers that drain glaciers yield very large sediment loads. The major point sources of sediments in the northeastern Gulf of Alaska are the Copper River and the Bering and Malaspina Glaciers. The Copper River is the 17th largest river in the world in terms of sediment load to the ocean (70×10^6 tons/yr), but has a very small drainage basin area of 6×10^4 km^2 (Milliman and Meade, 1983). Small mountain rivers tend to have great fluctuations in discharge due to their small basins, which have low capacity to absorb peak episodic events, such as storms and floods.

The sediment distribution along the shelf and slope is variable. Molnia *et. al.* (1977) found that the dominant sediment is clayey silt. The highest concentration of sand (> 90%) was found westward, at the mouth of the Copper River (Reimnitz 1966). The Yakatut

Island platform and the nearshore regions off the Malaspina Glacier and eastward off Yakatut are also sand-dominated regions. Glacial, glacial-marine, and glacial-fluvial sediments were widely deposited on the shelf by the glaciers during the last ice-age.

Extremely high annual precipitation in the coastal Alaskan mountains produces a large coastal fresh water discharge, which is a driving mechanism contributing to local shelf circulation. Rivers, glaciers and precipitation make up the fresh water sources. The major land inputs of fresh water in the studied region, as point sources, are the Copper River and the Malaspina and Bering Glaciers, but numerous small mountain rivers and streams enter the ocean as a cumulatively greater line source (Royer, 1982).

The Alaska Current lies offshore from the Alaska Coastal Current and is the dominant transport system of surface water in the Gulf of Alaska. These two currents, the Alaska Current and Alaska Coastal Current, transport sediments northwestward alongshore. Some Copper River sediment is transported into Prince William Sound through the channel between Montague and Hinchinbrook Islands (Burbank, 1974; Carlson and Molnia, 1978). The dipole eddies found near Kayak Island may play an important role in cross-shelf mixing and can transport terrigenous material to the southwest as much as 50 km offshore (Feely *et al.*, 1979).

The central Gulf of Alaska has annual primary productivity of ~ 170 g C/m^2, as estimated from *in situ* measurements at a station located at 50 °N, 145 °W (Welschmeyer, *et al.*, 1993), yielding over 3 times the productivity estimate of Sambrotto and Lorenzen (1987). However, few data are available for this region, so the temporal and spatial productivity variations are not well-characterized. Shelf areas are moderately productive with annual production ranging from 140 to over 200 g C/m^2 (Sambrotto and Lorenzen, 1987). Alaskan fjords often tend to have decreasing primary production from the mouth to the head, due to high suspended particulates and low nutrients in glacially-fed streams (Matthews and Heimdal, 1980).

§ 1.3 Sampling and Methods

Sediments were sampled in late August, 1994 (station numbers < 200) and early July, 1995 (station numbers > 200). Samples for this study were collected with a box corer (0 - 25 cm) and stored frozen. Samples were analyzed after acidification to remove carbonate. After drying at 70 °C, sediments were ground and stored in 5-ml vials until analysis. The analytical precision between duplicate samples, as the average deviation, is 0.016 mg/g for total nitrogen (TN), 0.17mg/g for total organic carbon (TOC), 0.11‰ for $\delta^{13}C$, and 0.5‰ for $\delta^{15}N$. The average relative deviation is < 4% for TN and TOC, < 0.5% for $\delta^{13}C$, and < 15% for $\delta^{15}N$. TOC, TN, $\delta^{15}N$ and $\delta^{13}C$ were measured using a Europa Model 20/20 mass spectrometer with a Roboprep $^{(TM)}$ automated combustion device.

The $\delta^{13}C$ and $\delta^{15}N$ values represent the relative difference in carbon and nitrogen isotopes between sample and standard. Sedimentary isotope ratios are reported as follows:

$$\delta X = \{ \frac{R_{sam}}{R_{sta}} - 1 \} \times 1000$$

X is ^{13}C or ^{15}N, R_{sam} is the $^{13}C/^{12}C$ or $^{15}N/^{14}N$ of samples, and R_{sta} is the $^{13}C/^{12}C$ or $^{15}N/^{14}N$ of the standard. Samples with low $\delta^{13}C$ or $\delta^{15}N$ values are often referred to as isotopically "light", since they contain more of the lighter isotopes.

The sediment accumulation rates and sediment clay and sand content were provided by Drs. J. Jaeger and C. Nittrouer, at State University of New York, Stony Brook. Accumulation rates were determined using excess ^{210}Pb, and verified in some cases with ^{137}Cs (Jaeger *et al.*, 1998). The geographic patterns of sediment accumulation rate are generally consistent with the thickness of Holocene sediment accumulation presented by Molnia (1989).

§ 1.4 Results

The data presented in figures are tabulated in Table A-1 (Appendix III). TOC in surface sediment samples from the 72 stations ranged from 1.5 - 9.4 mg/g and TN from 0.1

- 1.0 mg/g. The average C/N ratio was 9.9. TOC and TN showed similar patterns in the study region (Figures 1-2 and 1-3). Both were usually greater in areas with larger Holocene sediment accumulations (Molnia, 1989), including the Kayak Trough (immediately east of the Copper River mouth), Egg Island, Alsek and Bering Troughs, and the Hinchinbrook and Yakutat Sea Valleys. The major exceptions to this pattern were low-organic, rapidly accumulating upper Copper River Delta sediments and glacially- derived sediments within and near the mouth of Icy Bay, within Yakutat Bay and central Prince William Sound, and just off the Seal River (which drains the Bering Glacier).

Isotopically light carbon ($\delta^{13}C < -23.5‰$) was generally found in the areas of fresh water discharge, such as the Copper River Delta region, Kayak Trough, and near the Bering and Malaspina Glaciers, but not in the Yakutat Valley and Prince William Sound (Figure 1-4). Unusually "light" carbon was found just off the Bering Glacier and beneath the Kayak Island eddies. Isotopically light nitrogen ($\delta^{15}N < 4$ ‰) was usually associated with light carbon (Figure 1-5), as was high C/N ratio (Figure 1-6). These patterns (Figure 1-7) indicate a significant terrigenous OM accumulation on the shelf.

Very high burial fluxes of OM were found in Kayak Trough and across the west part of Egg Island Trough (Figure 1-8), due to the high sedimentation rate. Relatively high OM burial fluxes were also found just off Bering Glacier and near the entrance of Prince William Sound between Hinchinbrook and Montague Islands. Kayak Island eastward, except for Bering Trough, was mostly a region of extremely low OM accumulation with a maximum burial flux of 40 g $m^{-2} y^{-1}$. Figure 1-9 shows the terrestrial TOC accumulation in surface sediments. The percentage of organic carbon derived from a terrestrial source was calculated with a mixing model using $\delta^{13}C$ end member values of -20‰ for marine OM and -26‰ for terrigenous OM (see discussion). The patterns indicate that the Copper River is a major contributor to the OM accumulation on the shelf and slope between Kayak Island and Prince William Sound, and that most of the OM from the Copper River was transported southeastward as far as Kayak Trough and deposited beneath the Kayak eddies.

Three groups of shelf stations were selected to study the OM accumulation pattern

across the shelf and slope. These groups are located off the Malaspina Glacier, Icy Bay and the Bering Glacier (Figure 1-10). All of them show similar patterns, increasing TOC and TN and decreasing terrigenous OM content with increasing distance from shore (Figure 1-11).

§ 1.5 Discussion

§ *1.5.1 Physical Environment*

Circulation in the Gulf of Alaska is controlled by continental winds and fresh water discharge. The Aleutian Low and Pacific High dominate the Gulf, bringing storms in winter and fairer weather in summer (Bogdanov, 1963; Royer, 1975; Xiong and Royer 1984). The currents in the Gulf of Alaska generally parallel the continental slope. Offshore water circulation first takes a northward direction (the Alaska Current off SE Alaska) and then turns westward (the Alaska Stream; Reed and Schumacher, 1987).

Royer (1979, 1981a, 1981b, 1982) concluded that the nearshore, westward coastal current in the Gulf of Alaska results from salinity gradients that are controlled by freshwater discharge. The surface geostrophic flow (referred to 50 - 100 db) seems to be an approximation of actual circulation (Royer *et al.*, 1979; Reed *et al.*, 1981). In the northern hemisphere, greater dynamic height lies to the right of the flow. The dynamic height contours, calculated from 1994 and 1995 hydrographic data (Figure 1-10), show water flow consistent with earlier findings, generally westward, but with eddies near Kayak Island. The flow direction in the Copper River Delta region was variable, but the mean flow was also westward. A small portion of the flow entered Prince William Sound through the entrance among small islands to the east of Hinchinbrook Island, in addition to that entering between Hinchinbrook and Montague Islands.

The physical environment around Kayak Island is complex. Figure 1-13 shows that the deep water on the west side and south of the island was formed from cold and salty water, probably due to an invasion of the Alaska Current. Significant mixing of surface water with waters of substantial fresh water content was also found at the Kayak eddies,

but the subsurface and deep water were quite uniform. Except for the water deeper than 50 m, the subsurface water westward of the island seems to be affected by fresh water.

High bottom water salinity and low oxygen concentrations are present in troughs and valleys that are perpendicular to the shoreline (Figures 1-14 and 1-15). This oxygen minimum is not due to local O_2 utilization, but rather to the global circulation and the very low-O_2 water at intermediate depths just offshore (Sambrotto and Lorenzen, 1987). Surface sediment OM tends to be greater in low-O_2 and high-salinity bottom water areas (Figure 1-16). Thirty-nine of 72 stations were located at stations with higher bottom water O_2 content (> 5 mg/L) and a mean water depth of 110 m, and had a mean TOC content of 3.5 mg/g. Sixteen stations were located in low-O_2 (< 3 mg/L) zones, with a mean water depth of 230 m and TOC of 5.5 mg/g.

The role of bottom water oxygen content in OM preservation has been debated. Henrichs and Reeburgh (1987) and Cowie and Hedges (1993) found that bottom-water oxygen had little effect on OM burial efficiency. On the other hand, there are numerous reports of enhanced OM preservation under anoxic relative to oxic conditions (e.g., Benner *et al.*, 1984; Lee, 1992). In most cases these patterns exist only for sediments where the bottom water oxygen is lower than that found here, ≤ 20 μM. The tendency to higher surficial sedimentary OM in higher salinity and lower oxygen areas in this study is probably a result of physical rather than biological and chemical processes. In shallower areas, strong water column mixing resuspends fine organic-rich particles from the sediment-water interface, ultimately resulting in their transport to more quiescent areas. There was a positive relationship between clay content and sedimentary TOC (Figure 1-17), consistent with the proposed physical mechanism. This negative correlation of TOC and grain size is commonly observed in continental margin sediments, and may also be due to OM preservation by adsorption on clay mineral surfaces (Mayer, 1994a and b).

§ *1.5.2 Organic Matter in Surface Sediments*

Figure 1-7 shows linear correlations between total nitrogen and total organic carbon, $\delta^{13}C$ and $\delta^{15}N$, and $\delta^{13}C$ and C/N ratio. Most of the surface sedimentary OM in the NE Gulf

of Alaska is from a mixture of land and marine sources. The average fraction of terrestrial OM was 47%, 42% and 44%, using $\delta^{13}C$, $\delta^{15}N$ and C/N ratios as source indicators, respectively. These estimates are based on a linear mixing model, using 10 samples chosen from the Copper River and its prodelta and near Bering Glacier to represent the terrigenous source, and 4 samples from the farthest offshore stations for the marine source.

Generally, higher OM content sediments were associated with greater sediment accumulation rates and finer-grained (larger surface area per unit mass) sediments. Lower OM contents were found in some high sediment accumulation regions, such as the upper delta of the Copper River, some fjords, and central Prince William Sound. The upper delta is sandy, and the smaller surface area/g sediment would tend to decrease preservation if adsorption to particle surfaces is the major mechanism (Mayer, 1994a and b), or the large accumulation of organic-poor sandy sediment could simply dilute the available OM. The glacial sediments, due to sparse vegetation on the land bordering the fjords and low fjord primary production resulting from extremely high turbidity, probably contain little OM because of very low supply.

High sediment accumulation rates (>10 mm/yr) were found near the Seal and Kaliakh Rivers, which drain Bering and Malaspina Glaciers, respectively, and west of Kayak Island. The rest of the shelf has lower sedimentation rates, from several mm/yr in midshelf to zero on diamictons and at the shelf break, and little sediment is accumulated in the cross-shelf valleys (< 3 mm/yr; Jaeger *et al.*, 1998). The distribution of sediment accumulation was explained in relation to grain size and current patterns, particularly the along-shelf transport by the strong Alaska Coastal Current (Jaeger *et al.*, 1998). Figure 1-18 shows the clay content in surface sediments. In the Bering-Malaspina region, small glacial meltwater streams deliver 25% of the sediments to the shelf directly southwest of the glacier, and the rest accumulates in Icy and Yakutat Bays, Yakutat Trough and proglacial lakes (Jaeger *et al.*, 1998). Between Bering Glacier and Icy Bay, small rivers contribute a substantial supply of clay to the shelf, where TOC, TN, the C/N ratio and OM burial flux were somewhat higher than in regions to the east and west.

The Copper River seems to be a major clay source between Hinchinbrook Island and the west side of Kayak Island. There, greater clay content is generally associated with higher surface sediment TOC, except for the upper Copper River Delta. The extremely high OM content in Kayak Trough could also be due to a high sediment accumulation rate (10-15 mm/yr) (Reimnitz and Carlson, 1975; Carlson *et al.*, 1977), since OM burial efficiency increases with sediment accumulation rate (Henrichs and Reeburgh, 1987). A similar pattern was also found in the Bering Trough, Yakutat Sea Valley and Alsek Trough. Roughly, there is a positive linear relationship between clay content and sediment surface area (Mayer and Fink,1980). The correlation between sedimentary OC and surface area has been ascribed to OM adsorption to clay mineral surfaces, which may protect some OM against biodegradation (Mayer,1994a and 1994b).

Figure 1-19 shows the sand content in surface sediments. Sand with an extremely low OM content was input from the Alsek River. High salinity, low oxygen content, low C/N ratio, and less negative $\delta^{13}C$ and high $\delta^{15}N$ indicated a mostly marine sedimentary OM source, diluted by the organic-poor sand. Fairly high sand content was found to the southeast off the Bering Glacier, also associated with low OM content.

A greater C/N ratio and isotopically light OM were found in sediments westward of Kayak Island. The Copper River-derived sediments appear to be transported southeastward as far as Kayak Island. The recurrent Kayak eddies of the Alaska Coastal Current seem to play an important role in transporting terrigenous OM offshore. $\delta^{13}C$ (Figure 1-4), $\delta^{15}N$ (Figure 1-5), and C/N ratio (Figure 1-6) show the effects of Kayak Island eddies clearly.

Eastward of Kayak Island, substantial terrigenous OM in surface sediments was found just off the Bering Glacier. This was apparently deposited during the Bering Glacier surge from 1993 to 1995 (Roush, 1996). The surging glacier resulted in the input of a large amount of sediments via the Seal River to the shelf. Relatively low sediment OM content was also found in this region, which is probably due to dilution by low organic content glacial sediments. Effects of Bering Glacier surges on sediment organic content are discussed further in Chapter 2.

Extremely high C/N ratios were found in Yakutat Bay (YB) and Icy Bay(IB). Higher carbon to nitrogen ratios were probably contributed by fossil OM, contained in glacially eroded rocks; OM in ancient rocks tends to have high C/N, due to preferential decomposition of nitrogen compounds. From Figures 1-4 and 1-6, it is clear that IB has more typically terrestrial OM, while YB has unusually heavy nitrogen suggestive of a fossil marine source (see Chapter 2 for further discussion). YB sediment may also have some phytoplankton-derived OM because YB productivity is high, at least in the outer bay.

Jaeger *et al.* (1998) estimated the regional fine sediment (silt and clay) input using the sediment accumulation rates. I calculated the TOC and TN budgets based on their data (except in fjords). Table 1-1 shows that about 45 - 70 × 10^4 tons/yr of TOC and 5 - 7 × 10^4 tons/yr of TN were accumulated in the past century. About 40% of the TOC and 45% of the TN were accumulated in Bering-Malaspina region, 50% of TOC and 45% of TN were accumulated in the Copper River Delta region, and the rest was in Prince William Sound. Jaeger *et al.* (1998) also estimated the proportions of Kayak Trough sediment derived from the Copper River and Bering Glacier, based on clay mineralogy and seismic profile data (Molnia and Hein, 1982; Milliman *et al.*, unpubl.). Assuming that OM and mineral particles are transported together, the portion of Kayak Trough sedimentary TOC from the Copper River is about 70% higher than that from Bering Glacier. The two are equal sources of TN, however, reflecting the higher C/N ratio in the Copper River.

In the Copper River region, large amounts of TOC and TN were accumulated in the prodelta region due to the extremely high sediment accumulation rate, and that accounted for ~20% of the total TOC accumulation in the entire studied area. In the Kayak Trough, OM from the Copper River contributed about 17% of the total regional TOC accumulation. TOC from the Bering/Malaspina Glacier outflow accumulating on the shelf was about 20% of the regional TOC accumulation, and some additional TOC from the same sources was deposited in the Kayak Trough, about 10% of the total regional accumulation. This calculation indicates that the Copper River and Bering and Malaspina Glaciers are the dominant sedimentary OM sources in the studied area (40% and 30% of the total

respectively). Most of the sedimentary OM from the Copper River was deposited in the prodelta region, but a substantial portion was transported southeastward to Kayak Trough and a significant fraction northwestward into Prince William Sound. Most of the sedimentary OM from the Bering and Malaspina Glaciers was deposited in nearshore regions, and a substantial portion was transported northwestward by Alaska Coastal Current to Kayak Trough.

Globally, the annual fluvial sediment load is about 20 - 50 × 10^9 tons (Holeman, 1968), and rivers transport about 500 × 10^6 tons of organic carbon to the ocean, about half as POC (Spitzy and Ittekkot, 1991). Of the total organic carbon input from rivers, 43% enters the Atlantic Ocean, 34% the Pacific Ocean, 15% the Indian Ocean, and 8% the Arctic Ocean. The 10 largest rivers contribute about 28% of total carbon discharge (Ludwig *et al.*, 1996). Smith and Hollibaugh (1993) concluded that approximately 1/3 of the total riverine organic carbon is lost to the lithosphere, while 2/3 returns to atmosphere by respiration. For fluvial organic carbon, the ratio of burial to respiration in the coastal region is 3 : 2, while it is 1 : 9 in the open ocean (Ludwig *et al.*, 1996). The average sedimentary OM accumulation rate in the Copper River Delta region is 11.6 × 10^4 tons/yr. Fluvial POC data are not available in this region. Roughly, assuming that 60% of the fluvial POC is buried in marine sediments (Ludwig *et al.*, 1996), and 75% of the TOC in surface sediment was terrigenous (from the Copper River), the POC flux from the Copper River drainage area is 14 g m^{-2} y^{-1}.

Table 1-2 shows the POC flux from other rivers. The data listed in the table include values for most of the major rivers in the world, and some smaller rivers, depending upon the availability of POC data. Compared to other rivers in North America, the estimated OC yields from the Copper and Susitna Rivers were unusually large, corresponding to their large sediment yield (sediment discharge / drainage area). Milliman and Syvitski (1992) attribute the high erosion rate in such rivers to the influence of drainage basin elevation on erosion rates. It might be expected that rivers draining mountains of glaciated areas would carry organic-poor sediments, since these areas lack vegetation and organic-rich soils.

However, there is no particular pattern in the POC concentration of suspended sediments. The POC yield of the Copper River basin is high, relative to much larger rivers like the Columbia and St. Lawrence Rivers, so that the Copper River delivers a comparable amount of carbon to the shelf. The NE Gulf of Alaska regional terrigenous C accumulation, based on 60×10^4 tons TOC/yr accumulated and an estimated 50% terrigenous material, is about 10% that supplied by the Mississippi. Globally, only the Ganges/Brahmaputra has an annual POC yield (g POC/m^2 of drainage basin) greater than that of the Copper and Susitna Rivers. The information in Table 1-2 indicates that sediment yield, rather than vegetation, soil development, or other characteristics of the drainage basin, may be the main determining factor in POC yield. This, in turn, suggests that available sediment surface area largely governs POC delivery by rivers.

§ 1.6 Summary and Conclusions

1) Greater surface sedimentary TOC and TN were found in areas with larger Holocene sediment accumulations, except in upper Copper River Delta sediments, and in glacially-derived sediments within and near the mouth of Icy Bay, and within Yakutat Bay and central Prince William Sound.

2) Sediment OM of lower $\delta^{13}C$ and $\delta^{15}N$ and greater C/N were associated with greater TOC and TN.

3) Series of cores, collected along transects extending across the shelf, showed increasing OM contents in surface sediments and decreasing terrigenous OM seaward.

4) Annual TOC accumulation is $45 - 70 \times 10^4$ tons, and that of TN is $5 - 7 \times 10^4$ tons, during the past century on the NE Gulf of Alaska shelf and upper slope. Of this, approximately 50% was terrestrially-derived and the remainder of marine origin.

5) Sediment yield of river drainage basin has a positive relationship to POC accumulation on continental margins.

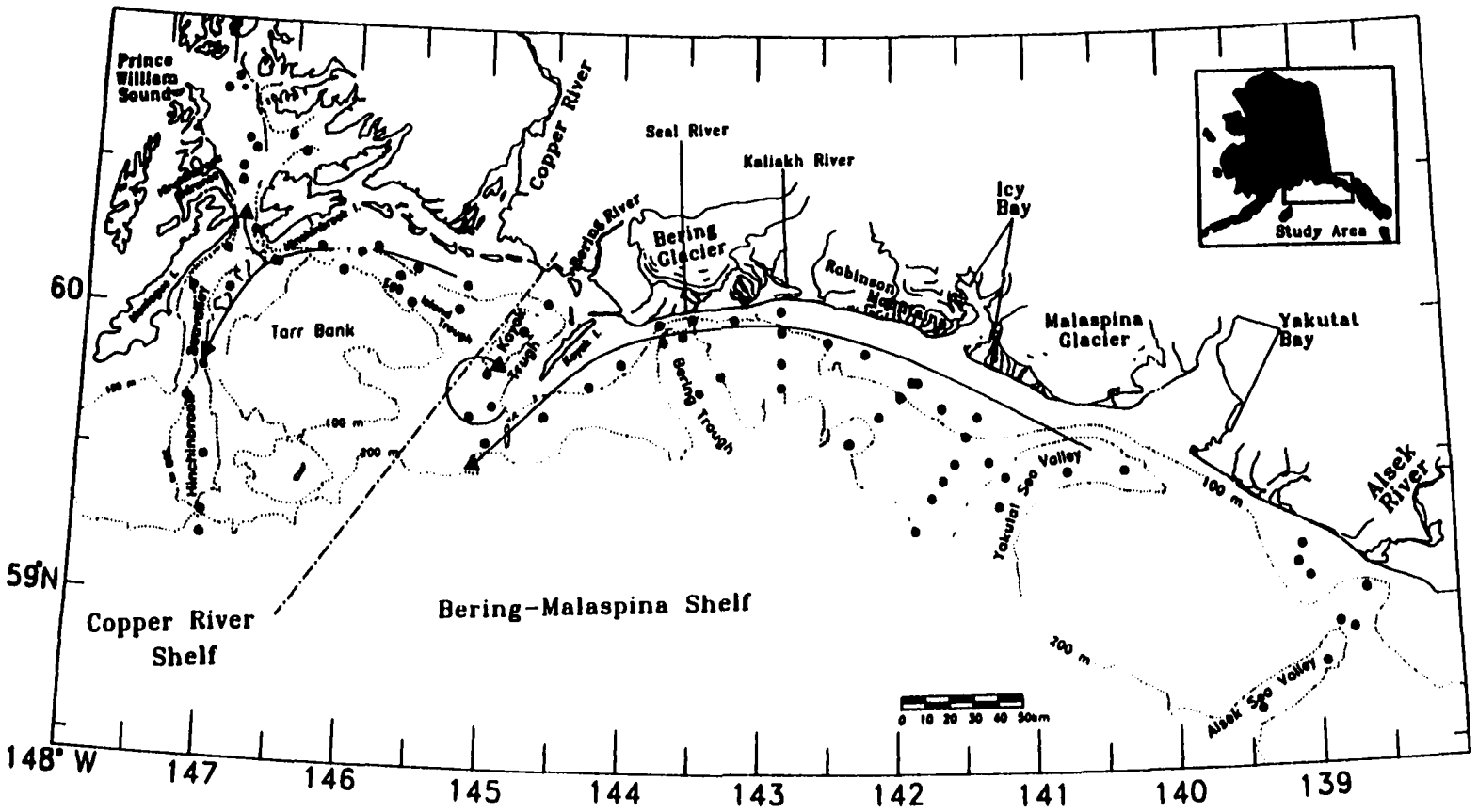

Figure 1-1. Sampling stations in the northeastern Gulf of Alaska. Arrows show the location and flow direction of the Alaska Coastal Current. Kayak eddy is in the lee of Kayak Island. The isobath contour lines show the bathymetric features (modified from Jaeger *et al.*, 1998).

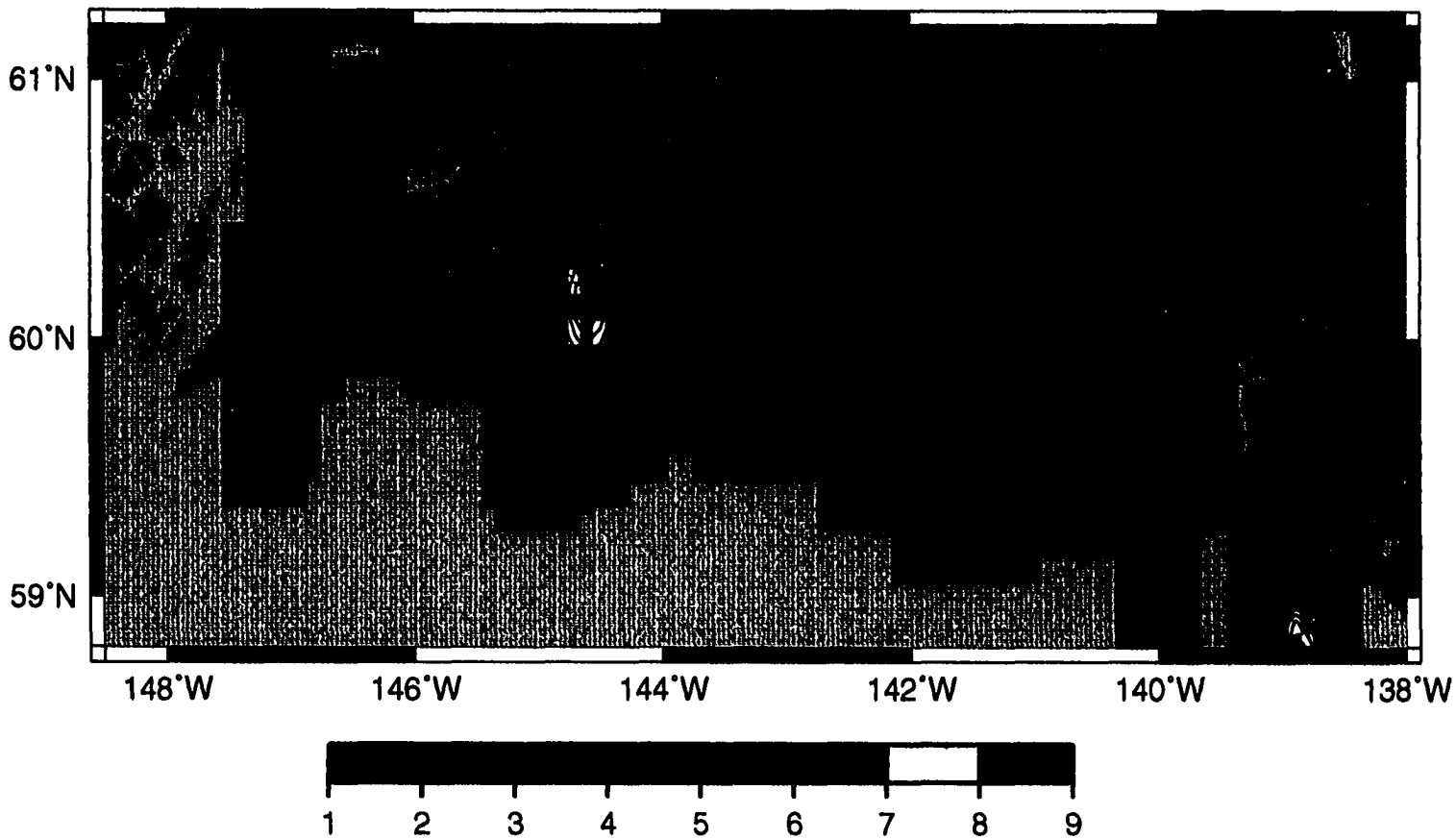

Figure 1-2. Surface sediment (0-2 cm) TOC content (mg/g) in the Gulf of Alaska.

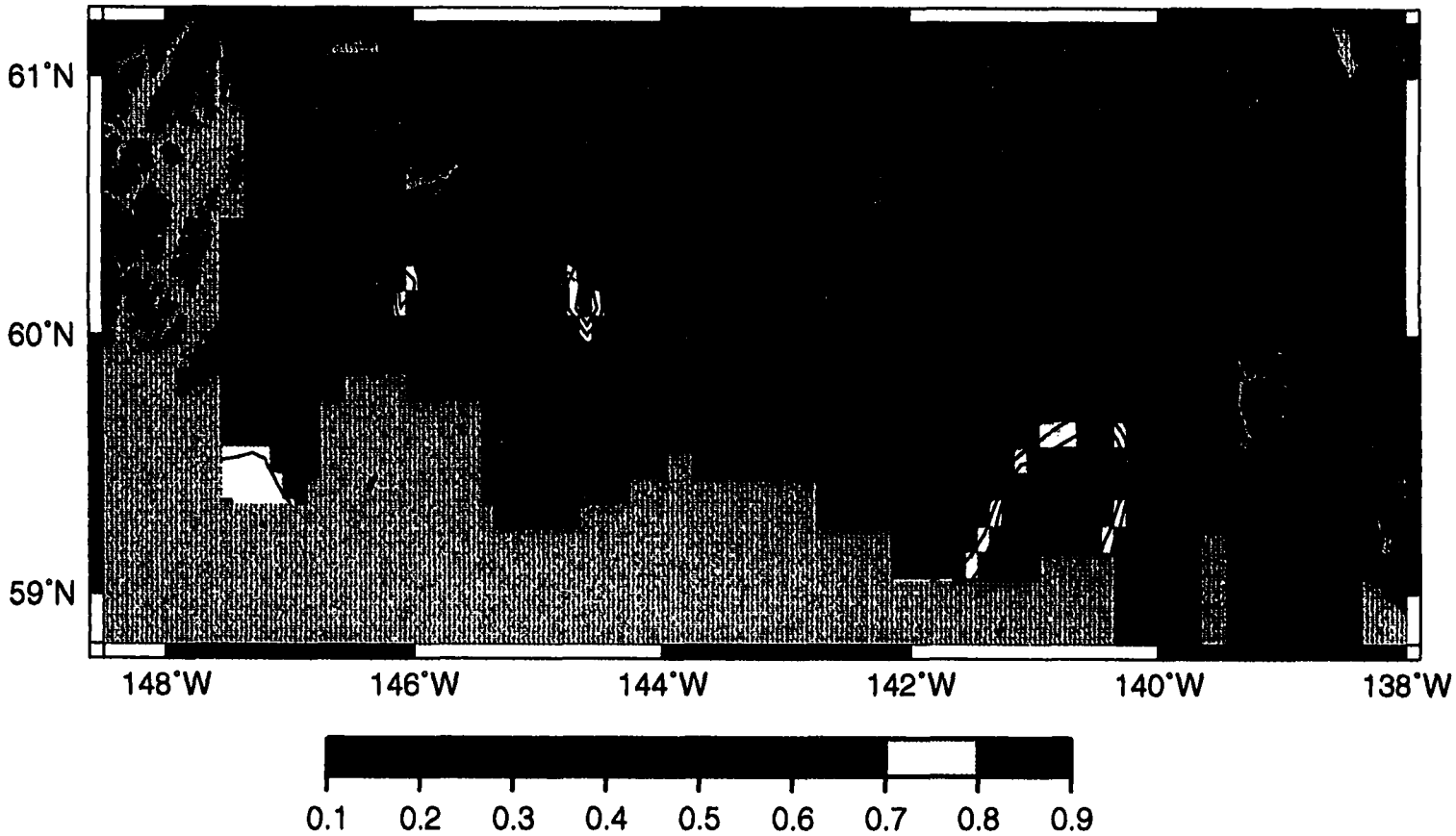

Figure 1-3. Surface sediment (0-2 cm) TN content (mg/g) in the Gulf of Alaska.

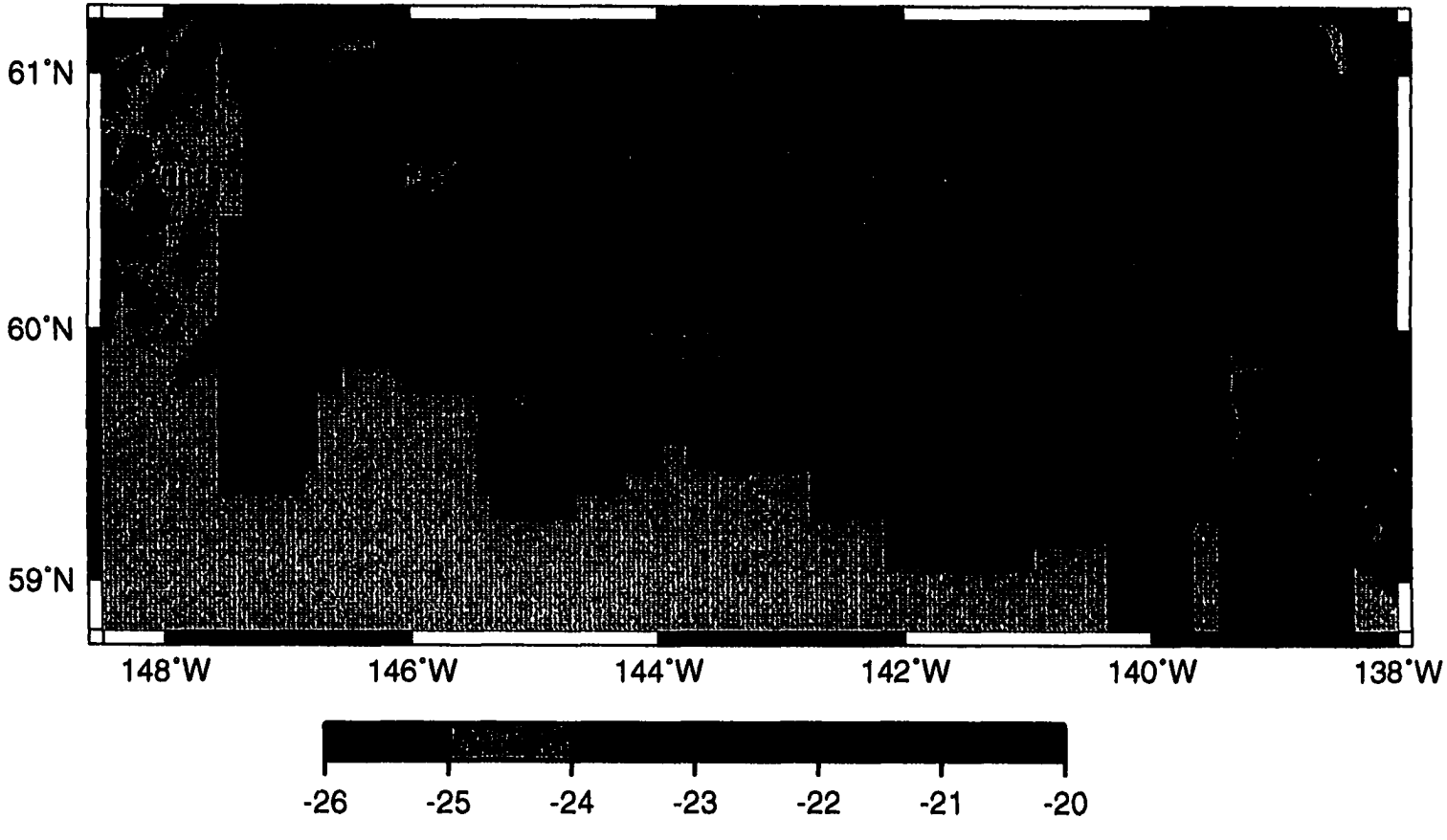

Figure 1-4. Surface sediment (0 - 2 cm) $\delta^{13}C$ (‰) in the Gulf of Alaska.

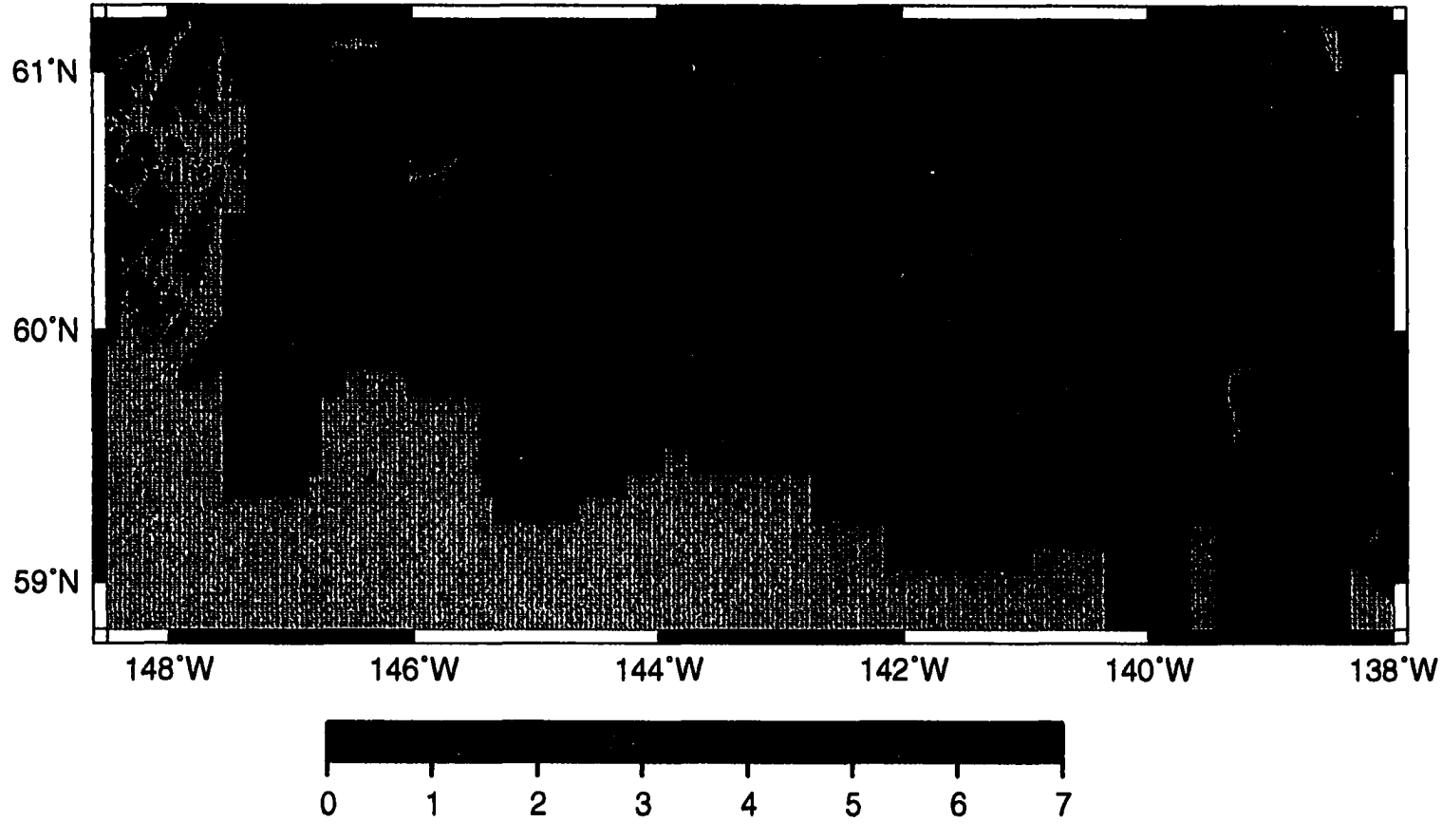

Figure 1-5. Surface sediment (0 - 2 cm) $\delta^{15}N$ (‰) in the Gulf of Alaska.

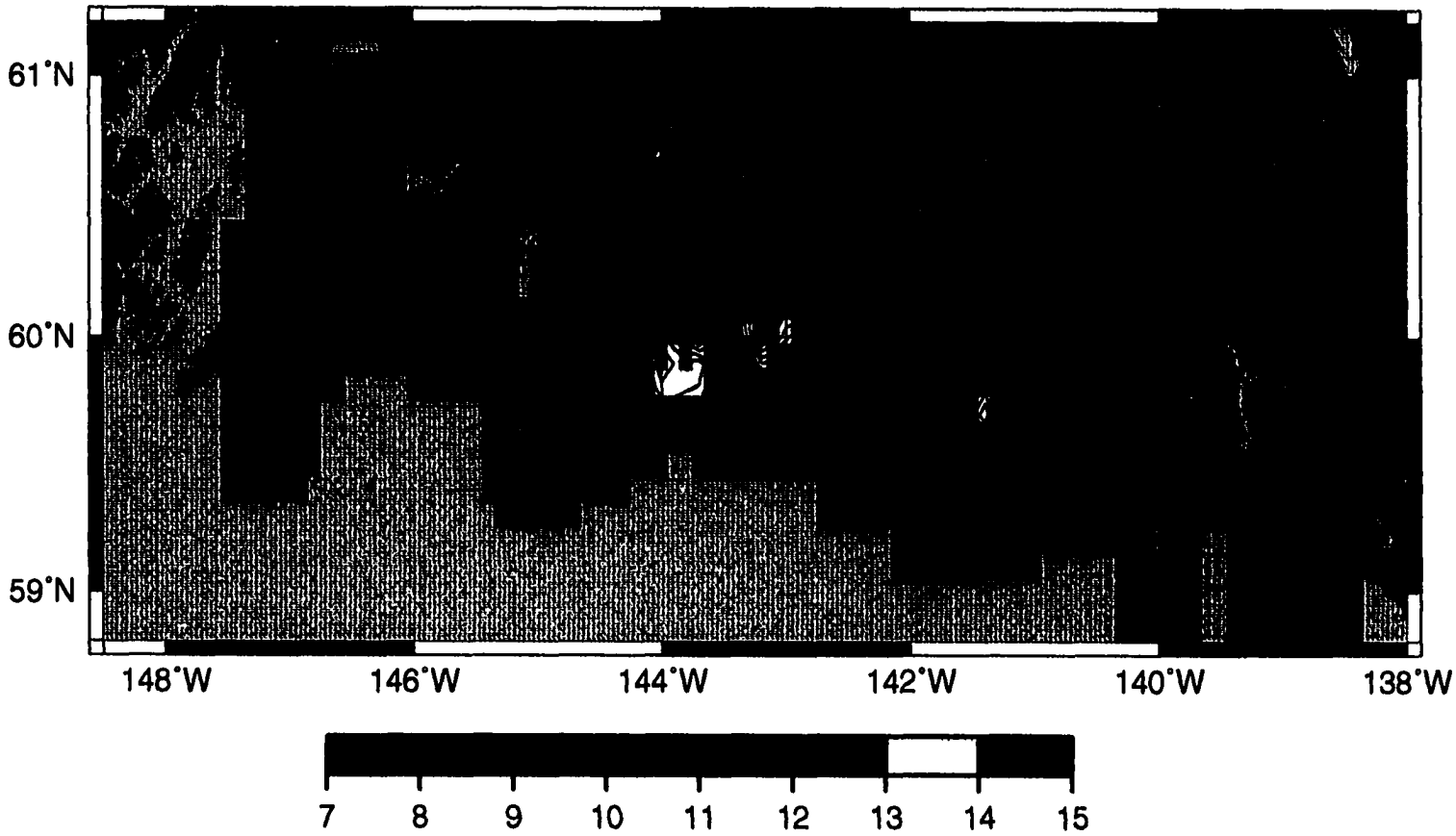

Figure 1-6. Surface sediment (0-2 cm) C/N ratio in the Gulf of Alaska.

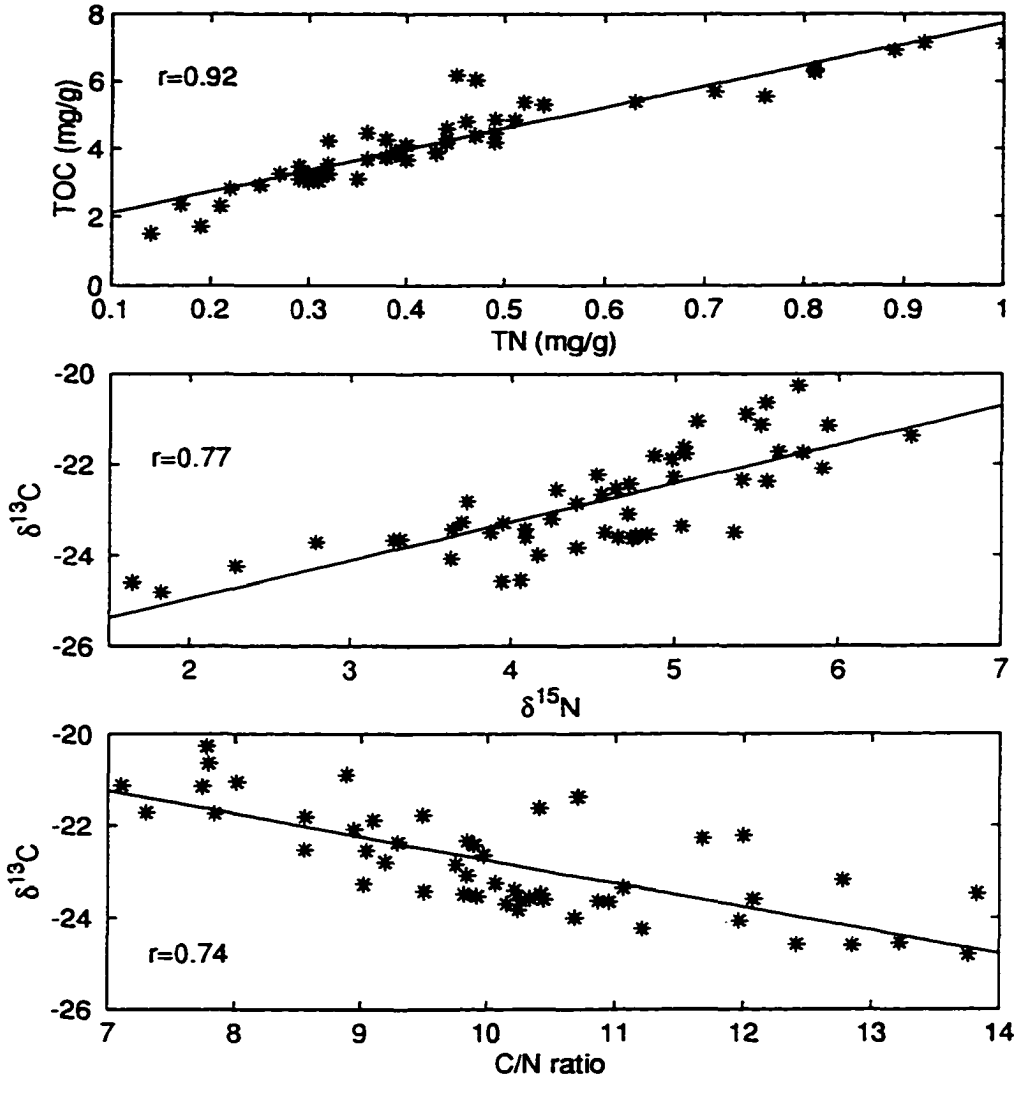

Figure 1-7. Correlations of TOC vs. TN, $\delta^{13}C$ vs. $\delta^{15}N$, and $\delta^{13}C$ vs. C/N ratio.

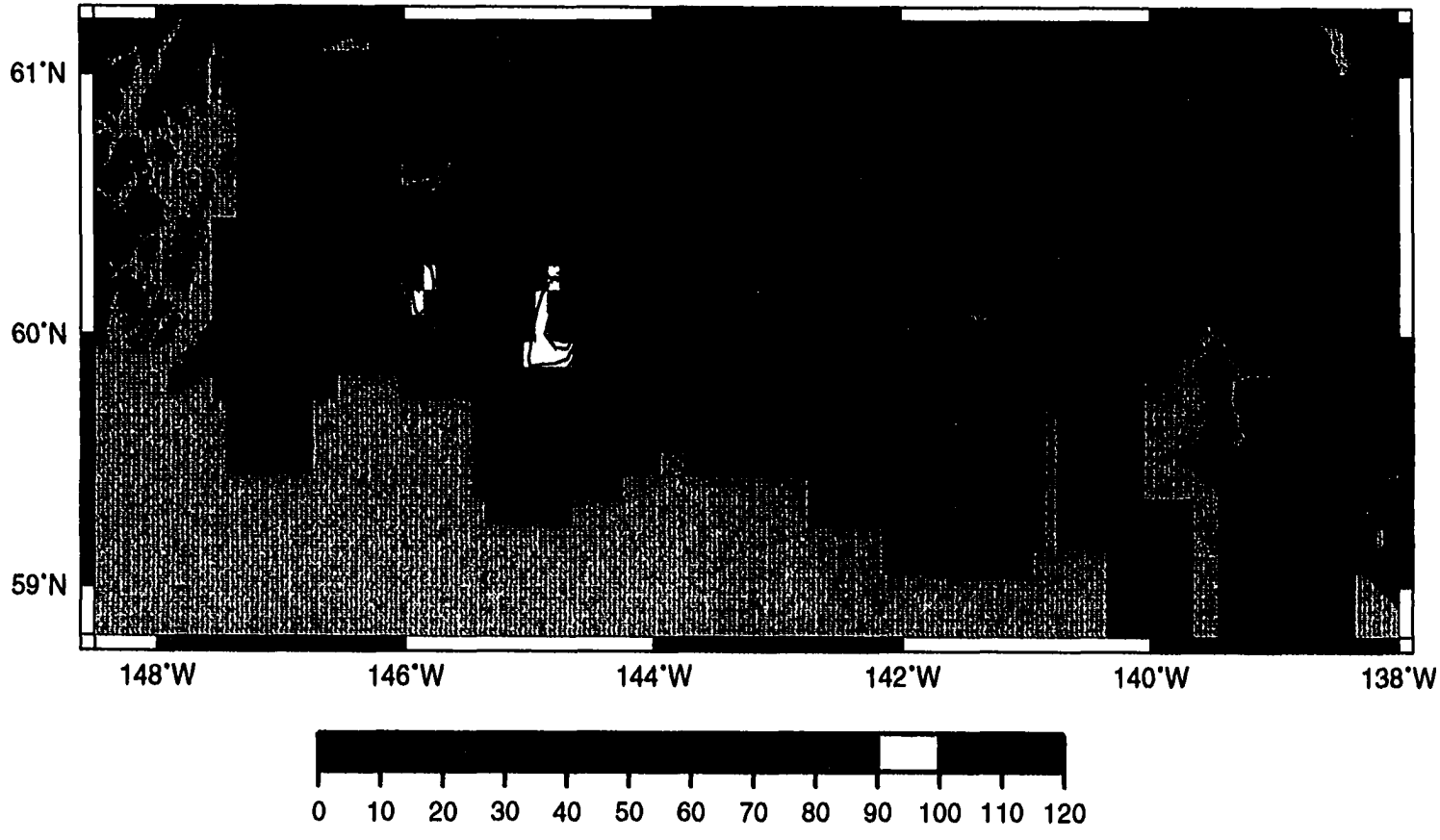

Figure 1-8. TOC burial flux (g m^{-2} y^{-1}) in the Gulf of Alaska.

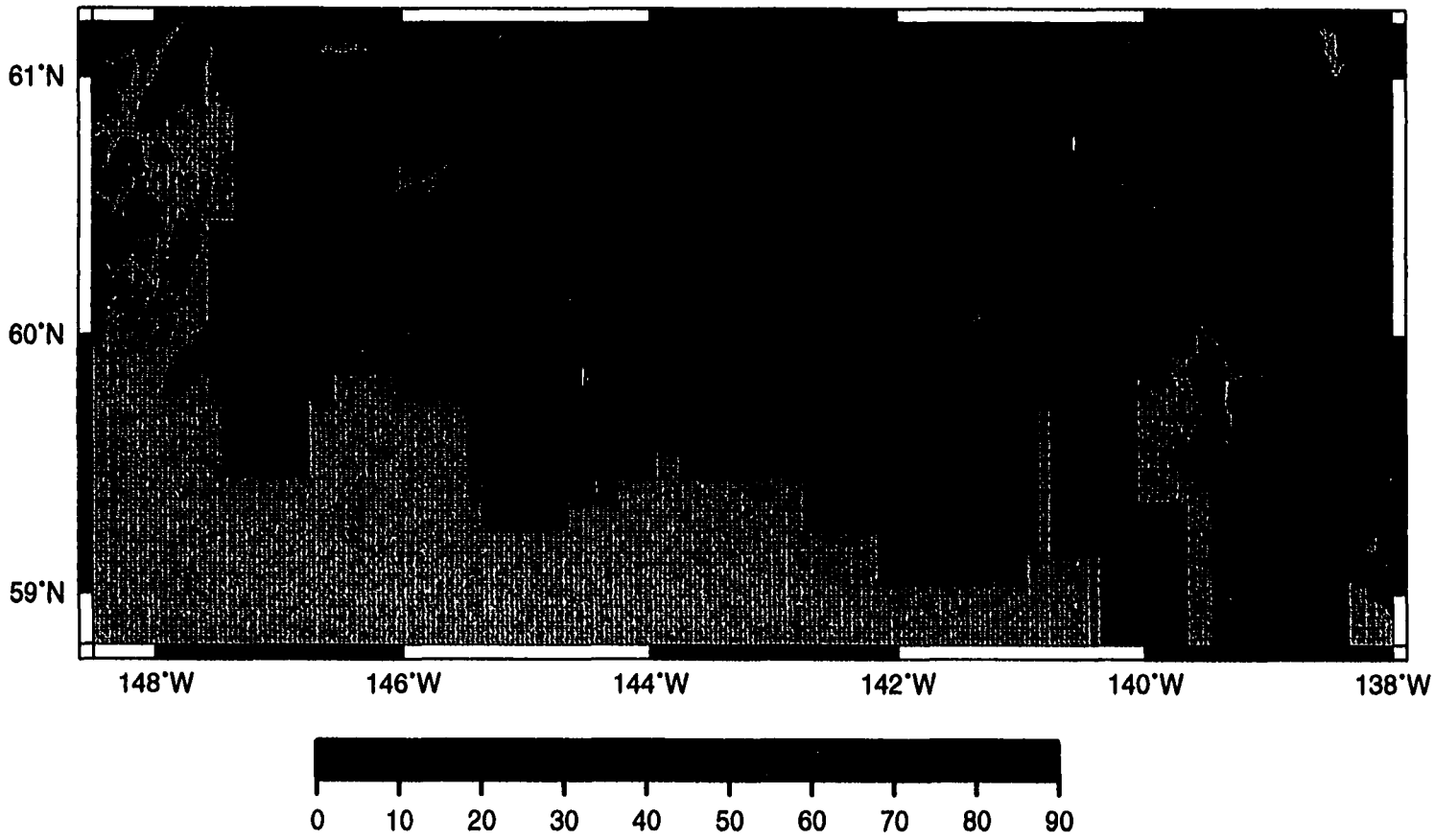

Figure 1-9. Terrestrial TOC burial flux (g m^{-2} y^{-1}) in the Gulf of Alaska.

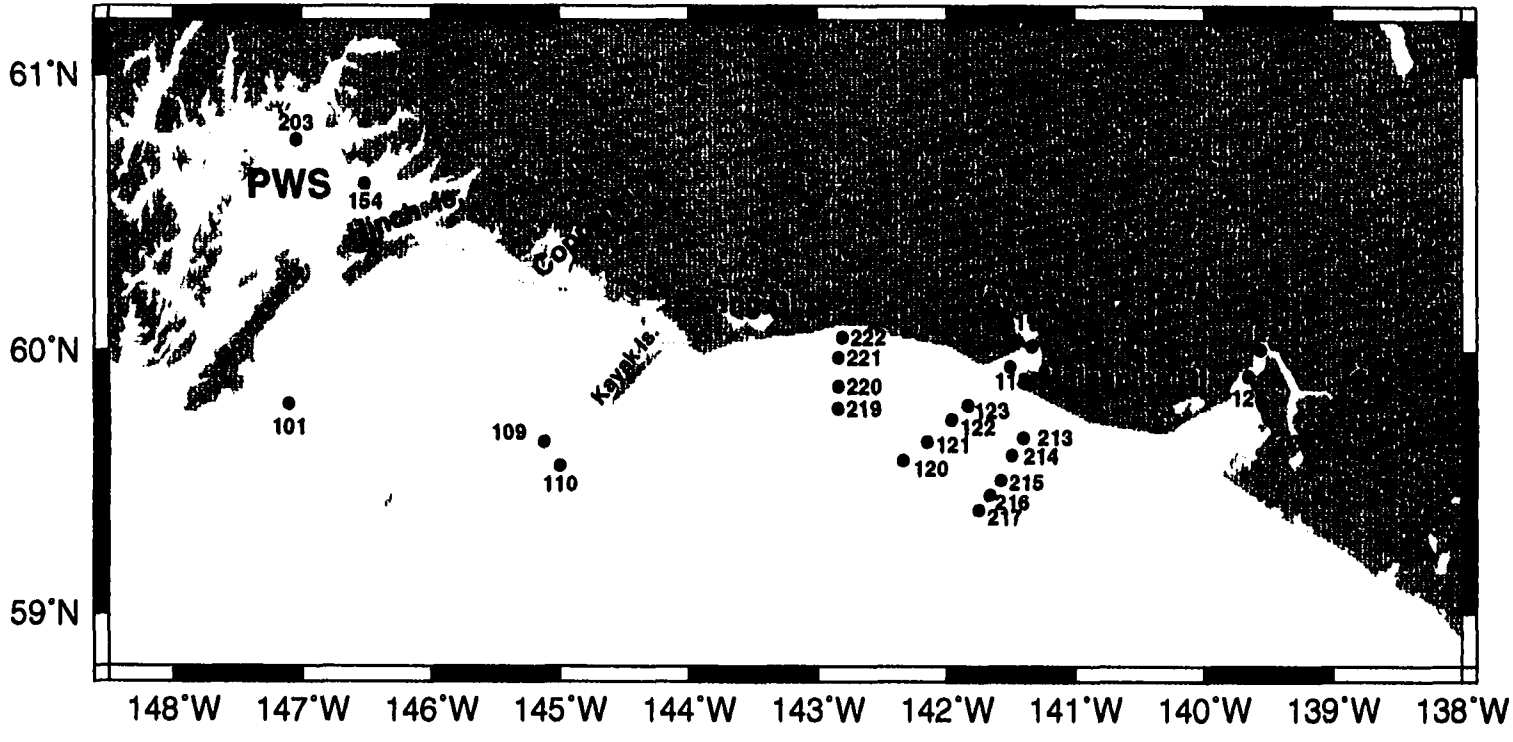

Figure 1-10. Selected sampling stations in the Gulf of Alaska.

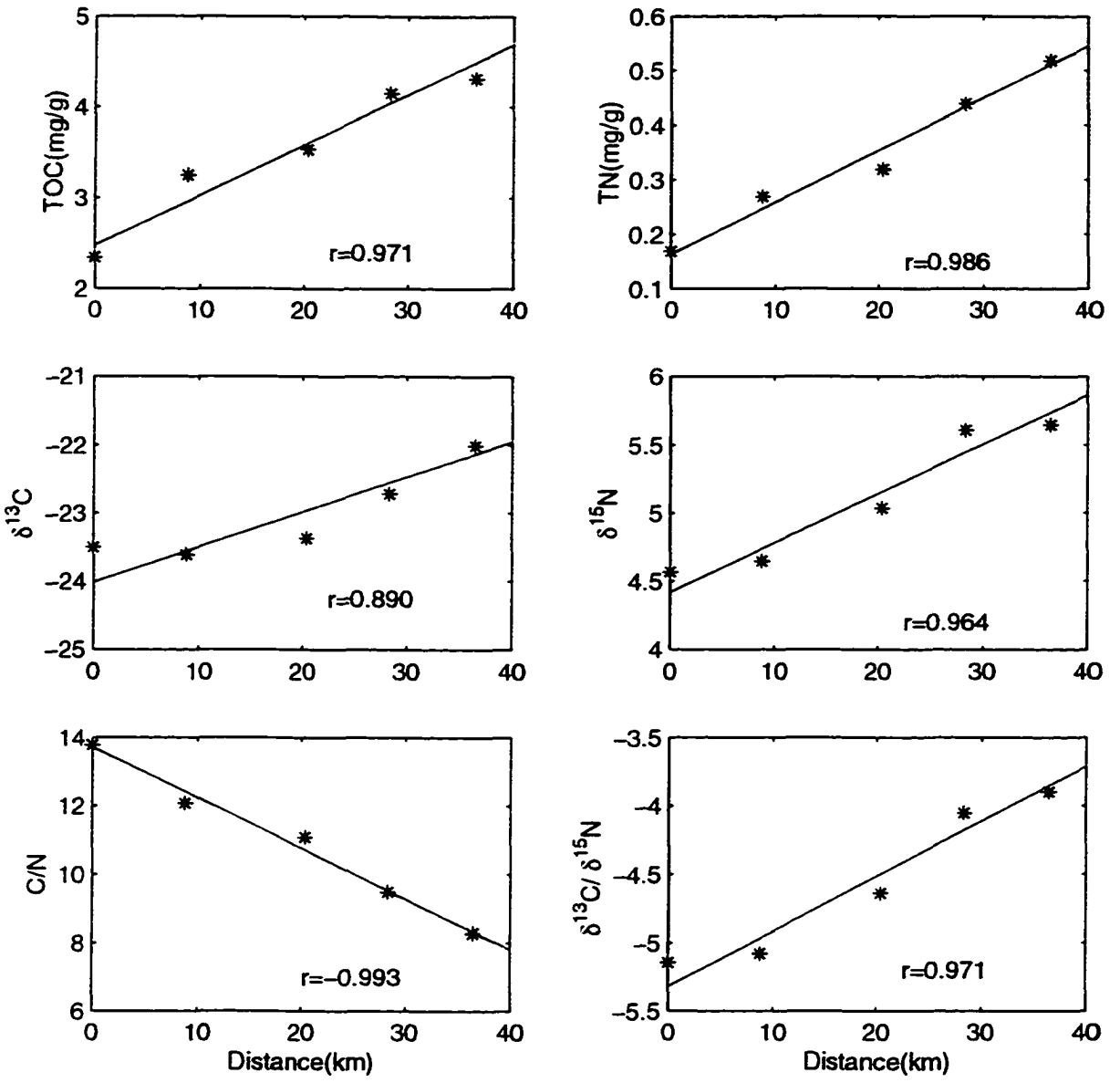

Figure 1-11. Variations from Station 213 to 217 (seaward).

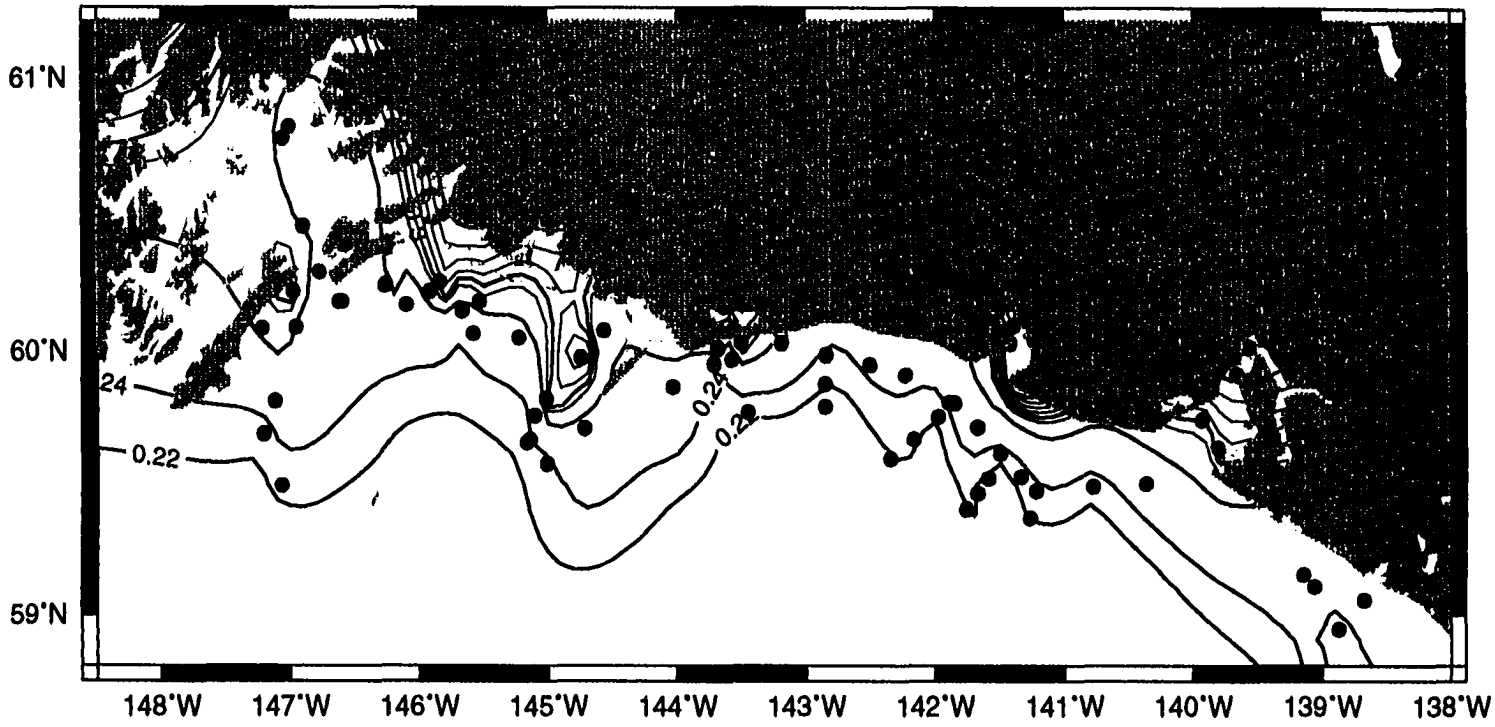

Figure 1-12. Dynamic height (0 - 75 db) contours in the Gulf of Alaska.

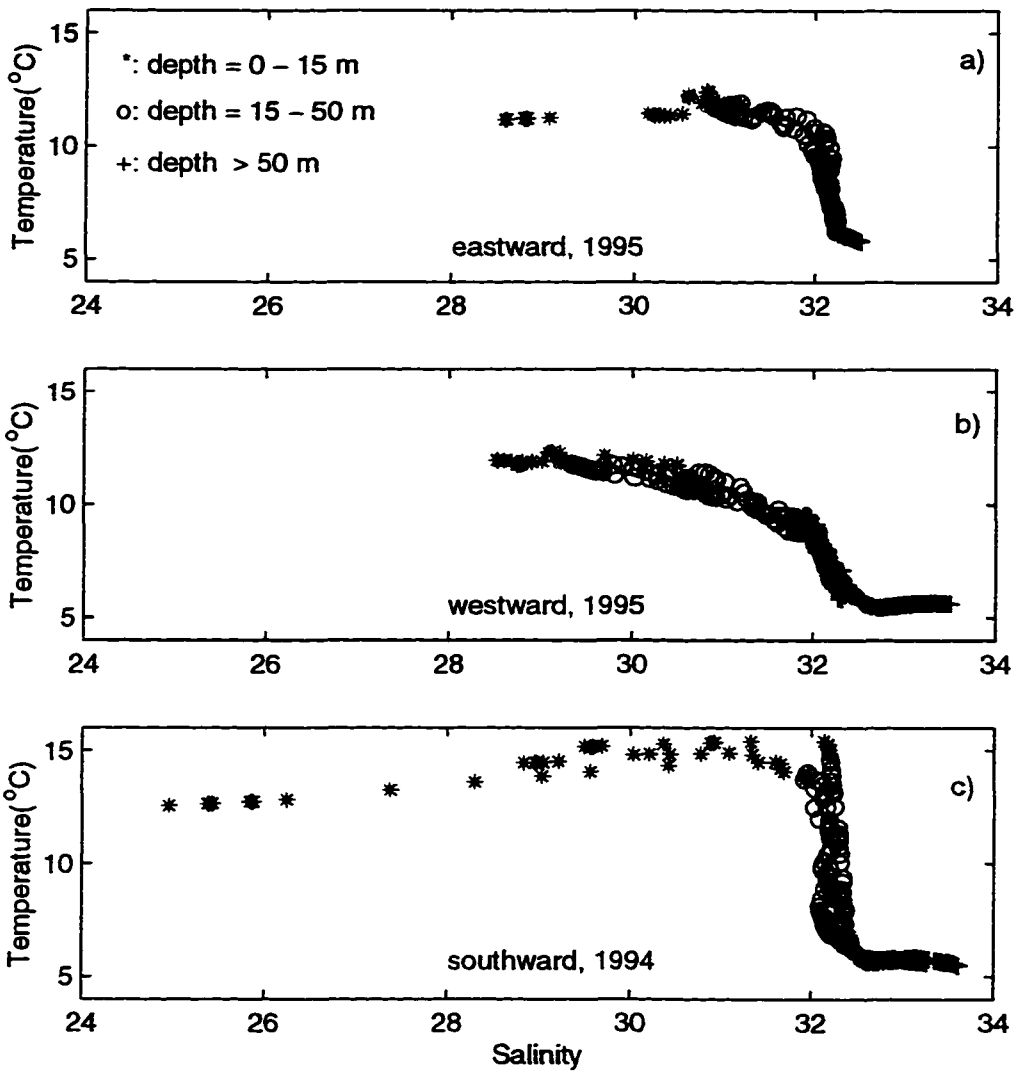

Figure 1-13. T-S curves of stations near Kayak Island.

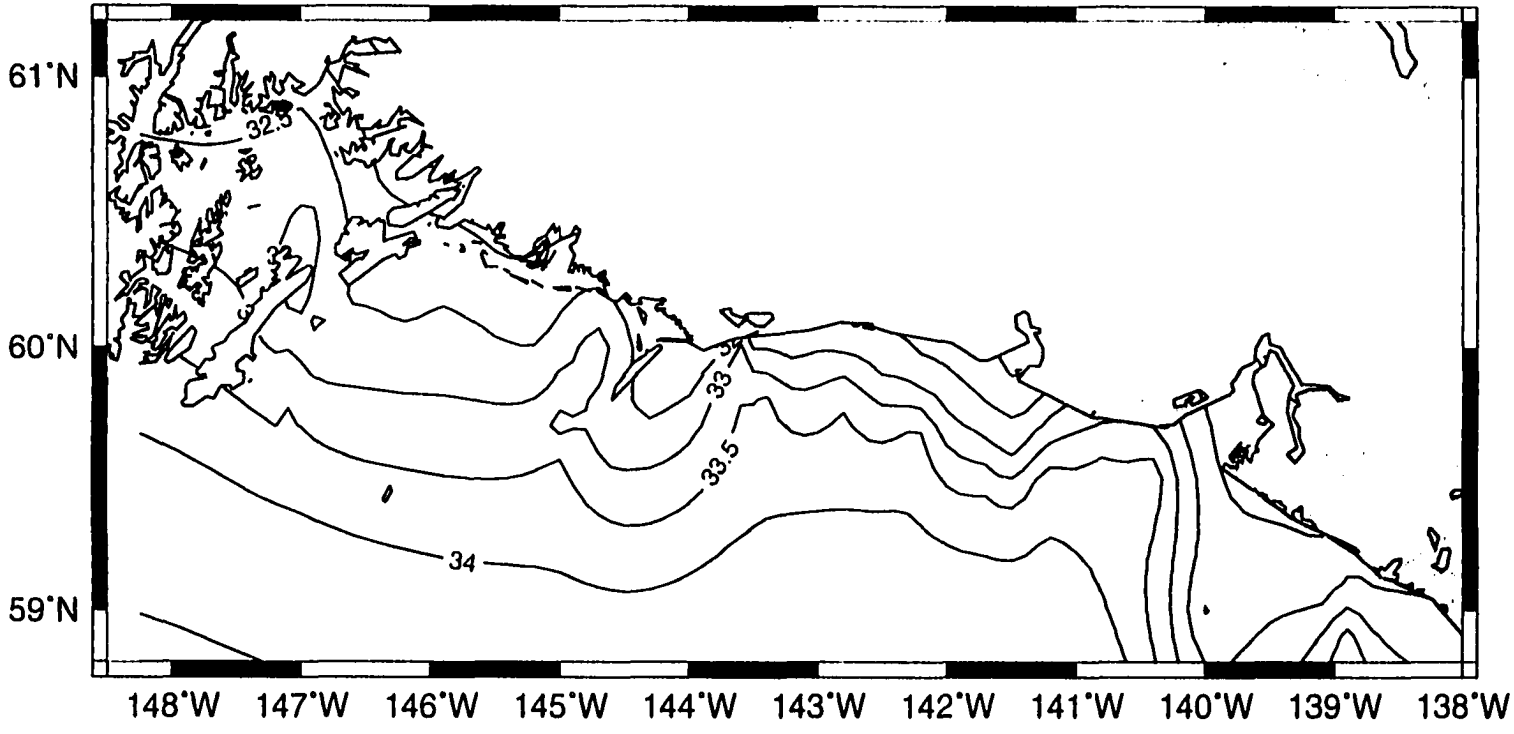

Figure 1-14. Bottom water salinity in the Gulf of Alaska.

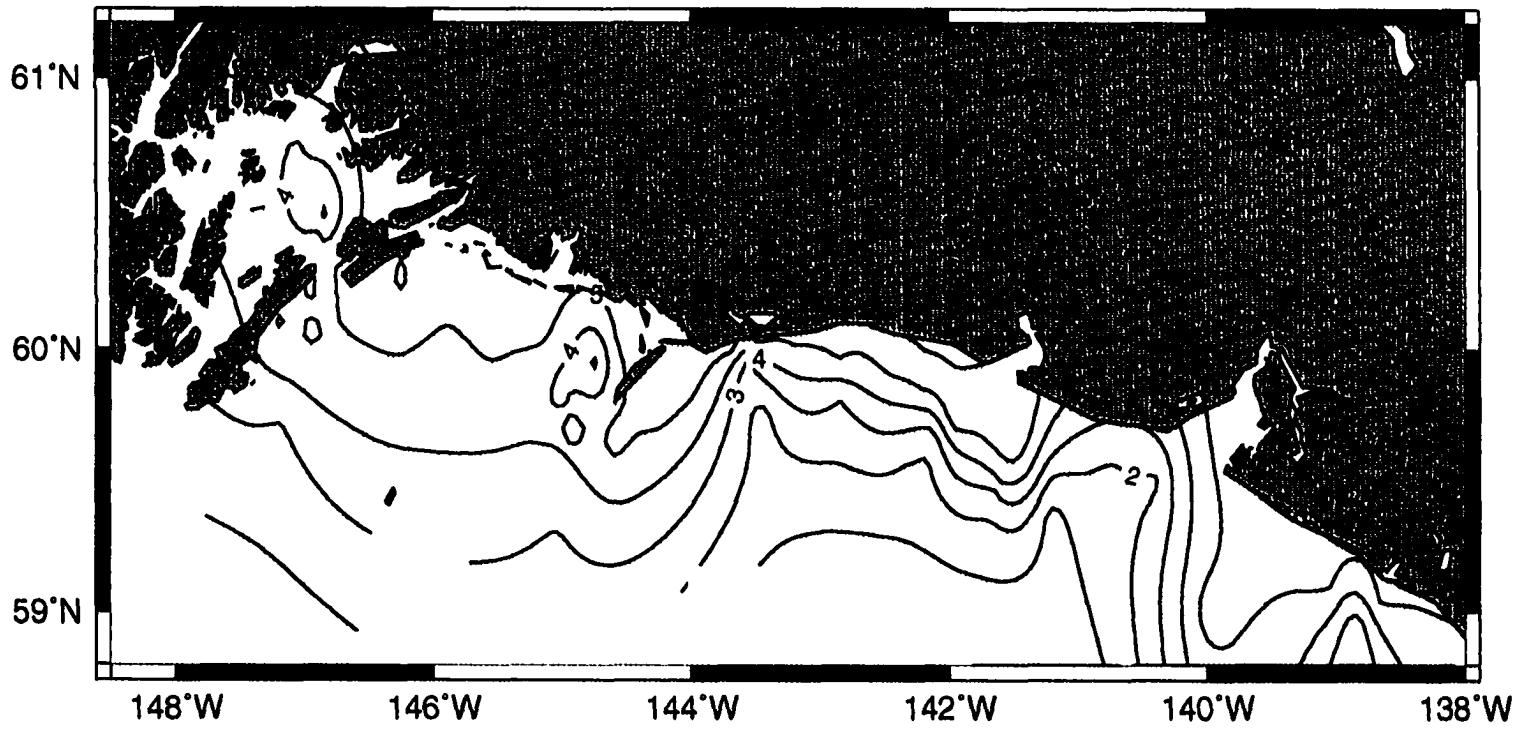

Figure 1-15. Botom water oxygen content (mg/L) in the Gulf of Alaska.

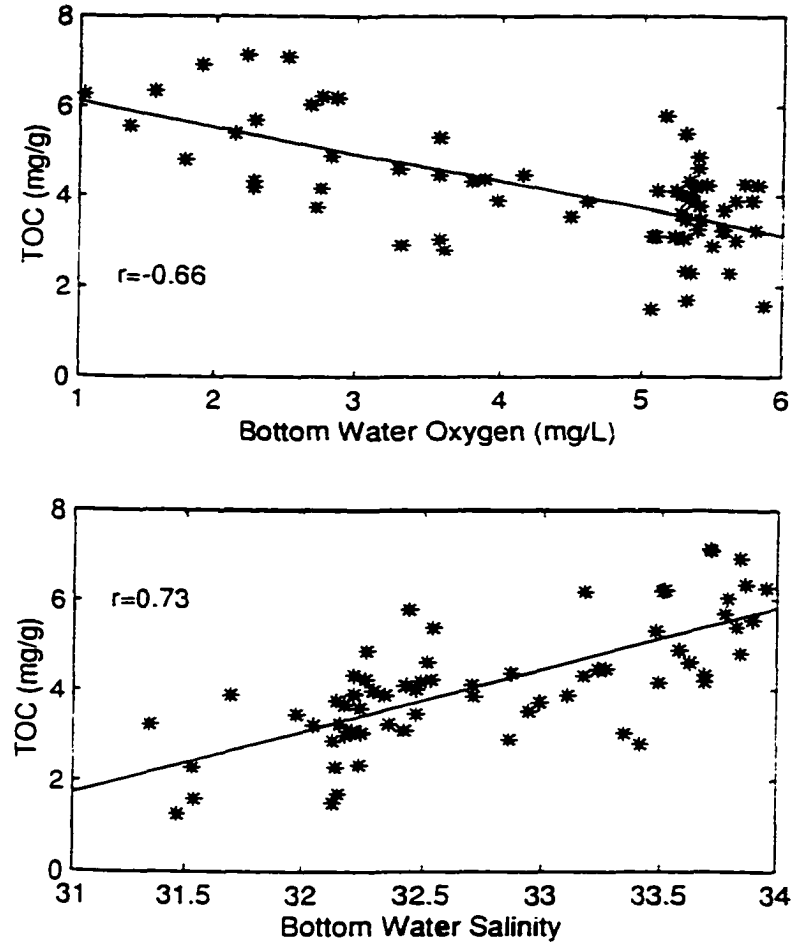

Figure 1-16. Correlations of TOC vs. bottom water salinity and oxygen content.

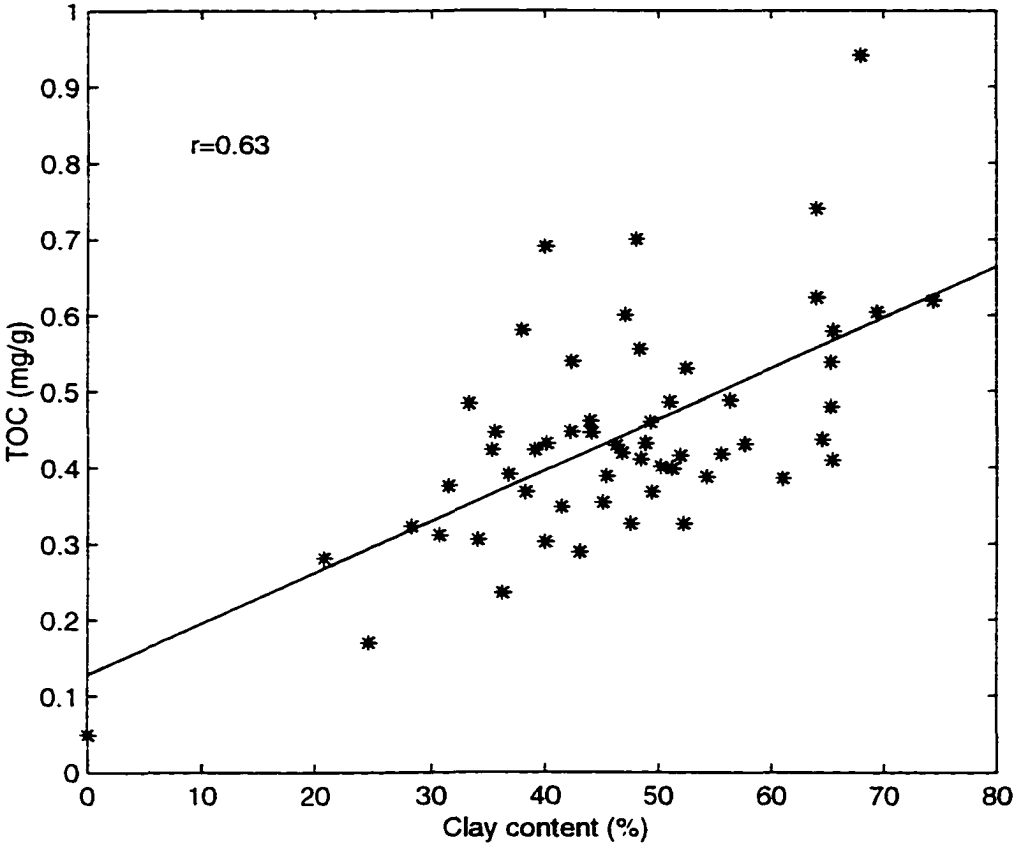

Figure 1-17. Correlation between clay content and TOC.

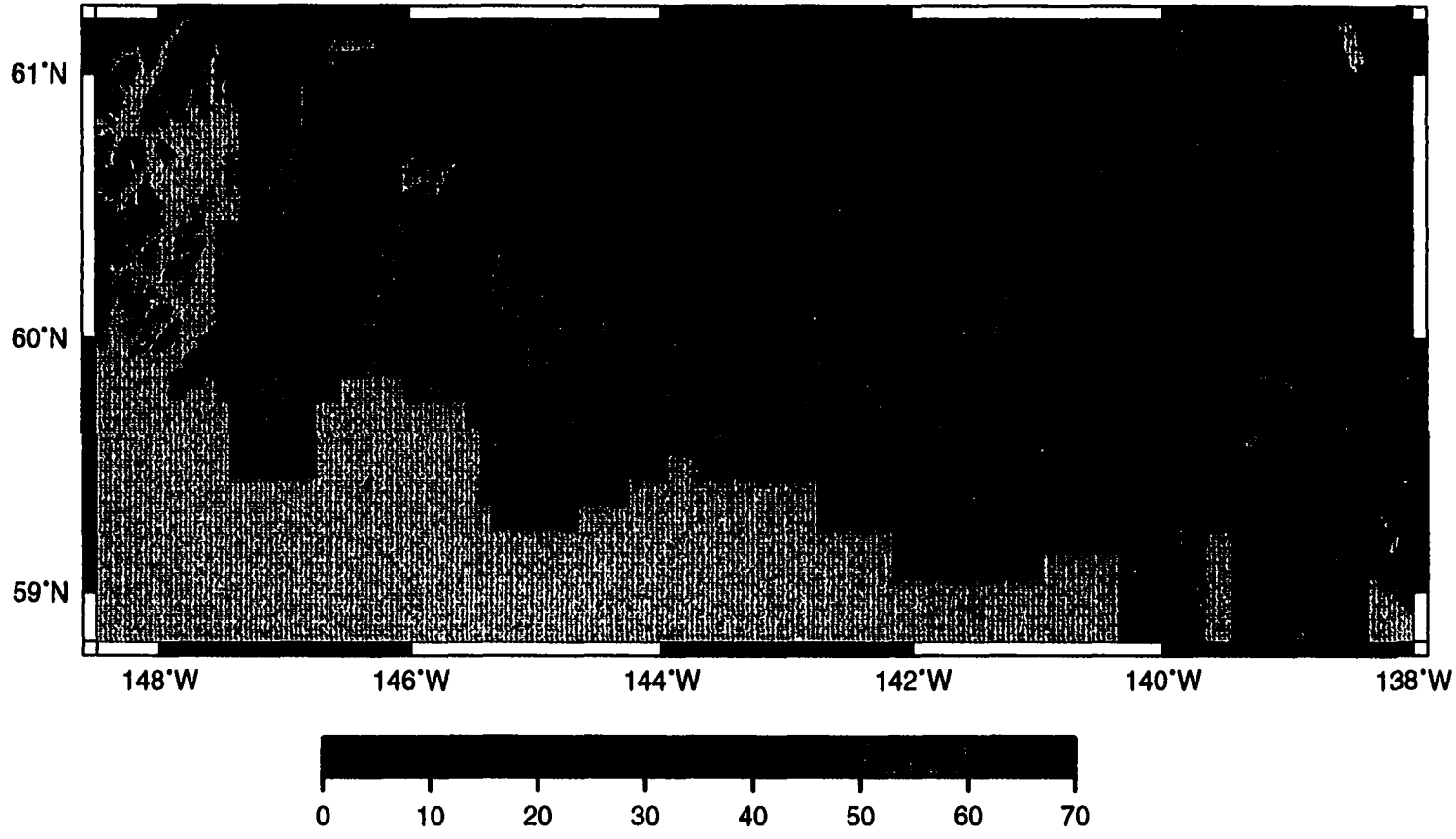

Figure 1-18. Surface sediment (0-2 cm) clay content (%) in the Gulf of Alaska (data from Jaeger et al., 1998).

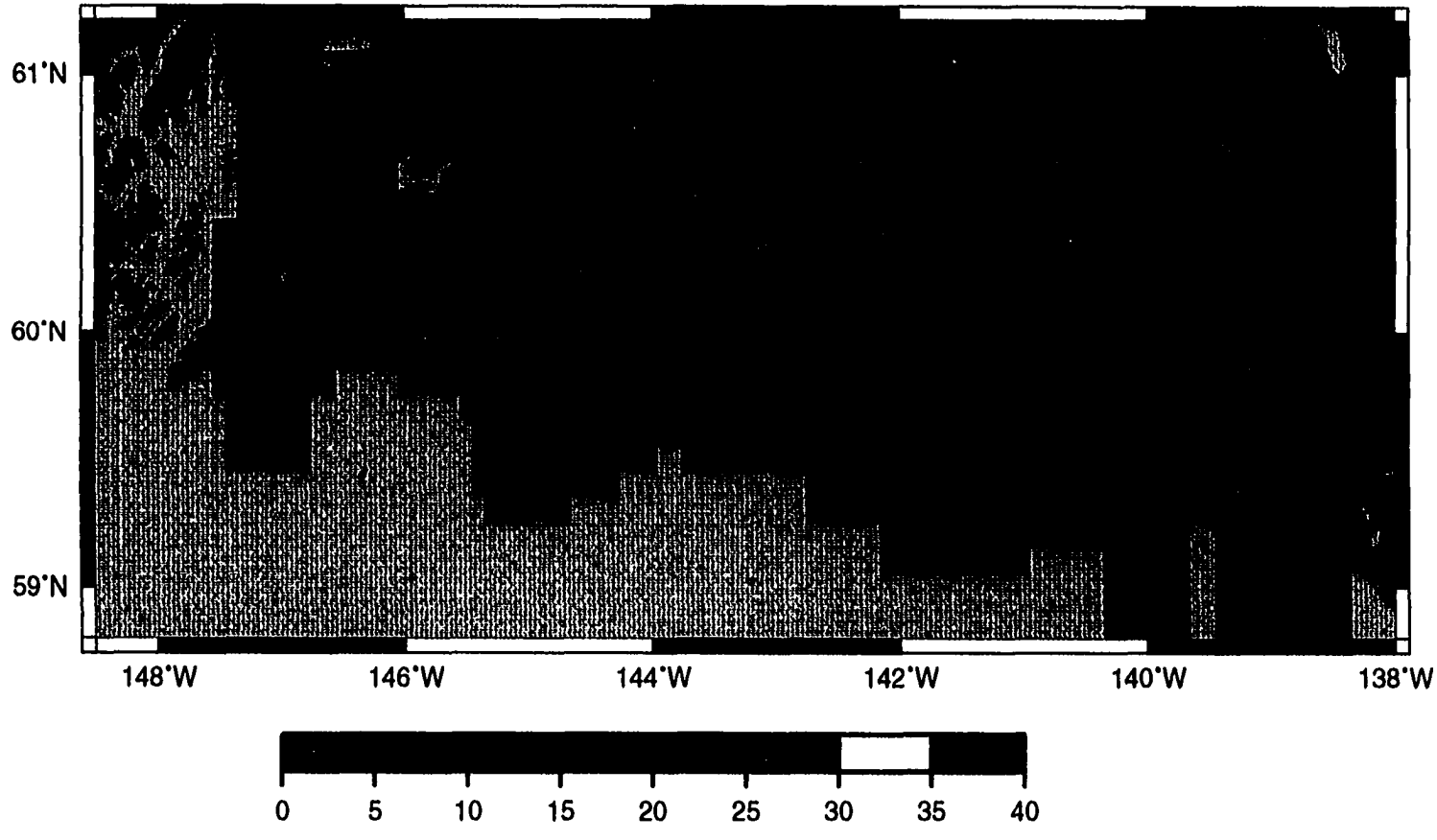

Figure 1-19. Surface sediment (0-2 cm) sand content (%) in the Gulf of Alaska (data from Jaeger et al., 1998).

Table 1-1. TOC and TN buried with fine sediments (silt and clay) on the shelf and upper slope of the northeastern Gulf of Alaska (100-yr time-scale).

	Sediment load (10^6 tons/yr)*	TOC (10^4 tons/yr)	TN (10^3 tons/yr)
Bering-Malaspina System			
Shelf	27 - 38	14 - 19	16 - 23
Kayak Trough (from Bering Glacier)	11 - 17	5 - 9	7 - 10
	38 - 55	19 - 28	23 - 33
Copper River Delta System			
Prodelta	27 - 40	9 - 14	10 - 14
Kayak Trough (from Copper River)	9 - 13	8 - 12	7 - 10
Hinchinbrook Sea Valley	8 - 12	5 - 8	6 - 9
	44 - 65	22 - 34	23 - 33
Prince William Sound	11 - 17	4 - 7	4 - 6

*: data from Jaeger, *et al.* (1998).

Table 1-2. Suspended organic carbon transported by rivers to the ocean.

River	Drainage area ($\times 10^6$ km^2)[a]	Sed. yield (t/km^2/yr)[b]	POC yield (g/m^2/yr)[c]	POC (10^6 t/yr)[d]	POC (% TSS)[e]	Ref.
North America						
St. Lawrence	1.03	4	0.2	0.2	4.3	Pocklington, 1982
Mississippi*	3.27	64	2.6	8.5	2.7	Leenheer, 1982
Brazos-	0.11	146	6.8	0.7	4.7	Meybeck, 1982
Columbia-	0.67	12	1.6	1.1	9.0	Leenheer, 1982
Yukon+	0.84	71	4.1	3.4	5.8	Leenheer, 1982
Copper+	0.06	1170	14	0.8		This work
Susitna+	0.05	500	15.6	0.8	3.1	Leenheer, 1982
Mackenzie-	1.81	55	1.8	3.3		Telang *et al.*, 1982
Kuskokwim-	0.08	90	4.0	0.3	4.3	Leenheer, 1982
Klamath-	0.022	160	2.3	0.05	2.1	Leenheer, 1982
South America						
Orinoco*	0.99	150	2.1	2.1	1.6	Nemeth, A. *et al.*, 1982
Amazon*	6.15	146	6.2	38.1	4.2	Richey, 1982
Paraná*	2.6	30	0.5	4.2	1.6	Depetris and Cascante, 1985
Europe						
Rhone+	0.09	111	0.2	0.02	2.4	Cauwet and Martin, 1982
Po-	0.07	214	0.9	0.06		Pettine *et al.*, 1985
Rioni+	0.013	630	4.0	0.05		Romankevich, 1984
Don-	0.42	18	0.04	0.02		Romankevich, 1984
Loire+	0.115	13	0.1	0.01	3.5	Cauwet and Martin, 1982
Rhine+	0.17	4	1.2	0.2	2.1	Eisma *et al.*, 1982
Asia						
Huangho (Yellow)-	0.77	1403	5.8	4.5	0.5	Cauwet and Mackenzie, 1993
Yangtze*	1.94	246	2.7	5.2	1.1	Cauwet and Mackenzie, 1993
Ganges/Brahmaputra*	1.48	1128	13.5	20.0	1.1	Safiullah *et al.*, 1985
Indus*	0.97	103	0.4	0.4	1.8	Arain, 1985
Africa						
Nile-	2.96	38	0.4	1.2	1.1	Meybeck, 1982
Niger-	1.21	33	1.1	1.3	3.3	Martins, 1983
Zaire+	3.82	11	0.5	1.9	4.7	Cadée, 1982
Orange+	1.02	17	<0.1	<0.1	1.2	Hart, 1985

*: high mountain rivers (>3000m); +: mountain rivers (1000-3000m); -: upland (500-1000m).

a: from Milliman and Mead, 1983; Milliman and Syvitski, 1992.

b: sediment yield = sediment discharge / drainage area.

c: POC yield = total POC discharge / drainage area.

d: annual POC discharge.

e: total suspended sediment.

Chapter 2

Temporal Variation of Sedimentary Organic Matter in the Northeastern Gulf of Alaska

Abstract

Total organic carbon (TOC), total nitrogen (TN), and nitrogen and carbon stable isotopic composition were measured in 374 core subsamples from 29 stations in the NE Gulf of Alaska. Both TOC and TN were usually greater in areas with larger sediment accumulation rates. Subsurface isotopically light carbon ($\delta^{13}C < -23.5‰$) and nitrogen ($\delta^{15}N < 4‰$) were generally associated with higher surface organic matter (OM) content. Terrigenous organic matter in surface sediments and low organic content were found just off the Bering Glacier, associated with the Bering Glacier surge from 1993 to 1995. Significant changes in organic matter content and sources associated with the Great Alaskan Earthquake of 1964 are reflected in some cores near the Copper River Delta. Indications of the "Regime Shift" associated with interdecadal environmental changes in the Gulf of Alaska were found in a core with a predominantly marine organic matter source. However, most sediment cores from the NE Gulf of Alaska showed little variation in organic matter content or isotopic composition with depth and time. This indicates that geographic patterns of sedimentary OM accumulation and sources have not changed substantially over the time spans represented by the cores, generally 100 - 200 years.

§ 2.1 Introduction

Examination of organic matter concentrations, isotopic composition, and C/N ratio in surface sediments have shown that the sedimentary organic matter of the NE Gulf of Alaska consists of a mixture terrestrial and marine OM sources, with some fossil material, especially in the fjords (Chapter 1 of this thesis). In this chapter, I will relate temporal changes in the characteristics of sedimentary organic matter to geological events in this region.

Sedimentary organic matter isotopic composition and C/N ratio have been frequently used to indicate organic matter sources, which in turn reflect oceanographic conditions and processes. For example, Peters *et al.* (1978) reported the correlation of carbon and nitrogen stable isotope ratios in sedimentary organic matter, probably due to a mixture of terrigenous (isotopically light) and marine (isotopically heavy) organic matter in their samples. Rau (1994) used the variations of sedimentary $\delta^{13}C$ as a proxy to study past changes in ocean and atmospheric CO_2 concentration. Altabet and Francois (1994) found a relationship between surface sedimentary $\delta^{15}N$ and nitrate concentrations in surface water. Wu *et al.* (1997) determined food-web structure in the northeast Pacific based on N stable isotopic compositions, since the $\delta^{15}N$ increases with trophic level.

The northeastern Gulf of Alaska is a major site of Holocene sediment deposition (Jaeger *et al.*, 1998; Molnia, 1979) and recent organic carbon accumulation (see Chapter 1). In the Gulf of Alaska, sediments are derived mostly from physical weathering of rocks. The sedimentation rate is extremely high in some fjords and the Copper River Delta region (Molnia, 1989). The Copper River is the major point source of fresh water and sediments in the area west of Kayak Island, while east of Kayak Island, a large number of small rivers and streams contribute, termed a "line" source (Royer, 1982). In the northeastern Gulf of Alaska coastal region, glaciation began about 6 million years ago (Molnia, 1986), and glaciers now cover about 20% of the coastal area (Royer, 1982). Many of these glaciers experienced their maximal terminal advances during the past 2,000 years, including

Malaspina Glacier. In many cases, the retreat of modern tidewater glaciers into coastal fjords started at the beginning of this century (Molnia, 1986). Glacial, glacial-marine, and glacial-fluvial sediments were deposited in some shelf areas as the ice advanced during the last ice-age.

The Bering Glacier is the largest surge-type glacier in North America. It has surged approximately once every 20 years during this century (Molnia and Post, 1995). The most recent surge began in the spring of 1993 and lasted until the summer of 1995, with two pulses of fast ice motion (accelerated ice displacement offshore); the first ended in August of 1994, and the second began in the spring of 1995 and lasted until late that summer. These resulted in the advance of the Bering Glacier terminus approximately 8 km (Roush, 1996) over two years.

Due to the north-northwest movement of the Pacific Plate relative to the North American Plate, at a rate of 5-7 cm/yr, the Gulf of Alaska is tectonically one of the most active regions in the world (Jacob, 1987). The Great Alaskan Earthquake, one of the largest earthquakes ever recorded with a M_w = 9.2, occurred in March, 1964. The earthquake caused several large local tsunamis in arms and inlets of Prince William Sound (Committee on the Alaska earthquake, 1972). An uplift of the sea floor, by as much as 15 m, occurred to the west of Montague Island (Malloy and Merrill, 1972). There was a general 2-m uplift in the Copper River Delta region (Reimnitz, 1972), which tilted an area stretching from northwest of Montague Island to southeast of the Copper River Delta.

As indicated by the irregular sea-floor morphology and disrupted bedding, an unusual number of sediment slides have occurred in the northeastern Gulf of Alaska compared with other shelf areas (Hampton *et al.*, 1987). After the earthquake, the slumps were found over an area of 1,730 km and extended 20 km offshore between Hinchinbrook Island and Kayak Island (Carlson and Molnia, 1977). Low-angle slump scars, dipping at 2°30' to 5°, a thick accumulation of Holocene sediments in certain areas, and evidence of earthquake-generated seiches in shallow-water regions were found in and near Copper River Delta (Reimnitz, 1972).

Some of these geological events are reflected in lithogenic sediments of the region (Jaeger *et al.*, 1998; Jaeger and Nittrouer, submitted). However, sediment organic matter may have different sources from the lithogenic material, and thus reflect different aspects of the geologic events. Also, organic matter is subject to decomposition by sediment organisms, and this may alter the preserved record. The purpose of this study is to delineate the source changes and diagenetic alternations of OM, and the influence of major geologic events on OM content, in the NE Gulf of Alaska.

§ 2.2 Sampling and Methods

Sediments were sampled in late August, 1994 (station numbers < 200) and early July, 1995 (station numbers > 200). Samples for this study, from continental shelf regions in the Gulf of Alaska and Prince William Sound (26 cores), and fjords (3 cores) were collected with a box corer (0 - 25 cm) or a Kasten core (0 - 250 cm), and stored frozen. Samples were analyzed after acidification to remove carbonate. After drying at 70 °C, sediments were ground and stored in 5-ml vials until analysis. The analytical precision, as the average deviation of duplicate samples, is 0.016 mg/g for total nitrogen (TN), 0.17mg/g for total organic carbon (TOC), 0.11‰ for $\delta^{13}C$, and 0.5‰ for $\delta^{15}N$. The average relative deviation is 4% for TN and TOC, 0.5% for $\delta^{13}C$, and 15% for $\delta^{15}N$. TOC, TN, $\delta^{15}N$ and $\delta^{13}C$ were measured using a Europa Model 20/20 mass spectrometer with Roboprep(TM) automated combustion device.

§ 2.3 Results

TOC and TN and stable carbon and nitrogen isotopic composition were measured in 20 cores > 1m in length and 9 cores < 1m in length. Locations of the selected stations are shown in Figure 2-1. In 85% of the 374 downcore samples, TOC ranged from 2.5 - 6.5 mg/g, with a mean value of 4.4 mg/g, and TN varied from 0.2 - 0.6 mg/g with a mean value of 0.40 mg/g. In 75% of the samples, $\delta^{13}C$ ranged from -25.0 to -22.0‰, with a mean

value of -23.5‰, and $\delta^{15}N$ was between 2.0 - 5.2‰, with a mean value of 3.5‰. Both TOC and TN were usually greater through out cores in areas with larger surface sedimentary OM accumulation. Surface and subsurface isotopically light carbon ($\delta^{13}C$ < -23.5‰) and nitrogen ($\delta^{13}N$ < 4 ‰) were generally associated with higher surface sediment OM content (Table A-3).

About 35% of the 20 cores > 1m in length showed trends in $\delta^{13}C$, $\delta^{15}N$ and C/N indicating that more terrigenous organic matter was accumulated at earlier times. TN and TOC did not change significantly with depth in these cores. In 45% of the cores > 1m in length $\delta^{13}C$, $\delta^{15}N$ and C/N ratio varied only slightly with time and showed no consistent change in organic matter source (e.g., Table A-3; also see Figure 2-4). The remaining cores showed variations in terrigenous OM, but no consistent temporal trend, or had compositional changes due to diagensis.

§ 2.4 Discussion

§2.4.1 Diagenetic Changes

During mineralization, nitrogen-rich OM tends to lose N due to preferential decomposition of N-rich compounds, resulting in increased C/N ratios with time (Tyson, 1995a). In the 20 cores > 1m in length, 15 cores showed a slight increase in C/N ratios with time. Only 2 cores, from just off the Bering Glacier, showed a significant decrease in C/N ratios. Six cores showed a larger change in C/N coupled with a > 1.5‰ variation in $\delta^{13}C$ between top and bottom of the cores, indicating a source change with time (Figure 2-2A). The changes in $\delta^{13}C$ and C/N with depth in cores are illustrated for 3 representative stations (Figure 2-2B). At Station 122, where $\delta^{13}C$ showed a small change, but C/N increased markedly with time, the changes are due to a combination of diagenesis and varying OM source. Figure 2-3 shows that there was a rapid decrease in TOC and TN in the upper 4 cm, coupled with an increase in C/N, and slight enrichment of both ^{13}C and ^{15}N. This pattern is very likely due to organic matter decomposition. Subsequently TOC and TN change

little, but $\delta^{13}C$ and $\delta^{15}N$ become lighter and C/N increases, indicating that more terrigenous organic matter was accumulated at earlier times. This pattern may also reflect the gradual retreat of the Malaspina Glacier, and less deposition of glacially-derived sediments on the shelf more recently.

The Station 111 core showed relatively large variations in both C/N and $\delta^{13}C$ (Figure 2-2B) but no clear overall trends with time (Figure 2-6). Station 126 showed little change with time and a stable isotopic composition typical of a marine source. The pattern from Station 126 to 122 to 111, an along-shelf transect from east to west, is of increasing terrigenous OM throughout the cores.

The samples from Station 205 (Figure 2-4) showed relatively constant values of $\delta^{15}N$, $\delta^{13}C$ and C/N ratio with depth. Meanwhile, both TN and TOC decreased slightly with time, probably due to remineralization processes. The samples from Station156 (Figure 2-5) showed constant values of TN, TOC, $\delta^{15}N$, $\delta^{13}C$ and C/N ratio with depth, probably reflecting a uniform biogeochemical and physical environment. This station is far from large glaciers and rivers, which comprise the major fresh water and sediment sources, avoiding direct influences of large variable point sources. The OM at this station is predominantly of marine origin. These two cores are typical of 45% of those longer than 1 m in length, which apparently had nearly constant organic matter sources with time.

§2.4.2 *Isotopic Compositions and their Variations*

Table 2-1 shows that, generally, marine-derived organic matter has a heavier $\delta^{13}C$ (mean = -22.16‰), while samples containing more terrigenous OM are isotopically lighter (e. g., Bering Glacier, Copper River Delta). This is consistent with other studies of sediment sources using stable C isotopes (O'Leary, 1988; Tyson, 1995b). $\delta^{15}N$ shows a similar pattern, and in addition has greater variability within cores. This reflects the fact that sedimentation in nearshore regions is greatly affected by local events, such as variation of fresh water discharge and glacial sediment output, etc., leading to more temporal

variability. In the Copper River Delta region, most of the cores showed a mixture with more terrigenous than marine sources. The increasing $\delta^{15}N$ westward from the mouth of the Copper River indicates decreasing terrigenous organic matter away from the Copper River. Core 241 was 250 cm long, while 158 was only 20 cm long. The $\delta^{15}N$ in 241 at ≥ 25 cm was about 2.1, while in top 20 cm of both cores it was about 3.6. The average $\delta^{15}N$ and $\delta^{13}C$ in the cores off Bering Glacier were less light than those from the Copper River Delta.

The greatest temporal variability in $\delta^{15}N$ and $\delta^{13}C$ was found in the cores from the mouths of IB and YB. These cores are both long (1.5 m for 152 and 2 m for 147). Due to very low sedimentation rates, the oldest sediments are hundreds to thousands of years old (Jaeger *et al.*, 1998). During this long period, the great retreat of the Malaspina Glacier is reflected in the cores, accounting for their variability.

Jaeger *et al.* (1998) divided the sediment cores from the studied area into four types according to their ^{210}Pb profiles: I: steady-state accumulation; II: event-layer deposition; III: change in steady-state accumulation; IV: varying activity without trend. These types are indicated in Table 2-1. (See Figure 2-1 for their locations). Most of the II and IV sedimentation types were located in the Copper River Delta region and off the Bering Glacier, where organic matter had a substantial terrigenous character and where fresh water discharge affected the input of organic matter, along with geological events such as the earthquake and glacial surges. In the area off Bering Glacier, only core 227 had type I sedimentation, which matches our observations of Bering Glacier surge being recorded in the organic matter of all of the cores except in core 227 (see next section). Most of the type I and III cores were located at places far from freshwater discharge, with typical characteristics of a constant marine organic matter source. The exceptions to this pattern were two cores from Alsek Sea Valley (149 and 150), where $\delta^{15}N$ and $\delta^{13}C$ were marine, but the sedimentation type was II.

Stations 205, 201 and 156 were located at the entrance between Montague and Hinchinbrook Islands, where part of the Alaska Coastal Current enters Prince William

Sound. All these cores are type III. This suggests that Alaska Coastal Current has changed with time. From Core 205 to 201 to 156, the average $\delta^{15}N$ increased and its variability decreased, probably reflecting increasing distance away from the Copper River. Since all of these cores showed no or little change in organic matter source over time, alterations in sedimentation rates apparently were not connected to major changes in sediment source.

The $\delta^{15}N$ and $\delta^{13}C$ ratios of most of our samples from cores of types I and III showed no or little source change with time, while type II and IV cores showed greater fluctuations with time, or sharp event-related changes (Figures 2-15 and 2-16). The $\delta^{15}N$ and $\delta^{13}C$ ratios in type II cores showed changes at depths similar to those where event layers were found in ^{210}Pb data (Jaeger *et al.* 1998). Some such events apparently resulted from sudden change in sediment accumulation, due to glacier surges and/or sediment slides. However, most of the non-steady state ^{210}Pb profiles appear to be mainly related to changes in the source of sediments, as indicated by changes in sediment OM.

§*2.4.3 Bering Glacier Surges*

A glacier surge is defined as a brief period of very rapid flow, usually lasting one to four years, between normal flow periods which last 10 to 100 years (Kamb *et al.*, 1985). During a surge, ice within a glacier can be displaced several kilometers or more, resulting in a dramatic advance of its terminus (Heinrichs *et al.*, 1995). This behavior is not thought to be linked to climate change, but rather is related to the failure of subglacial water drainage (Kamb, 1987). This results in trapping and redistribution of water in cavities, and causes elevated subglacier water pressure and thus accelerates basal sliding. Also, Alaskan surge-type glaciers are located in complex tectonic settings. An unstable ground layer beneath them may be an important factor influencing surge activity (Harrison, 1994). A surge of the Bering Glacier was observed between March, 1993, and August, 1994, and it resumed in April, 1995, continuing until late summer that year (Roush, 1996). Almost at the same time, there was an outburst of sediment-laden water from the glacier base along its eastern margin. A flood occurred in the same location following a 1967 surge. Possibly,

an unusually large channel or trough present in the bed topography trapped most of the subglacial drainage water and carried it to one point of discharge (Roush, 1996).

The samples from the core just off the Bering Glacier (Figure 2-6) showed evidence of its surge from 1993 to 1995. In the surface layer, lighter carbon and nitrogen and greater C/N ratio were found during the time interval that increased land-derived sediment was probably deposited. Unusually low OM in the surface layer was due to the dilution by glacial sediments. In sediments deposited about 30 years ago, a similar pattern, a slight increase in C/N and decrease in $\delta^{15}N$, was found, which was probably associated with another Bering Glacier surge in 1957-1960, when the terminus advanced almost 8 km. This was followed by a minor surge in 1965-67, which advanced the terminus 1 km farther (Roush, 1996).

§2.4.4 *Fjords*

Many short but high-discharge streams drain the Malaspina Glacier, loading substantial quantities of glacially-derived sediments directly into the marine environment (Molnia, 1989). At the beginning of this century, following 500-700 years of retreat, Malaspina Glacier experienced a period of advance related to surging (Plafker and Miller, 1958).

Yakutat Bay (YB), a fjord located to the east of the Malaspina Glacier, was completely filled by a glacier several hundred years ago (Molnia, 1989). An extremely high C/N ratio was found in surface sediment from the head of YB, and the ratio (21.5) decreased to 8.8 at its mouth (see Chapter 1). TOC and TN tended to increase from head to mouth, indicating that old organic-poor sediment was input at the head. Also, high $\delta^{15}N$ was associated with the high C/N ratio, and $\delta^{15}N$ decreased from the head to mouth, from 12‰ to 4‰. The surface sedimentary $\delta^{13}C$ was not unusually light, with a mean value of -22.6‰, and the change from the head to mouth was from -22.2‰ to -23.9‰. The variations of isotopic composition and C/N in YB suggested that the old organic carbon

input from its head may be of marine origin, from sedimentary rocks eroded by the glacier. Miller (1953) recognized that some deposits of the Yakataga Formation were derived under marine conditions from a rafting ice shelf, from icebergs, or both.

Rapid erosion on both sides of the mouth of Icy Bay (IB) was reported by Molnia (1977). My data show that the surface sedimentary C/N ratio tended to decrease from its head to the mouth (18.9 to 10.2, Chapter 1), again suggesting that old organic matter was input at its head. Differing from YB, $\delta^{15}N$ and $\delta^{13}C$ increased from head to mouth (1.3‰ to 6.1‰ and -26.1‰ to -23.5‰, respectively). The low $\delta^{15}N$ and $\delta^{13}C$ suggested that old terrigenious organic matter was input at the head. A dropstone found at the mouth of IB showed even lower $\delta^{15}N$ and $\delta^{13}C$ (-0.2‰ and -25.0‰, respectively) than those in sediment, also indicating a fossil terrigenious source. Porter (1989) described Icy Bay: "In steeper terrain, gulches carved in the bedrock hills are partially filled with glacial and nonglacial sediments that are being exposed by stream erosion. Organic remains are ubiquitous: subfossil tree trunks, root systems, and branches are widely scattered over the surface, and remains of many trees are found rooted in place and enclosed by till. Buried soil, rich in plant detritus, are visible in many natural exposures, especially along stream cuts".

Stations 128 and 117 (Figure 2-7 and 2-8) were located in YB and IB, respectively, where sediment accumulation rates are extremely high (Molnia, 1989). Due to an extremely large sediment accumulation rate in the head of YB (1.75 m/yr, Molnia, 1989), the sample from Station 128 may only reflect seasonal variations in organic matter content and isotopic composition. Unusually low TOC and TN in surface sediment were probably due to dilution by organic-poor glacially-derived sediments in summer. At Station 117, except for slight variations in the upper few cm, all TOC, TN, $\delta^{13}C$, $\delta^{15}N$ and C/N ratios showed relatively constant values with time. A gradual increase of sedimentary TOC from the YB head to mouth may also reflect the primary productivity in the overlying water column, which should be greater near the mouth due to less turbid water. In IB, TOC

tended to decrease from head to mouth, indicating terrigenous, fossil materials were the major carbon source, especially near the head.

§2.4.5 *Great Alaskan Earthquake*

The samples from Station 105 in the Copper River Delta region (Figure 2-9) showed a possible effect of the 1964 Great Alaskan Earthquake. Sharp changes in sediment composition around 30 years ago reflected a sudden event happening at that time. This change may be associated with the ejection of sediments from below the delta surface, which could have occurred when the grains in the upper layer were more tightly packed together due to vibration, releasing pore water that mixed with sand, silt and clay and ejected to the surface. Or, changes in sediment texture could be due to an earthquake-generated slump found from Egg Island Trough landward (Reimnitz, 1972). A sharp increase of $\delta^{13}C$ indicated that an event resulted in more marine-derived sediment deposition for a short period. An increased C/N ratio suggested that the OM had been extensively decomposed. The decrease of TOC is also suggestive of older sediment in which much of the OM had decomposed.

The samples from Station 101 may also reflect sediment redeposition related to the Great Alaskan Earthquake (Figure 2-10). A significant change in both TOC and TN was found, which could be due to redistribution of sediment from a more organic-rich site at that time. However, $\delta^{13}C$, $\delta^{15}N$ and C/N ratios do not show a significant change in OM source.

Alternatively, sediment variation could be due to changes in runoff. Water circulation in the Gulf of Alaska is characterized by the cyclonic flow of the Alaska Gyre, which includes the eastward Subarctic Current at about 50°N, the Alaska Current in the northern Gulf, and the Alaskan Stream, a southwestward outflow from the Gulf of Alaska along the Alaska Peninsula. The Alaska Coastal Current is baroclinic flow affected by fresh water discharge, and it greatly depends on the Copper River runoff in that region.

Around 1981 and 1971, the core showed sharp changes in TOC, TN, $\delta^{13}C$ and $\delta^{15}N$. This may be associated with high runoff in the corresponding years. In 1981, the Copper River discharge near Chitina was the greatest of the years 1956 - 1990. The second greatest discharge was found in 1971 (data from United States Geological Survey, World Wide Web). In 1981, the peak daily runoff reported by USGS was about 10×10^3 m^3 s^{-1}; in 1971, it was about 7×10^3 m^3 s^{-1}, and that for the remaining years was about 4×10^3 m^3 s^{-1}.

§*2.4.6 Copper River Delta*

A group of cores (Stations 241, 239, 106, 236 and 235, Figure 2-1) from a transect across the Copper River Delta region (Table 2-2) showed that the highest TN and TOC contents were near Kayak Island due to deposition beneath the Kayak eddies. $\delta^{13}C$ and $\delta^{15}N$ from the same transect showed that some terrigenous OM from the Copper River was transported northwestward, as expected due to the flow of the Alaska Coastal Current, but that some was transported toward Kayak Island. The calculation of the contribution of terrestrial sources, based on the mixing model, also indicated a similar pattern. Also, the greater the terrestrial source, the more rapid was sediment accumulation, reflecting the contribution of the Copper River since its sediment load is large (Chapter 1). Consistent with my findings on OM transport and deposition, it was found that highest Holocene sediment accumulation, 325 m thick, lay just southeast of the main channel of the Copper River, and that a relatively thick layer of Holocene sediments, 150 m thick, are located in the upper delta region, decreasing seaward (Hampton *et al.*, 1987). This suggested that at least some of sediments from the Copper River were transported southeastward and deposited beneath the Kayak island eddies, and that this transport has persisted through the Holocene.

§*2.4.7 "Regime Shift" in the Gulf of Alaska*

There are various hypotheses about causes of interdecadal changes in the ocean and atmosphere, including the increase of greenhouse gases in the atmosphere, El Niño

Southern Oscillation (ENSO) events, and changes in solar, volcanic, or magnetic activity. The effects of many of these are thought to be amplified at high latitudes (Committee on the Bering Sea Ecosystem, 1996).

Interdecadal changes in the sea surface temperature of the Gulf of Alaska (Figure 2-11) demonstrate a relatively warm period (>1 °C variance) around 1958, then a temperature decline until 1973, when it was about 1 °C colder than normal. From 1973 to 1984 there was a relatively rapid temperature increase (~ 0.1 °C/yr), and then temperature declined until 1989 (Committee on the Bering Sea Ecosystem, 1996). The North Pacific sea level anomalies (Figure 2-11), the North Pacific index, and the catch of sockeye salmon (Committee on the Bering Sea Ecosystem, 1996) also showed the "Regime Shift" within this time frame.

Figure 2-12 shows the changes of $\delta^{15}N$ with time from two marine cores (Stations 101 and 149). Basically, the Station 101 data indicate interdecadal variations, and higher temperatures are associated with greater $\delta^{15}N$, except for 1-5 years' difference in timing compared with the temperature variation. This is well within the uncertainty of the sedimentation rate used in the calculation of sediment ages. A constant sediment accumulation rate based on the ^{210}Pb and ^{137}Cs data (Jaeger *et al.* 1998) was assumed. Station 149 data are not inconsistent with the patterns of Station 101, but the sedimentation rate of this core is lower and the record is more blurred by bioturbation. Altabet and Francois (1994) reported that as NO_3^- was depleted, the $\delta^{15}N$ of phytoplankton rose, thus increasing the $\delta^{15}N$ of newly produced particulate N. Also, they found a latitudinal pattern of lower surface ocean [NO_3^-] and greater $\delta^{15}N$ in sediment across productivity gradients. So, times of greater NO_3^- depletion should be associated with greater $\delta^{15}N$ in Gulf of Alaska sediments. Greater NO_3^- depletion might reflect stronger stratification, due to warmer temperatures or increased fresh water inflow.

It is premature to speculate further on the causes of the $\delta^{15}N$ changes observed, since the data available within my cores are limited. To avoid any influence of geological events, I chose only the stations among the cores in the marine source group with suitable

accumulation rates and core lengths. Very low accumulation rate (e. g., Core 119. 0 mm/yr) results in loss of signal, while fast sediment accumulation (e. g., Core 201. 12 mm/yr) results in insufficient time within the core to record the change. The two cores shown are the only ones in our study area that met the criteria. They suggest that it may be possible to find long-term records of decadal climatic change in NE Gulf sediments.

§ 2.5 Conclusions

1) Greater TOC and TN in the subsurface sediments were found in areas with larger surface sedimentary OM.

2) Isotopically light carbon and nitrogen and high C/N ratios in subsurface sediments were generally correlated with surface signatures; this indicates that the geographic patterns in sedimentation discussed in Chapter 1 have been persistent for the time spans represented by the cores.

3) The Great Alaskan Earthquake, Bering Glacier surge and a climatic "Regime Shift" were recorded in some cores.

4) However, most of the cores collected in the NE Gulf of Alaska showed little variation in OM content or sources with time.

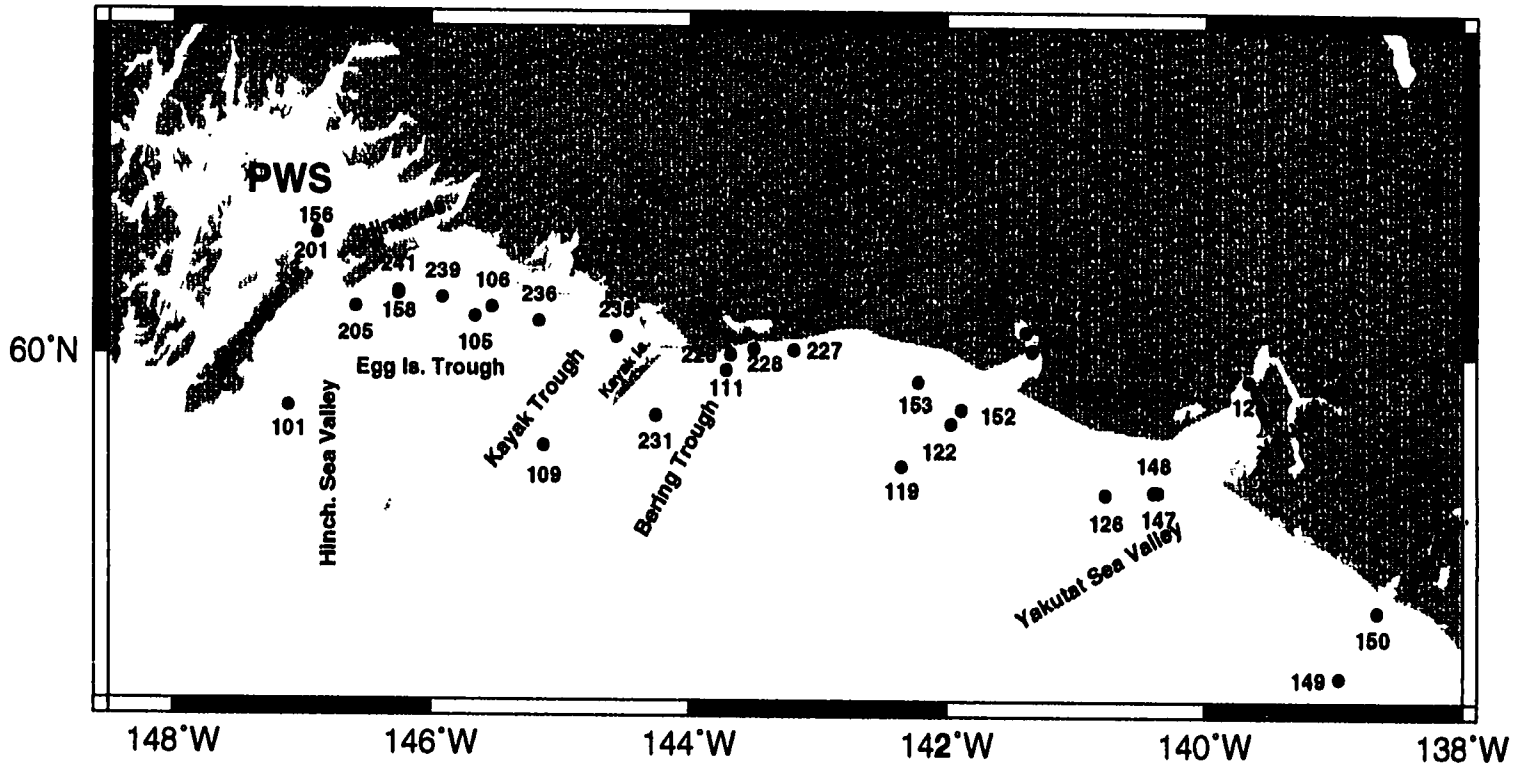

Figure 2-1. Selected sampling stations in the Gulf of Alaska.

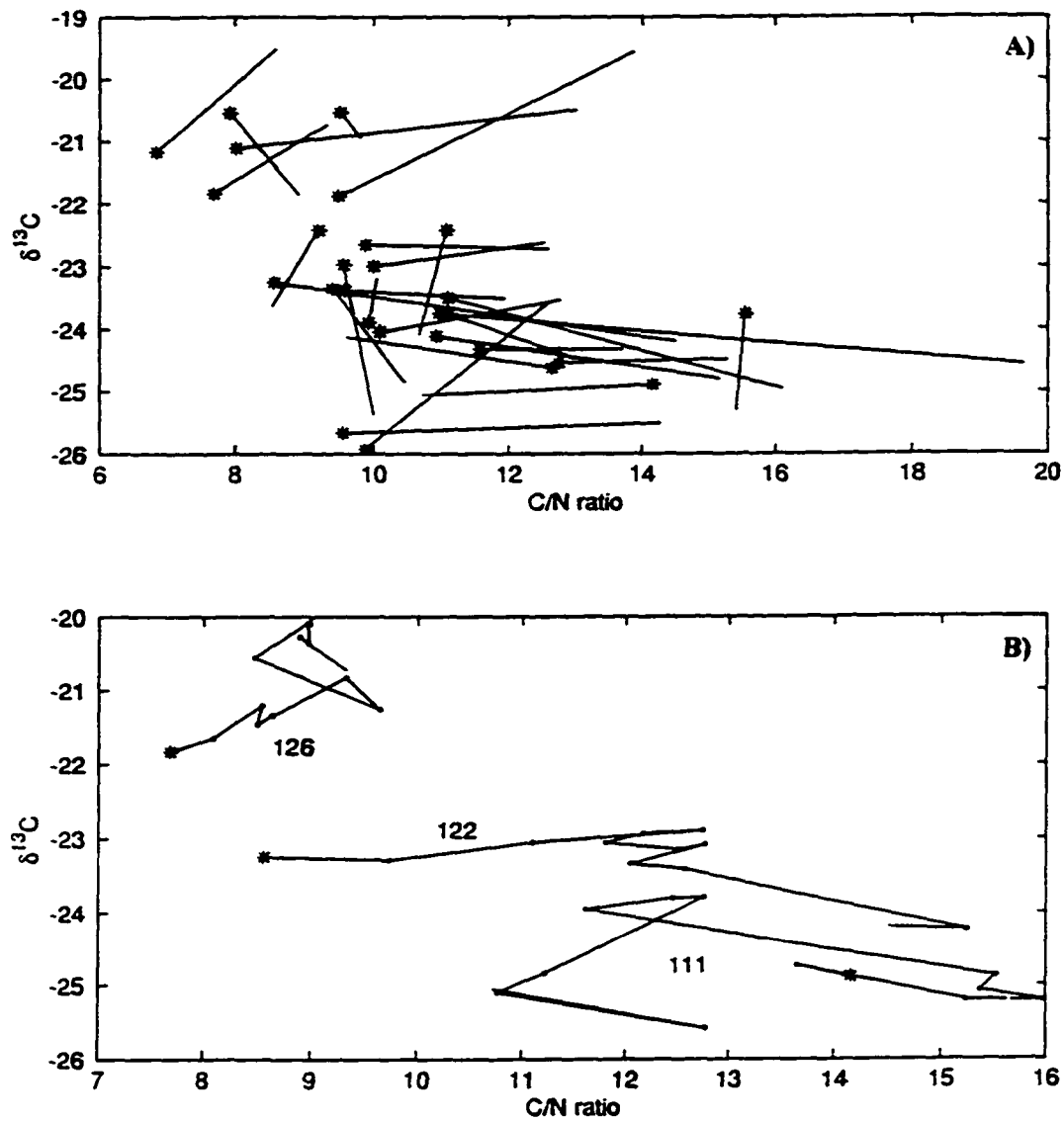

Figure 2-2. Changes in $\delta^{13}C$ and C/N ratio with depth in A) all cores and B) three representative cores. The asterisk represents data for surface sediments; points indicate subsurface samples.

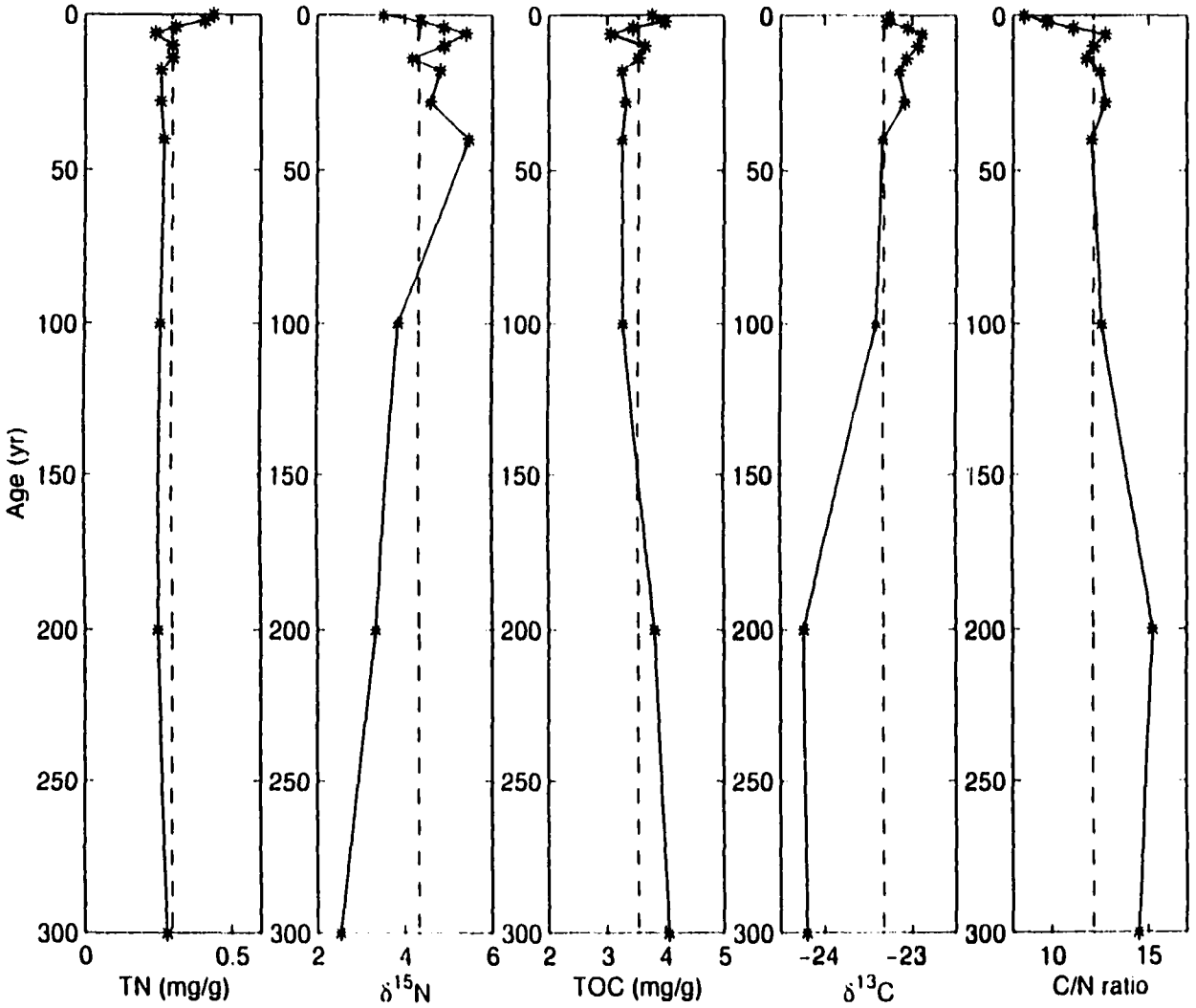

Figure 2-3. Variation in organic matter content and isotopic composition with time in the core from Station 122.

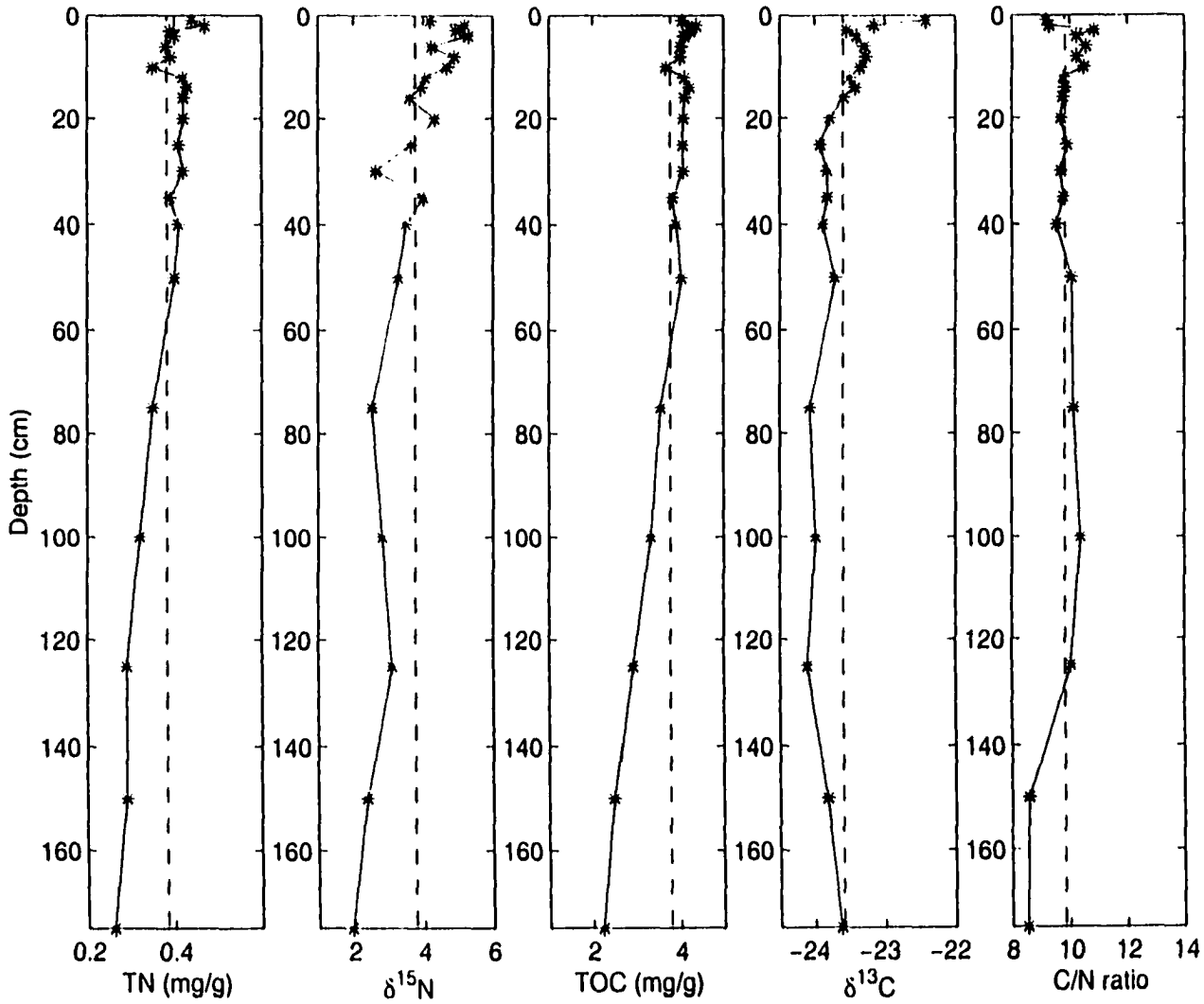

Figure 2-4. Variations in organic matter content and isotopic composition with depth in the core from Station 205.

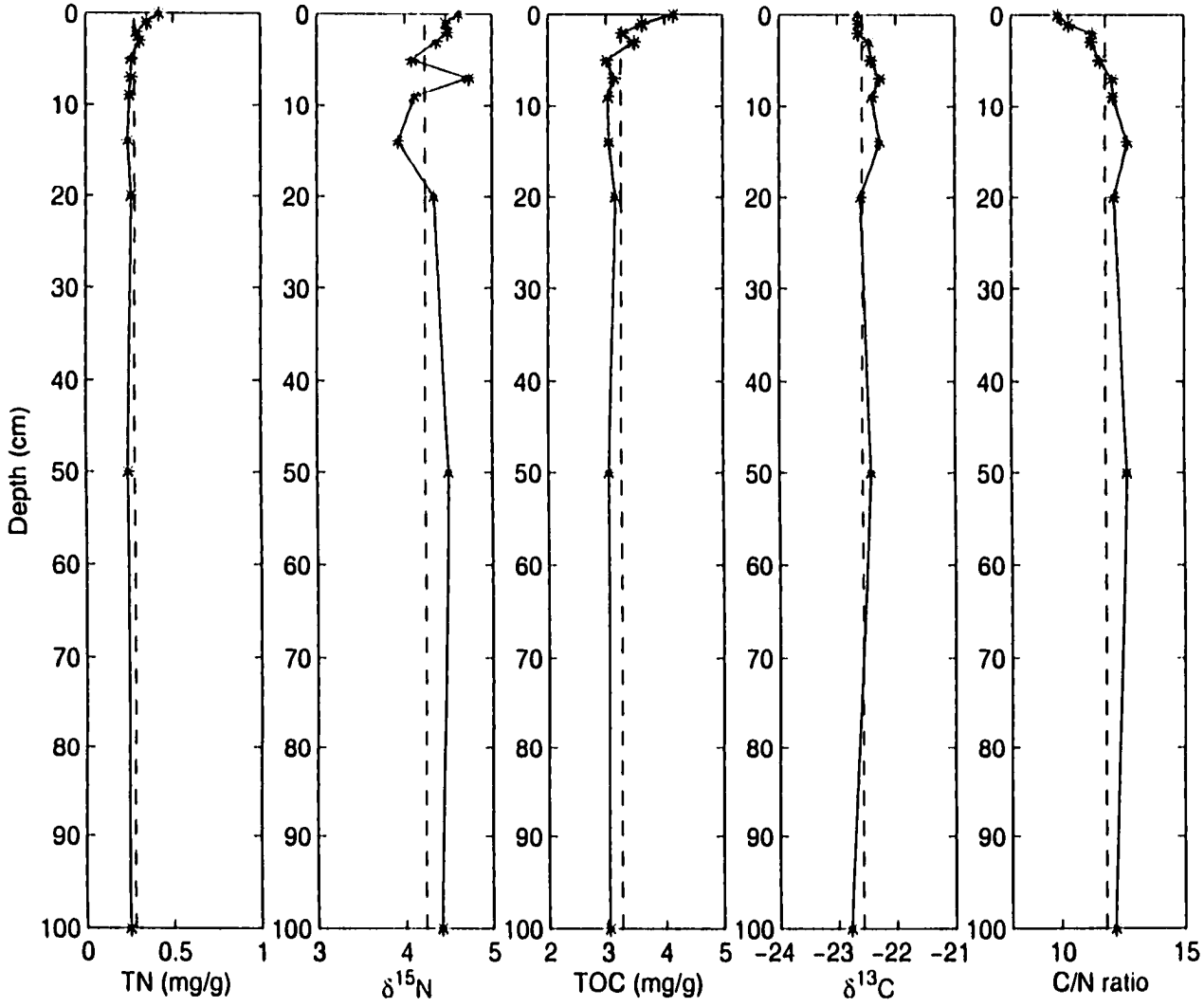

Figure 2-5. Variations in organic matter content and isotopic composition with depth in the core from Station 156.

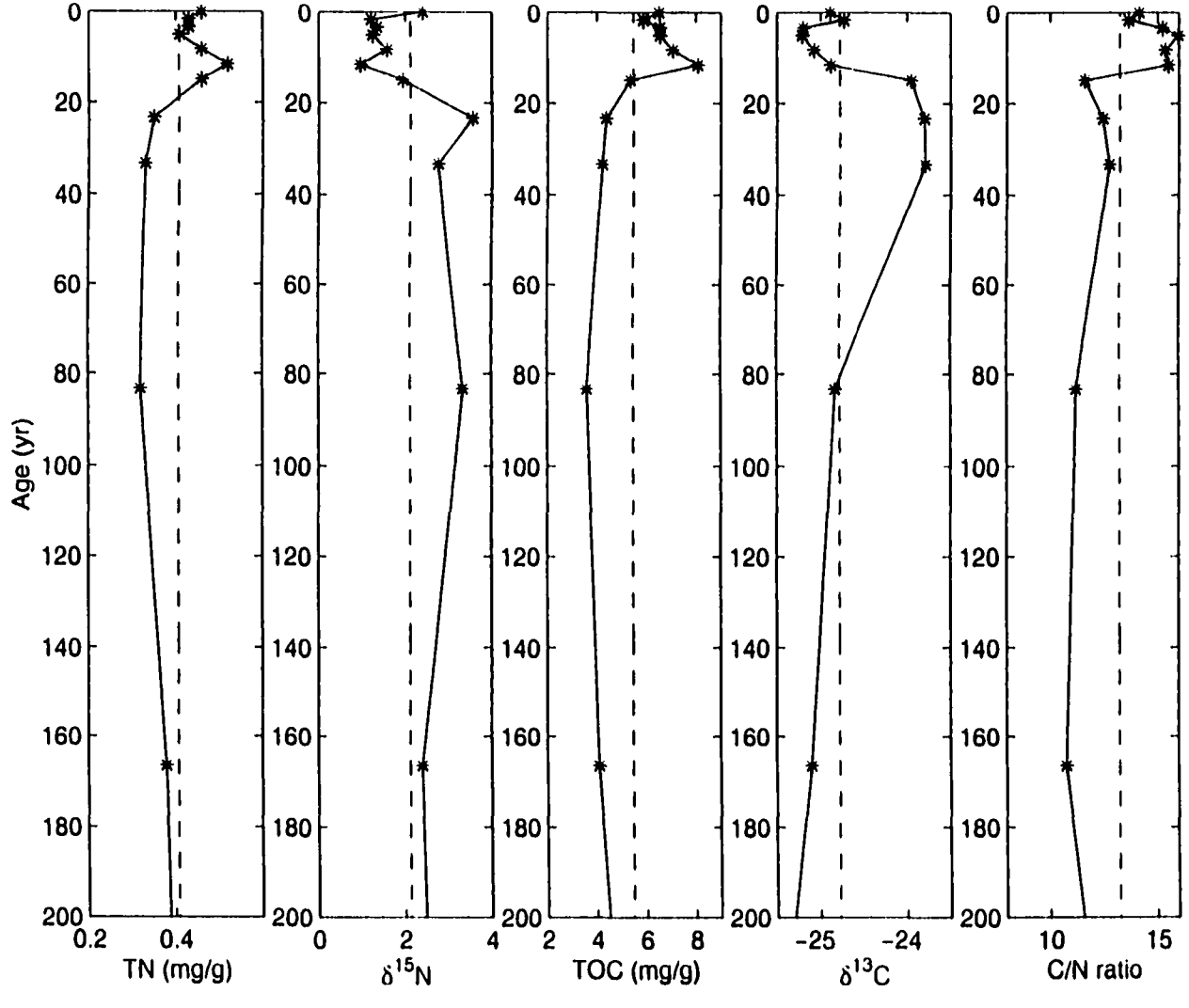

Figure 2-6. Variations in organic matter content and isotopic composition with time in the core from Station 111.

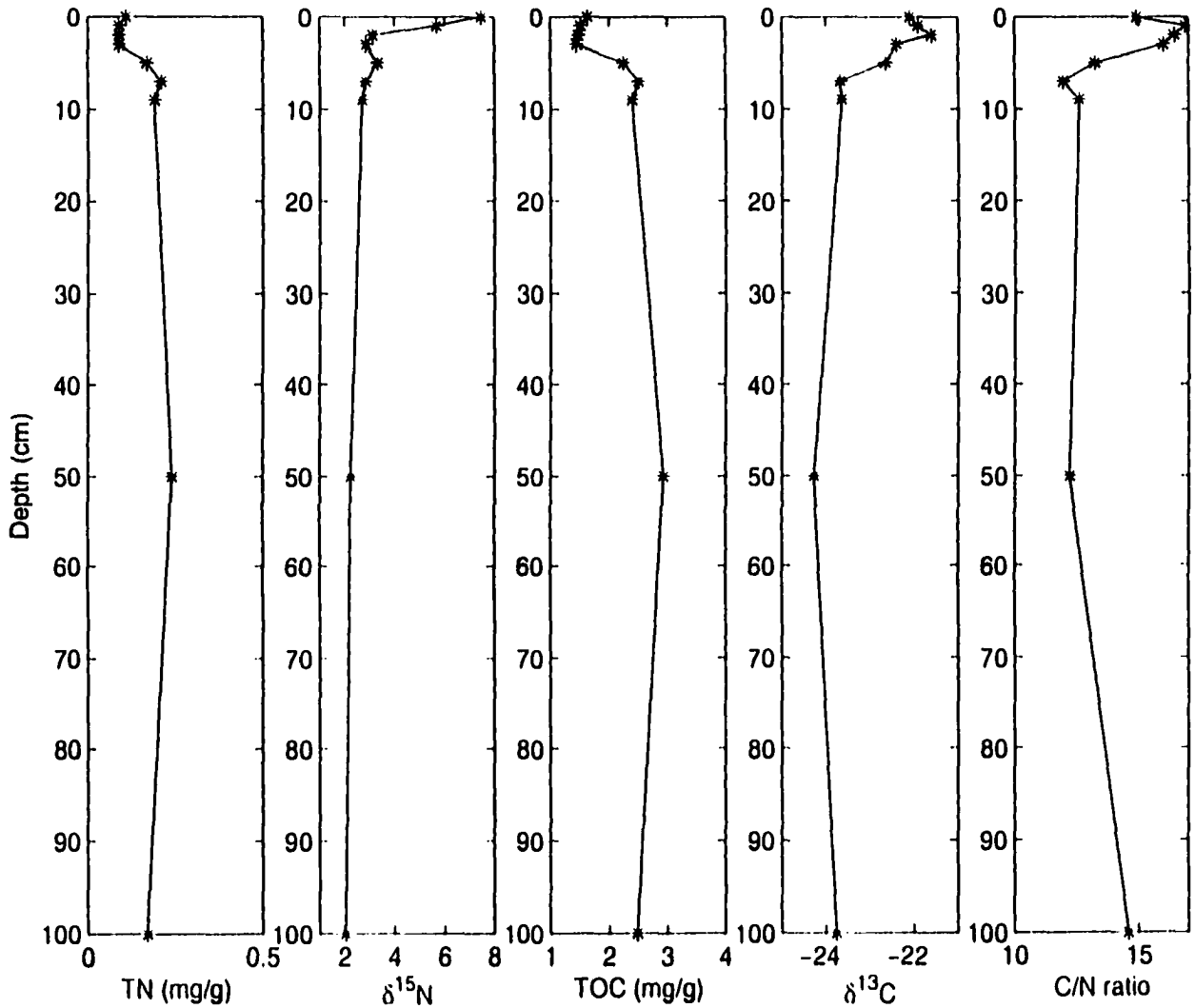

Figure 2-7. Variations in organic matter content, and isotopic composition with depth in the core from Station 128.

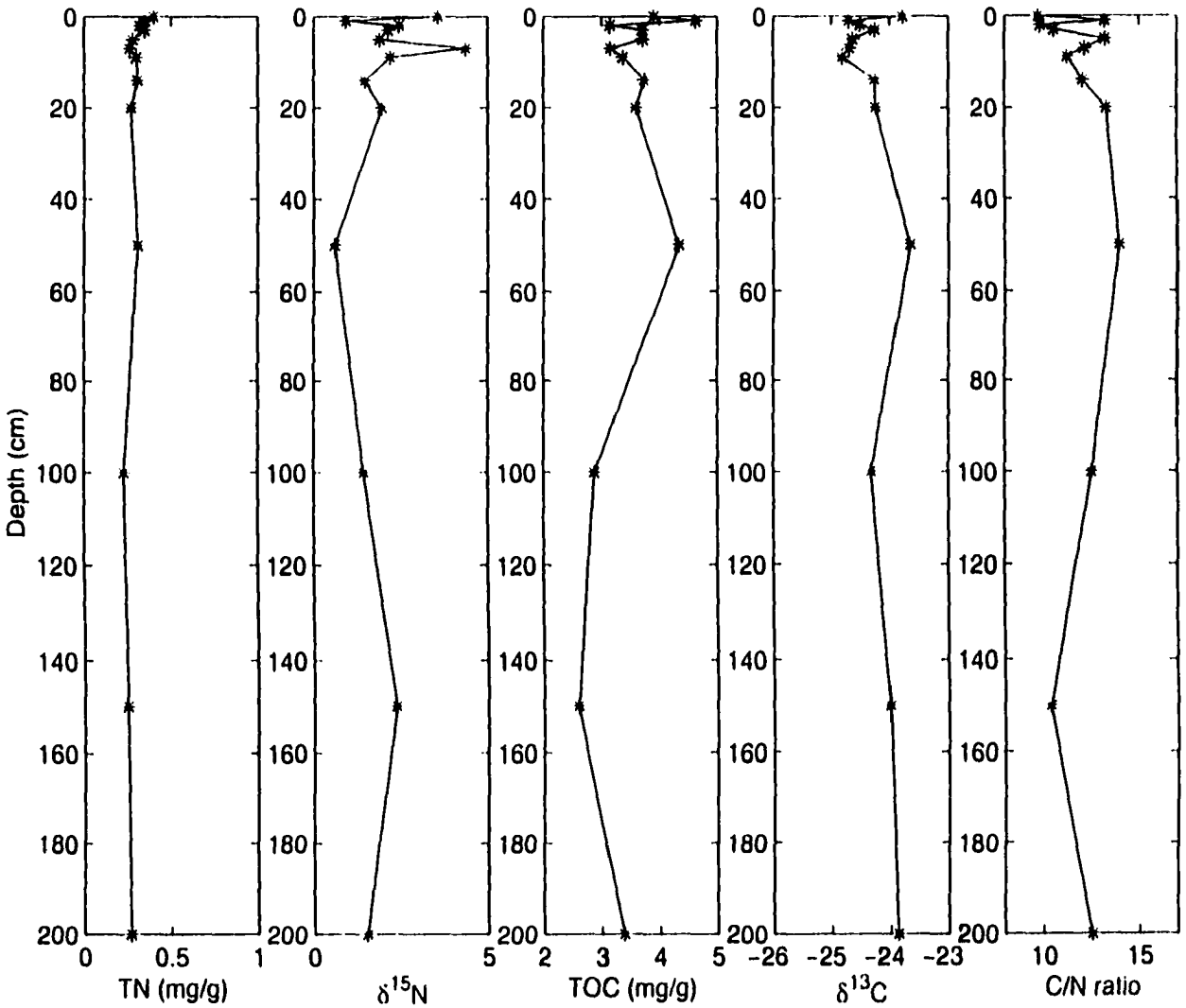

Figure 2-8. Variations in organic matter content and isotopic composition with depth in the core from Station 117.

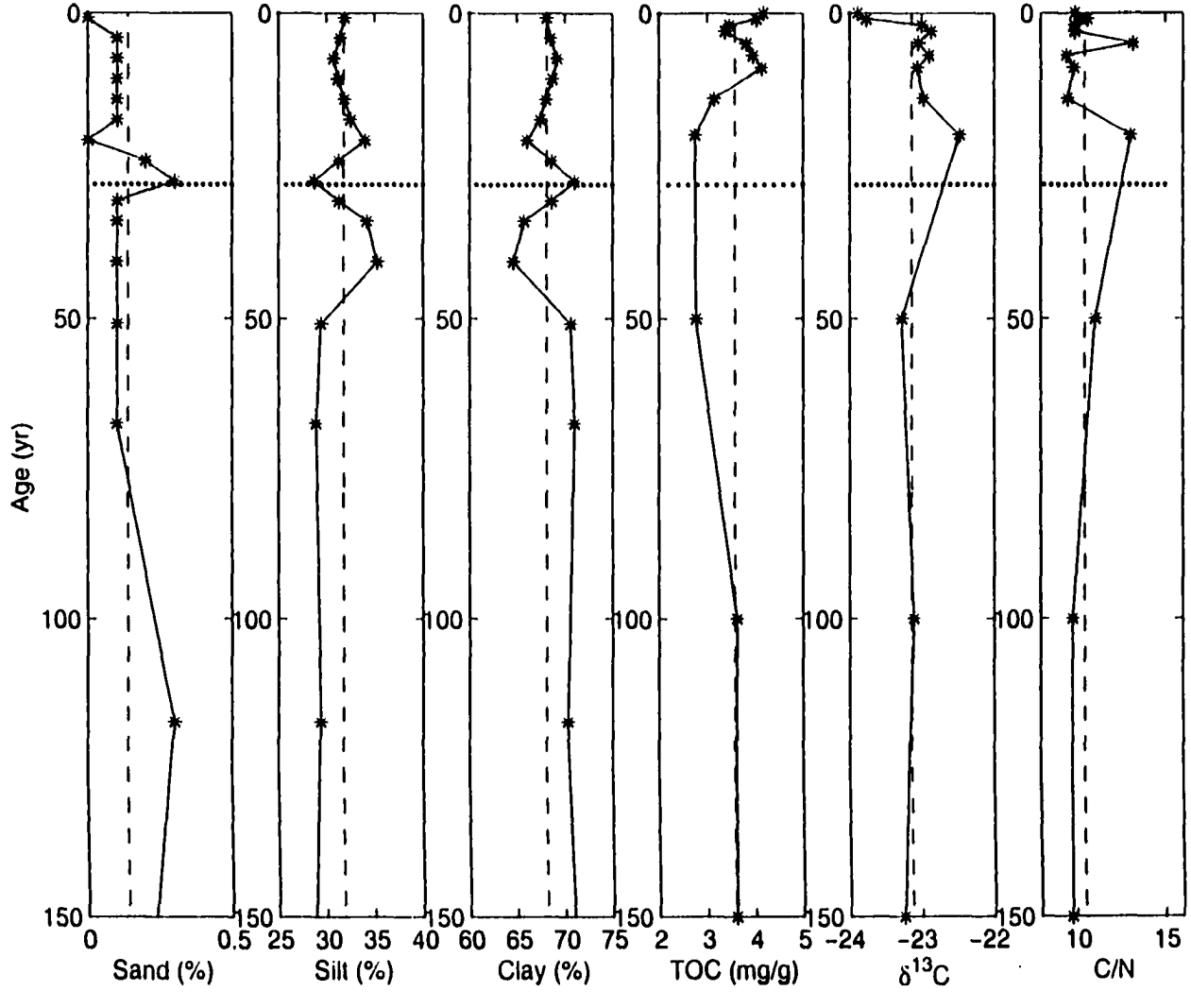

Figure 2-9. Variations in organic matter content and isotopic and sedimentary composition with time in the core from Station 105.

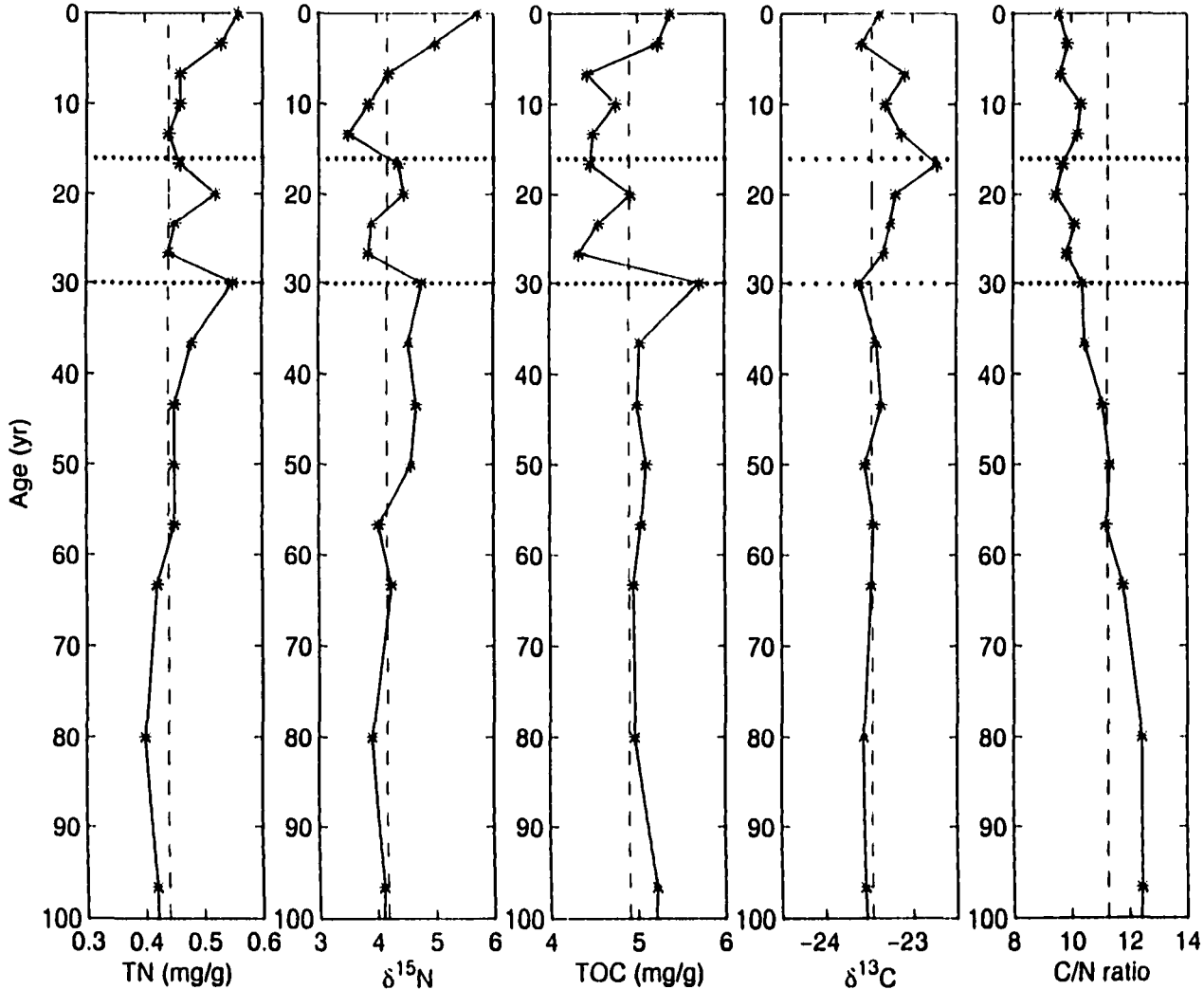

Figure 2-10. Variations in organic matter content and isotopic composition with time in the core from station 101.

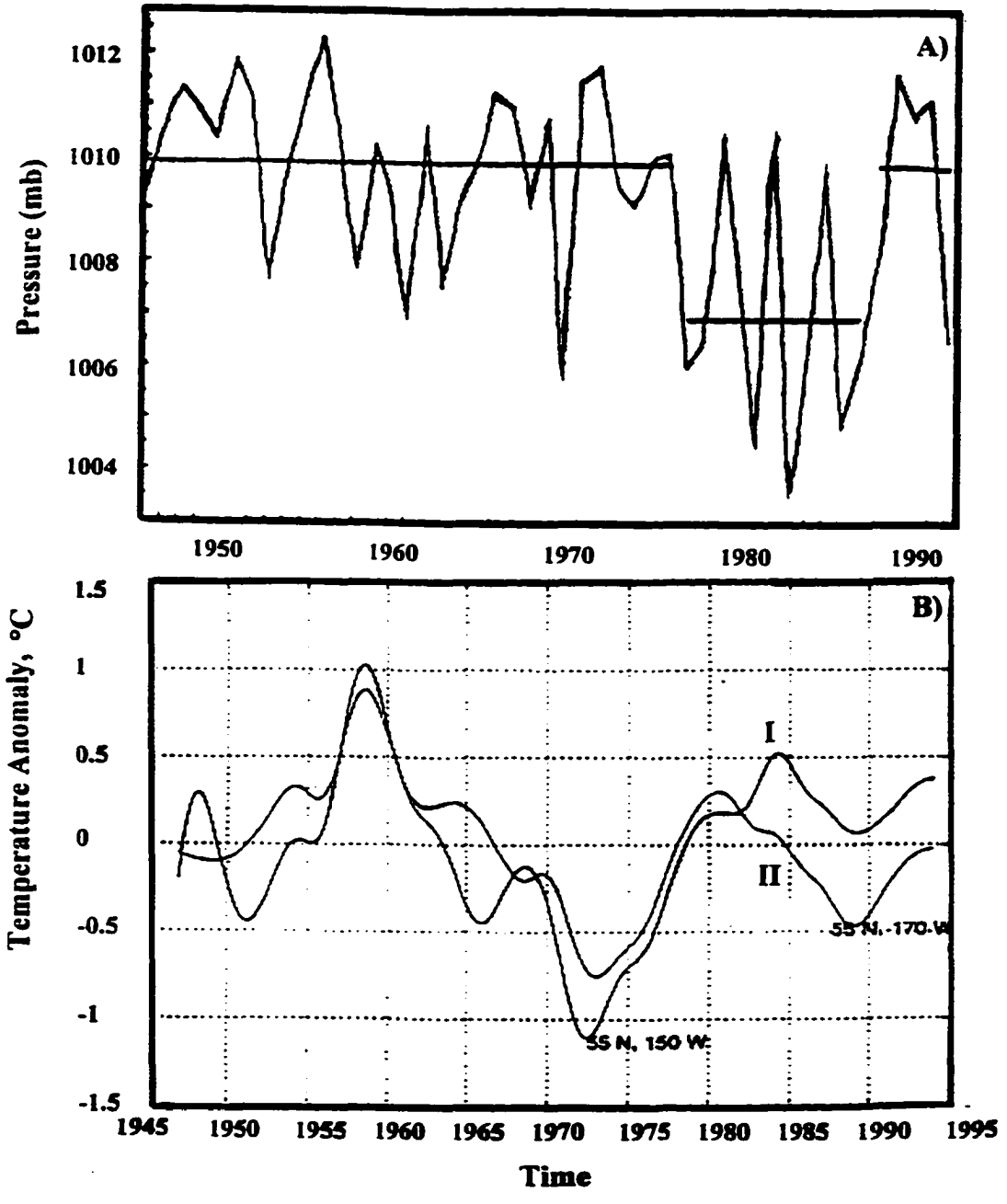

Figure 2-11. A) North Pacific sea level pressure anomalies averaged over 30°-65°N, 160°E to 140°W for the months of November through March and B) Interdecadal changes in the sea surface temperature of the Gulf of Alaska (I) and Bering Sea (II) since 1947 (modified from the Committee of the Bering Sea Ecosystem, 1996).

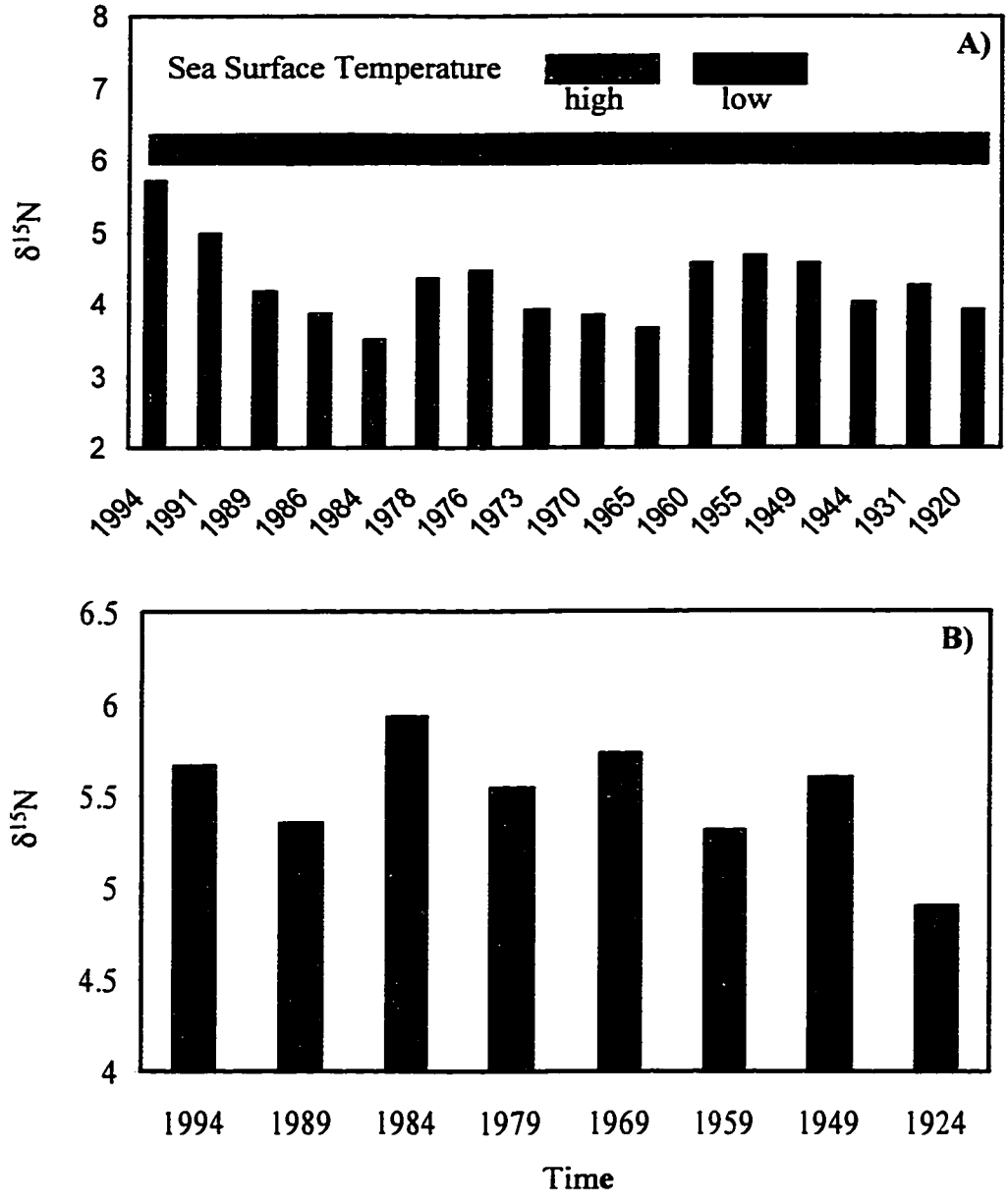

Figure 2-12. $\delta^{15}N$ in cores A) 101 and B) 149 shows interdecadal changes related to the "Regime Shift" in the Gulf of Alaska.

Table 2-1. Stable isotopic composition and C/N ratios in the cores from northeastern Gulf of Alaska.

Station	Mean $\delta^{13}C$	Std[a] of $\delta^{13}C$	Mean $\delta^{15}N$	Std. of $\delta^{15}N$	Mean C/N	Std. of C/N	Sed. type[b]
Copper R. Delta							
105	-23.14	0.37	3.27	0.87	10.46	1.25	II
106	-23.13	0.65	2.88	0.94	13.28	1.41	IV
158	-22.42	0.47	3.67	0.54	13.30	1.64	IV
235	-24.45	0.47	2.25	1.92	12.54	1.48	II
236	-23.98	0.27	3.04	0.94	12.20	0.94	IV
239	-24.34	0.44	3.84	0.82	10.43	0.62	II
241	-24.14	0.28	2.62	0.76	12.27	0.79	IV
average	**-23.66**	**0.42**	**3.08**	**0.96**	**12.07**	**1.16**	
Off Bering Gl.							
111	-24.78	0.57	2.13	0.82	13.25	2.13	II
227	-24.42	0.52	3.07	1.17	14.25	1.43	I
228	-24.68	0.79	1.61	2.82	11.15	1.13	II
229	-25.42	0.21	1.31	0.92	13.22	1.92	II
average	**-24.83**	**0.52**	**2.03**	**1.43**	**12.97**	**1.65**	
Kayak Is.							
109	-24.44	0.17	3.08	0.63	14.08	1.01	III
231	-24.31	0.49	3.16	1.25	12.49	1.62	I
average	**-24.38**	**0.33**	**3.12**	**0.94**	**13.29**	**1.32**	
Marine Source							
101	-23.47	0.25	4.18	0.53	11.25	1.21	I
119	-21.17	0.78	4.87	0.79	10.22	1.84	I
122	-23.32	0.45	4.32	1.81	12.15	1.81	I
126	-20.97	0.57	5.39	0.43	8.76	0.55	I
148	-21.62	0.58	5.34	0.53	8.17	0.36	I
149	-20.64	0.55	5.37	0.50	7.73	0.77	II
150	-20.65	0.51	4.90	0.77	8.67	0.60	II
156	-22.58	0.25	4.23	0.40	11.80	0.91	III
201	-23.60	0.72	3.86	0.77	11.31	0.79	III
205	-23.60	0.39	3.77	0.96	9.84	0.58	III
average	**-22.16**	**0.51**	**4.62**	**0.75**	**9.99**	**0.94**	

(Continued)

Table 2-1. (Continued)

Station	Mean $\delta^{13}C$	Std[a] of $\delta^{13}C$	Mean $\delta^{15}N$	Std. of $\delta^{15}N$	Mean C/N	Std. of C/N	Sed. type[b]
YB							
128	**-22.89**	**0.96**	**3.59**	**1.80**	**14.31**	**1.89**	
YB Mouth							
147	**-20.36**	**1.05**	**5.96**	**2.19**	**9.18**	**1.92**	I
IB							
117	-24.29	0.38	2.06	1.02	11.91	1.41	
224	-25.61	0.45	2.29	1.23	14.93	4.50	
average	**-24.95**	**0.42**	**2.18**	**1.13**	**13.42**	**2.96**	
IB Mouth							
152	-23.92	1.07	2.81	2.52	10.75	1.21	I
153	-23.93	0.44	2.70	0.70	16.17	3.14	I
average	**-23.93**	**0.76**	**2.76**	**1.61**	**13.46**	**2.18**	

a: standard deviation of samples in a core.
b: data from Jaeger *et al.* (1998).

Table 2-2. OM content (average of the past 100 y) and sources and sedimentation rates in the transect cores across the Copper River Delta.

Station	TN (mg/g)	TOC (mg/g)	$\delta^{15}N$	$\delta^{13}C$	C/N	SR[a] (mm/y)	Terrestrial[b] (%)
241	0.28	3.40	2.95	-24.0	12.1	8	67
239	0.43	4.46	3.92	-24.2	10.4	12	70
106	0.23	3.08	3.08	-23.0	13.4	7	50
236	0.29	3.47	3.05	-23.9	12.2	20	65
235	0.63	7.58	2.50	-24.4	12.1	16	73

a: sedimentation rate. Data are from Jaeger *et al.* (1998).
b: percentage of terrestrial source, calculated from $\delta^{13}C$ using the mixing model.

Chapter 3

Adsorption and Desorption of Proteins on Clay Minerals and Goethite

Abstract

Protein adsorption on illite, goethite, and montmorillonite was investigated. Three ^{14}C-labeled hydrophilic proteins, Rubisco from *C. reinhardtii*, and GroEL and GroES from genetically modified *E. coli*, were synthesized and purified for use in the adsorption studies. The proteins were strongly and rapidly adsorbed by the clay minerals. SDS extraction and separation by SDS-PAGE and sucrose density gradients showed that Rubisco and GroEL were adsorbed on illite in their original forms. The activity remaining in the supernatant after adsorption was mostly associated with smaller proteins present as impurities in the original protein solution. The apparent adsorption partition coefficients of the proteins, calculated from the adsorption isotherm slope, were in the order Rubisco > GroEL ≥ GroES. Adsorption was in the order of on goethite ≥on montmorillonite > on illite. Cytochrome *c* from horse heart showed reversible sorption due to its small molecular weight and high purity, but the other proteins exhibited adsorption that was not reversible under the experimental conditions used.

Generally, basic poly-amino acids had greater adsorption partition coefficients than acidic poly-amino acids. Molecular size did not affect the electrostatic interaction between poly-amino acids and mineral surfaces. Positively charged poly-amino acid adsorption on montmorillonite was greater than that on goethite; negatively charged poly-amino acid adsorption on goethite was greater than that on montmorillonite. BSA and negatively charged poly-amino acids inhibited Rubisco adsorption on illite, goethite and montmorillonite, reflecting competition for similar adsorption sites. Positively charged cytochrome *c* and poly-amino acids increased Rubisco adsorption significantly, because Rubisco bound to these adsorbed organic molecules more strongly than to the mineral surface. Overall, these results indicated that electrostatic interactions, rather than van der Waals forces, dominate in protein adsorption. They also show that adsorbate-adsorbate interactions can be important.

§3.1 Introduction

The interaction of organic matter (OM) with solid surfaces is an important process in the global carbon cycle. Adsorption of OM to marine sediment particles can decrease its availability to microbial degradation, and thus could lead to its preservation (Sugai and Henrichs, 1992; Luo, 1994; Mayer, 1994a; Hedges and Keil, 1995). Adsorption to particles also is apparently a key process in the transport and deposition of organic matter (Hedges and Keil, 1995; Henrichs, 1995).

Proteins are major constituents of Recent sediment OM (e.g., Henrichs and Farrington, 1987; Burdige and Martens, 1988; Cowie and Hedges, 1993). Proteins, the most abundant macromolecules in living cells (Lehninger *et al.*, 1993b), consist of chains of amino acids, each joined to its neighbor by a specific type of covalent bond, the peptide bond. Since up to 20 amino acids can join in many different combinations and sequences, proteins have strikingly variable properties and activities. Generally, the amino acid composition is unique and specific to each particular protein, and amino acid sequence plays a fundamental role in determining the structure and function of the protein.

The adsorption of proteins onto a particle surface is a complicated process, which is affected by inorganic and organic constituents of the adsorbent, as well as the structure of the adsorbate. Figure 3-1 (from Andrade, 1985) summarizes protein interactions with a well-characterized surface. Once proteins bind to a surface, unfolding of the protein and practically irreversible adsorption are sometimes observed. The physical state of adsorbed proteins (Grinnel and Feld, 1982), chemical interactions on the particle surface accompanied by alteration in protein molecular conformation or spatial ordering (Voller *et al.*, 1980), and hydrophobic interactions (Kirchman, *et al.*, 1989) are thought to be important in influencing protein adsorption. Samuelsson and Kirchman (1990) found that protein adsorption on glass and plastics tends to increase with decreasing surface energy, i.e., decreasing work of adhesion and increasing hydrophobicity. However, the mechanism of protein adsorption on the kinds of mineral particles found in marine sediments is poorly

understood.

Henrichs (1995) has shown that only very strong adsorption can explain organic matter preservation in marine sediments. The purpose of this study was to determine if protein adsorption to common sedimentary mineral phases (illite, montmorillonite, and goethite) was sufficiently strong to be consistent with their preservation in sedimentary deposits. Also, adsorption of several proteins with varying properties was studied, in order to discover how protein characteristics might affect their adsorption and preservation. Detailed examination of protein adsorption, for example, its reversibility and competitive inhibition, shed some light on probable protein adsorption mechanisms.

§3.2 Materials

Several proteins were chosen based on their stability, relative ease of purification, and hydrophilic properties. ^{14}C-labeled Rubisco, GroEL and GroES were prepared for this study.

Rubisco is a bifunctional enzyme that catalyzes the carboxylation or oxygenation of ribulose-1,5-bisphophate (RuBP) during photosynthesis and photorespiration (Plumley *et al.*, 1986; Roesler and Ogren, 1990; Chen and Spreitzer, 1991). In higher plants and most algae, the enzyme comprises up to 65 % of the total protein (Park and Pon, 1961; Jensen and Bahr 1977; Ellis, 1979). The Rubisco holoenzyme contains eight large subunits (LS) of 55 kDa and eight small subunits (SS) of 15kDa. Rubisco is localized homogeneously in the pyrenoid and chloroplast stroma (Kuchitsu *et al.*, 1990), where it plays an important role in the photosynthetic fixation of CO_2 by the chloroplast. Because of its great abundance, key role in stimulating carboxylation or oxygenation, and interesting biochemical properties, Rubisco is one of the most thoroughly studied proteins.

GroEL and GroES are heat shock proteins whose synthesis rate increases at higher temperatures (Gross *et al.*, 1990). The *E. coli* GroEL, an oligomeric particle, contains 14 identical subunits of 57.3 kDa (Hemmingsen, *et al.*, 1988), and its helper-protein GroES

contains 7-membered ring of identical subunits of 10 kDa (Chandrasekhar *et al.*, 1986; Hemmingsen, *et al.*, 1988). Together with ATP, GroEL stabilizes an unfolded state of newly synthesized proteins and releases them upon ATP hydrolysis (Bochkareva *et. al.*, 1988; Georgopoulos, 1992), preventing aggregation (Kovalenko *et al.*, 1994).

Cytochrome *c* has been isolated from many aerobic organisms - animals, plants and fungi. Cytochrome *c* is a basic protein which is relatively stable to heat and acids. The structure of this cytochrome varies somewhat in different organisms, but generally it consists of a single peptide chain with M.W. of about 12.4 - 13 kDa (White *et al.*, 1968a). Cytochrome *c* can be reversibly denatured by heat and alcohols, indicating that the amino acid sequence determines conformation. Also, the hydrophobicity of cytochrome *c* plays a major role in determining the conformation (White *et al.*, 1968a). An aqueous solution of horse heart cytochrome *c* is orange-colored, with a sharp absorbance peak at 406 nm. Cytochrome *c* (from horse heart), bovine serum albumin (BSA), and poly-amino acids used in my experiments were purchased from Sigma. They were used without further purification.

Illite, goethite and montmorillonite were used as standard minerals in my study because they all are common in natural marine sediments. Goethite was provided by Dr. Susan Sugai. The goethite was made by slowly adding with stirring 50 g $Fe(NO_3)_3 \cdot 9H_2O$, dissolved in 825 mL low-organic, deionized water, to 200 mL 2.5 M KOH, over 30 min. The suspension was aged for 24 h at 60 °C, and then the precipitate was recovered by centrifugation and rinsed repeatedly with low-organic deionized water. It is quite stable at room temperature. Structural rearrangement of goethite during dehydration occurs at 300 °C:

$$2\alpha\text{–FeOOH} \xrightarrow[\Delta]{} \alpha\text{–}Fe_2O_3 + H_2O$$

However, this reconstructive transformation from yellow goethite to red hematite can occur slowly at much lower temperatures by dissolution and re-precipitation under changing environmental conditions (Schwertmann and Taylor, 1977; Taylor, 1987).

The illite was API (American Petroleum Institute) #35, and the montmorillonite, API #25. Nearly all organic matter on the illite and montmorillonite used in this study was removed by H_2O_2 treatment before use. For each 2 g of clay mineral, 10 mL of 30 % H_2O_2 were added, and the mixture left overnight; this was repeated once. Then, the solution was heated at 70°C for 24 hr. After rinsing with distilled water, the clays were heated at 70°C until dry. The TOC of the minerals was < 0.1 % after this treatment. TOC content of the goethite for this study was less than 0.1%, so goethite was used without further treatment. All minerals were passed through a 64 μm sieve before use.

§3.3 Experimental Procedures

§3.3.1 Protein Purification

C. reinhardtii cultures Cells of *C. reinhardtii* (137GB125+) were kindly donated by Dr. G. Plumley at University of Alaska Fairbanks. Algae were grown photoautotrophically at 25°C in 3 L of minimal medium (Appendix I) in a 4 L flask. The cultures were stirred gently and continuously, and illuminated with cool-white fluorescent tubes. CO_2 was supplied to the system by sparging from a reservoir which contained ^{14}C labeled sodium bicarbonate solution at pH 10.2, which insured a continuous supply of low-level CO_2. The CO_2 reservoir contained 65 g ^{14}C-labeled sodium bicarbonate (2,500 μCi), 9.1 g sodium hydroxide, and 47.5 g sodium borate in 10 L distilled water. The whole system was sealed to prevent ^{14}C from leaking and to recycle $^{14}CO_2$.

Isolation of Rubisco from cells The culture was harvested by centrifuging at 3,000 rpm for 5 min at 4 °C. For each 10 mL packed cell volume, the cells were resuspended in 150 mL of ice-cold water, mixed gently, and then centrifuged at 3,000 rpm for 5 min. The cells were resuspended in 25 mL of 50 mM sodium phosphate (NaPi) buffer at pH 7.2, mixed, then frozen at -60°C for 24 hours. The solution was thawed at room temperature to break the cells, centrifuged at 15,000 rpm for 10 min and decanted, and the supernatant was saved. The cells were resuspended in 50 mL of 50 mM NaPi buffer, and placed on ice for

10 min, then centrifuged at 15,000 rpm for 10 min. This was repeated once, and all supernatants were combined.

Rubisco purification The procedure used to purify Rubisco for this study was modified from Plumley *et al.* (1986). Briefly, for each 120 mL of crude extract solution, 21 g of ammonium sulfate was added slowly, over 15 min, to the solution, while stirring gently and continuously. Stirring was continued for 30 min to complete the reaction, then the solution was centrifuged at 15,000 rpm for 10 min. Over 15 min, an additional 22 g of ammonium sulfate was added to give 60% $(NH_4)_2SO_4$, and the solution was stirred for 30 min. After centrifuging at 15,000 rpm for 10 min, the precipitate was resuspended in 3 mL of 20 mM NaPi buffer. One mL of solution was removed from the top of each of three 13-mL sucrose linear gradients (0% - 30%) and replaced with 1 mL of Rubisco solution. The sucrose gradients were centrifuged at 39,000 rpm for 20 h at 4°C. The bottom 3 mL of each gradient (11 to 13 mL from the top) were combined and precipitated by 60 % $(NH_4)_2SO_4$. The pellets were stored in a -60 °C freezer, or resuspended in 25 mM NaPi buffer, pH 7.2, for use.

Electrophoresis Rubisco purity was examined by 15% sodium dodecyl sulfate-polyacrylamide gel electrophoresis (SDS - PAGE), as described by Bio-Rad laboratories in the *Electrophoresis Cell Instruction Manual*. Gels were stained with Coomassie Brilliant Blue. Molecular weight standards were purchased from Bio-Rad laboratories.

Protein concentration Protein concentration was measured as in Bradford (1976), via the binding of Coomassie Brilliant Blue G-250 dye to protein. Absorbance of the stained protein solution was measured using a spectrometer at 596 nm. BSA was used as the standard.

E. coli cultures Cells of *E. coli* TG2 containing pOA were kindly donated by Dr. A. Horovitz of the Weizmann Institute, Israel. *E. coli* cells were grown at 37 °C in an incubator with continuous shaking for a few days in 1 L of minimal medium (Atlas and Parks, 1993; Appendix II) plus 50 μg/mL ampicillin. In the culture medium, ^{14}C labeled

glucose (50 μCi) was used as the only carbon source, thereby to homogeneously label the desired proteins.

GroEL purification The method used to purify GroEL is modified from Kamireddi *et al.* (1997). Cells were harvested by centrifugation at 6,000 rpm for 10 min and washed with Tris-HCl buffer, pH 8.0. The cells were resuspended in buffer A, which contained 50 mM Tris-HCl, pH 8.0, 1 mM EDTA, 1 mM DTT and 0.1 mM phenylmethylsulfonyl fluoride, and lysed under sonication for 30 min. The lysate was centrifuged at 15,000 rpm for 20 min. The supernatant was subjected to the 30 - 60 % ammonium sulfate cut-off procedure as described for Rubisco. The protein pellets were resuspended in buffer A, and loaded onto three linear 0 - 30 % sucrose density gradients. The top 5 mL of each gradient was saved for obtaining GroES. The bottom 2 mL of each gradient (12 and 13 mL from the top) were combined, and the proteins were precipitated using 60% $(NH_4)_2SO_4$. The precipitate was dissolved in buffer A, and then treated with 1 mL (packed volume) of DE-52 anion exchanger equilibrated to pH 8.0. The supernatant was subjected to 60% $(NH_4)_2SO_4$, and the pellets were stored in a -60 °C freezer or resuspended in 25 mM NaPi buffer, pH 7.2, for use.

GroEL purity was determined by SDS-PAGE on 15% polyacrylamide gels. Its concentration was determined as in Bradford (1976).

GroES purification The solutions from the top 5 mL of the gradient saved from the GroEL purification were combined and precipitated by 60% $(NH_4)_2SO_4$. The protein pellets were resuspended in buffer A, and heated in a water bath to 80 ± 2°C for 20 min. Centrifuging at 14,000 rpm for 15 min removed coagulated proteins. The supernatant was treated to 60 % $(NH_4)_2SO_4$, and the pellets were stored in a -60°C freezer or resuspended in 25 mM NaPi buffer, pH 7.2, until use. GroES purity was examined by SDS - PAGE on 15% polyacrylamide gel, and its concentration was determined as in Bradford (1976).

Hydrophobic proteins from E. coli The cell detritus after extraction of GroEL and GroES was mostly hydrophobic membrane proteins. Twenty mL of 2:1 (v/v) chloroform and

methanol were added to 2 g of cell pellets and mixed well, then the mixture was incubated on ice for 30 min. After centrifuging at 6,000 rpm for 10 min, the supernatant was removed. $MgSO_4$ was added to the supernatant to remove water, and it was stored at -60 °C until use.

§3.3.2. *Adsorption and Desorption Experiments*

Adsorption - desorption ^{14}C-labeled protein adsorption on minerals was assessed at 4 °C. Protein solution (15 - 60 μg) and water (2 mL) were added to 5 mg of mineral with frequent mixing or continuous shaking of the solution for 2 h. After centrifugation, the ^{14}C activity in the supernatant was measured. Desorption was determined by replacing a portion of the supernatant with an equal volume of water. Control experiments, intended to check for losses of protein via processes other than adsorption to the mineral phase, were carried out in the same manner except that no mineral was added.

Cytochrome *c* concentration was determined by measuring the absorbance at 406 nm. The measurements of adsorption of cytochrome *c* on illite were conducted as above. Because spectrophotometric detection was less sensitive than radiometric, cytochrome *c* was added at concentrations up to three times greater than those of the ^{14}C-labeled protein solutions.

The adsorption of poly-amino acids on goethite and montmorillonite was carried out in the same way as that of proteins. The assay of dissolved concentration was modified from North (1975). Briefly, for acidic poly- Glu and Asp, 0.5 mL of sodium borate buffer (pH 9.5) was added to 250 μL of sample solution. Next, 0.5 mL of fluorescamine in acetone (20 mg/100mL) was added. The sample must be vigorously mixed for 1 minute during addition because fluorescamine is unstable in aqueous solution. Fluorescence was measured in a SPF 500™ spectrofluorometer using an excitation wavelength of 390 nm and an emission wavelength of 480 nm. For basic poly- Lys and Arg, 0.5 mL of citric buffer (pH 4.0) was added to 250 μL of sample solution. After addition of 0.5 mL of

fluorescamine and mixing for 1 minute. 2 mL and 4 mL of water were added to the poly-Lys and Arg solutions, respectively, to dissolve the precipitate produced by acetone. The fluorescence measurement was the same for poly-Glu. The blank was less than 10% of sample fluorescence.

Inhibition experiments One mL of a solution containing BSA, cytochrome *c*, or a polyamino acid was added to glass vials which contained 5.0 mg of mineral. The suspension was left for 12 hours at 4°C after mixing. After centrifuging and removal of the supernatant, protein adsorption experiments were carried out as described above. The inhibition of protein adsorption by other proteins or poly-amino acids was calculated relative to experiments without pre-adsorption.

§3.3.3 *Extraction of Rubisco from Minerals*

Rubisco was adsorbed on the minerals as described above. After removal of the supernatant and measurement of the ^{14}C activity, the minerals were rinsed with water, and then 2.5% sodium dodecyl sulfate (SDS) or 2.5 % Triton X-100 (t-octylphenoxypoly-ethoxyethanol) solution was added. The solution and minerals were either placed on ice for 2 h after thoroughly mixing, or heated in boiling water for 30 minutes. The suspensions were centrifuged at 10,000 rpm, and then ^{14}C activity in the supernatant was measured. The extraction efficiency was calculated as the percentage of adsorbed ^{14}C extracted by the detergent solution.

§3.3.4 *^{14}C Analysis of Proteins Using Gel Electrophoresis*

^{14}C labeled proteins were loaded on a 15% SDS - PAGE gel, and the mini-gel was run under a constant voltage of 200V for 45 min. After staining by Coomassie Blue, the gel was destained by rinsing with an aqueous solution of acetic acid and methanol. The separating gel was cut into pieces, according to the location of molecular weight standards and target proteins, 500 μL of 30% H_2O_2 was added to the stacking and separating gel

slices, and then the solution was heated at 70 °C for several hours to dissolve the gel. Sixteen mL of scintillation cocktail was added to the gel solution with shaking. If the mixture was not clear, a small volume of concentrated HCl was added. The proportions of different molecular size fractions in the protein solution were measured by counting ^{14}C activity in bands equivalent to protein size groups located by means of standards. Natural proteins extracted from sediment were also loaded on the same gel as a reference. The blanks of background gel slices were subtracted.

§3.3.5 ^{14}C Analysis of Proteins from Sucrose Density Gradients

One mL of ^{14}C-labeled protein solution was loaded on the top of a linear sucrose density gradient (0 - 30 %). After centrifuging at 39,000 rpm and 4°C for 20 h, 1 mL increments of the protein-containing sucrose solution were pipetted into scintillation vials, and ^{14}C activity was measured. Addition of HCl was necessary for the most concentrated sucrose solutions (≥ 8 mL from top) to clarify the cocktail. After removal of the sucrose solution, 1 mL of 5% SDS solution was added to the empty tube. After thorough mixing, the ^{14}C activity in the solution was measured to check for loss of ^{14}C to the container walls.

§3.4 Results

§3.4.1 Composition of Protein Solution and Effects of Adsorption on Protein Structure

GroEL and GroES are highly expressed in some mutant *Escherichia coli* vectors, e. g., about 60% and 40% of total cell protein respectively in the pRE vector (Kamireddi *et al.*, 1997). In this work, GroEL and GroES expressed in *E. coli* TG2 were only 10 % and 5 % of total hydrophilic proteins, respectively. The low expression was due to the minimal culture medium used, and the resulting longer growth period.

The purity of Rubisco used in this study was about 90%, and that of GroEL and GroES was about 85 % according to SDS-PAGE. The ^{14}C specific activity of Rubisco varied from 80 to 150 dpm/μg, and those of GroEL and GroES were about 10 to 25

dpm/μg. However, the Coomassie Blue used to stain the gel reveals only proteins. The purity of the protein solution was checked by cutting the electrophoresis gel into pieces, and counting their ^{14}C activity. The results showed that originally, 77% and 71% of the total activity in solution was associated with the target proteins, Rubisco and GroEL (Table 3-7). The ratio of Rubisco large subunit (LS) and small subunit (SS) was about 4.1, which is similar to that theoretically calculated, 3.7 (8 × 55 kDa /8 × 15 kDa). Originally, about 10 % of the total activity was found in the stacking gel, which probably consisted of coagulated and/or uncharged proteins or other organic matter with high M.W. (The purification methods should have eliminated small molecules).

The composition of the supernatant from the Rubisco adsorption experiment showed significant alteration compared with the original solution. The ratio of LS to SS was about 0.92, << 3.7, and the major proteins were smaller ones with M.W. < 55 kDa (about 40% of the total, including SS). The adsorbed material was similar to that in the original solution, which is due to the high percentage of target protein in the original solution and the strong Rubisco adsorption on illite. The absolute percentages of smaller (15 - 55 kDa) and larger (> 55 kDa) proteins in the separating gel and the stacking gel were 2.3, 1.7 and 2.5 fold greater, respectively, in the supernatant than in the adsorbed material under comparable conditions. In the GroEL supernatant after adsorption, larger impurity proteins (> 58 kDa) comprised 39% of the total activity. Adsorbed GroEL showed similar ^{14}C activity composition to that of the original protein solution.

The SDS-PAGE was done with denatured proteins. Therefore, the original molecular size was not determined by this method. However, Triton X-100 does not induce conformational changes, which is probably because its rigid structure can not penetrate the crevices of protein as efficiently as the flexible alkyl chains of SDS. The results from sucrose density gradients of Triton X-100 extracts (Table 3-6) showed that 1) adsorbed Rubisco was distributed in the gradients in almost the same way as the original solution (11 - 13 mL from top); 2) the supernatant after removal of the adsorbed Rubisco and

GroEL was mostly smaller proteins; 3) The supernatant of the Rubisco adsorption experiment contained about 22% of M.W. < 150 kDa (≤ 3 mL from top); 14% of M.W. between 150 and 350 kDa (4 - 6 mL from top); 40% of M.W. between 350 and 550 kDa (7 - 10 mL from top), and 25% of M.W. > 550 kDa (≥ 11 mL from top). The corresponding GroEL supernatant percentages were 6%, 18 %, 37% and 39%. The recovery of ^{14}C activity was 80 - 90% of the total loaded.

§3.4.2 *Adsorption and Desorption of Proteins*

The adsorption partition coefficient (K) is the ratio of adsorbed to dissolved protein:

$$K = \frac{\text{activity adsorbed } (\mu g) \text{ / g dry mineral}}{\text{activity dissolved } (\mu g) \text{ / mL solution}}$$

^{14}C activity in solution was measured, and the protein concentration on the mineral phases was calculated under the assumption that the activity not in solution was adsorbed to the minerals.

Rubisco adsorption on illite was a rapid process which reached steady state in < 1.5 hours (Figure 3-2). Rubisco, GroEL, GroES and cytochrome *c* were all strongly adsorbed by the clay minerals illite, goethite and montorillonite (Figures 3-3, 3-4, 3-5 and 3-6). The control experiments showed that about 2 - 8% of total added protein (mainly depending on protein concentration) was lost due to adhesion to glass vessels. The adsorption data reported are the apparent results without correction for the control experiment.

All of the adsorption isotherms were linear. But, except for cytochrome *c*, much of the adsorbed protein was not readily desorbed. After several dilutions, adsorbed protein concentrations tended to remain at constant values, indicating the presence of components which exhibited irreversible adsorption behavior under the conditions employed. The isotherm of cytochrome *c* showed quite linear adsorption and desorption.

We used SDS to extract both hydrophilic and hydrophobic proteins from clay minerals (Table 3-3). SDS is a strong surfactant which can denature and dissociate

proteins. SDS contains a long hydrocarbon chain of twelve carbon atoms, which interacts with the relatively non-polar interior of globular proteins to unfold the native structure. The charged sulfate group remains exposed to the solution, and this results in a large net negative charge for the protein-SDS complex (Abeles *et al.*, 1992). Generally, a 2.5% SDS solution had the greatest extraction efficiency, and after two such extractions about 90% of the total adsorbed Rubisco was extracted. Hydrophilic protein (Rubisco) tended to be more readily extracted than hydrophobic proteins at a lower temperature (4°C). However, at a higher temperature (95°C) there was no significant difference. These results are similar to Bothner and Horbett (1986), indicating that the molecular conformation of adsorbed proteins depends on hydrophobicity or surface energy.

Figure 3-7 shows that extraction of Rubisco from illite by 2.5% SDS is a rapid process. Only 5 min after the extraction was begun, 85% of the steady state efficiency was reached, and no further Rubisco was extracted after 1.5 hour.

Triton X-100 is a mild detergent which can extract protein by non-ionic interactions in which a molecule of acid and of alcohol react reversibly to yield one molecule of ester and water:

$$\mathrm{R\text{-}\overset{\overset{O}{\|}}{C}\text{-}OH + HOR' \rightleftharpoons R\text{-}\overset{\overset{O}{\|}}{C}\text{-}OR' + H_2O}$$

This esterification is extremely slow without catalysis; heat or addition of hydrogen ion, or both, can speed the reaction (White, *et. al.*, 1968b).

At 4°C, the extraction efficiency of Rubisco by Triton X-100 was greater for illite than for goethite or montmorillonite (Table 3-4). At 95°C, extraction from illite and montmorillonite increased about 30% and 86% respectively, but that from goethite did not change. Overall, Triton extraction efficiency was much lower than that of SDS.

We used chloroform/methanol (v:v, 2:1) to extract hydrophobic proteins. After

removal of hydrophilic proteins, most of the proteins in cell detritus were membrane proteins with high hydrophobicity. Table 3-5 shows that Rubisco did not dissolve in chloroform/methanol at neutral pH, and even in very acidic solution, only 5% was dissolved. The hydrophobic proteins used in this work produced a broad band on a SDS-PAGE gel, indicating that a range of molecular sizes was present.

After one set of adsorption experiments, at a total protein concentration of 20 μg in 2 mL of water containing 5 mg of illite, the adsorbed proteins were extracted with 2.5% SDS. The extracted proteins and proteins remaining in the supernatant were separated by SDS-PAGE. Figures 3-8 and 3-9 show that Rubisco and GroEL were adsorbed by illite in their original forms, indicating that they bind on the illite surface without irreversible conformational alteration. The activity remaining in the supernatant after adsorption was largely composed of smaller proteins, which probably were impurities in the original protein solution or were present due to protein decomposition. The results indicated that Rubisco and GroEL were almost entirely adsorbed by the illite and exhibited practically irreversible adsorption. The smaller proteins were reversibly sorbed. These results were confirmed by Triton X-100 extraction and sucrose density gradient M.W. separation. Table 3-6 shows that adsorbed Rubisco, after extraction by Triton X-100, is distributed the same way as the original Rubisco in a sucrose density gradient, indicating that it was adsorbed without dissociation. The supernatant activity of both Rubisco and GroEL adsorption experiments mostly consisted of smaller proteins.

§*3.4.3 Poly-amino Acid Adsorption*

Poly-amino acid adsorption on goethite and montmorillonite is shown in Figures 3-10, 3-11 and 3-12, and the adsorption partition coefficients are listed in Table 3-8. For negatively charged poly-Glu, adsorption on goethite was the same for three different

molecular weights, varying from 7.7 kDa to 71.7 kDa, but their adsorption on montmorillonite tended to be greater at lower molecular weight. The adsorption on goethite was about 1 - 6 times greater than that on montmorillonite. A similar trend was found for negatively charged poly-Asp adsorption, but the magnitude was about half of that of poly-Glu. For positively charged poly-Lys, the adsorption on goethite tended to be lower with decreasing molecular size, but there only was a slight size effect on adsorption to montmorillonite. A similar result was found for the adsorption of positively charged poly-Arg. Generally, basic poly-amino acids had much greater adsorption than acidic poly-amino acids. Comparing goethite and montmorillonite, acidic poly-amino acids have slightly greater adsorption on goethite, while basic poly-amino acids have slightly greater adsorption on montmorillonite.

§*3.4.4 Inhibition of Rubisco Adsorption by Pre-adsorbed Poly-amino Acids and Proteins*

Table 3-9 presents data on the inhibition of Rubisco adsorption by poly-amino acids and proteins. Pre-adsorbed poly-Glu and BSA inhibited Rubisco adsorption. Cytochrome *c* enhanced Rubisco adsorption significantly, behaving similarly to poly-Lys. Both effects increased with the amount of pre-adsorbed BSA or cytochrome *c*.

Results of the inhibition experiments on goethite were similar to those on illite, except the magnitudes of the effects were somewhat different. Poly-Glu (49 kDa) and BSA inhibited Rubisco adsorption on goethite about 25% and 29% more than on illite, poly-Lys (20.7 kDa) enhanced adsorption about 17% less, and cytochrome *c* had almost the same effect. Larger poly-Glu greatly inhibited adsorption of Rubisco, but the effects of poly-Lys size were complicated. Larger poly-Lys inhibited Rubisco adsorption, while smaller poly-Lys enhanced it.

Pre-adsorption of cytochrome *c* and poly-Arg on montmorillonite enhanced Rubisco adsorption much more than they did on illite and goethite, while poly-Asp inhibited

adsorption 42% less and BSA only slightly affected adsorption. Larger poly-Glu greatly inhibited Rubisco adsorption, but the molecular size of poly-Lys did not affect the magnitude of its enhancement of adsorption.

§3.5 Discussion

§3.5.1 Protein Adsorption on Clay Minerals

Andrade (1985) described the non-covalent forces and interactions in the organization and stabilization of protein structure in aqueous solution, which include: 1) ionic or electrostatic forces due to the attraction of two or more groups carrying opposite charges; 2) hydrophobic interaction, which is basically an entropically driven process; 3) hydrogen bonding, which is a dipole/dipole interaction with an associated energy change comparable to very weak covalent bonds; and 4) other interactions, which are usually dominated by π-π interactions.

When organic matter adsorbs on solid surfaces, there is a layer of adsorbate directly in contact with the absorbent, and then possibly a number of layers of adsorbate condensed onto the first layer. If all of the adsorbate is in one layer on the surface, it is called monolayer adsorption, and if in several layers, multilayer adsorption. For multilayer adsorption, the first layer of molecules physically or chemically binds to the surface. Therefore, the interaction between absorbent and adsorbate is stronger compared to that in outer layers. However, the adsorbate-adsorbate attractive interaction is relatively larger in outer layers than in a monolayer. Typically, multilayer adsorption occurs at lower temperatures than monolayer adsorption (Masel, 1996).

The adsorption-desorption isotherms (Figures 3-3, 3-4 and 3-5) show linear adsorption but incomplete desorption. Only about 13.5% of total adsorbed Rubisco was desorbed from illite, 4.7% from goethite, and 2.3% from montmorillonite. Ensminger and Gieseking (1939) studied protein adsorption on montmorillonite, and found large spacings

which were not related to molecular size and configuration, suggesting that the "stretched" adsorbed proteins on it may bind at multiple sites, and thus resist desorption. The very strong adsorption of Rubisco is likely due to binding at multiple sites, so smaller proteins present in the Rubisco solution as impurities should be desorbed first.

While van der Waals interactions could be a factor in increased binding of Rubisco relative to smaller proteins in the mixture, the similarity of partition coefficients of Rubisco, GroEL and GroES, which have different molecular sizes, argues that electrostatic interactions predominate (see next section). Also, results of inhibition experiments (see Section 3.5.3) indicate that electrostatic interactions are important in Rubisco adsorption.

Influence of the properties of proteins on adsorption In addition to the terminal amino and carboxylic acid groups in a protein, some amino acid side chains are ionized under normal conditions. These side chains are generally located at the surface, where protein-water interactions occur. Charged sites are, on average, surrounded by oppositely charged ones, thus stabilizing the protein (Perutz, 1978). In addition to the identity and sequence of amino acids in a protein, the three-dimensional and surface structures are also important, since adsorption to a solid surface is likely to result in a conformation change (Voller *et al.*, 1980). Some amino acids, e. g., valine, isoleucine and leucine, have rigid side chains, while glycine is flexible since it has no side chain (Schulz and Schirmer, 1979). A dissolved polypeptide chain tends to minimize the surface area between nonpolar groups and the aqueous phase and so polar and charged amino acid side chains are on the protein surface to interact with water.

For Rubisco from spinach, and GroEL and GroES from *E. coli*, 14.6%, 12.1% and 13.1% of total surface atoms are hydrophobic atoms (calculated from RasMol, Volume 2.5, World Wide Web). The mean area buried on transfer from the standard state to the folded protein is proportional to the hydrophobic contribution to the conformational free energy. For 1000 amino acid residues in Rubisco, GroEL and GroES, the total area buried on this transfer is 127×10^3 Å^2, 118×10^3 Å^2, and 120×10^3 Å^2, respectively (Table 3-1). The

hydrophobicity change during conformational alteration may help to explain the trend in the adsorption, Rubisco > GroEL ≥ GroES.

Table 3-1 shows that Rubisco has more negatively charged (acidic) amino acid residues than GroEL, which may also cause the slightly stronger adsorption of Rubisco. Even though the molecular size of GroES « Rubisco < GroEL, the high proportion of negatively charged amino acid residues in GroES results in comparable adsorption partition coefficients to those of GroEL and Rubisco, reflecting a stronger role of electrostatic forces than van der Waals forces in adsorption. Greater content of non-polar residues in GroES may result in a relatively larger folded state, compared with those of GroEL and Rubisco, resulting in more attachment points on the GroES surface.

Cytochrome *c* adsorption and desorption isotherms were quite linear, and coincided, exhibiting reversible sorption under my experimental conditions. The reversible adsorption, in contrast to that for the other proteins studied, may be due to 1) its lower molecular weight (12 kDa), so that van der Waals forces between it and mineral surfaces are smaller and fewer attachment points occur; 2) its stability; the more stable a protein is, the more reversible its adsorption will be (Andrade, 1985); 3) binding of a large portion of cytochrome *c* on illite surfaces via cation exchange at near-neutral pH.

Influence of mineral properties on adsorption The pH value at which the net surface charge of mineral is zero is referred to as the zero point of charge (ZPC). Below the ZPC the surface is positively charged, and it is negatively charged above the ZPC. At the ZPC, coagulation and sedimentation rates are greatest, and the anion exchange capacity is equal to the cation exchange capacity and both are at their minimal values (Parks, 1967). The ZPC of goethite is 6.9 (Taylor, 1987). The inhibition and adsorption experiments were conducted in distilled water, so the pH was a little less than the ZPC, and goethite was slightly positively charged.

Generally, no O atoms will persist at the surfaces of iron oxides under normal environmental conditions when exposed to water; O atoms are shared by other metal

cations. Charges develop on the goethite surface either by dissociation of surface hydroxyls, or adsorption of either H^+ or OH^- ions. Positively charged polyamino acids and proteins may bind on the goethite surface as H^+ donors.

Montmorillonite contains a large proportion of expandable interlayer, where water surrounds the interlayer cations in a partly ordered structure (Newman, 1987). Illite does not hydrate under mild conditions because the hydration energy of the interlayer K^+ is insufficient to overcome the cooperative structural forces at the coherent edges of a cleavage surface (Newman and Brown, 1969). Goethite has hexagonal close packing, and broken bonds occur only at edge surfaces where hydroxylation occurs. However, the area of these edges is generally small (1% of the total surfaces, according to Dyal and Hendricks, 1950), so that the sorption of water on goethite is smaller than that on montmorillonite. The larger content of sorbed water on montmorillonite results in greater cation exchange capacity.

The apparent adsorption partition coefficients of the proteins were greater on goethite than on montmorillonite than on illite. In addition to van der Waals forces, the slightly positively charged goethite may bind with proteins through electrostatic forces. Hydrogen bonds may also form, and because these interactions are stronger than other non-ionic ones, and multi-site adsorption is expected to occur, the adsorption of protein on goethite should be strong. Montmorillonite cation exchange capacity (CEC) is about 3 - 5 times higher than that of illite (Grim, 1968a). Hendricks (1941) found that organic ions were oriented between the montmorillonite layers in order to cause minimum expansion of the layers, and tended to be adsorbed in multiple layers. Organic matter is thought to be adsorbed by illite only on the exterior surfaces, i. e., organic ions do not replace the cations between the silicate layers (Grim, 1968b). Therefore, goethite and montmorillonite should adsorb the protein more strongly than illite, the pattern which was observed.

§3.5.2 *Adsorption of Poly-amino Acids*

The greatest adsorption was found for poly-Lys on montmorillonite (Table 3-9). The adsorption of small positively charged amino acids, peptides, and amines onto negatively charged mineral surfaces is via cation exchange, and adsorption partition coefficients are controlled by their basicity (Van Olphen, 1977; Wang and Lee, 1993; Luo, 1994). The CEC of montmorillonite is 40 times higher than that of kaolinite, so equally strong adsorption of Lys by both montmorillonite and kaolinite was explained by both amino and carboxyl functional groups affecting Lys adsorption (Wang and Lee, 1993). Strong electrostatic attraction between the cationic amino group and the negatively-charged clay surface, and interaction of the carboxyl group of the amino acid and the amino group of another adsorbed amino acid, may explain the very high adsorption capacity of clay minerals for Lys (Cloos *et al.*, 1966; Henrichs and Sugai, 1993) and, by extension, poly-Lys. Negatively charged poly- Glu and Asp showed slightly greater adsorption on goethite than on montmorillonite, which is due to stronger interaction between negatively charged poly-amino acids and the positively charged goethite surface.

Table 3-8 shows that there was no consistent molecular size effect on adsorption. Both the negatively charged poly-Glu adsorbing on positively charged goethite, and the positively charged poly-Lys adsorbing on negatively charged, high CEC montmorillonite, had similar partition coefficients for all polymers tested, even though their molecular weights ranged over an order of magnitude. The decrease in the partition coefficient with molecular weight for poly-Glu adsorption on montmorillonite could result from there being fewer amino groups per unit mass at higher molecular weight, if N-terminal amino groups are much more strongly bound than carboxyl groups. The relative adsorption change with molecular weight, and the large difference between poly-Lys and poly-Glu adsorption, is reasonably consistent with this explanation. The increase in poly-Lys adsorption on goethite with molecular weight, and the fact that poly-Lys adsorption on goethite is greater than or about equal to poly-Asp and poly-Glu adsorption, indicates that there are many

adsorption sites available for poly-Lys. This is presumably related to the amphoteric nature of the goethite surface, so that amino groups may exchange with H^+, leading to multi-site adsorption of the larger molecules. However, this does not seem to occur with poly-Lys adsorption on montmorillonite, perhaps because flocculation of the montmorillonite occurred in this solution, decreasing available surface area. It is not clear why poly-Glu adsorption on goethite is constant with molecular size if multi-site adsorption can occur.

§3.5.3 *Inhibition of Rubisco Adsorption by Poly-amino Acids and Proteins*

Table 3-9 shows that poly-Glu, poly-Asp, and BSA inhibited Rubisco adsorption, while poly-Lys and cytochrome *c* nearly always enhanced adsorption, for all three mineral phases. Both of the effects increased with the amount of protein or poly amino acid pre-adsorbed, which was largely related to their partition coefficients (Table 3-8). The enhancement of Rubisco adsorption by poly-Lys could be due to its positive surface charge. Poly-Glu is negatively charged (Schulz and Schirmer, 1979). Since these two poly-amino acids had opposite effects on Rubisco adsorption, absorbent-adsorbate and adsorbate-adsorbate electrostatic interactions may be important in affecting Rubisco adsorption. I propose that the negatively charged poly-amino acids compete with Rubisco for mineral surface adsorption sites, while Rubisco adsorbs more strongly to the adsorbed poly-Lys and poly-Arg than to the mineral. This explanation is supported by the small effects of neutral poly-amino acids (poly-Ala, poly-Phe, and poly-Leu) on adsorption (Table 3-9). Lacking charged side-chains, these poly-amino acids adsorb weakly and do not compete for adsorption sites with Rubisco, and neither do they provide strong Rubisco adsorption sites. The enhancement of Rubisco adsorption by cytochrome *c* is also consistent, since all of the Lys in cytochrome *c* probably is on the surface (White *et al.*, 1968a), making its similarity to poly-Lys plausible. BSA may be adsorbed on the same sites as Rubisco, thus competitively inhibiting Rubisco adsorption.

The molecular weight of poly-amino acids did not have much influence on their effects on Rubisco adsorption in most cases. The main exception is that the two larger sizes of poly-Lys inhibited Rubisco adsorption on goethite, rather than enhancing it like the smallest poly-Lys, poly-Arg, and cytochrome *c*. Notably, these two larger poly-Lys compounds had much greater partition coefficients on goethite than the smaller one. If this resulted in multiple layers of adsorbed lysine, weaker adsorption in the outer layers could have resulted both for poly-Lys and Rubisco.

§3.6 Conclusions

1) Proteins were strongly adsorbed by illite, montmorillonite, and goethite. This process was rapid and reached steady state in < 1.5 hour. Rubisco and GroEL were adsorbed on illite in their original forms. The activity remaining in the supernatant after adsorption was mostly smaller proteins.

2) Protein with more negatively charged amino acid residues may have stronger adsorption on goethite due to extra electrostatic interaction. The apparent adsorption partition coefficients of our proteins were in the order Rubisco > GroEL ≥ GroES, and on goethite ≥ on montmorillonite > on illite.

3) Generally, basic poly-amino acids have greater adsorption partition coefficients than acidic poly-amino acids. Acidic poly-amino acids were adsorbed slightly more on goethite than on montmorillonite, while basic poly-amino acids were adsorbed slightly more on montmorillonite than on goethite. Molecular size did not affect the electrostatic interaction between poly-amino acids and mineral surfaces.

4) Pre-adsorption of negatively charged poly- Glu, Asp and BSA inhibited Rubisco adsorption, indicating competition for the same binding sites. Positively charged poly- Lys, Arg, and cytochrome *c* usually enhanced Rubisco adsorption. Both influences were greater when more poly-amino

acid or protein was pre-adsorbed. Larger and/or more negatively charged poly-amino acids tended to inhibit Rubisco adsorption more.

5) The results indicate that electrostatic interactions between adsorbates and the particle surfaces, and between adsorbate molecules, are important in protein adsorption to clay minerals and goethite.

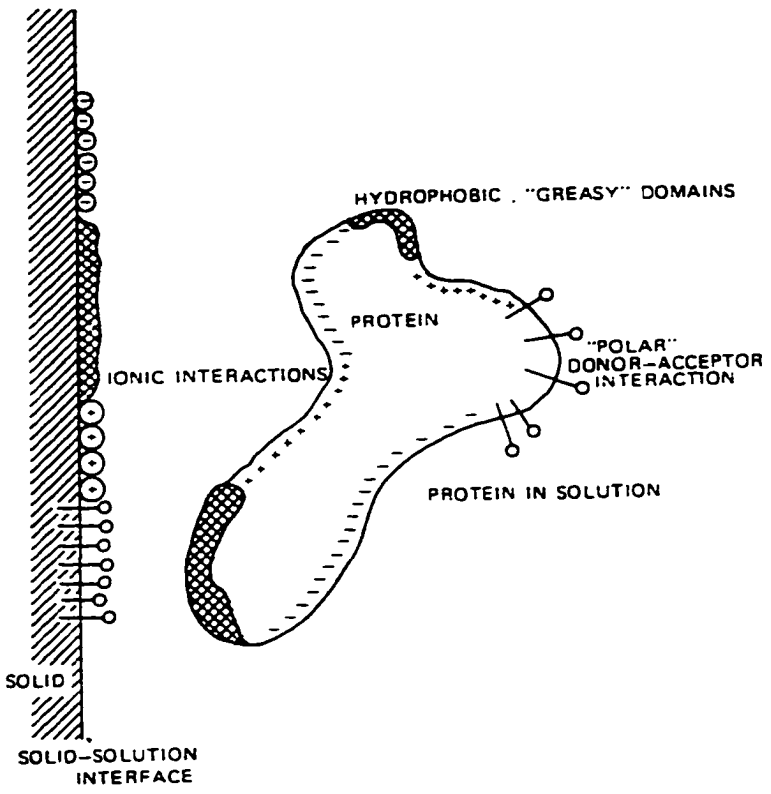

Figure 3-1. A schematic view of a protein interacting with a well-characterized surface (from Andrade, 1985).

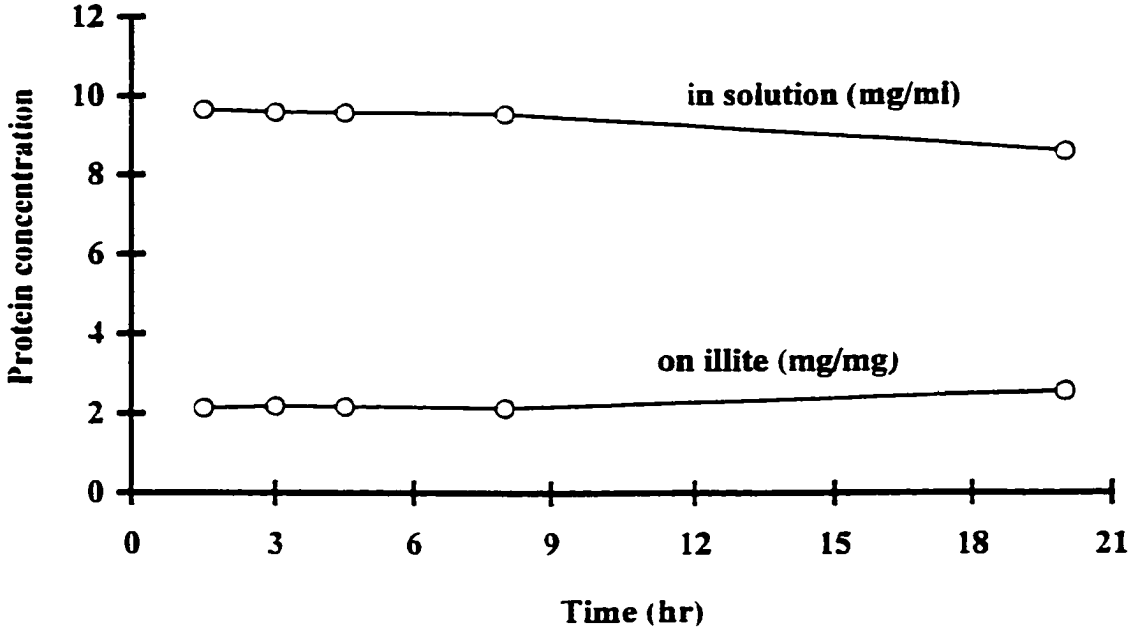

Figure 3-2. Time-course of Rubisco adsorption on illite

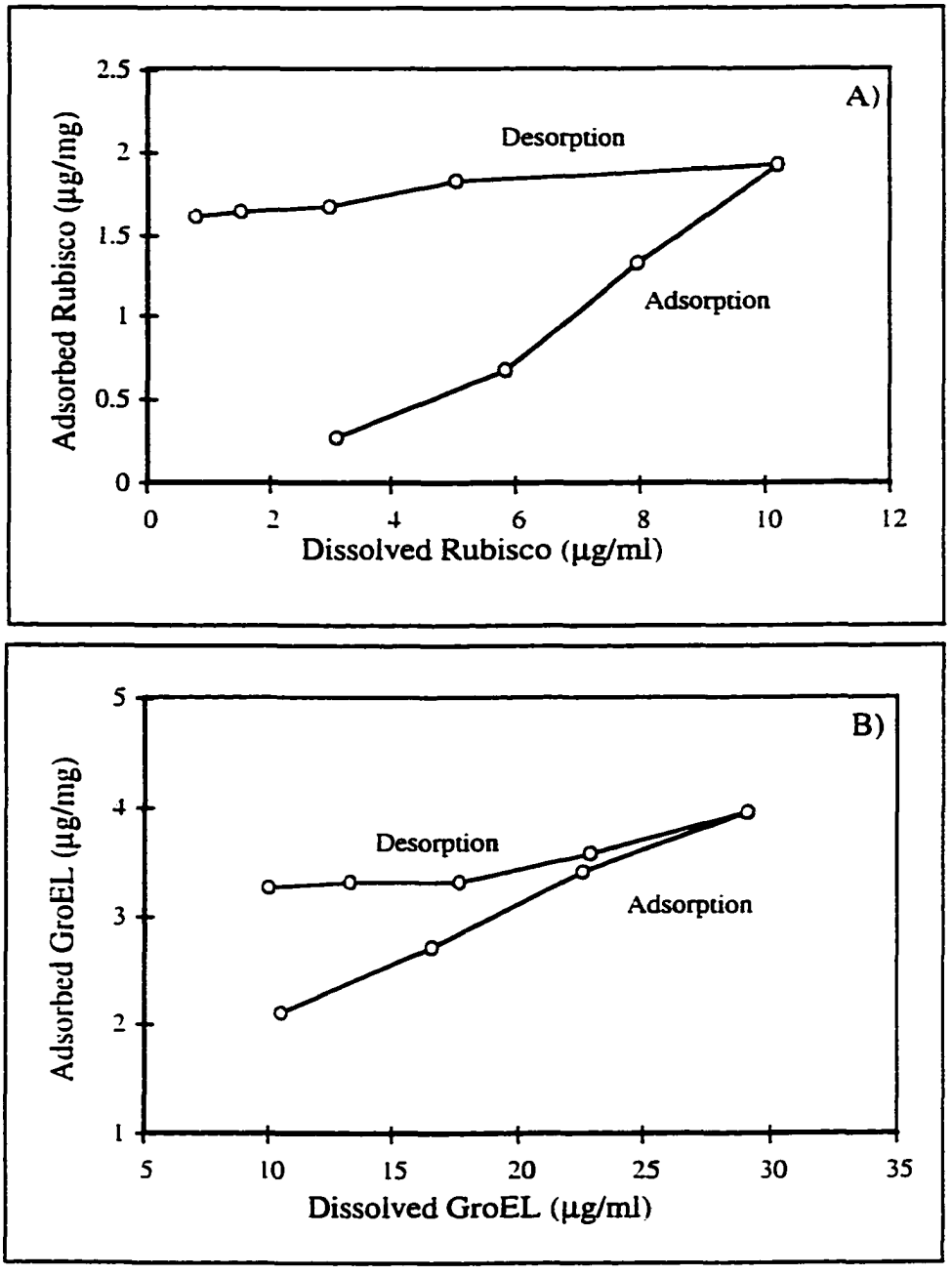

Figure 3-3. A) Rubisco and B) GroEL adsorption on and desorption from illite.

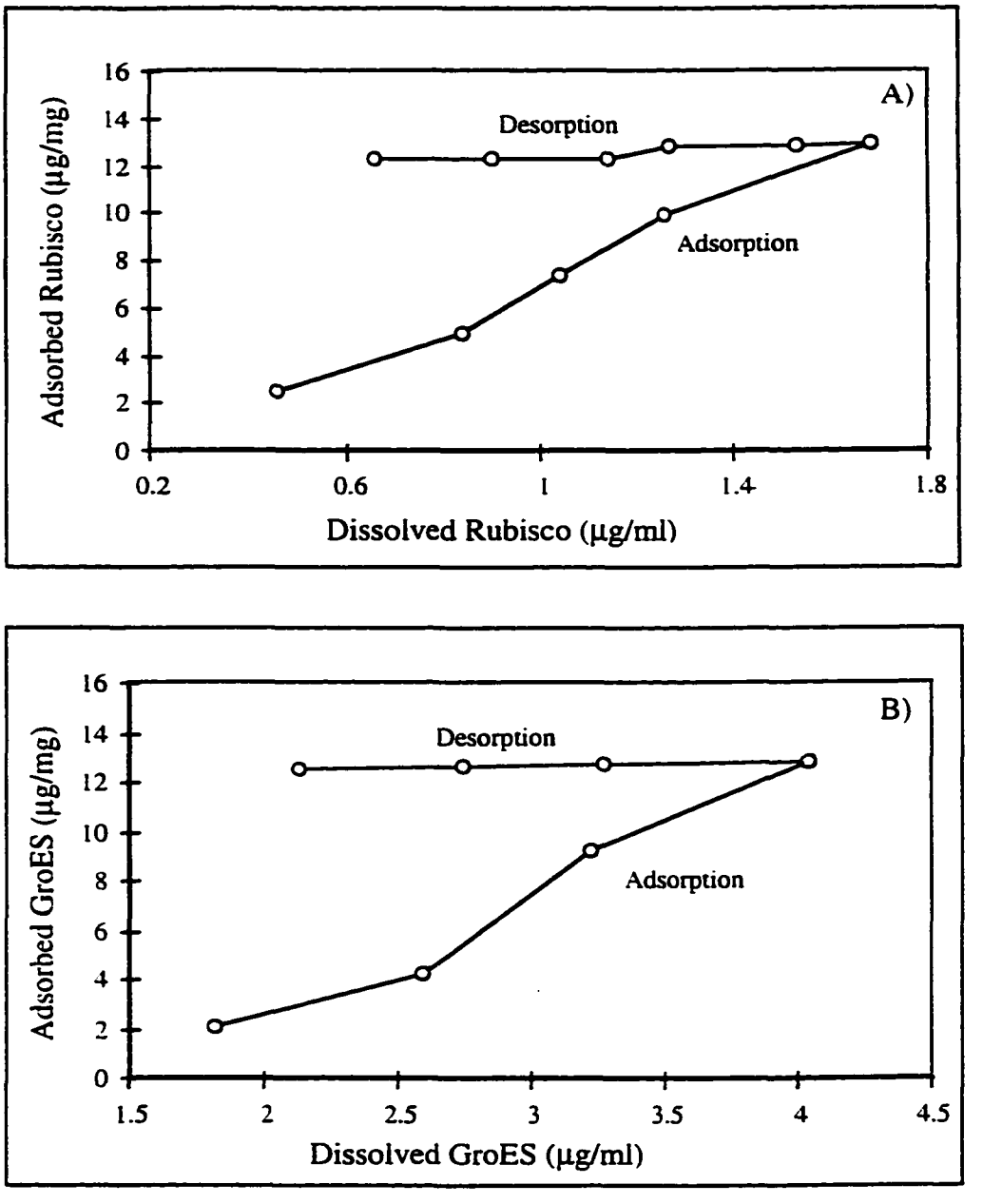

Figure 3-4. A) Rubisco and B) GroES adsorption on and desorption from goethite.

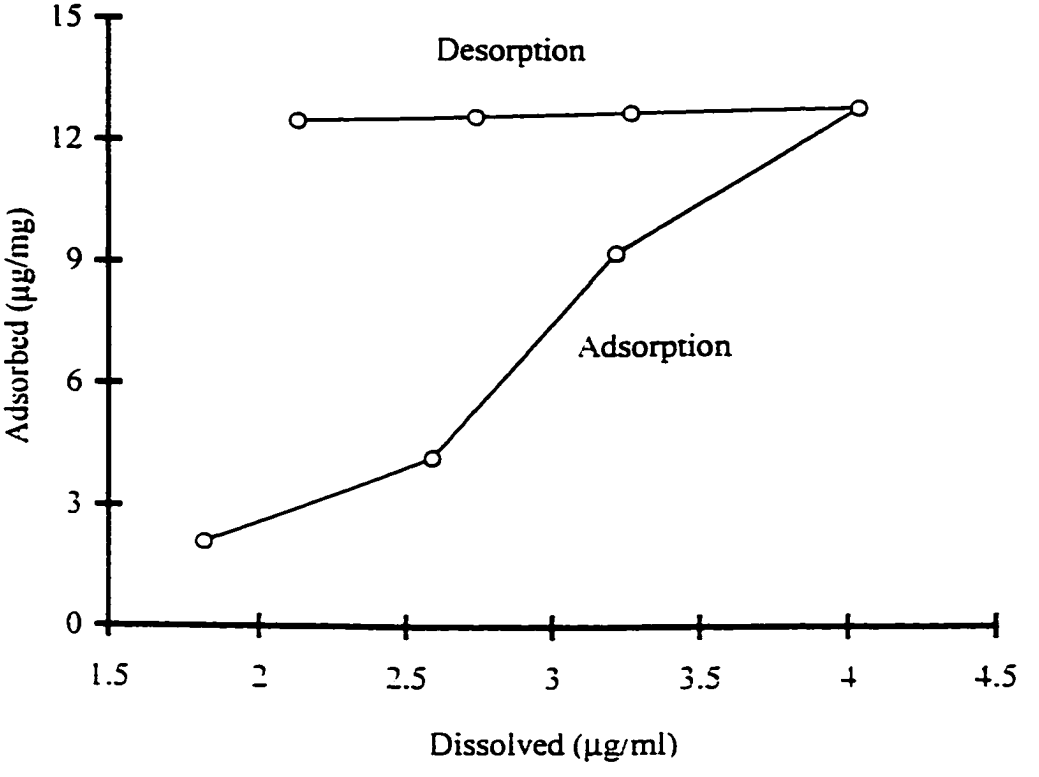

Figure 3-5. Rubisco adsorption on and desorption from montmorillonite.

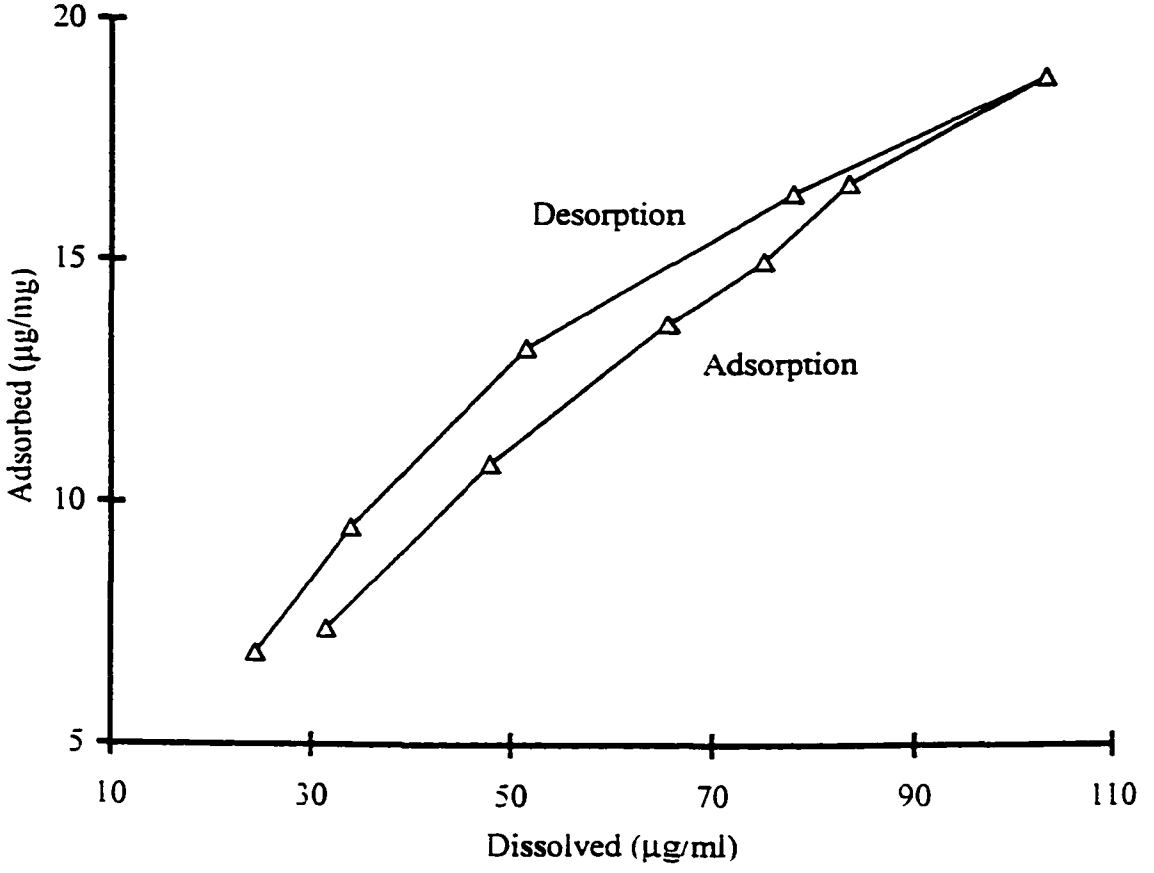

Figure 3-6. Cytochrome c adsorption on and desorption from illite.

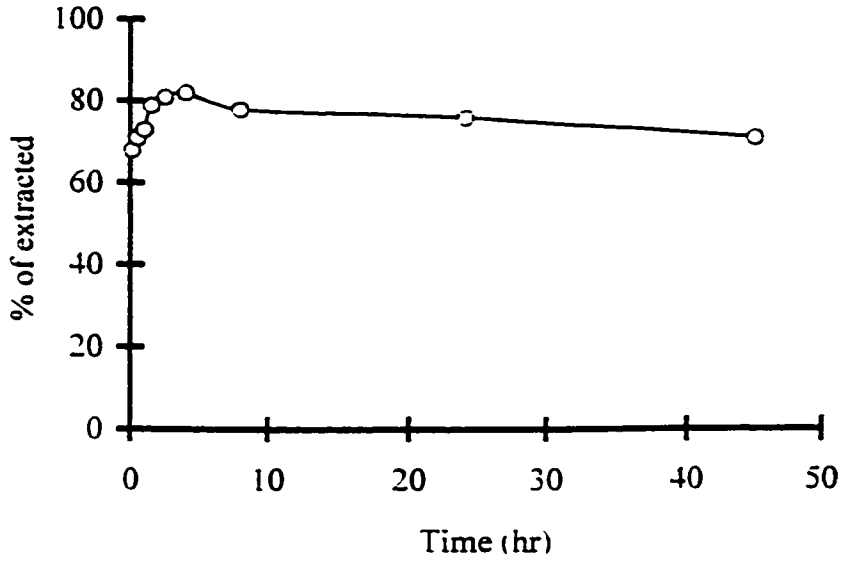

Figure 3-7. Time-course of Rubisco extraction from illite by 2.5 % of SDS.

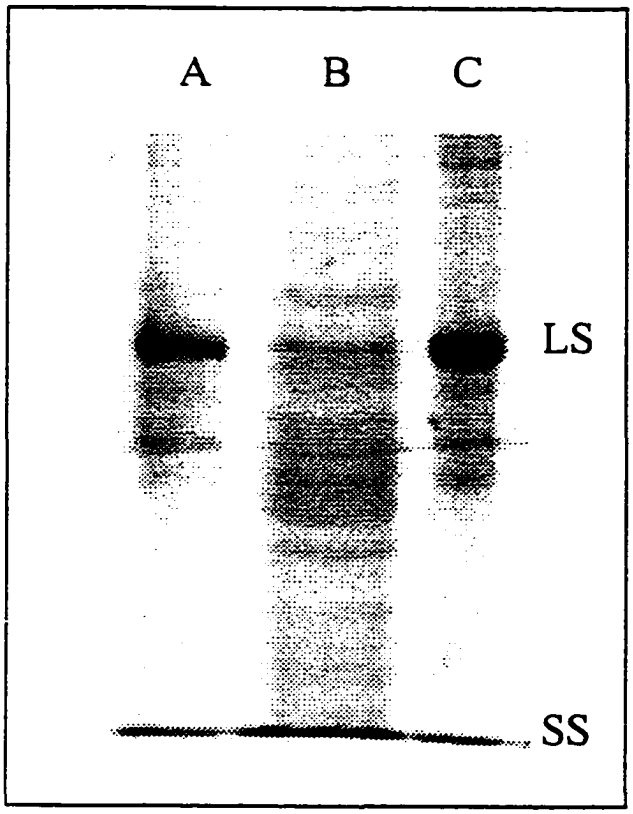

Figure 3-8. SDS-PAGE of Rubisco. A) original Rubisco; B) supernatant after adsorption on illite; C) adsorbed Rubisco after extraction from illite.

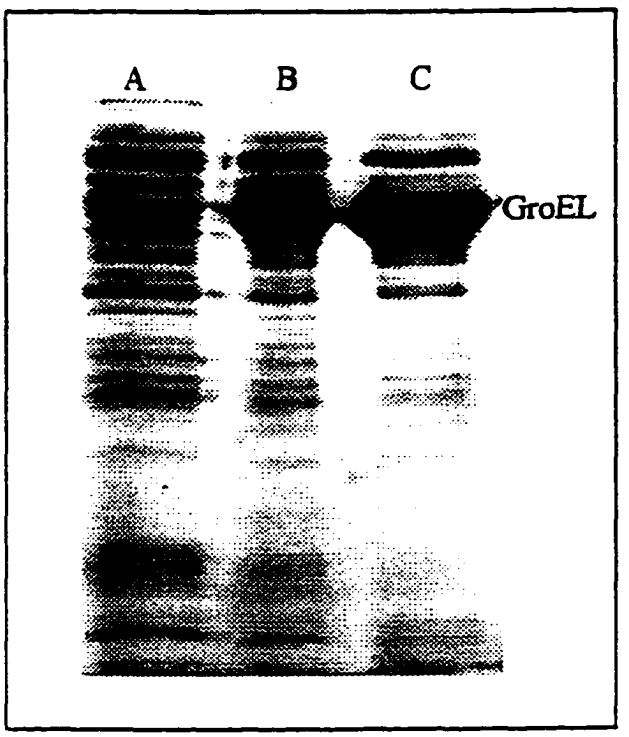

Figure 3-9. SDS-PAGE of GroEL. A) supernatant after adsorption on illite; B) adsorbed GroEL after extraction from illite; C) original GroEL.

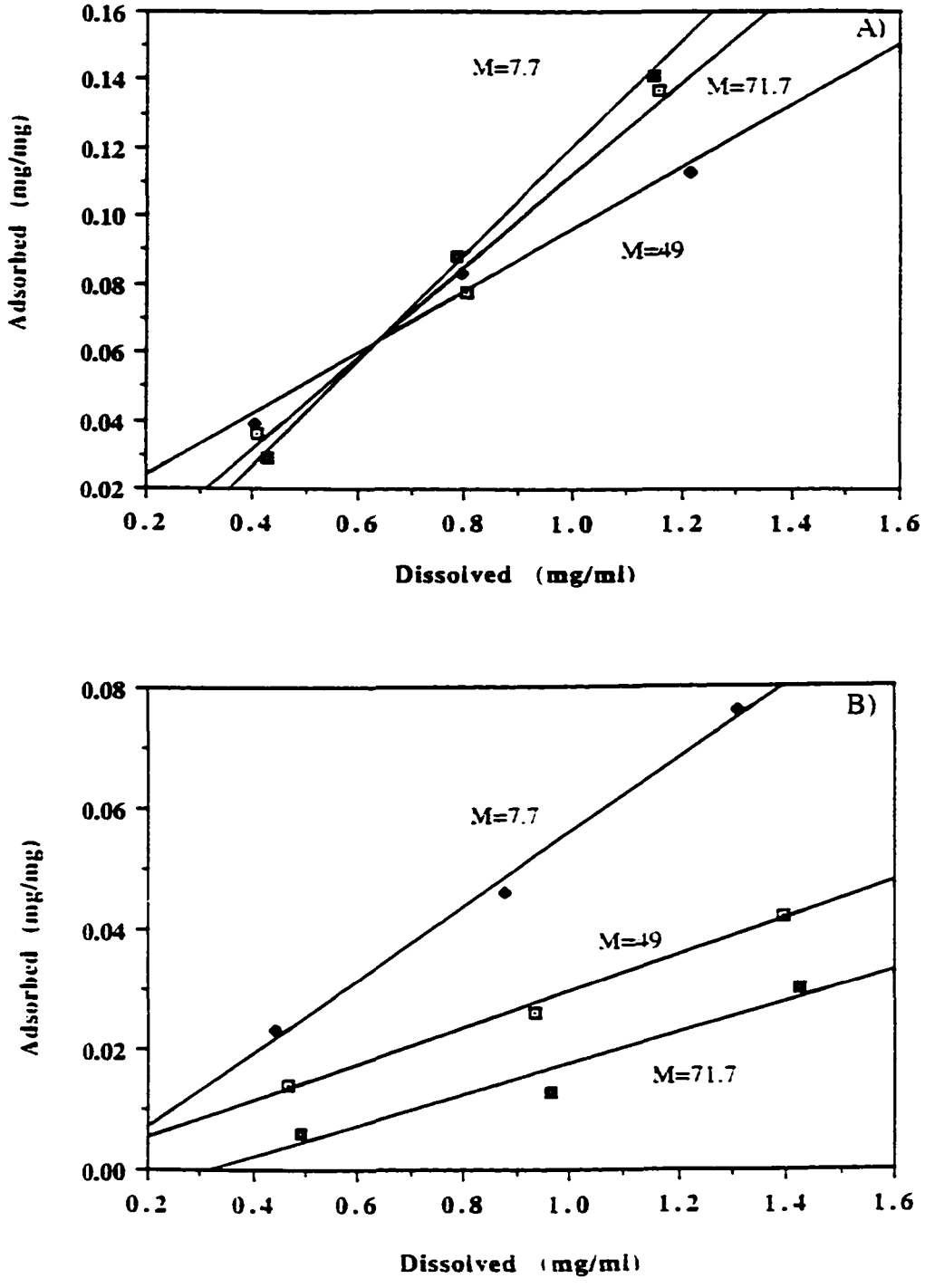

Figure 3-10. Adsorption of poly-glutamic acids on A) goethite and B) montmorillonite.

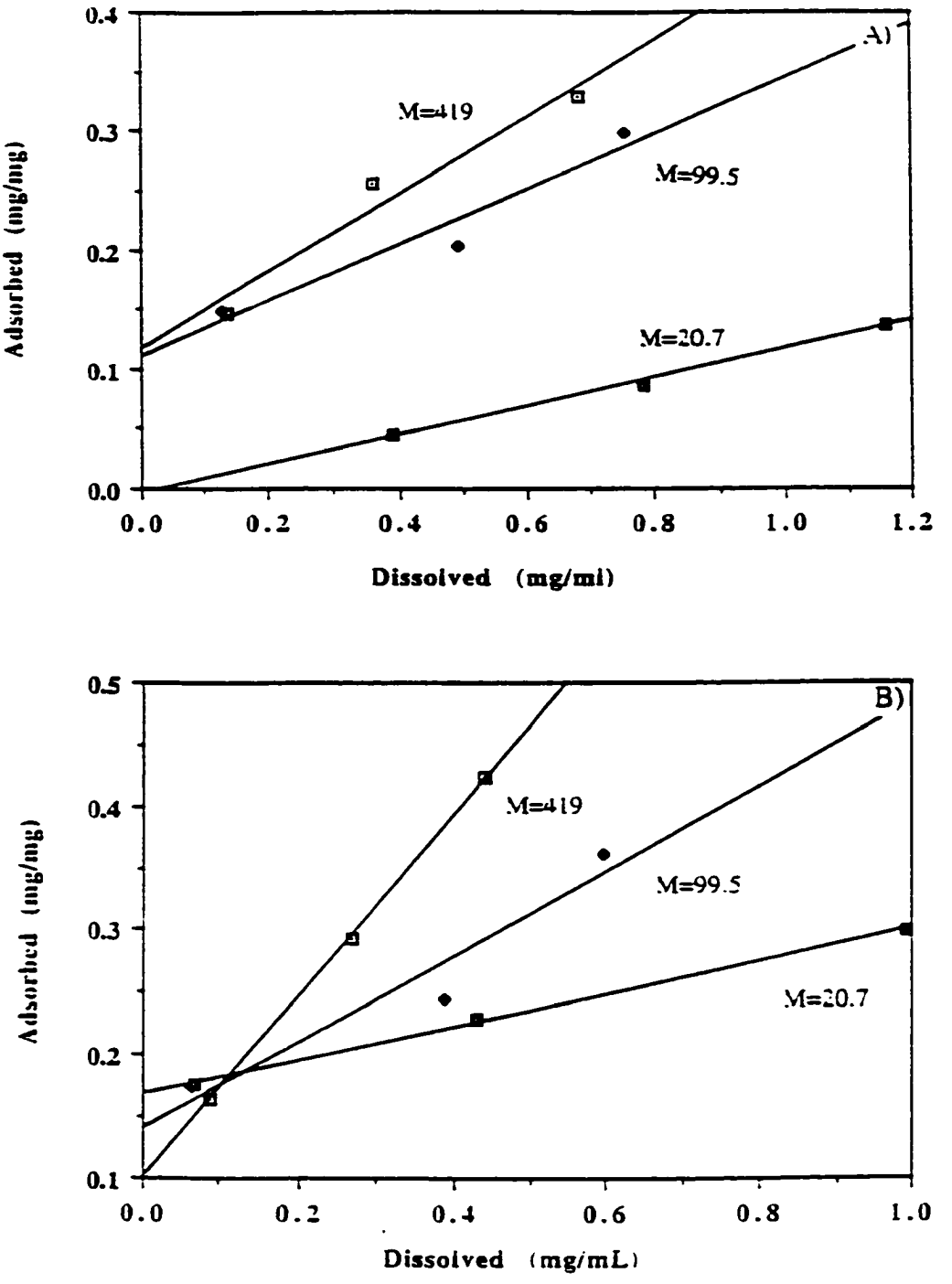

Figure 3-11. Adsorption of poly-lysine on A) goethite and B) montmorillonite.

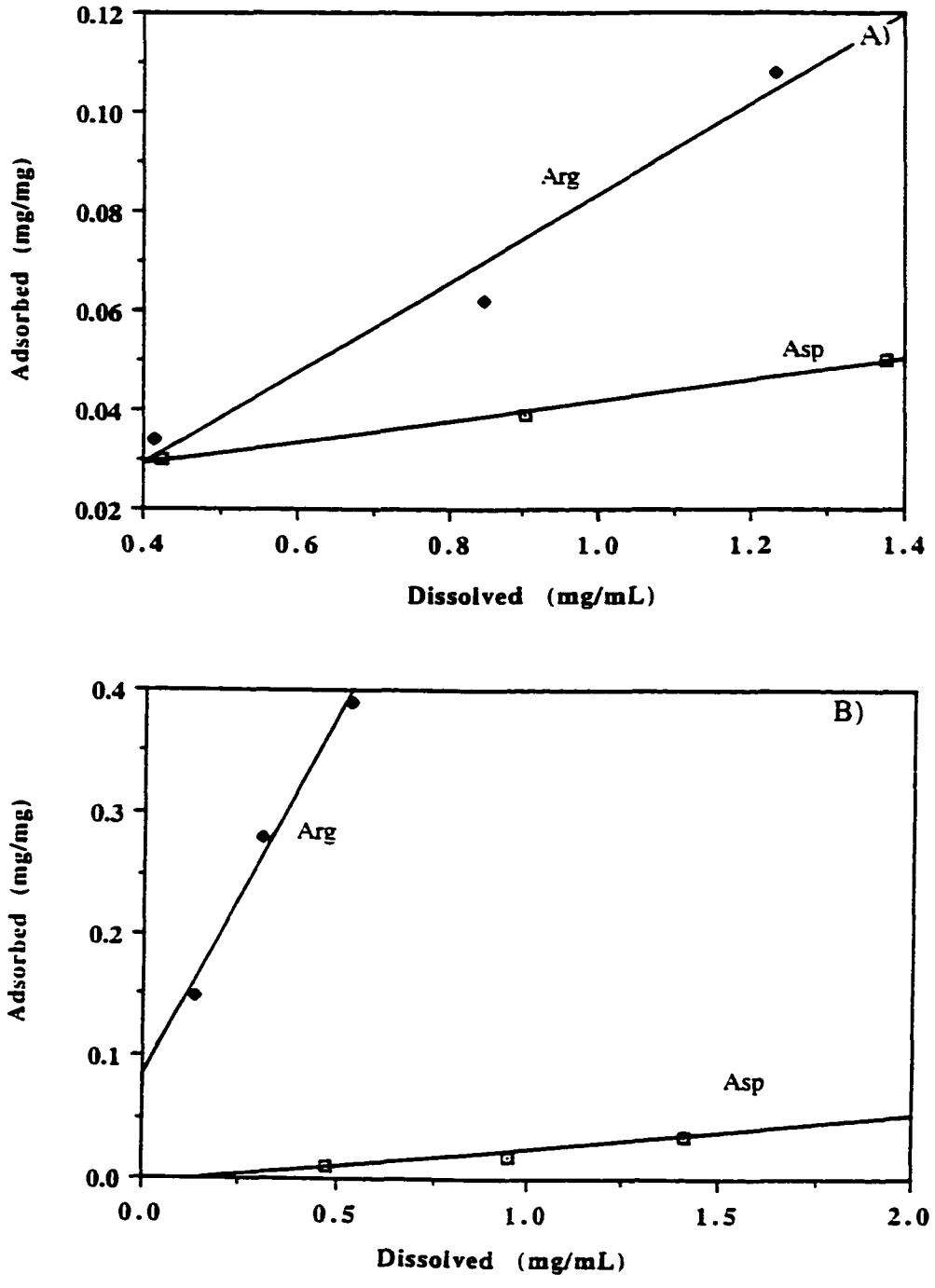

Figure 3-12. Adsorption of poly-asparate and arginine on A) goethite and B) montmorillonite.

Table 3-1. Amino acid compositions of proteins (No. of residues/1000 amino acids).

Amino acid Residue	3-letter symbol	M.W. at pH 7.0 (daltons)[a]	LS[b]	SS[c]	Ru	GroEL[d]	GroES[e]	ΔA^f (Å^2)	pI[g]
Alanine	Ala*	71	103	89	97	200	72	86.6	6.01
Glutamate	Glu-	128	69	43	57		103	113.9	3.22
Glutamine	Gln#	128	23	57	38			119.2	5.65
Aspartate	Asp-	114	74	57	66	100	62	97.8	2.77
Asparagine	Asn#	114	23	50	35	100	52	103.3	5.41
Leucine	Leu*	113	74	57	66		72	164.1	5.98
Glycine	Gly*	57	120	29	80	100	103	62.9	5.97
Lysine	Lys+	129	40	50	44	200	82	115.5	9.74
Serine	Ser#	87	40	54	46		62	85.6	5.68
Valine	Val*	99	63	93	76	100	134	141.0	5.967
Arginine	Arg+	157	69	57	64		52	162.2	10.76
Threonine	Thr#	101	34	36	35		31	106.5	5.87
Proline	Pro*	97	29	64	45		21	92.9	6.48
Isoleucine	Ile*	113	51	43	47		103	158.0	6.02
Methionine	Met#	131	29	50	38	100	21	172.9	5.74
Phenylalanine	Phe*	147	51	61	55	100	10	194.1	5.48
Tyrosine	Tyr#	163	11	50	28		10	177.7	5.66
Cysteine	Cys#	103	29	29	29			132.3	5.07
Tryptophan	Trp#	186	29	32	30			224.6	5.89
Histidine	His+	137	40	0	22		10	155.8	7.59
Σ Acidic					123	100	165		
Σ Basic					130	200	144		
Σ Non-polar					466	500	515		
Σ Polar, uncharged					279	200	176		

Abbreviations: Ru: Rubisco; LS: large subunit of Rubisco; SS: small subunit of Rubisco; -: acidic; +: Basic; #: polar, uncharged; *: non-polar.

a: from Andrade, 1985.

b: calculated from Yang *et al.*, 1986.

c: calculated and averaged between two genes from Clermont and Rahire, 1986.

d: calculated from Horovitz *et al.*, 1993.

e: from Hemmingsen, *et al.*, 1988.

f: the mean area buried on transfer from the standard state to the folded protein (Rose *et. al.*, 1985).

g: Isoelectric point, from Lehninger *et al.*, 1993a.

Table 3-2. Analysis of Rubisco stability in acidic solution after 2 hours at 4 °C, using sucrose density gradients (relative composition).

Location (mL from top)	H_2O (%)	Buffer, pH 4 (%)	6 N HCl (%)
1	1.4	1.9	2.5
2	1.4	2.0	5.1
3	1.6	3.0	6.6
4	1.2	4.1	6.6
5	2.1	3.5	4.3
6	2.8	3.3	6.2
7	4.8	5.7	5.0
8	6.6	5.7	5.4
9	8.0	5.3	4.5
10	8.0	7.0	5.2
11	9.3	12.7	8.5
12	20.1	19.7	18.0
13	32.7	26.1	22.1

Table 3-3. Conditions of SDS extraction of proteins from minerals.

Minerals	Protein	SDS(%)	T (°C)	Extraction efficiency (%)	
				First	Second
illite	Rubisco	1	4	73	
		2.5	4	84	3
		5	4	69	
goethite	Rubisco	1	4	71	3
		2.5	4	85	7
		5	4	61	5
illite	hydrophobic	2.5	4	46	
		2.5	95	75	

Table 3-4. 2.5 % of Triton X-100 extraction efficiency of Rubisco from minerals.

Minerals	Temperature (°C)	Efficiency (%)
illite	4	5.4
	95	6.9
goethite	4	4.2
	95	4.1
montmorillonite	4	4.2
	95	7.8

Table 3-5. Chloroform/Methanol (2:1) extraction of Rubisco from illite

pH	extraction efficiency (%)
0	5
2	0.5
5	0.7
8	2.4
10	1.7

Table 3-6. Distribution of adsorbed proteins extracted from illite along sucrose density gradients. The adsorbed proteins were extracted by Triton X-100.

Location (ml from top)	Original Rubisco (%)[a]	Adsorbed Rubisco (%)	Supernatant of Rubisco (%)	Original GroEL(%)	Adsorbed GroEL (%)	Supernatant of GroEL (%)
1	1.4	3.0	5.4	2.5	1.1	1.0
2	1.4	5.0	5.8	5.3	6.8	2.0
3	1.6	6.2	10.3	5.6	7.3	3.1
4	1.2	3.2	3.5	3.1	0.6	5.0
5	2.1	6.2	6.6	5.5	0.6	5.6
6	2.8	6.4	3.7	0.1	4.8	7.6
7	4.8	4.3	5.6	5.1	0.6	10.5
8	6.6	5.1	10.8	2.7	4.5	8.9
9	8.0	4.5	10.4	5.3	7.6	9.2
10	8.0	7.2	13.1	5.2	8.0	8.4
11	9.3	8.5	4.6	7.7	11.4	10.5
12	20.1	10.6	11.0	15.1	18.8	17.5
13	32.7	28.5	9.1	36.8	29.3	10.7
Recovery[b]	91.1	87.0	84.0	85.3	90.9	91.4

a: % of total ^{14}C activity measured in the sucrose gradient.
b: % of total ^{14}C activity loaded on the sucrose gradient.

Table 3-7. Analysis of ^{14}C Activity in Proteins from SDS-PAGE gel.

Origin	location on gel	Proteins*	M.W. (kDa)	% of total added	relative composition (%)
original	separating	Ru-LS	55	41	62
		Ru-SS	15	10	15
		impurity		11	17
	stacking	impurity		4	6
				subtotal: 66	
supernatant	separating	Ru-LS	55	15	25
		Ru-SS	15	16	27
		impurity	15~ 55	8	13
		impurity	> 55	14	23
	stacking	impurity		7	12
				subtotal: 60	
adsorbed	separating	Ru-LS	55	52	58
		Ru-SS	15	16	18
		impurity	15 ~ 55	5	6
		impurity	>55	12	13
	stacking	impurity		4	5
				subtotal: 89	
original	separating	GroEL	57	33	71
		impurity		8	18
	stacking	impurity		5	11
				subtotal: 45	
supernatant	separating	GroEL	57	27	39
		impurity	< 20	8	11
		impurity	20 ~56	6	9
		impurity	> 58	27	39
	stacking	impurity		1	1
				subtotal: 69	
adsorbed	separating	GroEL	57	50	70
		impurity	< 20	6	8
		impurity	20 ~56	3	4
		impurity	> 58	10	15
	stacking	impurity		3	4
				subtotal: 72	

* Abbreviations: Ru-LS: Rubisco large subunit; Ru-SS: Rubisco small subunit.

Table 3-8. Adsorption partition coefficients of poly-amino acids.

poly-amino acids	minerals	molecular size (kDa)	partition coefficient (L/kg)
poly-Glu	goethite	71.7	101
		49	98
		7.7	101
	montmorillonite	71.7	15
		49	29
		7.7	54
poly-Lys	goethite	419	857
		99.5	652
		20.7	86
	montmorillonite	419	1316
		99.5	1305
		20.7	1144
poly-Asp	goethite	12.3	50
	montmorillonite		22
poly-Arg	goethite	42.4	185
	montmorillonite		945

Table 3-9. Inhibition of Rubisco adsorption on minerals by other macro-molecules.

Organic Material Pre-adsorbed	Minerals	M.W. (kDa)	Exposure to OM concentration (mg/ml)	% Change*
poly-Glu	illite	49	5	+68
poly-Lys		20.7	5	-51
poly-Ala		21.4	Sat**	-8
poly-Phe		16.8	Sat**	3
poly-Leu		29.4	Sat**	15
cytochrome *c*		12.4	0.05	-12
			1	-33
BSA		66	0.05	+12
			1	+45
poly-Glu	goethite	71.7	5	+95
		49	5	+93
		7.7	5	+56
poly-Lys		419.5	5	+62
		99.5	5	+31
		20.7	5	-39
poly-Arg		42.4	5	-16
poly-Asp		12.3	5	+77
cytochrome *c*		12.4	1	-34
BSA		66	1	+74
poly-Glu	montmorillonite	71.7	5	-64
		49	5	+57
		7.7	5	+47
poly-Lys		419.5	5	-19
		99.5	5	-18
		20.7	5	-20
poly-Arg		42.4	5	-48
poly-Asp		12.3	5	+40
cytochrome *c*		12.4	1	-70
BSA		66	1	+6

*: $(A_{pre} - A_{ref})/A_{ref}$, positive sign represents inhibition of Rubisco adsorption; negative sign represents enhanced adsorption. A_{pre}: % of adsorbed protein on mineral which is pre-adsorbed by poly-amino acid or protein; A_{ref}: % of adsorbed protein on mineral without pre-adsorption.
**: saturated solution (< 5 mg/ml).

Chapter 4

Modeling the Adsorption of Proteins on Minerals

Abstract

Adsorption and desorption isotherms of several proteins on clay minerals and goethite showed marked differences. Although adsorption was linear, desorption isotherms were concave upward and a substantial fraction of the original adsorption was apparently irreversible. Three possible explanations for these observations are: 1) The mineral surface had at least two different types of binding sites. 2) Some protein molecules adsorbed at multiple sites. 3) The protein solutions contained a mixture of proteins with varying adsorption properties.

Two models were developed to test these hypotheses. Comparing model predictions to the data indicated that the protein solution contained small amounts of weakly adsorbed protein in addition to very strongly adsorbed protein. This is consistent with the SDS-PAGE results showing that adsorbed proteins ware mainly large proteins, while those remaining in solution were smaller molecules present as impurities in the original solution.

The small impurities in the protein solutions caused partition coefficients to be underestimated from adsorption isotherms. More accurate partition coefficients for the strongly adsorbed proteins were calculated from desorption data. The adsorption partition coefficients calculated using a model were on the order of 10^4 L/kg for Rubisco and GroEL adsorption on illite, 10^5 L/kg for Rubisco on montmorillonite and GroES on goethite, and 10^6 L/kg for Rubisco on goethite. These partition coefficients are quite comparable to the experimental results at very low particle concentrations, as predicted by the model. The partition coefficients of weakly adsorbed proteins are on the order of 10 - 100 L/kg.

§4.1 Introduction

The reversibility of organic matter adsorption on particle surfaces is of fundamental importance in understanding their fate in natural environments. Adsorption of organic matter (OM) on particle surfaces has been proposed as a key process leading to their preservation (Mayer, 1994a and b; Hedges and Keil, 1995). A simple model of the role of adsorption in OM preservation has illustrated that only very strong adsorption can lead to preservation (Henrichs, 1995). On the time scales of >100 yr relevant to OM preservation in continental margin sediments, weakly-sorbed molecules would exchange with those dissolved in pore water, leading to decomposition by microorganisms or loss via diffusion. There is little direct evidence that strong OM adsorption occurs on the mineral phases commonly found in sediments, under conditions that are appropriate for predicting whether sedimentary preservation would occur. Proteins are of particular interest relative to the issue of OM preservation because they are the largest component of the biomass of most marine organisms and because they are known to be preserved in coastal sediments (Mayer *et al.*, 1986; Pantoja and Lee, 1998), although some proteins decompose rapidly in the marine environment (e. g., Kirchman *et al.*, 1989).

Protein adsorption has been the subject of past research, but mainly this work has focused on biomedical issues and on surfaces (like glass) not found in sediments. An exception is work conducted by soil scientists (Sims and Holden, 1996), which has shown strong adsorption to clay minerals and that adsorption protects protein from decomposition. However, these experiments were done under conditions (e. g., high concentrations, very low water/particle ratios) very different from those in marine sediments. Some of the past work has found very strong, or irreversible, adsorption of proteins on a variety of surfaces. One explanation for past results has been that proteins undergo conformational change when adsorbing to surfaces. The tendency for an adsorbed protein to undergo conformational change is dependent upon protein structure, characteristics of the solid-solution interface, and time. Soderquist and Walton (1980) characterized adsorption

processes in three stages : 1) short times when adsorption is reversible, and probably little or no time is available for conformational adjustment; 2) longer times, when slow conformation change may occur, the process is semi-reversible, and desorption is very slow; 3) long times, when the conformation change is completed, adsorption is irreversible, and desorption may be impossible. However, proteins with many binding sites on their surfaces can adsorb with a multi-point attachment, resulting high adsorption free energy, even without any conformation adjustment (Andrade, 1985). At low concentrations, the adsorbed proteins have sufficient time and room to adjust their conformation to achieve significant hydrogen bonding to the solid surface. At high concentrations adsorbed proteins have neither time nor room to optimize their interaction with the surface (Morrissey, 1977). The adsorption of a protein on hydrophilic surfaces, such as glass, is often at least partly reversible (Andrade, 1985).

Here, I develop a mathematical treatment which allows prediction of protein adsorption partition coefficients from experimental data, minimizing the influence of impurities which sorb weakly. My observations of protein adsorption on clay minerals and goethite (Chapter 3) showed that adsorption was linear with concentration, but that much of the protein was apparently adsorbed irreversibly. SDS-PAGE data presented in Chapter 3 show that these results are likely due to the presence of several proteins in the solutions used, one (the major and intended constituent) which was very strongly adsorbed, and the others (small impurities in the solution) which were weakly adsorbed. However, at least two other phenomena could be responsible for my observations: 1) the mineral surfaces could have two or more different types of adsorption sites, or 2) the strength of protein adsorption could increase with time because of conformational changes.

§4.2 Experiments

The adsorption experiments were conducted as described in Chapter 3, except that water volumes were varied to achieve several particle concentrations. The particle mass used was 5.0 mg, and the volumes used were 2, 10 and 166 mL. Resuspension and dilution

experiments were conducted similarly to those described in Di Toro *et al.* (1986).

One experiment was designed to increase particle concentration by decreasing solution volume, without other changes in the system. In this experiment three control and three experimental vessels were prepared. After steady state adsorption was achieved, the suspension was centrifuged at 3,500 rpm for 15 minutes to separate particles and supernatant. A portion of supernatant was removed from the experimental vessels to obtain the desired particle concentration and the ^{14}C activity counted. Note that the volume in control vessels did not change during this experiment. Then the particles in both control and experimental vessels were resuspended by mixing. After reacting, the particles and supernatant were separated by centrifugation at 3,500 rpm. Then, ^{14}C activity was counted. The results reported are the mean of triplicate assays, with a relative deviation < 10%.

The other experiment was designed to decrease the particle concentration by diluting supernatant with the same solution. In this experiment, six dilution and three experimental vessels were prepared identically. After adsorption reached steady state, the particle suspensions in the dilution vessels were centrifuged at 3,500 rpm. The experimental vessels were not centrifuged at this time. After counting the ^{14}C activity, the supernatant in the dilution vessels was added to the experimental vessels to achieve the desired particle concentration. After adsorption reached steady state, experimental vessels were centrifuged, and the supernatant ^{14}C activity counted. The results reported are the average of triplicate measurements, with a relative standard deviation < 10%.

§4.3 Results

Protein adsorption on clay minerals tended to increase with decreasing particle concentration (Figure 4-1 and Table 4-1). This result was not due to the small adsorption of protein on container walls (see Chapter 3). Calculations showed that the amount of protein loss due to wall adsorption did not significantly affect the measured partition coefficients. Similar results were found for heavy metal adsorption on clay minerals (Di Toro *et al.*, 1986), in that partition coefficients tended to decrease with increasing particle

concentration, and eventually their value depended only on particle concentration. Physical rather than chemical factors were suggested to play the controlling role in this system.

Table 4-2 shows the results of the resuspension and dilution experiments. The concentrations in the resuspension supernatant, after adsorption, were slightly lower in both control and experimental vessels. This could be due to the adsorption reaction being not quite complete during the reaction times used. The adsorption partition coefficients were the same as in the first stage of the experiment, indicating that once the protein adsorbed on clay, it did not desorb readily. The dilution experiment showed that the partition coefficients tended to be greater at lower particle concentrations.

§4.4 Discussion

§4.4.1 Effects of Particle Concentration on Protein Adsorption

The dilution experiments (Figure 4-1) show greater adsorption partition coefficients at lower particle concentrations. One explanation is that, even though the supernatant after adsorption contained mostly smaller proteins, there were still some strongly adsorbed proteins in solution. At lower particle concentrations, when adsorption sites become limiting, the strongly adsorbed proteins occupy an increasing proportion of the sites. Alternatively, if weaker and stronger adsorption sites are present on the particle surface, the stronger sites become saturated at higher concentrations. Therefore, 1) the variation in adsorption partition coefficients at different particle concentrations is largely due to the partitioning behavior of weakly adsorbed protein or weak adsorption sites; 2) measured apparent adsorption partition coefficients tend to be greater at lower particle concentrations; and 3) at lower particle concentrations, the adsorption partition coefficient is close to that of strongly-adsorbed protein, or protein adsorbed at strongly adsorbing surface sites.

Another explanation for the data is more optimal conformation of adsorbed proteins at lower protein concentration and longer reaction times, since they had room and time to interact optimally with the particle surface. This conformation change may include

formation of multiple attachment points to the surface, which can lead to reversible or even irreversible denaturation. Or, mono-layer adsorption on the particle surface can develop if there is stronger absorbent-adsorbate interaction than adsorbate-adsorbate attraction. Henrichs (1995) used a simple model to calculate a relationship between adsorption coefficients and number of attachment points for macromolecules; in general this model predicts very strong, practically irreversible, adsorption for more than about 10 attachment points.

§4.4.2 *Prediction of Adsorption Partition Coefficients*

For an ideal adsorption-desorption reaction, involving a single solute and a homogeneous surface, the adsorption and desorption isotherms should be the same. The ^{14}C-labeled proteins studied showed linear adsorption on clay minerals, but a complicated desorption. To explain this pattern, I hypothesized that there were either two or more adsorption sites on the particle surfaces, with different adsorption reaction energies, or two or more dissolved proteins, with different adsorption partition coefficients. To simplify the situation, I will discuss 1) a clay mineral with strong and weak adsorption sites, and 2) two kinds of proteins, one strongly and the other weakly adsorbed by the mineral.

Model A, a clay mineral with two types of sites Model A assumes a monolayer adsorption of protein on a mineral surface containing both strong and weak adsorption sites for proteins. Both types of sites exhibit linear adsorption and desorption, with differing adsorption and desorption partition coefficients. The adsorption and desorption partition coefficients are constants. Figure 4-2 illustrates reversible adsorption at two different sites. The abbreviations used in this model are defined as follows:

D_T: total dissolved concentration in solution (μg/mL)

P_T: total adsorbed concentration (μg/mg)

D_T': total dissolved concentration in solution, after dilution of supernatant (μg/mL)

P_T': total adsorbed concentration after dilution of supernatant (μg/mg)

P_1: adsorbed protein concentration at weak adsorption sites (μg/mg)

P_2: adsorbed protein concentration at strong adsorption sites (μg/mg)

P_1': adsorbed protein concentration at weak adsorption sites, after dilution of supernatant (μg/mg)

P_2': adsorbed protein concentration at strong adsorption sites, after dilution of supernatant (μg/mg)

K: observed adsorption partition coefficient

K': observed desorption partition coefficient after dilution

K_1: true adsorption partition coefficient of protein at weak adsorption sites

K_2: true adsorption partition coefficient of protein at strong adsorption sites

K_1': true desorption partition coefficient of protein at weak adsorption sites after dilution

K_2': true desorption partition coefficient of protein at strong adsorption sites after dilution

g: mg of mineral

n: mL of solution

k: mL of water replaced during dilution

From the definitions,

$$P_T = P_1 + P_2 \tag{1a}$$

$$K_1 = \frac{P_1}{D_T} \times 1000 \tag{2a}$$

$$K_2 = \frac{P_2}{D_T} \times 1000 \tag{3a}$$

So, $K = K_1 + K_2$

$$P_T' = P_1' + P_2' \tag{4a}$$

$$K_1' = \frac{P_1'}{D_T'} \times 1000 \tag{5a}$$

$$K_2' = \frac{P_2'}{D_T'} \times 1000 \qquad (6a)$$

So, $K' = K_1' + K_2'$

For a one-step dilution, the mass balance is:

$$n D_T' + g P_T' = (n - k)D_T + g P_T \qquad (7a)$$

$$n D_T' + g P_T' = nD_T' + gP_1' + gP_2'$$

$$= n D_T' + gP_1' + \frac{g D_T' K_2'}{1000} \qquad (8a)$$

Combining (9a) and (10a),

$$g P_T + (n - k)D_T = nD_T' + gP_1' + \frac{g D_T' K_2'}{1000}$$

$$\text{i.e.,} \quad P_1' = P_T + \frac{(n - k)}{g}D_T - \frac{n}{g}D_T' - \frac{D_T' K_2'}{1000} \qquad (4\text{-}9a)$$

From the definitions,

$$K_2' = \frac{P_2'}{D_T'} \times 1000 = \frac{P_T' - P_1'}{D_T'} \times 1000$$

$$\text{i.e.,} \quad P_1' = P_T' - \frac{D_T' K_2'}{1000} \qquad (4\text{-}10a)$$

Actually, Equations 4-9a and 4-10a should be the same for reversible sorption (from Eq. 7a). Our experimental results showed that there was only a small difference (<4% of P_T) between Equations 4-9a and 4-10a for almost all protein desorption experiments after one dilution step, which is within experimental uncertainty. The only exception was GroEL desorption from illite, with a 94% offset between 4-9a and 4-10a. This could be due to substantial reversible desorption occurring during the first few dilutions. When $k \to 0$, or $n \gg k$, $D_T' \approx D_T$, $P_T' \approx P_T$, and $K' = K$.

As the adsorbed protein concentration at the weak adsorption site (P_1') approaches 0, the observed adsorption partition coefficient of protein approaches that at strong adsorption sites. From equation 4-10a in this case K_2' is:

$$K_2' = \frac{P_T'}{D_T'} \times 1000 = K' \qquad (11\text{-}a)$$

This means that proteins adsorbed at strong adsorption sites control results of desorption experiments.

According to my data, K_2' calculated from 11-a was only slightly greater than K, and depended on the dilution volume k; as $k \to 0$, $K_2' \to K$. The predictions of adsorption partition coefficients by this model did not match my observations (Table 4-1, Figures 3-3, 3-4, 3-5). That is, the proteins are predominantly very resistant to desorption and must have much greater adsorption partition coefficients than those calculated from experimental data. In addition, observed protein adsorption isotherms are linear in a very large adsorbed protein concentration range (e. g., 0.3-7 μg/mg for Rubisco on illite, 7-20 μg/mg for cytochrome *c* on illite). This also indicates uniform adsorption sites, since no saturation was observed with increasing concentration. Here, we reject the hypothesis that our desorption results are due to two different adsorption sites on the particle surface.

However, at very low particle concentrations, P_1 can be neglected relative to P_2. So, from the definitions (Eqs. 1a, 2a and 3a),

$$\frac{K_2}{K} = \frac{P_2}{P_1 + P_2} \approx 1 \qquad \text{i. e.,} \qquad K_2 \approx K$$

This indicates that at very low particle concentrations, the observed adsorption partition coefficient is very large, reflecting strong interaction between protein and mineral surfaces. This prediction matches the observation that there is more adsorbed protein than expected at low particle concentrations, when dissolved protein concentration is close to 0. Note, the strong adsorption mentioned here could be related to multiple attachment, rather than different types of adsorption sites on the mineral surfaces.

Model B, two or more proteins with different adsorption properties Figure 4-3 is a scheme which shows adsorption that is partly reversible due the presence of at least two proteins with differing properties. According to Chapter 3, the target proteins were adsorbed in their original forms, and most of the weakly adsorbed proteins were smaller proteins present as impurities.

The abbreviations used in this model are defined as follows:

D_A: weakly adsorbed protein concentration in solution (μg/mL)

D_B: strongly adsorbed protein concentration in solution (μg/mL)

D_A': weakly adsorbed protein concentration in diluted solution (μg/mL)

D_B': strongly adsorbed protein concentration in diluted solution (μg/mL)

P_A: weakly adsorbed protein concentration (μg/mg)

P_B: strongly adsorbed protein concentration (μg/mg)

P_A': weakly adsorbed protein concentration after dilution of supernatant (μg/mg)

P_B': strongly adsorbed protein concentration after dilution of supernatant (μg/mg)

K_A: partition coefficient of weakly adsorbed protein

K_B: partition coefficient of strongly adsorbed protein

From the definitions:

$$D_T = D_A + D_B \tag{1b}$$

$$P_T = P_A + P_B \tag{2b}$$

$$K_A = \frac{P_A}{D_T} \times 1000 \tag{3b}$$

$$K_B = \frac{P_B}{D_T} \times 1000 \tag{4b}$$

$$D_T' = D_A' + D_B' \tag{5b}$$

$$P_T' = P_A' + P_B' \tag{6b}$$

$$K_A = \frac{P_A'}{D_A'} \times 1000 \tag{7b}$$

$$K_B = \frac{P_B'}{D_B'} \times 1000 \tag{8b}$$

For one-step dilution, the mass balance is:

$$g\,P_T' + n\,D_T' = g\,P_T + n\,D_T - kD_T = g\,P_T + (n-k)D_T \tag{9b}$$

$$g P_T' + n D_T' = n D_A' + n D_B' + g \frac{K_A D_A'}{1000} + g \frac{K_B D_B'}{1000}$$

$$= (n + \frac{g K_A}{1000}) D_A' + (n + \frac{g K_B}{1000}) D_B'$$

$$= (n + \frac{g K_A}{1000}) (D_T' - D_B') + (n + \frac{g K_B}{1000}) D_B' \qquad (10b)$$

Combining (9b) and (10b),

$$g P_T + (n - k) D_T = (n + \frac{g K_A}{1000}) D_T' + \frac{g}{1000} (K_B - K_A) D_B'$$

$$D_B' = \frac{1000 P_T + \frac{1000(n - k)}{g} D_T - (\frac{1000n}{g} + K_A) D_T'}{(K_B - K_A)}$$

$$= \frac{1000\{P_T + \frac{(n - k)}{g} D_T - \frac{n}{g} D_T'\} - K_A D_T'}{(K_B - K_A)} \qquad (4\text{-}11b)$$

From the definition:

$$K_A = \frac{P_A'}{D_A'} \times 1000 = \frac{P_T' - P_B'}{D_T' - D_B'} \times 1000 = \frac{1000 P_T' - K_B D_B'}{D_T' - D_B'}$$

$$K_A (D_T' - D_B') = 1000 P_T' - K_B D_B'$$

$$D_B' = \frac{1000 P_T' - K_A D_T'}{(K_B - K_A)} \qquad (4\text{-}12b)$$

Equations 4-11b and 4-12b are the same for a reversible desorption (see Eq. 9-b). However, when $k \to 0$ or $n \gg k$, $D_T' \approx D_T$, $P_T' \approx P_T$. After deleting a small term which contains K_A, equations 4-11b and 4-12b are also the same, which means that after a small dilution, protein adsorption could appear reversible, since Eq. 4-12b was derived from a reversible sorption definition.

I assumed that D_B' accounted for about 1% of D_T', and $P_B' \approx P_T'$, since the purity of the proteins used was about 80 -90%, and on average about 10% of total adsorbed

proteins were desorbed during dilution. The adsorption partition coefficients for the strongly and weakly adsorbed proteins on illite were calculated using Equation 8b, as follows, and are listed in Table 4-3:

$$K_B = \frac{P_B'}{D_B'} \times 1000 = \frac{P_T'}{1\%\ D_T'} \times 1000 = 100K$$

Similarly, $K_A = K/100$, with the similar assumption that P_A' accounted for about 1% of P_T', and $D_A' \approx D_T'$ (Table 4-3). Since a maximum of 13.5% of Rubisco was desorbed from illite, and 4.7% and 2.3% from goethite and montmorillonite, respectively, we used $P_A' / P_T' = 0.4\%$ for goethite and 0.2 for montmorillonite. The results are listed in Table 4-3.

This model predicted that reversal of adsorption could occur after slight dilution, which is quite similar to our experimental results, i. e., partial reversal of adsorption was found after a few dilutions, but the protein that remained adsorbed was apparently irreversibly adsorbed. My studies of Rubisco decomposition in Skan Bay sediments (Chapter 5) showed that initially there was about 1 - 4% of the total adsorbed protein in interstitial water, which was contributed by reversibly adsorbed protein. So, the assumption that D_B' accounted for about 1% of D_T' is reasonable. The experimental results at low particle concentrations reliably predict adsorption partition coefficients. Also, model B described my observations much better than model A. This indicates that the differing adsorption and desorption isotherms were due to a mixture of at least two proteins, one strongly and one weakly adsorbed, with the weakly adsorbed protein being a minor component.

§*4.4.3 The Role of Adsorption in Protein Preservation*

A diagenetic model developed by Berner (1980) can be modified to predict the effect of adsorption on the decomposition of an organic substance (Henrichs, 1995):

$$\frac{dG}{dt} = -\frac{k_1 KG}{(K+1)} - \frac{k_2 G}{(K+1)}$$

where G is the total concentration of the organic substance in sediments, k_1 and k_2 are the first-order rate constants for the decomposition of adsorbed and dissolved organic matter, respectively, and K is a dimensionless adsorption coefficient which represents the adsorbed/dissolved ratio in sediment. This model, as discussed by Henrichs (1995), predicts the preservation of only strongly adsorbed organic substances. If the dissolved organic matter are mineralized at rates of 1 - 50 yr^{-1}, partition coefficients on the order of 10^2 - 10^4 are required. The proteins for this study have adsorption partition coefficients about 10^4 -10^6 kg/L for the strongly adsorbed ones, and 10 - 10 ^{2}kg/L for those that are weakly adsorbed. Selective decomposition of the more weakly adsorbed proteins is likely to occur in marine sediments. The partition coefficients of Rubisco, GroEL and GroES are consistent with their long-term preservation in continental margin sediments, provided that adsorbed proteins are not accessible to bacterial decomposition.

§4.5 Conclusions

1) The partition coefficients of proteins were 10^4 - 10^6 L/kg, and in the order Rubisco > GroEL ≥ GroES. Adsorption on goethite ≥ on montmorillonite > on illite.

2) Smaller proteins present in the protein solution as impurities showed reversible sorption, and their adsorption partition coefficients were from 10 - 100 L/kg.

3) Protein adsorption on clay minerals tended to increase with decreasing particle concentration. This was largely explained by a model which described the behavior of a mixture containing mostly strongly-adsorbed protein, with a minor component of weakly-adsorbed protein.

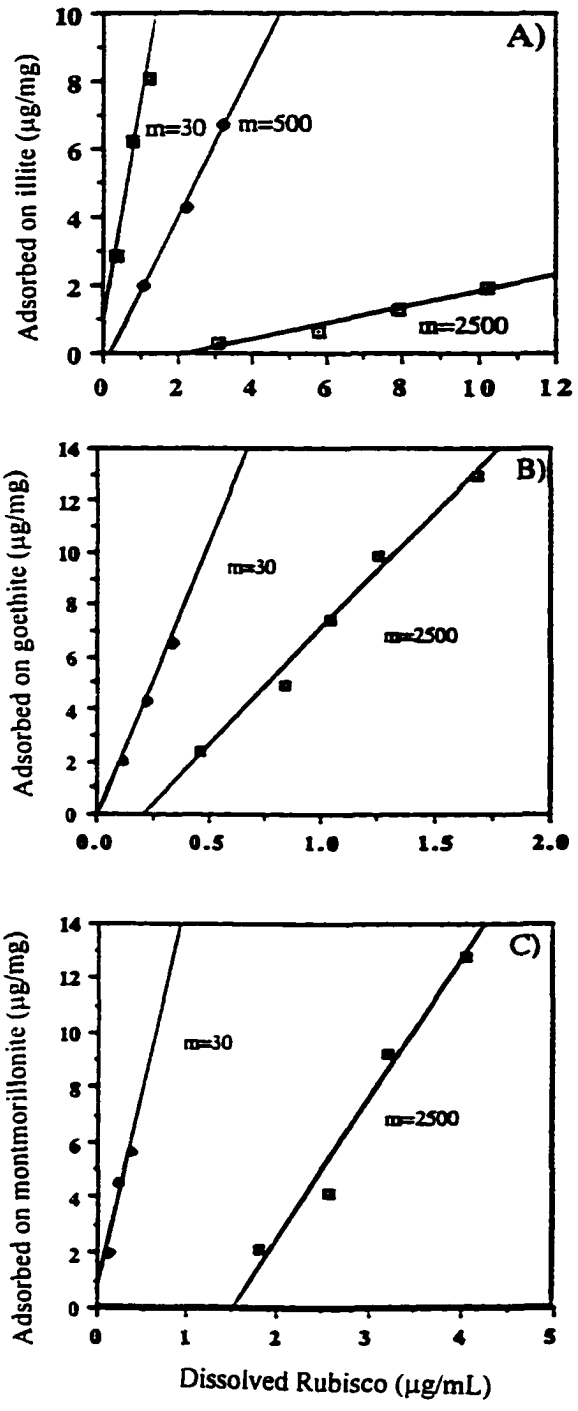

Figure 4-1. Rubisco adsorption on minerals at various particle concentrations = m (mg/L).

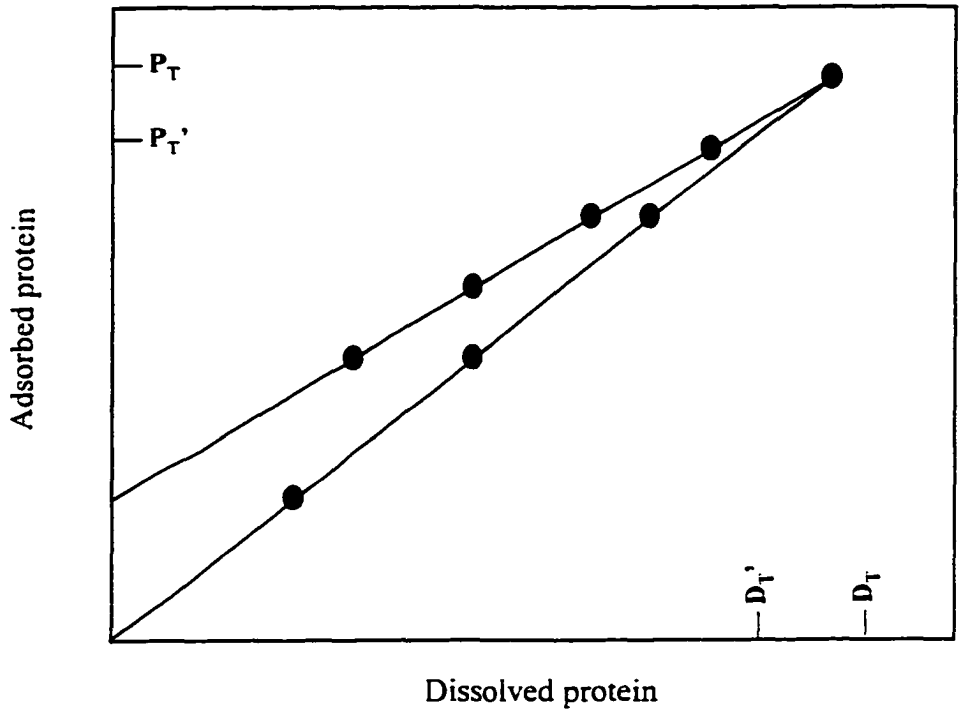

Figure 4-2. Reversible protein adsorption predicted by a model which describes adsorption at two different protein binding strengths.

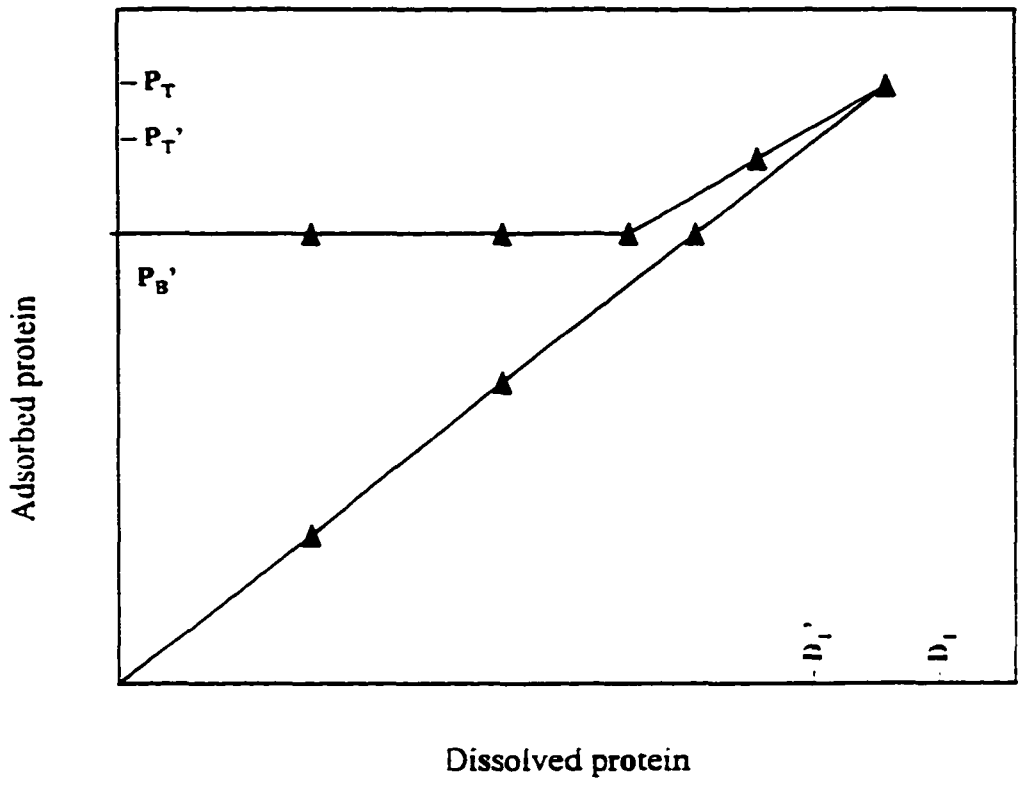

Figure 4.3. Protein adsorption on clay predicted by a model which describes the adsorption of a weakly and a strongly adsorbed protein on a homogeneous surface.

Table 4-1. Adsorption partition coefficients of Rubisco on minerals at varying particle concentrations.

Minerals	particle concentration m (mg/L)	Partition coefficients K (L/kg)
illite	2500	240
	500	2200
	30	6400
goethite	2500	8900
	30	21000
montmorillonite	2500	5100
	30	15000

Table 4-2. Apparent Rnbisco adsorption coefficients on goethite calculated using data from resuspension and dilution experiments at varying particle concentrations, m (mg/L).

Experiments	Supernatant concentration (C_A, μg/ml)	Supernatant concentration (C_{RES}, μg/ml)	C_{RES} / C_A	K_{AD}*
Resuspension				
control	0.62 / 0.63 / 0.65	0.56 / 0.57 / 0.58	0.91 / 0.94 / 0.89	1860 ± 65
experimental	0.62 / 0.63 / 0.65 (m = 500)	0.54 / 0.57 / 0.54 (m = 2500)	0.87 / 0.90 / 0.87	1943 ± 80
Dilution				
control (m = 2500)				1030 ± 240
experimental (m=1000)				1990 ± 300

* C_A: Rubisco concentration in supernatant; C_{RES}:Rubisco concentration in resuspension experiment supernatant; K_{AD}: the adsorption partition coefficient calculated from either resuspension experiment data or from data generated by dilution of the supernatant.

Table 4-3 . Adsorption partition coefficients of proteins on minerals calculated using model B.

Minerals	Proteins	D_B' / D_T' and P_A' / P_T'	K_B (L/kg)	K_A(L/kg)
illite	Rubisco	1	400	400
		0.1	4×10^3	40
		0.01	$\underline{4 \times 10^4}$	<u>4</u>
		0.001	4×10^5	0.4
	GroEL	1	200	200
		0.1	2×10^3	20
		0.01	$\underline{2 \times 10^4}$	<u>2</u>
		0.001	2×10^5	0.2
goethite	Rubisco	1	8×10^3	2×10^4
		0.04	2×10^5	2×10^3
		0.004	$\underline{2 \times 10^6}$	<u>200</u>
		0.0004	2×10^7	20
	GroES	1	5×10^3	5×10^3
		0.04	5×10^4	5×10^2
		0.004	$\underline{5 \times 10^5}$	<u>50</u>
		0.0004	5×10^6	5
montmorillonite	Rubisco	1	2×10^4	2×10^4
		0.02	2×10^5	2×10^3
		0.002	$\underline{2 \times 10^6}$	<u>200</u>
		0.0002	2×10^7	20

*: underlined values are the estimated adsorption partition coefficients for the strongly adsorbed proteins (K_B) named in the table and weakly adsorbed proteins present in the original solutions of these proteins (K_A).

Chapter 5

Decomposition of Rubisco in Anoxic Sediments

Abstract

Adsorption on mineral surfaces has been hypothesized to lead to organic matter preservation in marine sediments. Rubisco, a protein from *C. reinhardtii*, was strongly adsorbed by clay minerals and Skan Bay sediments. Rubisco adsorption on clay minerals decreased its decomposition rate up to 4 fold, compared with Rubisco that was added to sediments without pre-adsorption to a mineral phase. Rapid adsorption of Rubisco on the sediments themselves also resulted in slowed decomposition. The Rubisco solution used in the decomposition experiments contained small amounts of several other proteins which had varying adsorption properties and decomposition rates. In sediments from 6 cm depth, the turnover time for weakly adsorbed proteins was 6 days; for strongly adsorbed but labile proteins, 45 days; and for strongly adsorbed, refractory proteins, consisting mainly of Rubisco, 500 days. In almost all of the decomposition experiments, I found that the increase in $^{14}CO_2$ was slightly greater than the decrease of dissolved protein ^{14}C in interstitial water, suggesting that dissolved hydrolysis and fermentation products were assimilated quickly and completely by bacteria. Unexpectedly high CO_2 production was found during the decomposition of Rubisco pre-adsorbed on goethite, which could be due to desorption during reductive dissolution of iron oxides.

§5.1 Introduction

Understanding of the processes of preservation and remineralization of organic matter (OM) in marine sediments is incomplete. Henrichs and Reeburgh (1987) and Hedges and Keil (1995) reviewed the literature on sedimentary OM preservation. Most particulate OM produced by organisms is recycled in the photic zone (Suess 1980), and of the organic matter that reaches marine sediments, only a small fraction is preserved (Hedges *et al.*, 1988a; Lee, 1994). Much of the OM decomposition occurs at the water-sediment interface. The quality as well as the quantity of substrates that support bacterial growth could be an important factor affecting OM decomposition during early diagenesis (Westrich and Berner, 1984). Henrichs and Doyle (1986) found that different components of OM were decomposed at different rates, with the soluble fraction of a marine diatom and a bacterial polymer decomposing more rapidly than the natural sediment total organic carbon (TOC). Henrichs and Reeburgh (1987) found that organic matter burial efficiency (the ratio of the carbon burial rate and the carbon flux to the sediment surface) was enhanced by higher sedimentation rates that result in rapid burial. Mayer (1994a and b) found that many continental margin sediments have a similar ratio of organic carbon (OC) to sediment surface area (SA), suggesting that surface area controls OM content and that the OC/SA ratio represented a "mono-layer equivalent" coating of organic matter on the sediment particles.

The adsorption of OM to mineral surfaces is a rapid process which competes with decomposition during early diagenesis. The amount of adsorbed OM and the supply of dissolved OM at the water-sediment interface affect the rates of microbial processes. Adsorption of OM in sediments can decrease its availability to microorganisms, and thus its consumption rate, since adsorbed organic substances may be more difficult to degrade than dissolved OM (Christensen and Balckburn, 1980; Marshman and Marshall, 1981; Doyle, 1988; Kirchman *et al.*, 1989; Sugai and Henrichs, 1992; Keil and Kirchman, 1993).

Small dissolved molecules, such as free amino acids and peptides, are rapidly metabolized by sediment microorganisms. The numbers of bacteria decrease sharply with depth within the upper 100 cm (Price, 1976), so OM degradation by microorganisms is greatest near the sediment surface.

Remineralization of amino acids in coastal marine sediments has been investigated in detail (Henrichs *et al.*, 1984; Henrichs and Farrington, 1987; Sugai and Henrichs, 1992). Amino acids can account for about 30% of the carbon and 40 - 80 % of the nitrogen mineralized during OM decomposition (Henrichs and Farrington, 1987; Burdige and Martens, 1988). Generally, amino acids decompose rapidly, but their mineralization is slowed by adsorption (Sugai and Henrichs, 1992; Wang, 1993). Adsorption of amino acids by minerals and natural sediments generally increases with their basicity, and basic amino acids tend to decompose slowly (Sugai and Henrichs, 1992; Wang 1993).

Peptide decomposition and adsorption were also investigated. The decomposition of peptides involves two steps: the hydrolysis of peptides to free amino acids and the respiration of amino acids to CO_2 and H_2O. The adsorption of peptides is mainly controlled by the characteristics of the particle surface and the basicity of peptides. Adsorption partially protected peptides from biodegradation (Luo, 1994). Hydrolysis of small peptides in sediments was a rapid process, but was the rate-limiting step in the mineralization of several of the peptides investigated.

The remineralization of OM during early diagenesis in anoxic sediments has been extensively studied, with emphasis on the consumption of sulfate and the generation of CO_2 and CH_4 (Reeburgh, 1976, 1979 and 1980; Coleman *et al.*, 1993; Giordani *et al.*, 1996). It is thought that complete anaerobic decomposition requires the initial fermentation and hydrolysis of larger biopolymers to produce lower molecular weight compounds, (e.g., acetate), which are utilized by bacteria to finally produce CO_2 and CH_4 (Fenchel and Blackburn, 1979). Ferric iron (Fe(III)) reduction to ferrous iron (Fe(II)) is one of the most important geochemical reactions in anaerobic sediments (Lovley *et al.*, 1991). The

reduction of sulfate and ferric iron, coupled with the oxidation of important fermentation products such as acetate and hydrogen, has received increasing attention in recent years. H_2S produced by sulfate-reducing bacteria can reduce iron oxyhydroxides to form sulfides (Berner, 1984).

In this study, the decomposition and adsorption of a ^{14}C-labeled protein, Rubisco, in anoxic marine sediments and pore water were investigated. Illite (the second most abundant clay mineral in Skan Bay sediments, Luo, 1994) and goethite (a well-characterized iron oxide) were used as solid phases to pre-adsorb Rubisco and to investigate the influence of adsorption on protein decomposition. The objectives of this work were:

1) To determine the adsorption of Rubisco by anoxic sediments.

2) To determine the decomposition rates of Rubisco in anoxic sediments.

3) To compare the decomposition rates of proteins pre-adsorbed on clay minerals to those added to sediments in dissolved form, and thus determine the effect of adsorption on decomposition.

4) To compare the decomposition rates of weakly and strongly adsorbed proteins.

5) To compare the Rubisco decomposition rates in sediments from 6 cm and 12 cm depths.

§5.2 Site Description

Skan Bay, located on the northwestern side of Unalaska Island in the Aleutian chain, is a pristine embayment with no human habitation and infrequent visitation. Our study site is in the south arm (Figure 5-1), which is relatively narrow (1.2 km at its widest point) and has a 10 m sill at the mouth. The steep walls cause the basin to act as a sediment trap, accumulating terrestrial debris and marine particulates, and the broad and shallow sill across the inlet restricts horizontal exchange of basin bottom water with O_2-rich Bering

Sea water (Aiperin, 1988). In winter, storms renew bottom water. In summer, the water column is strongly stratified, preventing vertical mixing. The high influx of organic matter results in depletion of bottom water O_2 in late summer.

Skan Bay sediments are organic-rich with a surface TOC value of 5 - 6 %, partly due to large OM inputs from kelp. About 60% of the OM is consumed in the upper 40 cm of sediments (Alperin, 1988, Alperin *et al.*, 1992). The sediment porosity is high in surface sediment (> 0.99) and decreases with depth to a relatively constant value of 0.85 at ≥ 30 cm. The surface area of the sediments is 15 - 29 m^2/g (Mayer, 1994b). The sedimentation rate is about 0.24 - 0.26 g cm^{-2} yr^{-1}, with no bioturbation (Sugai *et al.*, 1994). The sulfate concentration decreases linearly, from 25 to 15 $mmol/L_{PW}$ over the upper 18 cm. The carbon flux from POC to DOC changed drastically, from about 500 to 30 μmol cm^{-2} yr^{-1}, between 6 cm and 12 cm depth (Alperin, 1988). Methane is produced at depths greater than 40 cm (Alperin, 1988), and its oxidation rate is two times greater at 11.5 - 14 cm than at 6.5 - 9.2 cm (Reeburgh, 1980). The first-order decomposition rate constant of acetate is 1.0 h^{-1} (Shaw *et al.*, 1984), of amino acids is 0.1 - 0.5 h^{-1}, and of peptides is 0.1 - 1.0 h^{-1} (Luo, 1994). Hydrogen production rates in SB were estimated at < 3 μmol $cm^{-2} \cdot yr^{-1}$ in the upper 30 cm (Alperin, 1988). Alperin (1988) determined a sulfate reduction rate of 27 $mM_{PW} \cdot yr^{-1}$ at a depth of 10 - 12 cm. Shaw and McIntosh (1990) concluded that 97% of acetate oxidation depended on sulfate reduction.

§5.3 Sampling

Sediments were collected from Skan Bay (SB), Alaska in August 1997. The sampling method was similar to that of Alperin (1988) and Luo (1994). For decomposition experiments, after collecting sediment with a MK-III box corer and removal of the overlying water, the sediments were horizontally subsampled, by using 10 - 12 mL plastic incubation syringes, at depths of 6 cm and 12 cm. After filling, the plastic syringes were sealed with rubber stoppers. Sediment samples for adsorption measurements were obtained

from box cores by manually scooping sediments from the appropriate depth into mason jars which were completely filled before sealing with a Teflon-lined lid. All samples for decomposition and adsorption experiments were stored in the dark in a 4 °C incubator until used. Decomposition experiments were conducted within one day after sample collection. Adsorption experiments were conducted within 2 months.

§5.4 Materials and Methods

^{14}C-labeled Rubisco and the clay minerals used for this study were prepared as described in Chapter 3. The purity and concentration of Rubisco were checked before and after the decomposition experiment. The clay mineral, illite, was treated with H_2O_2 to remove organic coatings. The goethite synthesis was done in glass distilled water and after preparation the solid was rinsed repeatedly with glass distilled water and centrifuged 4 times. All minerals were passed through a 64 μm sieve before use.

All of the decomposition experiments were conducted on board ship. The ^{14}C activity recovered as $^{14}CO_2$ and dissolved in pore water was measured by scintillation counting aboard ship and checked by recounting in our Fairbanks laboratory. Phenethylamine used to trap $^{14}CO_2$ produced persistent chemiluminescence in the scintillation cocktail used, so data were not accepted until counts repeated after at least 1 day were the same.

§5.4.1 Decomposition Experiments Using Non-preadsorbed Protein

In a glove bag under N_2, about 10 - 12 mL of SB sediments were transferred from a plastic syringe into a centrifuge tube, which contained 15 μg Rubisco in 2 mL of sea water. The sediment and protein solution were thoroughly mixed for 1 min. The sediments were incubated at 4 °C for 0.5, 24 and 50 h. After centrifugation at 4 °C for 10 min, the pore water was filtered through a 0.4 μm GF/F filter. The $^{14}CO_2$ in pore water was collected by placing 200 μL of phenethylamine on a filter paper wick suspended over 1 mL of

acidified pore water in a scintillation vial. Using a rubber serum vial cap, the vial was sealed immediately after 200 μL of 5 N H_2SO_4 was added into the pore water. After sitting for at least 24 h, the wick was placed in a separate scintillation vial and the activity remaining in the acidified pore water was also measured. To measure $^{14}CO_2$ in the sediments, 10 mL of glass distilled water was added. After thorough mixing, 2 mL of 5 N H_2SO_4 was added. The $^{14}CO_2$ in the sediments was stripped for 15 minutes by bubbling with N_2, and trapped in a mixture of 10 mL of scintillation cocktail and 4 mL of phenethylamine. After rinsing the trap with 1 mL of methanol, ^{14}C in the phenethylamine solution was counted. $^{14}CO_2$ produced by decomposition was calculated by summing the $^{14}CO_2$ measured in pore water multiplied by the total pore water volume and $^{14}CO_2$ stripped from the sediments.

§5.4.2 *Decomposition Experiments Using Pre-adsorbed Protein*

Adsorption of protein to the mineral phases was carried out as described in Chapter 3. Rubisco (22.5 μg) was added to a small glass vial which contained 5.0 mg clay and 2.0 mL of sea water. After 2 h of adsorption at 4 °C, particles and solution were separated by centrifugation at 3,200 rpm. The ^{14}C in the supernatant was counted, and the amount of ^{14}C on the clay mineral was calculated by subtracting the amount of ^{14}C in the supernatant from the total added activity.

Sea water (2 mL) was added to the vial after protein adsorption on clay. After mixing, the mixture was carefully transferred to a plastic centrifuge tube. Ten to 12 mL of SB sediments were added to the tube under N_2. After thoroughly mixing the slurry for 1 minute, the sediments were incubated for 0.5, 24 and 50 h. The measurements of ^{14}C in pore water and sediments were carried out in the same manner as in decomposition experiments without pre-adsorption.

The sediments used to compare the decomposition of weakly adsorbed protein and strongly adsorbed Rubisco had 75 μg of Rubisco added to ensure enough activity in the

supernatant. The supernatant was saved for the following experiment. The incubation times were 0.5, 5.5, 22, 45 and 75 h.

§5.4.3 *Decomposition Experiments Using the Supernatant Solution*

After adsorption of Rubisco to illite, the supernatant solution was transferred to a plastic centrifuge tube. Ten to 12 mL of SB sediment was added under N_2. After thoroughly mixing the slurry for 1 minute, the sediments were incubated for 0.5, 5.5, 22, 45 and 75 h. The subsequent measurements were the same as described previously.

§5.4.4 *Adsorption and Desorption of Rubisco by Skan Bay Sediments*

Two mL of H_2O and 10 - 50 μg of Rubisco solution were added to a small glass vial which contained 100 mg of SB sediment. After thoroughly mixing for 1 min and reacting for 2 h at 4 °C, ^{14}C activity in the supernatant was assayed. The pore water content was measured by drying a known mass of wet sediment at 75 °C for 48 hours, and measuring the dry sediment weight. Adsorption experiments were also conducted with sediments and pore water that had been autoclaved, to eliminate bacterial activity. Desorption of Rubisco from autoclaved SB sediments was determined by replacing a portion of the supernatant with an equal volume of water.

§5.5 Results

Skan Bay sediments from both 6 cm and 12 cm depth contained about 80% pore water. The sediment samples were black, with a strong sulfide odor, and no macrobenthos were found at either depth.

For the Rubisco decomposition experiments, the mean of duplicate measurements is reported, with an average absolute deviation of 0.4% and 1.2% of total added protein for Rubisco and weakly adsorbed protein, respectively. The average relative deviations were about 10% and 9% (Appendix III: Table A-4).

§5.5.1 *Rubisco Adsorption by Skan Bay Sediments*

Rubisco was strongly and rapidly adsorbed by the clay minerals illite, goethite, and montmorillonite (Chapter 3), and by SB sediments (Figure 5-2). Much of the adsorbed Rubisco was not readily desorbed. Some smaller proteins present as impurities in the Rubisco solution were weakly adsorbed by minerals and sediments, and this sorption was readily reversible. The apparent average adsorption partition coefficient for untreated sediments was 208 L/kg, and for autoclaved sediments was 191 L/kg. SDS (2.5%) was used to extract ^{14}C-labeled Rubisco from SB sediments. The recovery was 85% after a one-step extraction carried out at 4 °C for 2 h, which was similar to recoveries from illite and goethite.

§5.5.2 *Rubisco Decomposition in Skan Bay Sediments*

Here, I use [$^{14}CO_2$] to represent the $^{14}CO_2$ concentration, [IW-^{14}C] for ^{14}C activity in interstitial water, Δ[$^{14}CO_2$] for the $^{14}CO_2$ production, Δ[IW-^{14}C] for the ^{14}C activity decrease in interstitial water (IW), Δ_t[$^{14}CO_2$] for the $^{14}CO_2$ production rate, and Δ_t[IW-^{14}C] for the rate of ^{14}C activity decrease in IW. All of the results are listed in Tables 5-1, 5-2, 5-3 and A-4 (Appendix III).

Decomposition of weakly adsorbed proteins in 6 cm sediments Figure 5-3 shows that after 75 h, for pre-adsorbed Rubisco on illite (experiment Ru-Ill-6cm-A), only 6.2% of the total added activity was decomposed to CO_2, but for the weakly bound proteins in supernatant (experiment Ru-Sup-6cm), 27% was respired as $^{14}CO_2$. Initially, 25 times more activity was in the IW of Ru-Sup-6m compared with Ru-Ill-6cm-A. After removal of strongly adsorbed proteins, the supernatant contained smaller proteins that were less adsorbed by sediments. Rubisco adsorption on illite decreased the decomposition rate about 3.3 fold compared with weakly adsorbed proteins after 75 h incubation.

Decomposition of Rubisco in 6 cm sediments Figure 5-4 shows that for non-preadsorbed Rubisco (experiment Non-Ru-6cm), 5.6% of the total added activity was decomposed to CO_2 after 50 h incubation. For Rubisco pre-adsorption on illite (experiment Ru-Ill-6cm-B), 5.4% was decomposed to CO_2, and for Rubisco pre-adsorption on goethite (experiment Ru-Fe-6cm), 1.4 % was decomposed to CO_2. Initially, 2 - 3 times more ^{14}C activity was in the IW of non-preadsorbed Rubisco, compared to Rubisco pre-adsorbed on illite and goethite. Rubisco pre-adsorption on illite and goethite surfaces decreased its decomposition rates about 9% and 2.5 fold, respectively, compared with non-preadsorbed Rubisco.

Decomposition of Rubisco in 12 cm sediments Figure 5-5 shows that for non-preadsorbed Rubisco (experiment Non-Ru-12cm), 11.8% of total added activity was decomposed to CO_2 after 50 h incubation; for Rubisco pre-adsorption on illite (experiment Ru-Ill-12cm), 2.3% was decomposed to CO_2; for Rubisco pre-adsorption on goethite (experiment Ru-Fe-12cm), 6.7% was decomposed to CO_2. Initially, 2 - 4 times more ^{14}C activity was in the IW after addition of non-preadsorbed Rubisco, compared with pre-adsorbed Rubisco on illite and goethite. Rubisco pre-adsorption on illite and goethite surfaces decreased its decomposition rate about 4.1 fold and 66%, respectively, compared to non-preadsorbed Rubisco.

Overall, 6 of 8 decomposition experiments showed greater $^{14}CO_2$ production than ^{14}C activity decrease in IW after 50 -75 h incubation. Rubisco decomposition usually resulted in $\Delta_t[^{14}CO_2]$ greater than $\Delta_t[IW\text{-}^{14}C]$ in deep sediments and in pre-adsorption experiments. Weakly adsorbed proteins and non-preadsorbed Rubisco in shallow sediments tended to have $\Delta_t[^{14}CO_2]$ less than $\Delta_t[IW\text{-}^{14}C]$, especially a few hours after starting the experiments.

§5.6 Discussion

§5.6.1 Rubisco Adsorption and Desorption by Skan Bay Sediments

The isotherm of Rubisco adsorption on SB sediment were linear (Figure 5-2), but much of the adsorbed protein was not readily desorbed. After several dilutions, adsorbed protein concentrations tended to remain at constant values, indicating the presence of components which exhibited irreversible adsorption behavior under the conditions employed. This was similar to the behavior observed for adsorption on clays and goethite, as discussed in Chapter 3 and Chapter 4. The Rubisco solution used in this study contained about 15% weakly adsorbed proteins which were present as impurities (Chapter 3). The very strong adsorption of Rubisco is likely due to binding at multiple sites, so the smaller proteins present in the Rubisco solution as impurities should be desorbed first.

§5.6.2 Rubisco Decomposition in Skan Bay Sediments

Most of the OM enters marine sediments as polymers. These organic materials are degraded into low-molecular-weight substances, e. g., free amino acids (FAA) that can be assimilated by bacteria (Priest, 1984). The fate of the ^{14}C-labeled proteins in sediments is illustrated below:

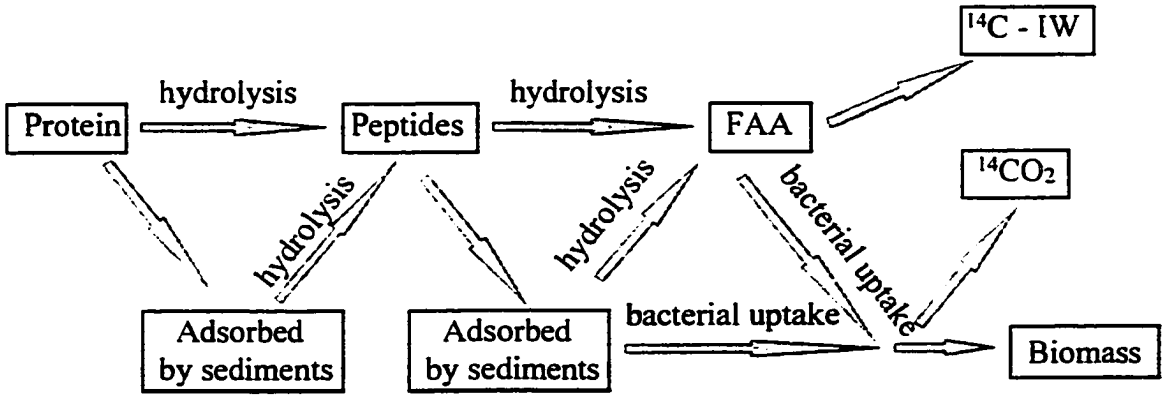

Here, adsorption and bacterial incorporation and respiration are the major sinks of dissolved proteins, and hydrolysis was the major source. Hydrolysis in marine sediments has been considered a rate-limiting step in decomposition (Meyer-Reil, 1991), but quantitative demonstrations of this are lacking. Luo (1994) found that the hydrolysis of peptides in SB sediments was rapid, but it could be a rate-limiting step in the decomposition of small alanyl and glutamyl peptides. The hydrolysis rates were positively related to peptide concentrations. Most of the extracellular enzymes in sediments are bound to solid surfaces, and are more active in hydrolyzing dissolved organic substances than particulate ones (Burns,1978; Ladd, 1978; Meyer-Reil, 1991).

Decomposition of weakly adsorbed proteins in 6 cm sediment In experiment Ru-Sup-6cm, $\Delta[^{14}CO_2] \approx \Delta[IW\text{-}^{14}C]$ after 75 hours' incubation (Table 5-1), indicating that dissolved proteins were selectively consumed by microorganisms. In experiment Ru-III-6cm-A, after removing the more strongly adsorbed Rubisco, $\Delta[^{14}CO_2]$ was about 5.8 times greater than $\Delta[IW\text{-}^{14}C]$, presumably due to decomposition of weakly adsorbed proteins present in the initial supernatant.

Tables 5-2 and 5-3 show that the $\Delta_t[^{14}CO_2]$ and $\Delta_t[IW\text{-}^{14}C]$ were both highest over the first few hours after the decomposition was started, and decreased with time. This reflects the fact that dissolved proteins were quickly decomposed by bacteria. In experiment Ru-Sup-6cm, a very high $\Delta_t[IW\text{-}^{14}C] / \Delta_t[^{14}CO_2]$ ratio (17.3) was found within 5 hours after the decomposition was started, which could be due to a loss of dissolved proteins to biomass during bacterial decomposition or to adsorption of IW ^{14}C by the sediment. The release of ^{14}C as dissolved hydrolysis products may be a rate-limiting process in complete mineralization of OM. From 22 to 45 hours, there was a relatively high $\Delta_t[IW\text{-}^{14}C]$ followed by a relatively high $\Delta_t[^{14}CO_2]$ (from 45 - 75 h), likely reflecting a process by which protein was hydrolyzed, assimilated by bacteria, and then released as CO_2. Over the total incubation time, 75 hours, the $[^{14}CO_2]$ production was about equal to

[IW-^{14}C] removal.

For weakly adsorbed proteins from the supernatant, the turnover time was about 10 days; for more labile adsorbed protein, it was about 45 days; and it was about 140 days for resistant, adsorbed protein. Compared with other "labile" organic substances, like free amino acids or peptides, even weakly adsorbed proteins were decomposed more slowly. For example, the respiration turnover times of amino acids are 1-100 hours in oxic sediments from Resurrection Bay (Doyle, 1988), Alaska, and those of peptides in anoxic sediments from SB are 2-10 days (Luo, 1994).

Decomposition of Rubisco in 6 cm sediments In experiments Ru-III-6cm-B and Ru-Fe-6cm, [$^{14}CO_2$] was ≥ [IW-^{14}C] after 50 hours' incubation (Table 5-1), indicating that dissolved protein was completely decomposed and a small portion of adsorbed protein was also decomposed. However, in non-Ru-6cm, [IW-^{14}C] was 64% greater than [$^{14}CO_2$]. Table A-4 (Appendix III) shows a similar pattern in Ru-Sup-6cm, i. e., after 46 h incubation, [IW-^{14}C] was 58% greater than [$^{14}CO_2$]. If $^{14}CO_2$ resulted mainly from metabolism of protein that was initially dissolved, these results suggest that ~ 1/3 of the assimilated activity is incorporated into microbial biomass. This is consistent with the $^{14}CO_2$ production / ^{14}C removal ratio for free amino acid decomposition in this sediment (Sugai and Henrichs, in prep.). The Δ_t[$^{14}CO_2$] and Δ_t[IW-^{14}C] were greatest from 0.5 to 25 h and decreased with time (Tables 5-2 and 5-3), reflecting a rapid response of bacteria to the available substrate. The results showed the same decomposition pattern. For the more labile proteins, the turnover time was 40 days, and it was 500 days for resistant protein.

Decomposition of Rubisco in 12 cm sediments Geochemically, anaerobic oxidation of fermentation products has been described by the following overall mass balance, which may represent many contributory reactions (Reeburgh, 1980; Coleman *et al.*, 1993).

$$CH_4 + SO_4^{2-} + 2H^+ \rightarrow H_2S + CO_2 + 2H_2O \qquad \text{(Eq. 5-1)}$$

$$4Fe_2O_3 + CH_3COO^- + 7H_2O \rightarrow 8Fe^{2+} + 2HCO_3^- + 15OH^- \quad \text{(Eq. 5-2)}$$

$$Fe_2O_3 + H_2 + H_2O \rightarrow 8Fe^{2+} + 4OH^- \quad \text{(Eq. 5-3)}$$

The reduction of Fe(III) to Fe(II) in natural marine sediments is more complex than is expressed in Eq. 5-3. Microorganisms can effectively couple the oxidation of organic compounds to enzymatic Fe(III) reduction (Lovley, 1987; Lovley and Phillips.1986a and 1986b; Lovley *et al.*, 1991). In the reactions shown, Fe(III) acts as the sole electron acceptor. Lovley *et al.* (1991) found that, in the presence of the appropriate Fe(III)-reducing and fermentative microorganisms, organic matter can be completely oxidized to CO_2. Even for organic compounds that can non-enzymatically reduce Fe(III), extensive microbial Fe(III) reduction was found. Munch and Ottow (1983) indicated that direct contact between bacteria and Fe(III) was required for Fe(III) reduction, suggesting that microorganisms enzymatically catalyze this process.

Complete oxidization of fermentation products to CO_2, with transfer of all of the electrons to Fe(III), is thermodynamically favorable, and hence possible (Lovley, 1987). During organic matter decomposition, Fe(III) is generally reduced before sulfate reduction and methane production. Fe(III) is not toxic to sulfate reducers or methanogens, but Fe(III) reducers may decrease substrate availability for them (Lovley, 1987). This suggests that Fe(III) reducing organisms can outcompete sulfate reducers and methanogens for hydrogen and acetate. Under non-limiting conditions, sulfate and Fe(III) were reduced simultaneously, while in low-H_2 aquatic sediments, Fe(III) may be the preferred electron acceptor (Lovley, 1987).

Table 5-1 shows that [$^{14}CO_2$] / [IW-^{14}C] ratios were 1.9, 1.6 and 11.2 in Non-Ru-12cm, Ru-Ill-12cm and Ru-Fe-12cm, respectively, reflecting rapid and complete decomposition of dissolved protein. Pre-adsorption on illite decreased the Rubisco decomposition rate about 4.6 fold compared to non-pre-adsorbed Rubisco, which illustrates that adsorption did decrease the rate if the solid phase was not reactive. But the

unexpectedly high $^{14}CO_2$ production during decomposition of Rubisco adsorbed on goethite could be due to adsorbed Rubisco oxidation being coupled to Fe(III) reduction. Desorption of Rubisco as the goethite dissolved could also be an important factor.

The turnover time remained constant during decomposition in 12 cm sediments. In contrast to the experiments using 6 cm sediments, all protein was metabolized at the same rate as the "labile" protein in experiments where the adsorber was clay. The increase in turnover time was much less in 12 cm than in 6 cm sediments when the adsorber was iron oxide. This also suggests that release of adsorbed protein was occurring in the 12 cm experiments.

Overall, the usually greater $\Delta[^{14}CO_2]$ than Δ[IW-^{14}C] at both 6 cm and 12 cm, and the fact that [IW-^{14}C] decreased to very low levels, indicated preferential decomposition of small, dissolved proteins, and that this decomposition was complete. Initially greater Δ_t[IW-^{14}C] than $\Delta_t[^{14}CO_2]$ in 6 cm sediments suggested that the labile proteins were quickly incorporated into biomass, or rapidly adsorbed, thus leading to a quick loss of ^{14}C activity from solution. Also, protein hydrolysis could be a rate-limiting process for bacterial incorporation, since after the initial part of the experiments, the [IW-^{14}C] remained low, even though slow $^{14}CO_2$ production continued.

Continuing slow $^{14}CO_2$ production late in the experiments at both 6 and 12 cm depth suggests that a portion of adsorbed Rubisco might be "cut" into smaller, soluble proteins by cell-surface enzymes, incorporated into biomass or released as $^{14}CO_2$. The observation of mostly small proteins in natural sediment (Chapter 7) implies that most protein is rapidly hydrolyzed compared to the time scales of sediment accumulation (a few years in the case of SB). Similarly, gradual hydrolysis and respiration of adsorbed peptides in SB sediments was found, reflecting slow adsorbed peptide decomposition with time (Luo, 1994).

§5.7 Summary and Conclusions

1) Rubisco was strongly and rapidly adsorbed by Skan Bay sediments. The 6 cm and 12 cm sediments showed the same adsorption patterns at the beginning of decomposition experiments.

2) Stronger adsorption of Rubisco on particle surfaces decreased its decomposition rate. These observations support the hypothesis that adsorption facilitates protein preservation in marine sediment.

3) Dissolved proteins were preferentially consumed by microorganisms. Weakly adsorbed proteins were decomposed much faster than strongly adsorbed proteins.

4) The $^{14}CO_2$ production tended to be greater than, but similar in magnitude to, the decrease of ^{14}C activity in IW, reflecting a rapid and complete decomposition of dissolved protein and slower, incomplete decomposition of adsorbed protein.

5) An unexpectedly large [$^{14}CO_2$] / [IW-^{14}C] ratio in the decomposition of Rubisco pre-adsorbed on goethite in 12 cm sediments was probably due to reductive dissolution of the solid phase, releasing adsorbed protein, or stimulation of microbial activity by the added iron oxide. Protein adsorbed to iron oxides and preserved in surface sediments could be decomposed in deeper, reducing sediments.

6) In 6 cm sediments, the turnover time was about 10 days for weakly adsorbed proteins, 45 days for the more labile adsorbed protein, and 500 days for refractory adsorbed proteins. The slowly-decomposing fraction of protein had a turnover time similar to that of natural sediment organic matter decomposing at this depth.

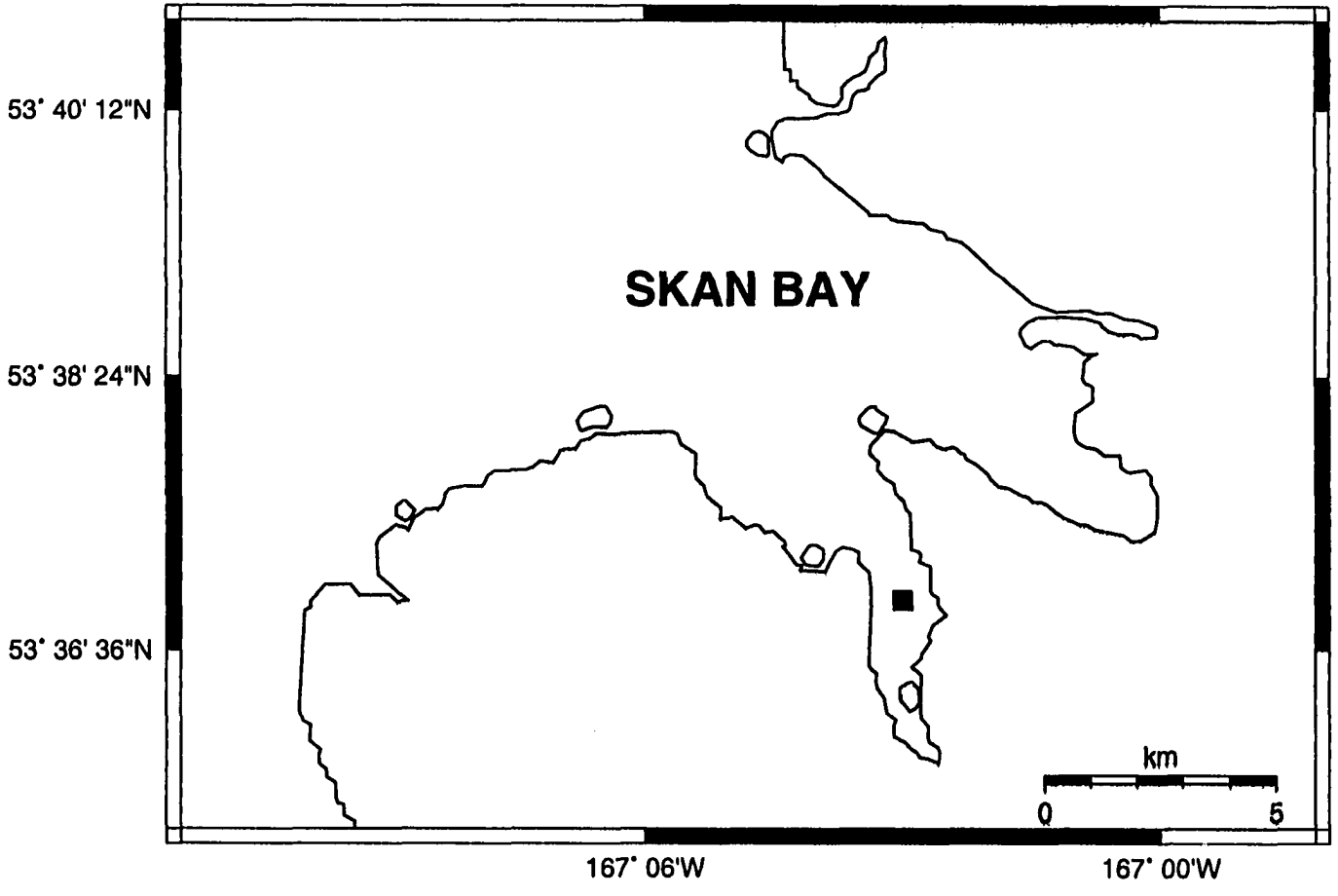

Figure 5-1. Map of Skan Bay.

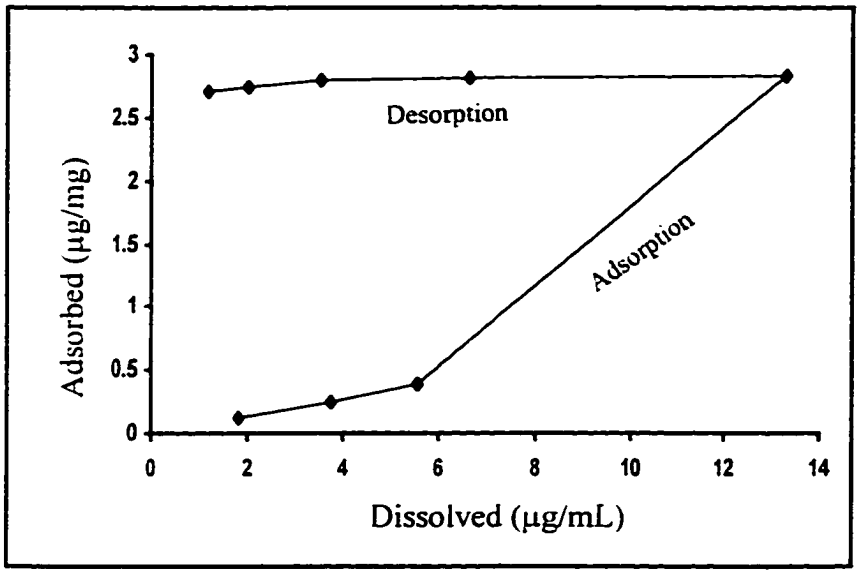

Figure 5-2. Rubisco adsorption on and desorption from Skan Bay sediments.

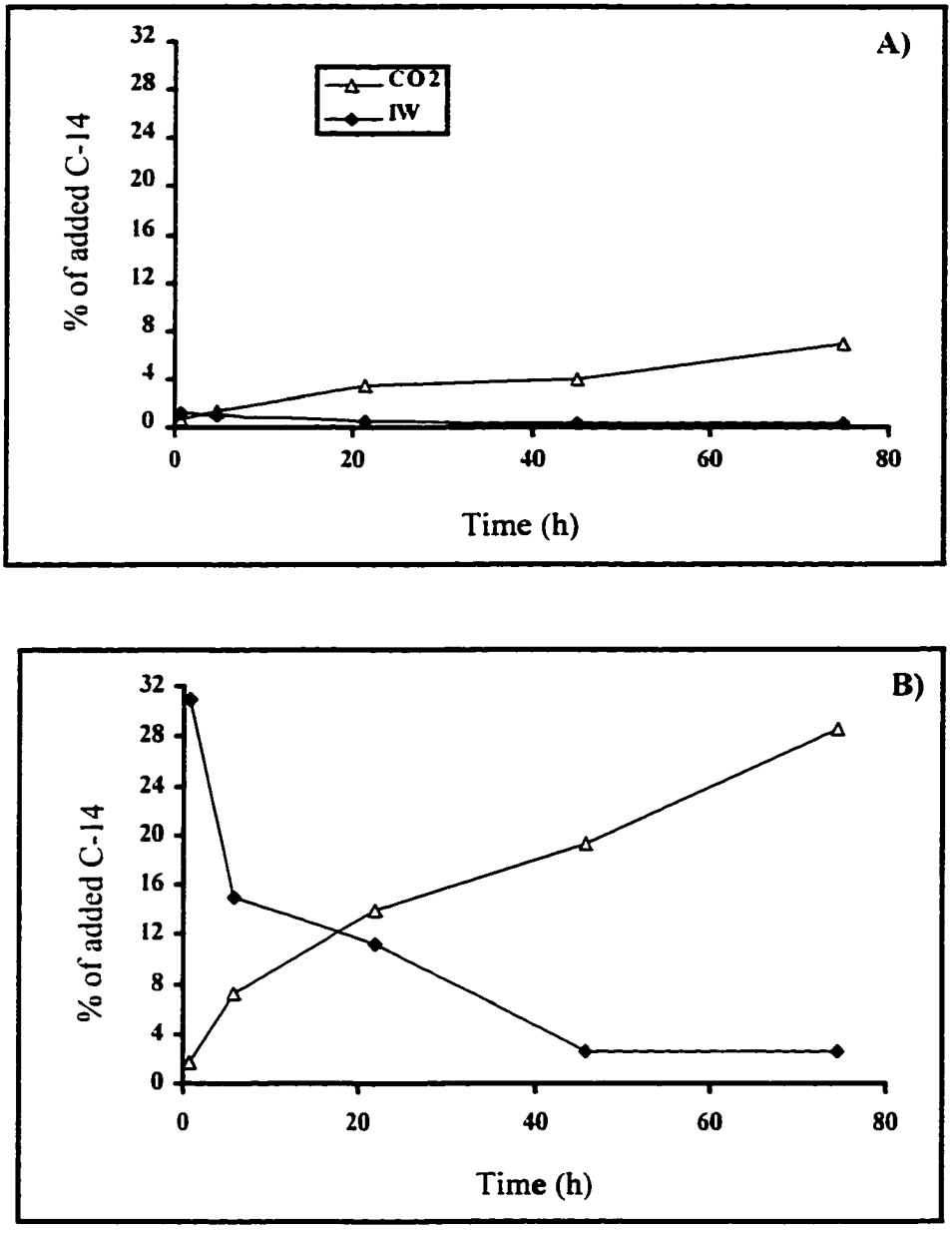

Figure 5-3. Decomposition of A) pre-adsorbed Rubisco on illite and B) supernatant of Rubisco ("weakly adsorbed proteins") after adsorption in Skan Bay sediments from 6 cm depth.

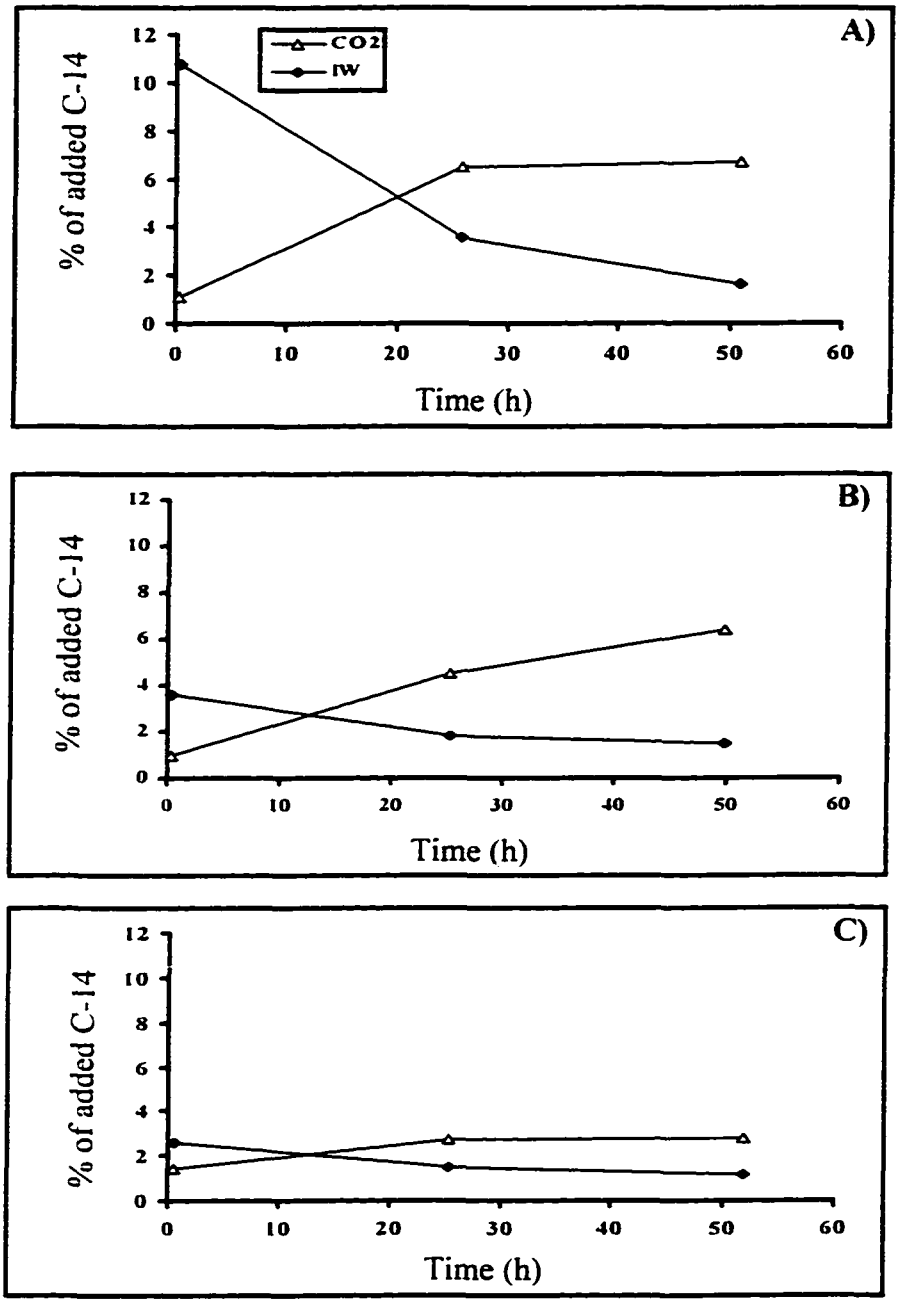

Figure 5-4. Decomposition of A) non-preadsorbed Rubisco; B) pre-adsorbed Rubisco on illite and C) pre-adsorbed Rubisco on goethite in Skan Bay sediments from 6 cm depth.

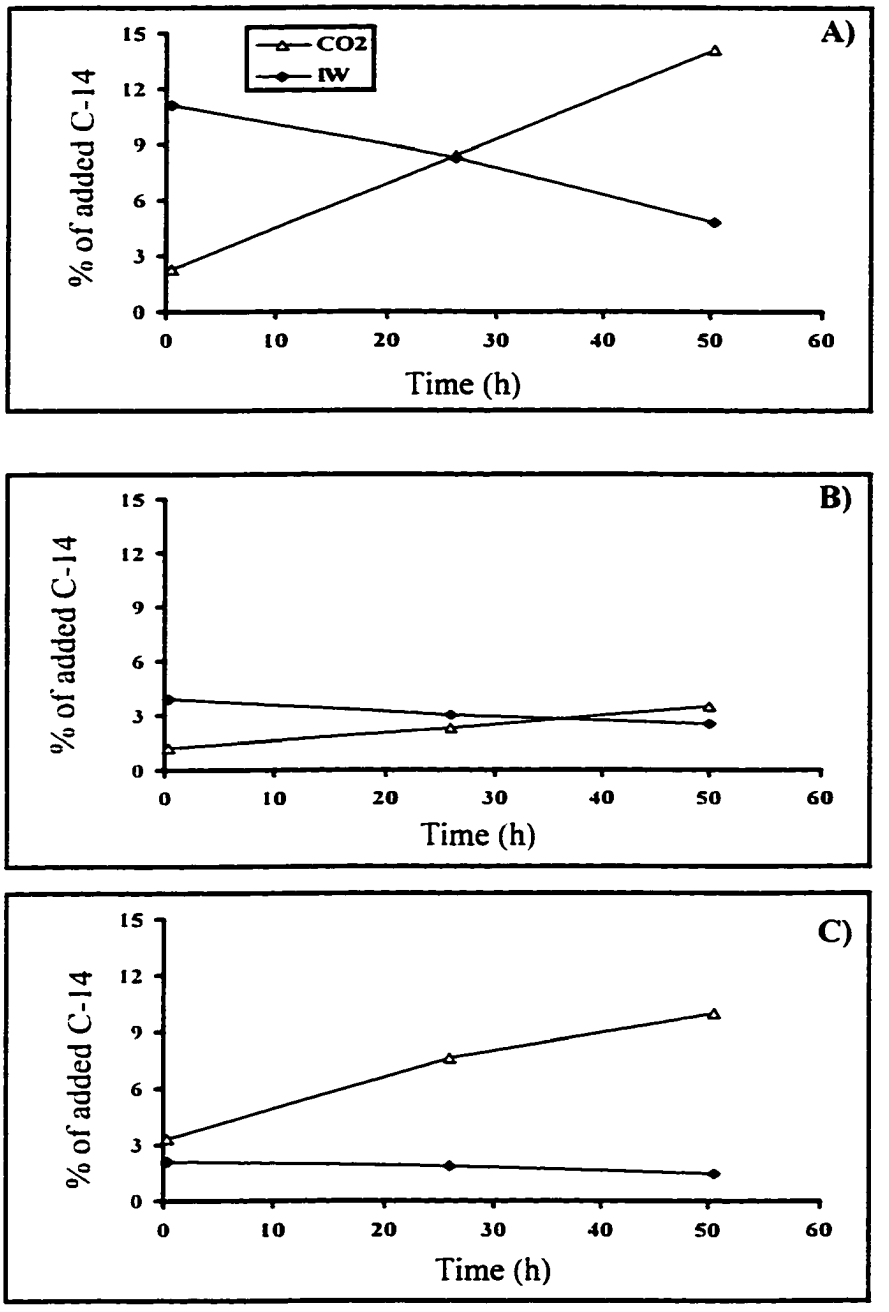

Figure 5-5. Decomposition of A) non-preadsorbed Rubisco; B) pre-adsorbed Rubisco on illite and C) pre-adsorbed Rubisco on goethite in Skan Bay sediments from 12 cm depth.

Table 5-1. Comparison of $^{14}CO_2$ production and decrease of dissolved ^{14}C activity in interstitial water during Rubisco decomposition.

Experiment*	Incubation time (h)	^{14}C activity decrease in IW (%)	$^{14}CO_2$ increase (%)
Ru-Ill-6cm-A	75	0.9	6.2
Ru-Sup-6cm	75	28.5	26.7
Non-Ru-6cm	50	9.2	5.6
Ru-Ill-6m-B	50	2.1	5.4
Ru-Fe-6cm	50	1.4	1.4
Non-Ru-12cm	50	6.3	11.8
Ru-Ill-12cm	50	1.4	2.3
Ru-Fe-12cm	50	0.6	6.7

*: abbreviations: Non: no preadsorption; Ru: Rubisco; Fe: pre-adsorption on goethite; Ill: pre-adsorption on illite; Sup: weakly adsorbed proteins from the supernatant after Rubisco adsorption.

Table 5-2. $^{14}CO_2$ production rate and dissolved ^{14}C decrease rate in interstitial water during Rubisco decomposition in Skan Bay sediments.

Experiment*	incubation time (h)	$^{14}CO_2$ production rate (% of added/h)		^{14}C decrease rate (% of added/h)	Turnover time (d)
Ru-Ill-6cm-A	1 - 5	0.18	>	0.05	23
	5 - 22	0.12	>	0.03	35
	22 - 45	0.03	>	0.01	140
	45 - 75	0.10	»	0.00	42
Ru-Sup-6cm	1 - 5	1.13	<	3.30	4
	5 - 22	0.41	>	0.23	10
	22 - 45	0.22	<	0.36	20
	45 - 75	0.32	»	0.00	15
Non-Ru-6cm	0.5 - 25	0.21	<	0.28	20
	25 - 50	0.01	<	0.08	420
Ru-Ill-6cm-B	0.5 - 25	0.14	>	0.07	30
	25 - 50	0.07	>	0.01	60
Ru-Fe-6cm	0.5 - 25	0.05	>	0.04	85
	25 - 50	0.00	<	0.01	1100
Non-Ru-12cm	0.5 - 26	0.24	>	0.11	20
	26 - 50	0.24	>	0.14	20
Ru-Ill-12cm	0.5 - 26	0.04	≈	0.04	105
	26 - 50	0.05	>	0.02	85
Ru-Fe-12cm	0.5 -26	0.17	»	0.01	25
	26 - 50	0.10	<	0.02	40

Table 5-3. Rate of dissolved, organic ^{14}C activity decrease in the interstitial water during Rubisco decomposition in Skan Bay sediments.

Experiment	incubation time (h)	^{14}C activity decrease rate (% of added/h)
Ru-Ill-6cm-A	1 - 5	0.05
	5 - 22	0.03
	22 - 45	0.01
	45 - 75	<0.01
Ru-Sup-6cm*	1 - 5	3.30
	5 - 22	0.23
	22 - 45	0.36
	45 - 75	<0.01
Non-Ru-6cm	0.5 - 25	0.28
	25 - 50	0.08
Ru-Ill-6cm-B	0.5 - 25	0.07
	25 - 50	0.01
Ru-Fe-6cm	0.5 - 25	0.04
	25 - 50	0.01
Non-Ru-12cm	0.5 - 26	0.11
	26 - 50	0.14
Ru-Ill-12cm	0.5 - 26	0.04
	26 - 50	0.02
Ru-Fe-12cm	0.5 -26	0.01
	26 - 50	0.02

*: weakly adsorbed proteins

Chapter 6

Protein Decomposition in Oxic and Suboxic Sediments

Abstract

The decomposition rate of three proteins, Rubisco, GroEL and GroES, was studied in sediments from Resurrection Bay, Alaska in order to examine the effects of adsorption to sediment particles. The proteins were strongly adsorbed by clay minerals and Resurrection Bay sediments. The influence of pre-adsorption of proteins on clay minerals, before addition to natural sediments, was investigated by comparing with the decomposition of proteins that were not adsorbed to a solid phase before addition. Adsorption on clay minerals decreased the protein decomposition rate by up to 60% after 50 h incubation. However, the rapid adsorption of the proteins on the natural sediments also apparently slowed their decomposition.

The proteins present in the supernatant after Rubisco and GroEL adsorption to clay or iron oxide were mostly small proteins, with fairly small adsorption partition coefficients of 10 - 100 L/kg. Decomposition of these proteins was compared to that of Rubisco and GroEL, which have partition coefficients of 10^4 - 10^6 L/kg. In surface sediments, the apparent protein decomposition rates were in the order of: weakly adsorbed proteins » Rubisco or GroEL added without pre-adsorption > pre-adsorbed Rubisco or GroEL on illite > pre-adsorbed Rubisco or GroEL on montmorillonite > pre-adsorbed Rubisco or GroEL on goethite. This indicates that stronger adsorption on minerals leads to slower decomposition of proteins. The trend of the decomposition rates was GroES > Rubisco > GroEL, so larger proteins were decomposed more slowly, again parallel to their adsorption behavior.

All of the studied proteins were relatively resistant to bacterial decomposition, e.g., only 10% of the Rubisco decomposed in 6 weeks. There was no difference in labile, weakly adsorbed protein decomposition in surface and 6 cm sediments. However, the decomposition rates of strongly-adsorbed proteins were 3 - 4 times greater in surface sediments than in 6 cm sediments. The turnover times were about 15 - 60 d for labile, weakly adsorbed proteins and 250 - 1000 d for strongly-adsorbed refractory proteins.

§ 6.1 Introduction

The factors controlling the decomposition of detrital organic matter (OM) in marine sediments are incompletely understood. One hypothesis is that adsorption of organic substances to sediment mineral phases may protect OM from decomposition by microorganisms, and thus lead to its preservation (Mayer, 1994a and b). There have been several previous studies of adsorption and decomposition of organic matter in marine sediments (e. g., Sugai and Henrichs, 1992; Wang, 1993; Luo, 1994). Generally, these studies have found that adsorption slows decomposition of small, labile molecules. Adsorption and decomposition of glucose, amino acids and peptides in sediments of Resurrection Bay, Alaska have been studied by Doyle (1988), McDaniel (1989), Sugai and Henrichs (1992), Henrichs and Sugai (1993), and Luo (1994). Both adsorption and bacterial uptake were major processes removing free amino acids from the dissolved pool. Adsorption of amino acids and peptides was found to be a rapid process and partly irreversible. Adsorbed amino acids and peptides decomposed more slowly than the dissolved substances.

Proteins are the most abundant biochemicals in living cells. Although proteins account for a considerable amount of the biomass on the Earth, understanding of their specific roles in the biogeochemical cycles of C and N is quite limited. Proteins can be divided into two different categories according to their water solubility: globular, hydrophilic proteins (e. g., enzymes, antibodies, nutrient storage proteins), and fibrous, or hydrophobic, proteins (e. g., most of the structural and protective proteins). Most proteins present in nature are very easily hydrolyzed to amino acids by proteolytic exoenzymes and peptidases (de Leeuw and Largeau, 1993).

Both theoretical considerations (Henrichs, 1995) and experimental evidence (Kirchman *et al.*, 1989; Chapter 3 of this thesis) indicate that macro-molecules such as proteins are strongly adsorbed by surfaces. Because they are abundant in nature and likely to exhibit strong adsorption to sediment particles, I chose to use several proteins to test the

hypothesis that adsorption can protect organic molecules from decomposition.

In this study, three ^{14}C-labeled hydrophilic proteins, Rubisco from *C. reinhardtii*, and GroEL and GroES from genetically modified *E. coli*, were prepared. Their molecular weights are 550, 800 and 70 kDa, respectively, and their partition coefficients for adsorption on clay minerals are much greater than those of amino acids and peptides (Chapter 3; Henrichs and Sugai, 1993; Luo, 1994). The purposes of this study were:

1) To investigate the adsorption behavior of three proteins on oxic and suboxic, glacially-derived sediment and to determine the influence of protein size on adsorption.

2) To determine the decomposition rates of the proteins in the sediments.

3) To compare the decomposition rates of proteins pre-adsorbed on clay minerals to those added to sediments in dissolved form, and thus examine the role of adsorption in controlling rates of OM decomposition.

4) To compare the decomposition rates of weakly and strongly adsorbed proteins.

§ 6.2 Study Site

The sampling site was Thumb Cove (60°0.4' N, 149° 18.3' W), a small embayment of Resurrection Bay (RB), Alaska, surrounded on 3 sides by steep mountains (Figure 6-1). The sediments are largely detrital silt, light grey or brownish-gray in color at the surface. The sediments contain 2 - 3 % of clay, which is an iron-rich chlorite (Doyle, 1988). The sediments contain 0.7 % organic carbon, and the C/N ratio is 8 - 10. The bottom water is oxic year-round.

§ 6.3 Materials and Methods

Three ^{14}C-labeled proteins, Rubisco, GroEL and GroES, were prepared as described in Chapter 3, and their purity and the concentrations of prepared solutions were checked

before and after they were used in decomposition experiments. Rubisco and GroEL were adsorbed by clay minerals in their original forms, with adsorption partition coefficients of about 10^4 - 10^6 L/kg (Chapters 3 and 4). The weakly adsorbed proteins, which remained in the supernatant solution after adsorbing Rubisco and GroEL to clay minerals and removing the particles by centrifugation, were mostly small molecules that were present in the protein solutions as impurities. The adsorption partition coefficients of the weakly adsorbed proteins were about 10 - 100 L/kg.

Two clay minerals and an iron oxide were used as solid phases for adsorbing proteins prior to their addition to natural sediments. The clay minerals, illite and montmorillonite, were treated with H_2O_2 to remove pre-existing organic coatings. Goethite was synthesized with special precautions to minimize organic content (see Chapter 5) and used without H_2O_2 treatment. All minerals were passed through a 64 μm sieve before use.

After collection with a box corer in April 1998, and removal of the overlying water, the sediments were horizontally subsampled at depths of 0 cm and 6 cm, using 10 or 12 mL plastic syringes with cut-off tips. After filling, the plastic syringes were sealed with rubber stoppers. Sediment samples for adsorption measurements were obtained from box cores by manually scooping sediments into mason jars. All samples for decomposition and adsorption experiments were stored in an incubator (4 °C) until used. Decomposition experiments were conducted within one day after sample collection. Adsorption experiments were conducted within 2 months.

§ 6.4 Experimental Procedures

§6.4.1 Adsorption and Desorption of Proteins on Resurrection Bay Sediments

Fifty mg of RB sediment, 2 mL of H_2O and 10 - 50 μg of Rubisco solution were added to a pre-weighed empty vial. After thoroughly mixing for 1 min and reacting for 2 h at 4 °C, ^{14}C activity in the supernatant was assayed. The pore water content was measured by drying a pre-weighed quantity of wet sediments at 75 °C for 48 hours, subtracting the

dry weight from the original weight, and correcting for pore water salt content.

Adsorption experiments were also conducted in the same way with sediments and pore water that had been autoclaved to eliminate bacterial activity. Two mL of water were added to 50 mg wet sediment in a small glass vial and autoclaved for 30 min. The water lost during autoclaving was measured, and then this amount of sterile water was added so that the water content would be the same as in the original sediments. Desorption of Rubisco from autoclaved RB sediments was determined by replacing a portion of the supernatant with an equal volume of water.

Two mL of an extraction solution, which contained 5% sodium dodecyl sulfate (SDS), 5% 2-mercaptoethanol, 0.1 M Tris buffer (pH 7.5) and 1 mM dithiothreitol were added to the sediments after removal of the supernatant. The sediment and extraction solution were thoroughly mixed, and then heated in boiling water for 20 min, and centrifuged at 3,200 rpm for 5 min. The ^{14}C activity in solution was counted and compared with the total adsorbed ^{14}C-labeled Rubisco to determine the extraction efficiency.

§6.4.2 *Decomposition Experiments Using Non-preadsorbed Protein*

About 10 - 12 mL of RB sediments were transferred under nitrogen from a plastic syringe into a centrifuge tube which contained about 75 μg Rubisco or GroEL, or 50 μg GroES, in 2 mL of sea water solution. The sediment and protein solution were thoroughly mixed for 1 min. The sediments were incubated at 4 °C for about 0.5, 12, 25 and 50 h. After centrifugation at 4 °C for 10 min, the pore water was filtered through a 0.4 μm GF/F filter. The $^{14}CO_2$ in pore water was collected by placing 200 μL of phenethylamine on a filter paper wick suspended over 1 mL of acidified pore water in a scintillation vial. Using a rubber serum vial cap, the vial was sealed immediately after adding 200 μL of 5 N H_2SO_4 to the pore water. After sitting for at least 24 h, the wick was placed in a separate scintillation vial and the activity remaining in the acidified pore water was also measured. To measure $^{14}CO_2$ in the sediments, 10 mL of glass distilled water was added. After thorough mixing, 2 mL of 5 N H_2SO_4 was added. The $^{14}CO_2$ in the sediments was stripped

for 15 min by bubbling with N_2, and trapped in a mixture of 10 mL of scintillation cocktail and 4 mL of phenethylamine. After rinsing the trap with 1 mL of methanol, ^{14}C in the phenethylamine solution was counted. $^{14}CO_2$ produced by decomposition of the protein was calculated by summing the $^{14}CO_2$ in the entire volume of pore water and the stripped sediments.

For all of the protein decomposition experiments, the mean of duplicate incubations is reported. These values had average absolute differences of about 0.1%, 0.1%, 0.4% and 0.9% of total added protein for Rubisco, GroEL, GroES and supernatant decomposition respectively, and the average differences relative to the mean values were about 7%, 9%, 12% and 10% (Appendix III: Table A-5).

§6.4.3 *Decomposition Experiments Using Pre-adsorbed Protein*

Adsorption of protein to the mineral phases was carried out as described in Chapter 3, except that the clays were rinsed with sea water to remove weakly adsorbed proteins before addition to sediments. 75 μg of Rubisco or GroEL, or 50 μg of GroES, were added to a small glass vial which contained 5.0 mg clay and 2.0 mL of H_2O. Protein solutions and clays were allowed to react for 2 h at 4 °C in the dark and then separated by centrifugation at 3,200 rpm. The ^{14}C in the supernatant was counted and the clay rinsed with 2 mL of seawater. After thoroughly mixing for 1 min, the slurry was centrifuged at 3,200 rpm and ^{14}C in the rinse supernatant was counted. The ^{14}C activity in the supernatant solution from the adsorption and rinse steps was summed, and the amount of ^{14}C on the clay was determined by subtracting the amount of ^{14}C in the supernatant from the total added activity.

Two mL of sea water were added to the vial after the protein adsorption on clay. After mixing, the mixture was carefully transferred to a plastic centrifuge tube. Ten to 12 mL of RB sediments were added to the tube under N_2. After thoroughly mixing the slurry for 1 min, the sediments were incubated for 0.5, 12, 24 and 50 h. The measurements of ^{14}C in pore water and sediments were the same as in decomposition experiments without pre-

adsorption.

§6.4.4 *Decomposition of Proteins from the Supernatant*

Seventy-five μg of Rubisco or GroEL were added to a small vial which contained 5.0 mg illite and 2.0 mL sea water. The adsorption procedure was the same as that described in the pre-adsorption experiment. The supernatant after Rubisco or GroEL adsorption on clay was transferred to a plastic centrifuge tube with 10 - 12 mL of sediment. After the sediment and solution were thoroughly mixed for 1 min, the sediments were incubated for 0.5, 13, 24, 80, 172 and 1050 h for Rubisco, or 0.5, 24 and 55 h for GroEL. The ^{14}C activity was measured as described previously.

§ 6.5 Results

The sediments from 6 cm depth and the surface both contained about 40% water. The sediments were brownish at the surface and grayish below 1 - 2 cm depth. The sediments had no sulfide odor, and macrobenthos were found at both depths.

Here, I use [$^{14}CO_2$] to represent the $^{14}CO_2$ concentration, [IW-^{14}C] for ^{14}C activity in interstitial water (IW) after $^{14}CO_2$ was removed, Δ[$^{14}CO_2$] for the $^{14}CO_2$ production, Δ[IW-^{14}C] for the ^{14}C activity decrease in IW, Δ_t[$^{14}CO_2$] for the $^{14}CO_2$ production rate, and Δ_t[IW-^{14}C] for the rate of ^{14}C activity decrease in IW. All of the decomposition results are listed in Tables 6-1, 6-2, and A-5 (Appendix III).

§ *6.5.1 Adsorption of Proteins by Resurrection Bay Sediments*

Rubisco was strongly adsorbed by RB sediments (Figure 6-2). For 0 - 3 cm sediments, the average adsorption partition coefficients for both untreated and autoclaved sediments were 75 L/kg. For 6 - 9 cm sediments, the partition coefficient was 72 L/kg for autoclaved sediments and 75 L/kg for untreated sediments. Much of the adsorbed Rubisco was not readily desorbed. Some smaller proteins present as impurities in the Rubisco solution were weakly adsorbed by minerals and sediments, and this sorption was readily

reversible. 5% SDS was used to extract ^{14}C-labeled Rubisco from RB sediments. After a one-step extraction at 95 °C for 30 min, the recovery was 80 - 85 % for autoclaved RB sediments from 0 - 3 and 6 - 9 cm depths, and 90% for untreated sediments.

§6.5.2 *Decomposition of Proteins*

Decomposition of Rubisco in 6 cm sediments When Rubisco was added directly to sediments (Figure 6-3A), 3.9% of total added activity initially was in IW, and 1.6% of the Rubisco was decomposed after 47 h incubation. Pre-adsorbing Rubisco on goethite (Figure 6-3B), resulted in 50% less activity being in IW initially, and reduced respiration to $^{14}CO_2$ by 31% after 47 h incubation, when compared to Rubisco decomposition without pre-adsorption (Figure 6-3A). The added activity initially present in pore water solution was reduced by 69% when Rubisco was pre-adsorbed onto illite (Figure 6-3C), and by 90% when pre-adsorbed on montmorillonite (Figure 6-3D), compared with the experiment without pre-adsorption. Although pre-adsorption significantly decreased the percentage of added activity initially present in the interstitial water, the effect on respiration over the course of the experiment was modest.

Decomposition of Rubisco in surface sediments When Rubisco was added directly to surface sediments (Figure 6-4A), 3.7% of total added activity was in IW initially, and 2.0% was respired as $^{14}CO_2$ after 45 h. When Rubisco was pre-adsorbed on goethite (Figure 6-4B), the percentage of activity initially found in IW was reduced by 76% over that in the experiment without pre-adsorption. Pre-adsorption on illite (Figure 6-4C) and montmorillonite (Figure 6-4D), reduced initial dissolved activity by 70% and 57%, respectively. Respiration to $^{14}CO_2$ after 48 h was decreased 45% by pre-adsorption on goethite, and by 25-30% by pre-adsorption on the clay minerals.

Six-week decomposition experiment in 6 cm sediments When Rubisco was added to RB sediments from 6 cm depth without pre-adsorption (Figure 6-5A), 4.0% of total added activity initially was in IW, and 10% was decomposed after 1050 h incubation. Although

pre-adsorption of Rubisco on illite (Figure 6-5B) resulted in a third less activity being present in IW compared to the experiment with Rubisco added directly to sediment, the activity recovered as $^{14}CO_2$ after 1050 h was not significantly different (10.2 ± 1.2% vs. 9.6 ± 0.1%). For the weakly adsorbed proteins in the supernatant from Rubisco adsorption (Figure 6-5C), the percent of total added activity in IW initially was 17 times greater than the non pre-adsorbed Rubisco experiment, and 6 times more was decomposed to CO_2 after 1050 h incubation.

Since the supernatant and adsorbed Rubisco were separated to do the experiments Ru-Ill-6cm-Long and Ru-Sup-6cm-Long, the combination of Ru-Ill-6cm-Long and Ru-Sup-6cm-Long should be the same as Non-Ru-6cm-Long. Actually, the $\Delta[^{14}CO_2]$ in the combination averaged 1.3 times that in the Non-Ru-6cm-Long experiment. So the results were quite similar, as expected.

Residual Rubisco and other ^{14}C-labeled substances remaining after 1050 h incubation were extracted using 6N HCl at 100°C. The recovery (including dissolved and adsorbed ^{14}C, and $^{14}CO_2$) for non pre-adsorbed Rubisco was 72 ± 2%; for pre-adsorbed on illite, it was 82 ± 1%; and for the weakly adsorbed in the protein supernatant, it was 113 ± 6%.

Decomposition of GroEL in 6 cm sediments As shown in Figure 6-6A, 2.9% of total added GroEL activity was initially in IW when added directly to 6 cm sediments. When GroEL was pre-adsorbed on goethite (Figure 6-6B) and illite (Figure 6-6C), 38% and 45% less of total added activity was in IW initially. When GroEL was pre-adsorbed on montmorillonite (Figure 6-6D), the dissolved activity initially present in the IW was enhanced by 45%, over that present when GroEL was added without pre-adsorption. Pre-adsorption of GroEL on both illite (Figure 6-6C) and montmorillonite (Figure 6-6D) depressed CO_2 respiration over 50 h more completely than pre-adsorption on goethite (Figure 6-6B), although very little decomposition was observed over this period for GroEL added directly to sediments (Figure 6-6A).

Decomposition of GroEL in surface sediments Contrary to the results of the other experiments, in surface sediments a larger percentage of the GroEL activity was found in the IW initially when the protein was pre-adsorbed to solid phases than when the protein was added directly. This enhancement in dissolved activity was greatest for GroEL pre-adsorbed to illite and montmorillonite (Figure 6-7C and D), for which 1.7 to 2 times as much dissolved activity was present. In spite of the greater initial dissolved GroEL activity, the percent of added activity that was respired to $^{14}CO_2$ after 49 h was only slightly greater for the proteins pre-adsorbed on the clay minerals than for untreated proteins. GroEL pre-adsorbed on goethite was respired less than GroEL that was not pre-adsorbed.

Decomposition of weakly adsorbed proteins from GroEL solution in 6 cm sediments For GroEL added directly to 6 cm sediments, 2.0% of total added activity initially was in IW (Figure 6-8A), and 1.4% was decomposed after 55 h incubation. When GroEL was pre-adsorbed on illite (Figure 6-8B), 80% less activity was in IW initially, and 43% less was decomposed to $^{14}CO_2$ after 55 h incubation. For small proteins from the supernatant after GroEL adsorption on illite (Figure 6-8C), 4.9 times more of total added activity was in IW initially, and 70% more was decomposed to $^{14}CO_2$ after 56 h.

Decomposition of GroES in 6 cm sediments For non pre-adsorbed GroES (Figure 6-9A), 4.1% of total added activity was in IW initially, and 3.1% was decomposed after 51 h. Pre-adsorption on goethite (Figure 6-9B) had the largest effect on the amount of added activity initially present in IW, with 68% more dissolved activity than that in untreated sediments. When GroES was pre-adsorbed on illite (Figure 6-9C) and montmorillonite (Figure 6-9D), about 20% less dissolved activity was found initially compared to untreated sediments. After 50 h, respiration was depressed by roughly a third in sediments where GroES was pre-adsorbed on illite, when compared with the other 3 conditions.

§ 6.6 Discussion

§6.6.1 Adsorption and Desorption of Rubisco

There was < 10% difference between autoclaved and untreated sediments from both 0 - 3 and 6 - 9 cm in depth and the partition coefficients are comparable to the apparent partition coefficients measured on clay minerals (Chapter 3). The strong adsorption of proteins by autoclaved sediments demonstrates that it is a non-biological process. The isotherm of Rubisco adsorption on RB sediment were linear (Figure 6-2), but much of the adsorbed protein was not readily desorbed. After several dilutions, adsorbed protein concentrations tended to remain at constant values, indicating the presence of components which exhibited irreversible adsorption behavior under the conditions employed. This was similar to the behavior observed for adsorption on clays and goethite, as discussed in Chapter 3 and Chapter 4. The Rubisco solution used in this study contained about 15% weakly adsorbed proteins which were present as impurities (Chapter 3). The very strong adsorption of Rubisco is likely due to binding at multiple sites, so the smaller proteins present in the Rubisco solution as impurities should be desorbed first.

§6.6.2 Decomposition of Proteins

The pool of sedimentary organic carbon is comprised of living biomass, labile (mostly dissolved) and refractory (I hypothesize, mostly adsorbed) organic molecules. Biomass and labile carbon account for only a few percent of the total carbon pool (literature cited in Neudörfer and Meyer-Reil, 1997), but are involved in most of the turnover of carbon. Neudörfer and Meyer-Reil (1997) concluded that available dissolved organic matter (ADOC) is the most important carbon and energy source for microorganism growth. Their study of glucose and acetate showed that < 0.1% of total organic carbon was immediately available for microbial metabolism, and the average turnover time of ADOC in surface sediments (< 1 mm) was about 50 min. As discussed in more detail below, my results were generally consistent with the idea that dissolved OM is more available to

microbial decomposers than adsorbed OM.

Decomposition of Rubisco in 6 cm sediments Pre-adsorption of Rubisco on 2 clay minerals and an Fe oxide slightly slowed its decomposition, by about 10 - 30% after 48 h incubation. However, rapid adsorption of Rubisco by RB sediments also apparently prevented protein biodegradation, and thus there was not a large effect of pre-adsorption.

For most experiments, the percent of added Rubisco activity respired as $^{14}CO_2$ was virtually identical to the loss of dissolved ^{14}C activity from the IW (Table 6-1). This suggests that dissolved proteins were readily mineralized, although little of the adsorbed protein was decomposed during the time frames of my experiments. Both $^{14}CO_2$ respiration rates and loss of ^{14}C from IW were greatest during the first 11 h, and after 27 to 47 h ^{14}C uptake and mineralization rates were minimal. Over the first 25 h, the most labile proteins were decomposed rapidly, with a turnover time of about 60 d. (The turnover time reported here was calculated as the time required to decompose all of the remaining proteins to $^{14}CO_2$). After about 25 h incubation, most of those remaining were resistant to decomposition, with an apparent turnover time of about 800 d.

Decomposition of Rubisco in surface sediments Table 6-1 shows that the $\Delta[^{14}CO_2]$ was $\leq$ 2 times the corresponding $\Delta[IW\text{-}^{14}C]$, for most of the experiments, indicating that dissolved protein was decomposed readily and completely, and adsorbed protein was decomposed to only a small extent. This result is similar to that for 6 cm sediments. Table 6-2 shows that the greatest $\Delta_t[^{14}CO_2]$ and $\Delta_t[IW\text{-}^{14}C]$ were during the first 11 h, as for sediments from 6 cm depth.

A difference between surface and 6 cm sediments was that pre-adsorption slowed decomposition slightly more in surface sediments. Another difference was that, after 25 h incubation, the turnover time of the resistant, adsorbed Rubisco in surface sediment was about 1/3 - 1/2 of that in 6 cm sediment. This difference is probably related to greater bacterial populations in surface sediments. Henrichs and Doyle (1986) found that the number of bacteria was about 3×10^9 cells/mL in RB surface sediments, and 1×10^9

cells/mL in 6 cm sediments.

Six-week decomposition experiment in 6 cm sediments When decomposition experiments for Rubisco in 6 cm sediments were continued for 6 wk, the amount of $^{14}CO_2$ respired was 4 and 5 times greater than the corresponding loss of dissolved ^{14}C in experiments, either with or without pre-adsorption on illite (Table 6-1). As was the case in shorter incubations, dissolved Rubisco was decomposed rapidly and completely, but the greater $^{14}CO_2$ production than loss of dissolved activity shows that some of the adsorbed Rubisco was also decomposing over this longer incubation time. The Δ[IW-^{14}C] was about the same as $\Delta[^{14}CO_2]$ for the weakly-adsorbed proteins (Ru-Sup-6cm-Long). The percent of added activity respired as $^{14}CO_2$ for the weakly-adsorbed proteins was much greater than that for Rubisco added directly to 6 cm sediment (Non-Ru-6cm-Long) and or Rubisco pre-adsorbed to illite (Ru-Ill-6cm-Long). Another unusual feature of the weakly adsorbed proteins (Figure 6-5B) was that $\Delta[^{14}CO_2] \ll \Delta$[IW-$^{14}C$] during the first 13 h. This indicates that either some of the proteins were lost by adsorption to sediment or that they were rapidly incorporated into bacterial biomass.

During the long incubation, all experiments generally showed a similar pattern during the initial 24 h of incubation (Table 6-2). As for the shorter experiments, respiration of $^{14}CO_2$ increased with time with the largest $\Delta_t[^{14}CO_2]$during the first 13 h; dissolved ^{14}C activity in the IW decreased rapidly in the first 13 h, due to rapid adsorption, with a more gradual microbial mineralization of adsorbed proteins. After 80 h, variations in dissolved and $^{14}CO_2$ pools were more complicated. An increase of Δ[IW-^{14}C], corresponding to higher $\Delta_t[^{14}CO_2]$, was found from 80 to 172 h in all 3 long experiments; the increase was especially notable for the weakly adsorbed protein (Ru-Sup-6cm-Long). This could represent a change in the sediment microbial community, (e.g., greater production of proteolytic enzymes). Or, the increase of ^{14}C in pore water could be due to bacteria which first assimilated ^{14}C into biomass, and then released it as fermentation products or other

soluble molecules. The $\Delta_t[^{14}CO_2]$ was very slow during the last phase of the experiment (1-6 wk), indicating that the protein remaining at this point was not readily decomposed. Except during the 80 - 172 h interval of the long experiment, [IW-^{14}C] either decreased rapidly or remained very low, even when some $^{14}CO_2$ production showed that decomposition was occurring. This suggests that hydrolysis, or other processes releasing dissolved organic materials, were limiting the rate of protein mineralization.

Decomposition of GroEL Table 6-1 shows that, like for Rubisco, the dissolved GroEL activity was always low. It was generally greatest initially, when it also decreased most rapidly, corresponding to a somewhat enhanced initial increase in $^{14}CO_2$. After 15 h (or 25 h), the first time point measured, $\Delta[^{14}CO_2]$ was usually small and [IW-^{14}C] low in the 6 cm sediments. However, in the surface sediments, $^{14}CO_2$ continued to increase at about the same slow rate throughout the experiment, while [IW-^{14}C] remained low and decreased very slowly after 16 h. As for Rubisco, these patterns are consistent with the small amount of dissolved protein being rapidly decomposed, while adsorbed protein decomposed much more slowly. Compared with Rubisco, GroEL decomposed less, which may be due to its larger molecular size, making it more strongly adsorbed or difficult to hydrolyze.

Decomposition in surface sediments was greater than that in deep sediments, except that GroEL showed greater decomposition when pre-adsorbed on goethite in 6 cm sediments. In surface sediments, the turnover time was 150 d for the more labile, and 250 d for more refractory protein; while in 6 cm sediments, the turnover times were 140 and 1000 d, respectively. There were no consistent differences among decomposition experiments using pre-adsorbed and non pre-adsorbed GroEL.

Similar to that for Rubisco, an experiment was conducted using the weakly adsorbed proteins from the supernatant after GroEL adsorption on illite. These proteins were rapidly removed from IW, probably by adsorption, since their overall mineralization was low. $\Delta[^{14}CO_2]$ was greater than for GroEL pre-adsorbed on illite or non pre-adsorbed GroEL, but only by 4 and 2.4 times, respectively. The "weakly" adsorbed proteins in the

GroEL solution were quite strongly adsorbed by the sediment, and this apparently led to their slow decomposition. This may reflect the fact that the impurities in GroEL present in the supernatant after adsorption included larger proteins than those from Rubsico (Chapter 3).

Decomposition of GroES Table 6-2 shows that both $\Delta_t[^{14}CO_2]$ and $\Delta_t[IW\text{-}\ ^{1}C]$ were greatest after 11 h incubation, and then decreased as for the other proteins, reflecting rapid utilization of the dissolved material. The GroES decomposition rate was about twice that of Rubisco and averaged five times that of GroEL. GroES is of lower MW and is not as strongly adsorbed as the two larger proteins, which may account for this difference. However, GroES also contained more low molecular weight impurities, which may have contributed to the greater $\Delta_t[^{14}CO_2]$.

§6.6.3 Comparison of Protein Decomposition Rates to those of Other Organic Substances

Sugai and Henrichs (1992) studied ^{14}C-labeled amino acid uptake and mineralization in RB sediments. They found that within 2 - 4 h, about 40 - 50% of added alanine (Ala), glycine (Gly) and serine (Ser) were mineralized to $^{14}CO_2$, but there was no additional decomposition between 4 - 8 h. 17% of glutamic acid (Glu) was mineralized in 12 h and 11% of lysine (Lys) in 54 h. Adsorbed and intracellular amino acids could be acid extracted from sediment, and in the acid extract Lys > Glu > Ser > Ala >Gly. The acid-extractable amino acids increased rapidly, as dissolved amino acids decreased, during the first 10 -15 min, then gradually decreased as decomposition to $^{14}CO_2$ occurred. This pattern was considered to be mostly due to adsorption, which was greatest for basic amino acids. Basic amino acids also were mineralized more slowly than acidic and neutral amino acids. The respiration rates of small peptides in RB sediments (Luo, 1994) decreased in the order $Ala_2 > Ala_3 > Glu_2 > Ala_6 > Lys_2$. This pattern also reflected their adsorption, with the more strongly adsorbed peptides decomposing more slowly. The turnover times of amino acids (Henrichs and Doyle, 1986; Sugai and Henrichs, 1992) and small peptides (Luo, 1994) in

RB sediments ranged from < 1 h to about 20 h, and were much shorter than for proteins (this study), as expected. The turnover time of adsorbed Rubisco was about 700 d, and that of weakly adsorbed small proteins was about 15 d. These were comparable to the turnover times of particulate and dissolved fraction of algae in RB sediments (Henrichs and Doyle, 1986).

§6.6.4 *Effects of Adsorption on Decomposition*

Because all proteins rapidly adsorbed to sediments, differences between pre-adsorption experiments and those in which protein solutions were added directly to sediments were small. Although the results suggested that pre-adsorption decreased decomposition slightly, all of the strongly adsorbed proteins decomposed slowly regardless of the type of experiment. Comparison between weakly adsorbed proteins and GroEL or Rubisco showed that the weakly adsorbed proteins did decompose more rapidly. However, this observation could also be related to a general tendency for lower molecular weight proteins to decompose faster, or to the supernatant proteins simply being more labile. There is a pattern in the experimental results of greater dissolved organic compound concentrations being associated with higher $^{14}CO_2$ production rates. Also, decreases in [IW-^{14}C] and increase in [$^{14}CO_2$] were often quantitatively related. Finally, SDS extraction of the Rubisco and GroEL after decomposition yielded a pattern of ^{14}C activity on sodium dodecyl sulfate-polyacrylamide gel electrophoresis (SDS-PAGE) gels and sucrose density gradients that indicated that much of the protein had survived intact, that is, most of the activity was still associated with the MW bands of the original compound (Chapter 7). Taken together, these results are consistent with the hypothesis that adsorption slows decomposition of proteins in RB sediments.

§ 6.7 Summary and Conclusions

1) Rubisco, GroEL and GroES were strongly adsorbed by RB sediments.

2) The decomposition rates of the proteins tended to be greater in surface

sediments due to their greater biological activity.

3) Pre-adsorption of proteins on minerals before addition to sediments slowed their decomposition up to 60%. But proteins added without pre-adsorption were strongly adsorbed to sediment and also decomposed slowly.

4) Weakly adsorbed, lower molecular weight proteins decomposed much more rapidly than GroEL and Rubisco.

5) Decomposition rates were in the order GroES > Rubisco > GroEL, reflecting their relative molecular size influence upon adsorption behavior.

6) These observations are consistent with adsorption being an important factor in slowing the decomposition of proteins in sediments.

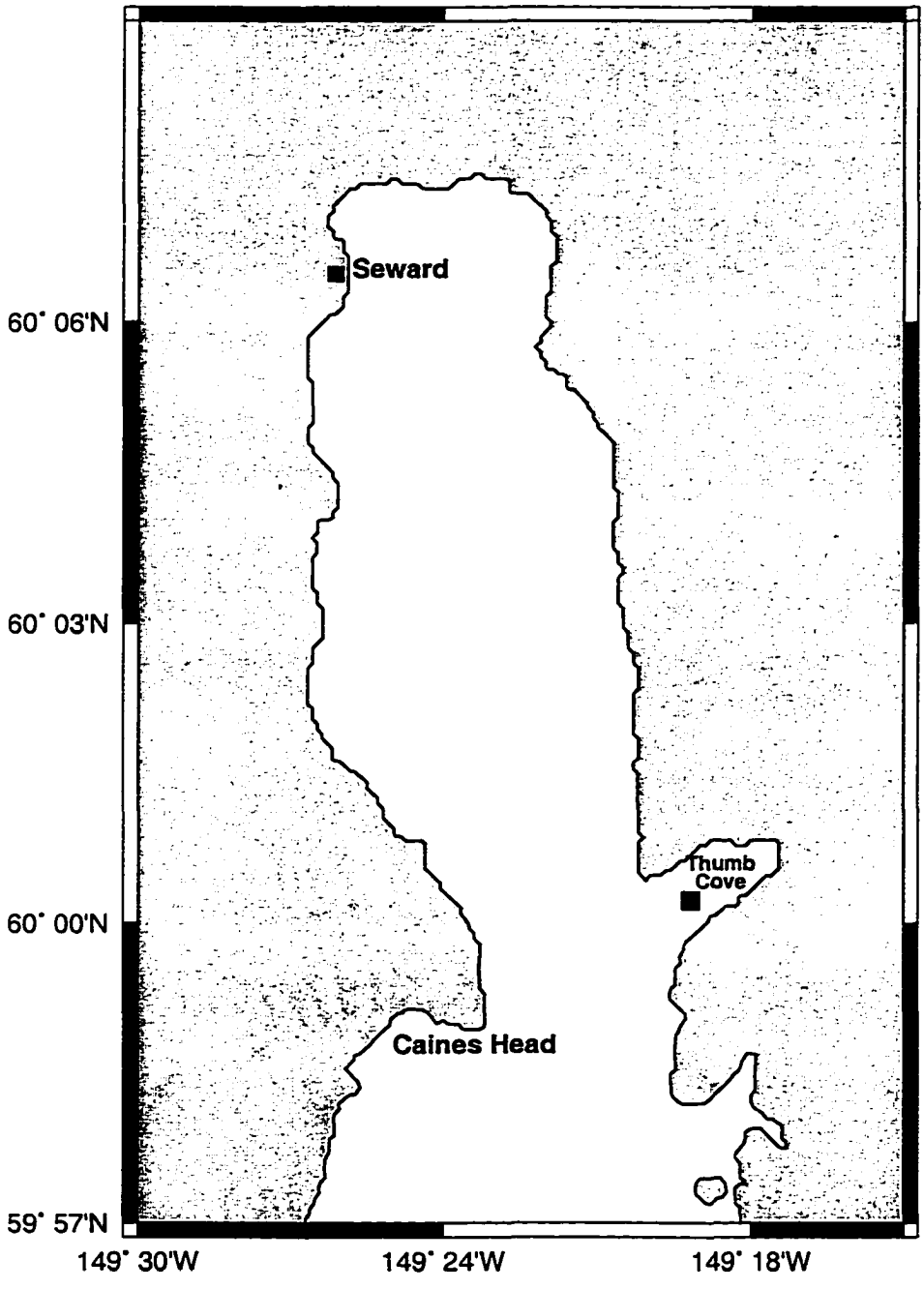

Figure 6-1. Map of Resurrection Bay.

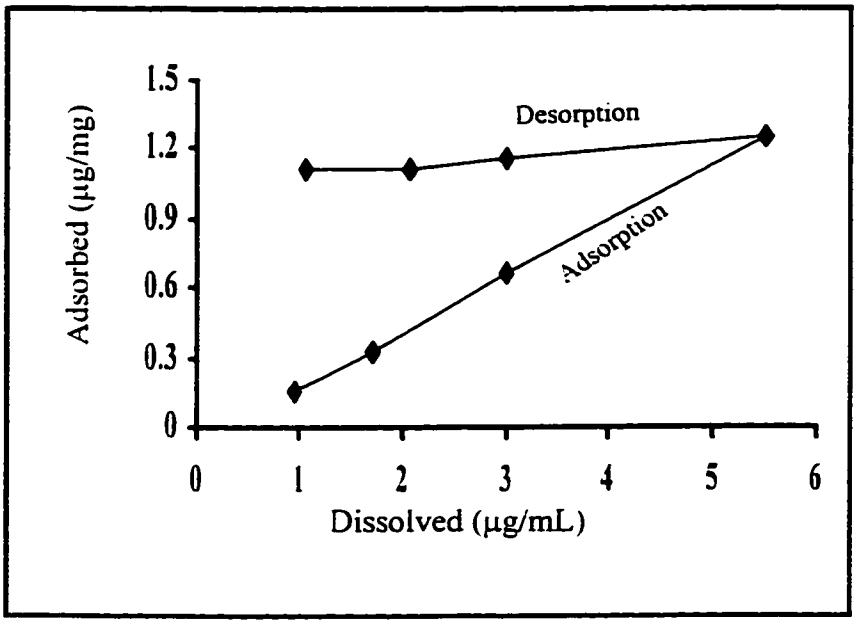

Figure 6-2. Rubisco adsorption on and desorption from Resurrection Bay sediments.

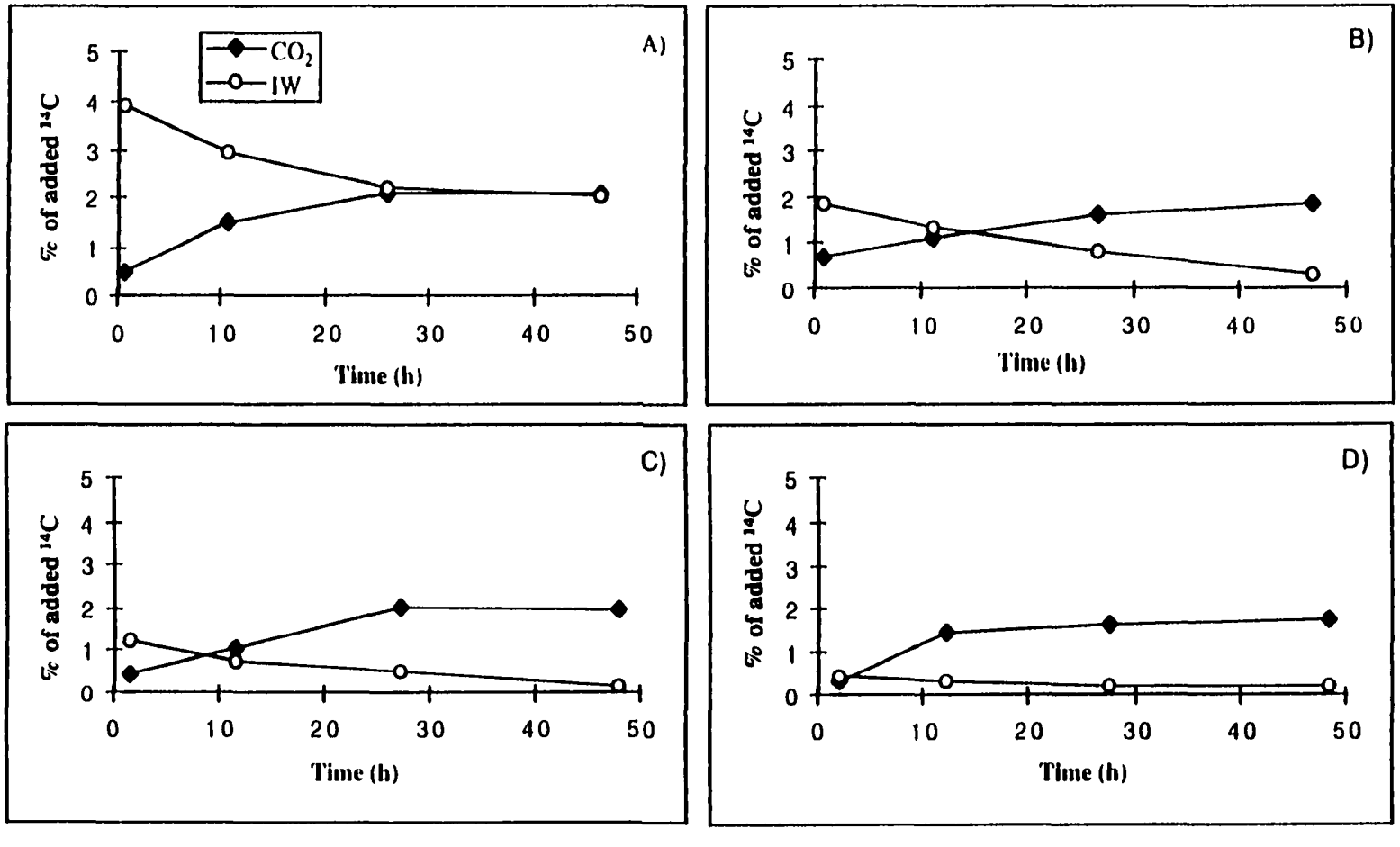

Figure 6-3. Rubisco decomposition in sediments from 6 cm depth. A) non-preadsorbed Rubisco; B) pre-adsorbed Rubisco on goethite; C) pre-adsorbed Rubisco on illite and D) pre-adsorbed Rubisco on montmorillonite.

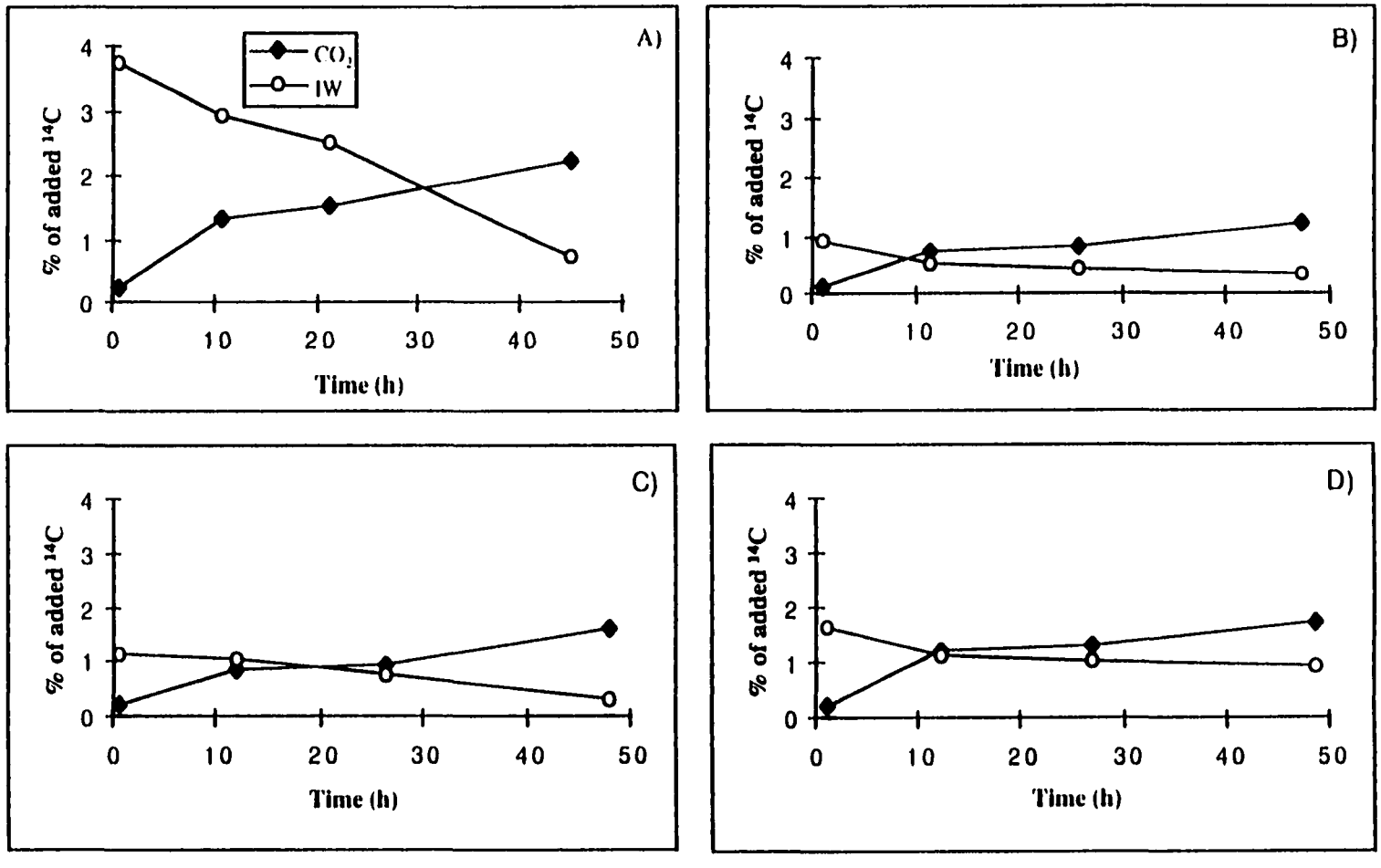

Figure 6-4. Rubisco decomposition in surface sediments. A) non-preadsorbed Rubisco; B) pre-adsorbed Rubisco on goethite; C) pre-adsorbed Rubisco on illite and D) pre-adsorbed Rubisco on montmorillonite.

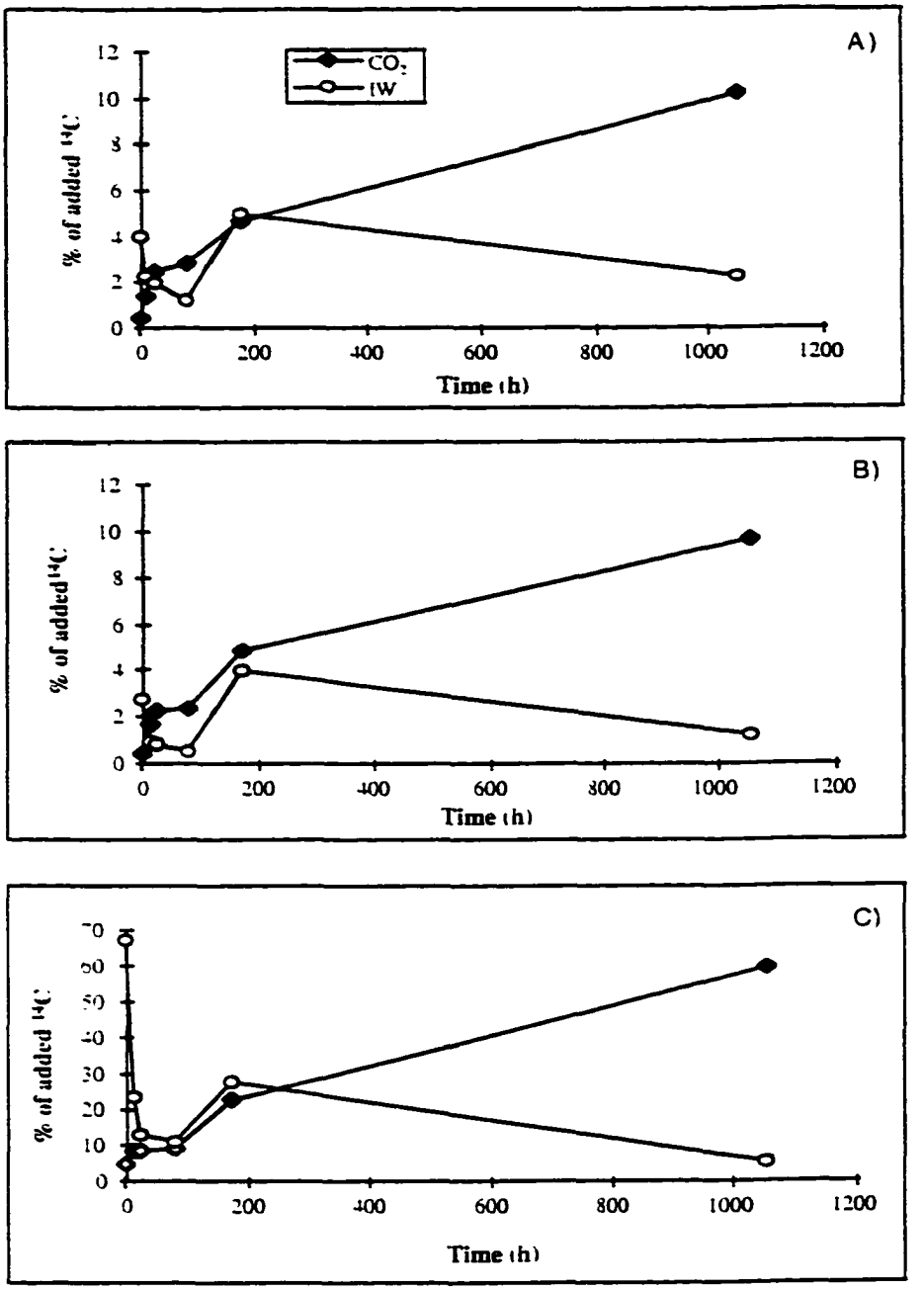

Figure 6-5. Rubisco long-term decomposition in sediments from 6 cm depth. A) non-preadsorbed Rubisco; B) pre-adsorbed Rubisco on illite and C) weakly adsorbed proteins from Rubisco supernatant after adsorption.

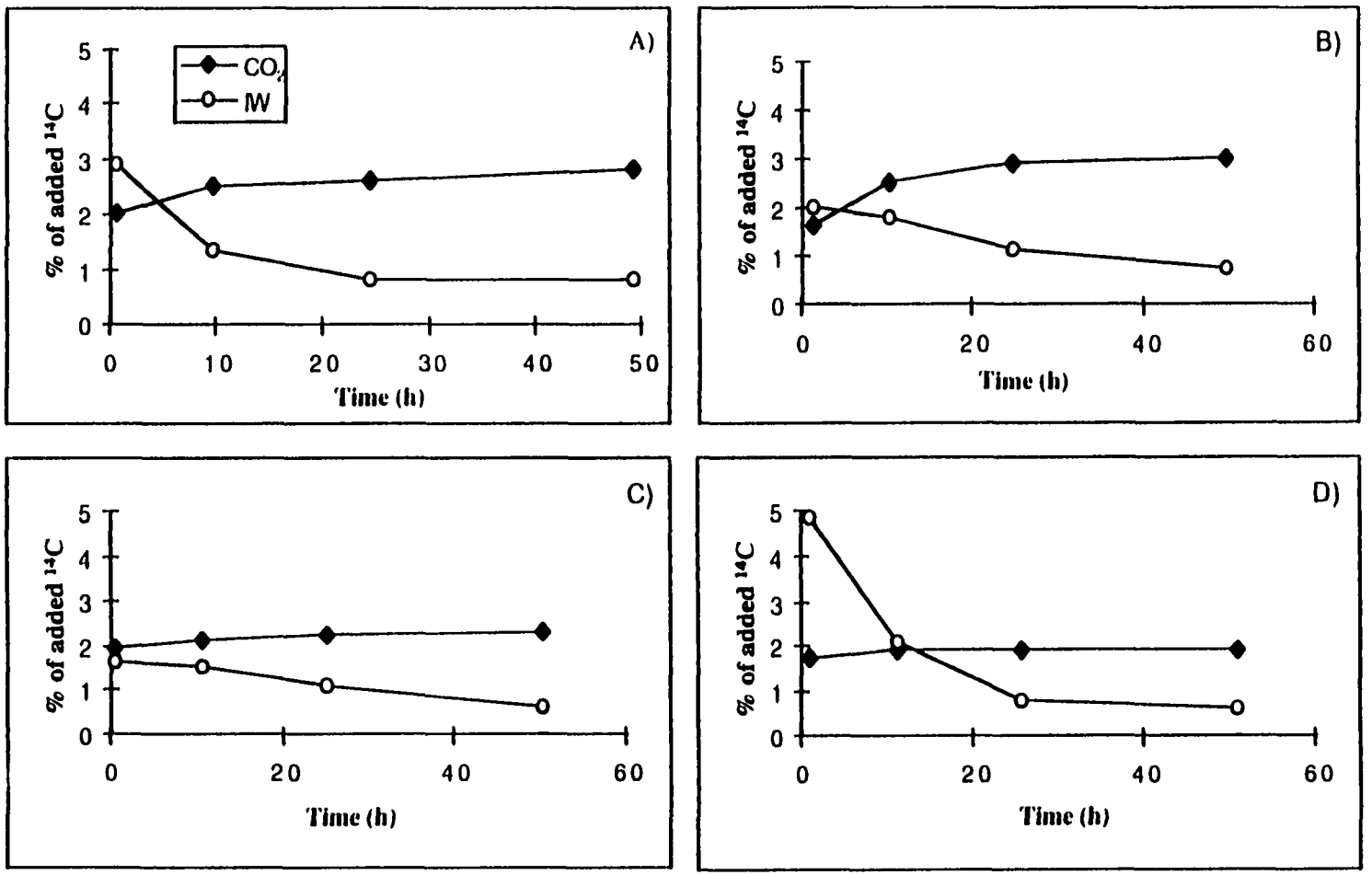

Figure 6-6. GroEL decomposition in sediments from 6 cm depth. A) non-preadsorbed GroEL; B) pre-adsorbed GroEL on goethite; C) pre-adsorbed GroEL on illite and D) pre-adsorbed GroEL on montmorillonite.

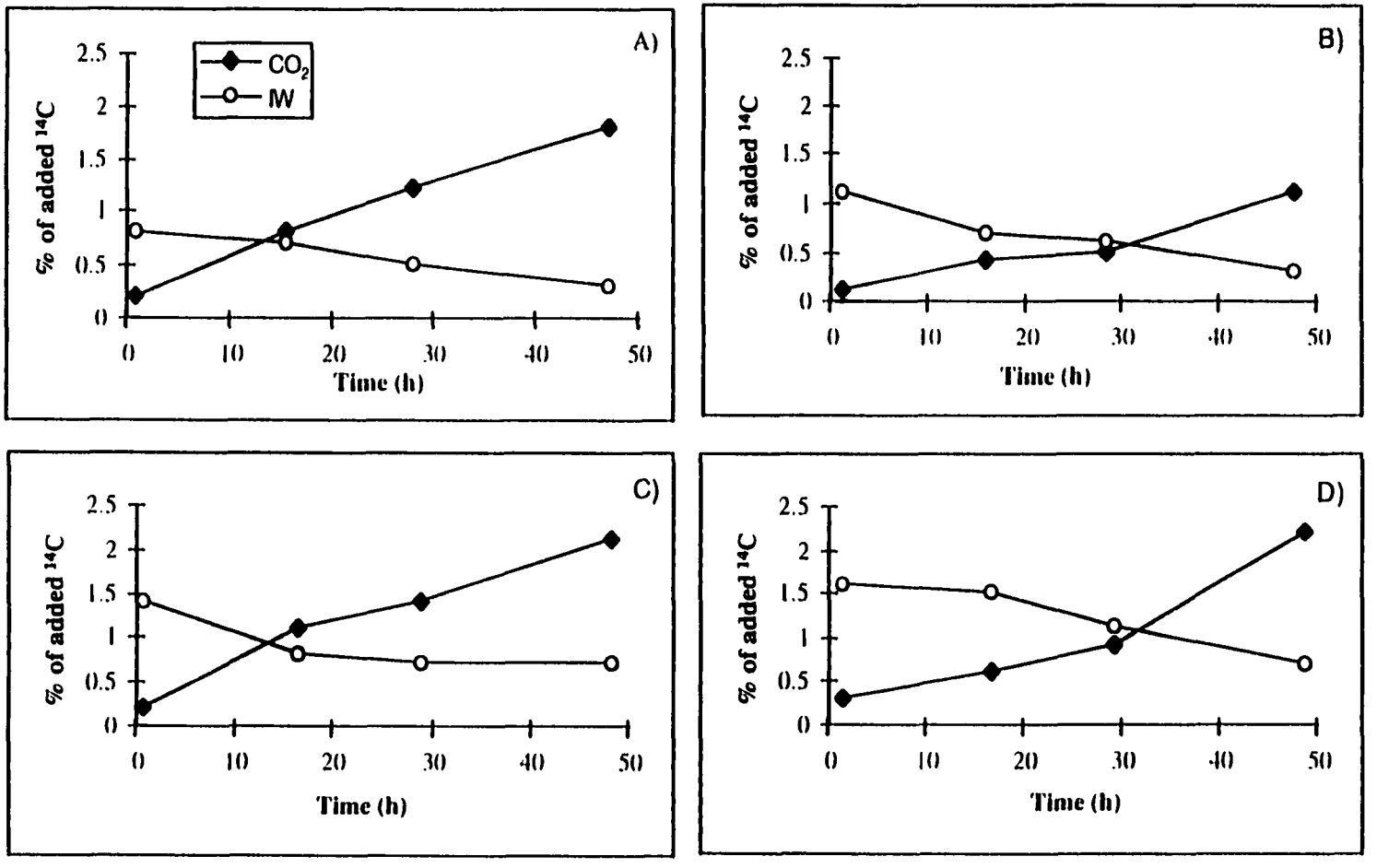

Figure 6-7. GroEL decomposition in surface sediments. A) non-preadsorbed GroEL; B) pre-adsorbed GroEL on goethite; C) pre-adsorbed GroEL on illite and D) pre-adsorbed GroEL on montmorillonite.

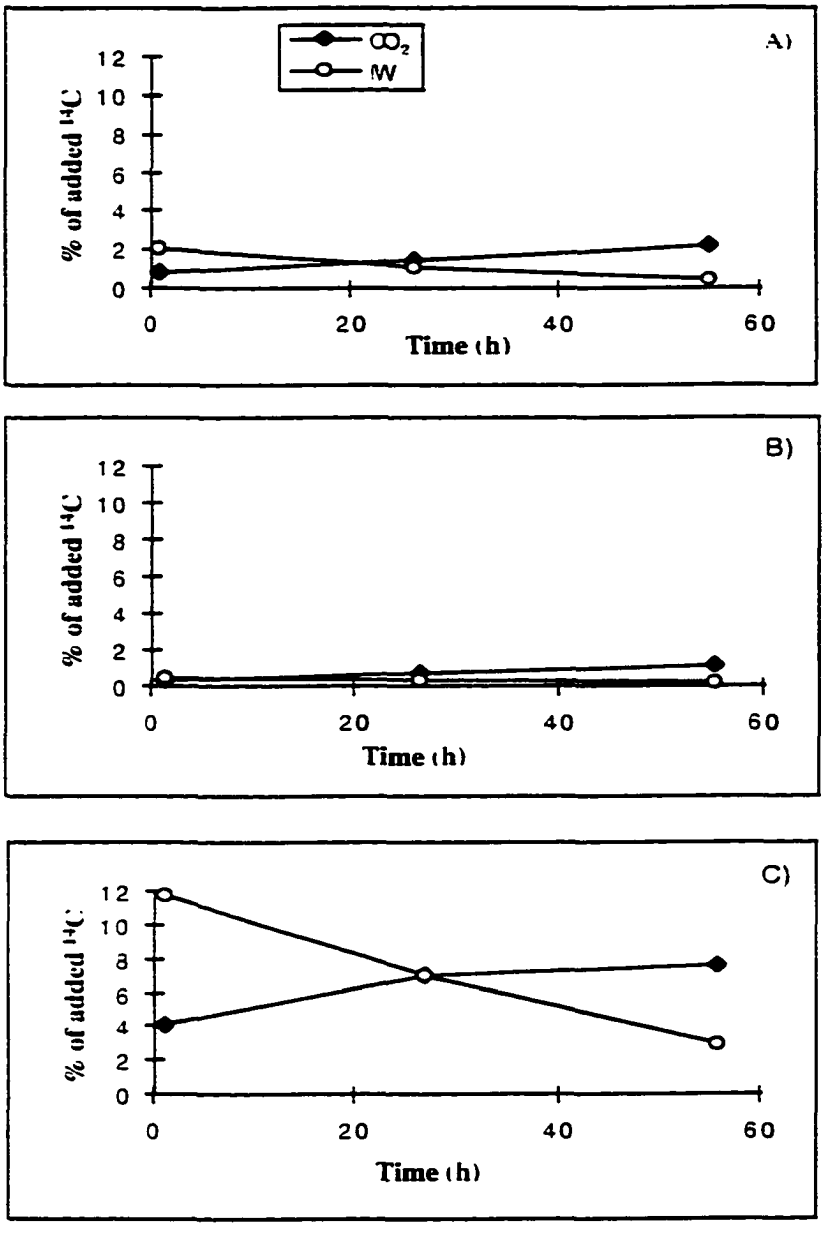

Figure 6-8. GroEL decomposition in sediments from 6 cm depth. A) non-preadsorbed GroEL; B) pre-adsorbed GroEL on illite and C) weakly adsorbed proteins from GroEL supernatant after adsorption.

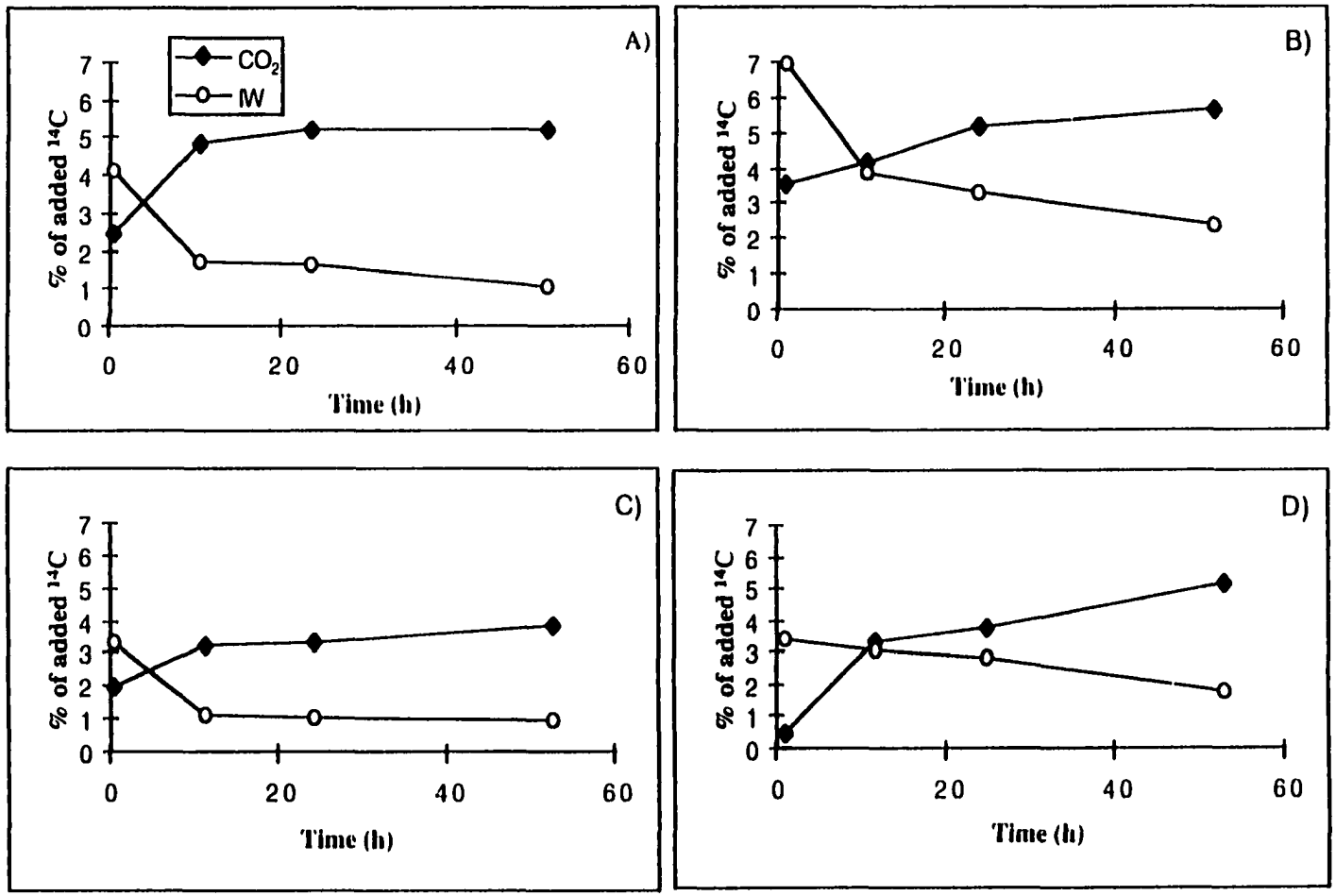

Figure 6-9. GroES decomposition in sediments from 6 cm depth. A) non-preadsorbed GroES; B) pre-adsorbed GroES on goethite; C) pre-adsorbed GroES on illite and D) pre-adsorbed GroES on montmorillonite.

Table 6-1. Comparison of $^{14}CO_2$ production and decrease of ^{14}C activity in pore water during protein decomposition.

Experiments*	Incubation Time (h)	^{14}C activity decrease in IW (%)		$^{14}CO_2$ increase (%)
Rubisco				
Non-Ru-6cm	47	1.9	>	1.6
Ru-Fe-6cm	47	1.5	>	1.1
Ru-Ill-6cm	48	1.1	<	1.5
Ru-Mon-6cm	48	0.2	«	1.4
Non-Ru-0cm	45	3.0	>	2.0
Ru-Fe-0cm	47	0.6	<	1.1
Ru-Ill-0cm	48	0.8	<	1.4
Ru-mon-0cm	49	0.7	<	1.5
Non-Ru-6cm-Long	1051	1.8	«	9.8
Ru-Ill-6cm-Long	1052	1.5	«	9.2
Ru-Sup-6cm-Long	1052	61.9	≥	55.0
GroEL				
Non-EL-6cm-A	49	2.1	>	0.5
EL-Fe-6cm	50	1.1	<	1.4
EL-Ill-6cm-A	50	1.0	>	0.4
EL-Mon-6cm	51	4.2	»	0.2
Non-EL-0cm	47	0.5	<	1.6
EL-Fe-0cm	48	0.8	>	0.6
EL-Ill-0cm	48	0.7	<	1.9
EL-Mon-0cm	49	0.9	<	1.9
Non-EL-6cm-B	55	1.6	≥	1.4
EL-Ill-6cm-B	55	0.2	<	0.8
EL-Sup-6cm	56	8.8	>	3.4
GroES				
Non-ES-6cm	51	3.1	≈	3.1
ES-Fe-6cm	52	4.6	>	2.1
ES-Ill-6cm	53	2.4	>	1.9
ES-Mon-6cm	53	1.7	<	4.7

* abbreviations: Non: no preadsorption; Ru: Rubisco; EL: GroEL; ES: GroES; Fe: pre-adsorption on goethite; Ill: pre-adsorption on illite; Mon: pre-adsorption on montmorillonite; Sup: weakly adsorbed proteins from the supernatant after Rubisco or GroEL adsorption.

Table 6-2. $^{14}CO_2$ production rates and ^{14}C decrease rates in interstitial water during protein decomposition in Resurrection Bay sediments*.

Experiment[a]	Incubation time (h)	$^{14}CO_2$ production rate (% of added/h)		^{14}C decrease rate[b] (% of added/h)	Turnover time (d)
Rubisco					
Non-Ru-6cm	1 - 11	0.10	≈	0.10	40
	11 - 27	0.04	≤	0.05	105
	27 - 47	0.00	≤	0.01	800
Ru-Fe-6cm	1 - 11	0.04	<	0.05	105
	11 - 27	0.03	≈	0.03	140
	27 - 47	0.01	<	0.02	420
Ru-Ill-6cm	1 - 11	0.06	>	0.05	70
	11 - 27	0.06	>	0.01	70
	27 - 47	0.00	<	0.02	800
Ru-Mon-6cm	1 - 11	0.11	»	0.01	40
	11 - 27	0.01	≈	0.01	420
	27 - 47	0.00	≈	0.00	860
Non-Ru-0-cm	1 - 11	0.09	>	0.08	45
	11 - 25	0.02	<	0.04	210
	25 - 48	0.03	<	0.07	140
Ru-Fe-0cm	1 - 11	0.06	>	0.04	70
	11 - 25	0.01	≈	0.01	420
	25 - 48	0.02	>	0.00	210
Ru-Ill-0cm	1 - 11	0.05	>	0.01	80
	11 - 25	0.01	<	0.02	420
	25 - 48	0.03	>	0.02	140
Ru-Mon-0cm	1 - 11	0.09	>	0.04	45
	11 - 25	0.01	≈	0.01	420
	25 - 48	0.02	>	0.00	210
Non-Ru-6cm-Long	1 - 13	0.09	<	0.16	45
	13 - 24	0.09	>	0.03	45
	24 - 80	0.01	≈	0.01	210
	80 - 172	0.02		-0.04	210
	172 - 1051	0.01	≥	0.00	650

(Continued)

Table 6-2. (Continued)

Experiment[a]	Incubation time (h)	$^{14}CO_2$ production rate (% of added/h)		^{14}C decrease rate[b] (% of added/h)	Turnover time (d)
Ru-Ill-6cm-Long	1 - 13	0.10	<	0.15	40
	13 - 24	0.06	>	0.01	70
	24 - 80	0.00	≤	0.01	2350
	80 - 172	0.03		-0.04	140
	172 - 1051	0.01	>	0.00	760
Ru-Sup-6cm-Long	1 - 13	0.28	«	3.55	15
	13 - 24	0.01	«	0.99	420
	24 - 80	0.02	<	0.04	210
	80 - 172	0.14		-0.18	30
	172 - 1051	0.04	>	0.03	105
GroEL					
Non-EL-6cm-A	1 - 11	0.05	<	0.18	80
	11 - 25	0.00	<	0.03	800
	25 - 50	0.00	≈	0.00	800
EL-Fe-6cm	1 - 11	0.10	»	0.02	40
	11 - 25	0.03	≈	0.03	140
	25 - 50	0.00	<	0.02	1050
EL-Ill-6cm-A	1 - 11	0.02	>	0.01	210
	11 - 25	0.01	<	0.03	420
	25 - 50	0.00	<	0.02	1050
EL-Mon-6cm	1 - 11	0.02	«	0.27	210
	11 - 25	0.00	«	0.09	800
	25 - 50	0.00	<	0.01	1000
Non-EL-0cm	1 - 16	0.04	>	0.01	105
	16 - 29	0.03	>	0.01	140
	29 - 48	0.03	>	0.01	140
EL-Fe-0cm	1 - 16	0.02	<	0.03	210
	16 - 29	0.01	≈	0.01	420
	29 - 48	0.01	<	0.02	420
EL-Ill-0cm	1 - 16	0.06	>	0.04	70
	16 - 29	0.02	>	0.01	210
	29 - 48	0.04	>	0.00	105

(Continued)

Table 6-2. (Continued)

Experiment[a]	Incubation time (h)	$^{14}CO_2$ production rate (% of added/h)		^{14}C decrease rate[b] (% of added/h)	Turnover time (d)
EL-Mon-0cm	1 - 16	0.02	>	0.01	210
	16 - 29	0.02	<	0.03	210
	29 - 48	0.07	>	0.02	60
Non-EL-6cm-B	1 - 26	0.02	<	0.04	210
	26 - 55	0.02	=	0.02	210
EL-Ill-6cm-B	1 - 26	0.02	>	0.01	210
	26 - 55	0.01	>	0.00	420
EL-Sup-6cm	1 - 26	0.11	<	0.19	40
	26 - 55	0.02	«	0.14	210
GroES					
Non-ES-6cm	1 - 11	0.24	=	0.24	17
	11 - 24	0.03	>	0.01	140
	24 - 52	0.00	<	0.02	500
ES-Fe-6cm	1 - 11	0.06	«	0.31	70
	11 - 24	0.08	>	0.04	50
	24 - 52	0.02	<	0.04	210
ES-Ill-6cm	1 - 11	0.12	<	0.21	35
	11 - 24	0.01	=	0.01	420
	24 - 52	0.02	>	0.02	210
ES-Mon-6cm	1 - 11	0.27	»	0.04	15
	11 - 24	0.03	>	0.02	140
	24 - 52	0.05	>	0.04	80

*: The differences between $^{14}CO_2$ production rate and ^{14}C decrease rate in interstitial water are also listed. The signs » and « represent absolute differences greater than 5 times; and = represents a relative difference less than 10%.

a: abbreviations: Non: non-preadsorption; Ru: Rubisco; EL: GroEL; ES: GroES; Fe: pre-adsorption on goethite; Ill: pre-adsorption on illite; Mon: pre-adsorption on montmorillonite; Sup: weakly adsorbed proteins from the supernatant after Rubisco or GroEL adsorption.

b: negative sign represents increase.

Chapter 7

Decomposition, Adsorption, and Preservation of Proteins in Marine Sediments

Abstract

Protein adsorption and decomposition in two different marine sediments, Skan Bay (anoxic) and Resurrection Bay (oxic), were compared. The Rubisco decomposition rate was greater in SB than in RB sediments, reflecting the greater organic matter (OM) content and higher overall rate of OM oxidation in SB sediment. Pre-adsorption to clays usually slowed decomposition in both sediments. Pre-adsorption to iron increased decomposition under conditions where Fe(III) reduction could occur. Rubisco was adsorbed by both marine sediments in its original form, and protein adsorption by SB and RB sediments was about the same. Similar Rubisco adsorption on untreated and autoclaved sediments was found for both SB and RB.

A new protein determination method was developed based on the Micro-Bradford method. This method showed that 30 - 50% of sediment THAA (Total Hydrolyzable Amino Acids) were from proteins. SDS was used to extract proteins from sediments. THAA in the SDS extract solutions were about half the THAA of the sediment. About 60 - 90% of the SDS-THAA was from proteins. Especially in organic-rich anoxic sediments, THAA and SDS-THAA somewhat overestimate protein concentrations, probably due to the presence of other amino acid containing materials. The THAA and SDS-THAA in both RB and SB sediments showed a similar distribution of amino acids, except for an order of magnitude difference in concentration, reflecting the greater TOC content of SB sediments. Most of the proteins extracted by SDS from both sediments (0-12 cm) were small (< 12 kDa). The sizes of preserved proteins match those of micropores on sediment surfaces, indicating that the parts of proteins adsorbed within such pores were protected from bacterial attack.

§7.1 Introduction

Major changes in organic matter (OM) concentration and composition occur at the sediment-water interface, and most OM diagenetic processes are rapid compared with geological time scales, occurring within 1000 years after deposition (Henrichs, 1993). OM decomposers include a wide variety of microorganisms such as bacteria, fungi and yeasts. In marine sediments, bacteria play the predominant role due to their universal abundance and broad degradative capacities (Deming and Baross, 1993).

Organic materials can be divided into two broad groups: substances soluble in water or organic solvents (generally low M.W. molecules, e.g., amino acids) and substances insoluble in both (generally high M.W. molecules, e.g., cell wall remains). Except for highly hydrophilic substances, such as sugars, which are largely present in dissolved forms, soluble OM in sediments tends to be adsorbed to particle surfaces. Hollerbach and Dehmer (1994) described the categories of organic molecules as follows:

1) Hydrophilic OM can be transported by pore water diffusion or advection to the sediment-water interface and is readily utilized by microorganisms.

2) Hydrophobic OM is usually adsorbed by the mineral matrix, and tends to be preserved once it escapes from the biologically active zone.

3) Hydrocarbons can only be broken down under aerobic conditions and thus are preferentially preserved.

4) Highly reactive OM can interact with functional groups present on particulate organic substances.

5) Other OM has been transformed into stable forms during diagenesis.

Figure 7-1 shows idealized zones of OM oxidation coupled with reduction of electron acceptors (from Deming and Baross, 1993). It is clear that the aerobic and anaerobic pathways are quite different. In aerobic respiration microorganisms directly oxidize OM to CO_2, while under anaerobic conditions, larger molecules are fermented into smaller ones and then oxidized to CO_2. Anaerobic oxidation is coupled with the reduction

of inorganic substances such as nitrate, iron, sulfate, etc.

In contrast to the terrestrial system, proteins are a major component of biomass in the aquatic environment. They make up about 50% - 75% and 35% - 55% of the total organic material in living bacteria and phytoplankton, respectively (Hollerbach and Dehmer, 1994). Amino acids are also the largest group of identifiable nitrogen-containing substances in marine sediments. Most amino acids are recovered from sediments only after acid hydrolysis, indicating that they were present as peptides, proteins, or another bound form. A small fraction of the total amino acids are dissolved in pore water or can be recovered by extraction with water. The concentrations of amino acids are highest near the sediment-water interface, and decrease rapidly with depth (Bada and Mann, 1980). Both free and bound amino acids play an important role in a number of biogeochemical processes. The composition of particulate OM in the water column differs from that found in sediments. For instance, almost 100% of organic nitrogen found in sediment-trap samples is amino acids (Biggs *et al.*, 1988; 1989), while only 2 - 12% of the nitrogen in many coastal surface sediments is identifiable as amino acids (Rosenfeld, 1979; Mayer *et al.*, 1988). However, particularly in anoxic coastal sediments, hydrolyzable amino acids do constitute a major fraction of total sediment nitrogen, up to 70% (Henrichs *et al.*, 1984).

The decomposition pathway of proteins involves hydrolysis to peptides and free amino acids (FAA), before metabolism to CO_2 and H_2O. The hydrolysis is accomplished by extracellular enzymes, which can either be free in solution or bound to the cell surface (Kim and ZoBell, 1974; Little *et al.*, 1979). Previous work in SB and RB sediments has shown that most peptides are not hydrolyzed in filtered sediment pore water, so most hydrolytic activity is confined to particles, probably bacteria (Luo, 1994). The turnover times of both dissolved, free amino acids and small ($\leq$ 5 residues) peptides are short (minutes to days) (Sugai and Henrichs, 1992; Luo, 1994), but these substances decompose more slowly when adsorbed by sediment particles. Basic amino acids are adsorbed most strongly and decomposed most slowly (Sugai and Henrichs, 1992).

Amino acid and peptide adsorption, decomposition and preservation in Skan Bay

(SB) and Resurrection Bay (RB) have been studied previously (Doyle, 1988; Sugai and Henrichs, 1992; Henrichs and Sugai, 1993; Luo, 1994; Sugai, *et al.*, 1994). Others (e. g., Burdige and Martens, 1990; Wang, 1993; Pantoja and Lee, 1998) have studied peptide and amino acid decomposition in different coastal sediments. The study of protein decomposition in marine sediments has been quite limited. In this study, we will compare the adsorption, oxidation and preservation of proteins in aerobic and anaerobic sediments. The results may be helpful in understanding the influence of biodegradation pathways on decomposition in different environments and on OM preservation mechanisms.

§7.2. Materials and Methods

Sediment samples were collected from SB, where bottom water and surface sediments are seasonally anoxic in late summer and fall, in August, 1997. Core samples were taken from RB, where surface sediments are oxic year-round, in April, 1998.

^{14}C-labeled Rubsico was purified as described in Chapter 3. The decomposition experiments were conducted on board ship within 24 h of sample collection. The sediments were stored in a refrigerator for about 2 months before use in adsorption and extraction experiments. The methods used in the protein decomposition experiments conducted with these sediments are presented in detail in Chapters 5 and 6, and briefly below.

§7.2.1 Adsorption and Decomposition of Rubisco

For the non-preadsorbed Rubisco experiments, 500 μL seawater and 55 μg Rubisco were added to 1 g wet sediments under N_2. After thorough mixing, the slurry was incubated at 4 °C for 48 hours. For the pre-adsorbed Rubisco decomposition experiment, 55 μg Rubisco were added to 5 mg mineral and a portion of the dissolved Rubisco then adsorbed to the mineral surface. The amount of adsorbed Rubisco was calculated by subtracting the amount of dissolved Rubisco remaining after reaction from the total added. After centrifugation and removal of supernatant, 500 μL sea water was added to the

mineral with the pre-adsorbed Rubisco, and 1.0 g of sediment was added under N_2. Sediments with added adsorbed Rubisco were also incubated for 48 hours.

§7.2.2 *Extraction of ^{14}C-Rubisco from Sediments*

After incubation and thorough mixing, the sediment mixture was centrifuged at 3,200 rpm for 10 minutes. The ^{14}C activity in the supernatant was counted. 250 μL of an extraction solution containing 5% SDS, 5% 2-mercaptoethanol, 0.1 M Tris buffer (pH 7.5), and 1 mM DTT was added to the sediment (SDS-1). After heating in boiling water for 30 minutes, the suspension was separated by centrifuging at 3,200 rpm. The ^{14}C activity in the supernatant was counted. This solution was also loaded on a SDS-PAGE gel to compare with the original Rubisco. Five mL of the extraction solution was again added to the sediment (SDS-2). After thorough mixing, the slurry was heated in an oven at 75 °C for 12 h, centrifuged, the supernatant saved, and 1 mL of the supernatant solution was loaded on a sucrose density gradient. The extraction was repeated again (SDS-3), and the total extracted ^{14}C was summed.

§7.2.3 *Assessment of ^{14}C-protein Composition Using an SDS-PAGE Gel*

^{14}C-labeled Rubisco extracted from sediments as previously described (SDS-1) was loaded on a 15% SDS - PAGE gel, and the mini-gel was run under a constant voltage of 200V for 45 min. The original Rubisco solution was treated in the same way, for comparison with the extracted Rubisco. The extraction conditions denatured and dissociated the Rubisco. For the denatured solution of the original Rubisco, about 600 dpm was loaded, and for extracted, adsorbed Rubisco 200-300 dpm. After staining using Coomassie Blue, the gel was destained by rinsing with an aqueous solution of acetic acid and methanol. The separating gel was cut into pieces, according to the locations of molecular weight standards and target protein spots. 500 μL of 30% H_2O_2 was added to the stacking and separating gel slices, and then the solution was heated at 70 °C for several

hours to dissolve the gel. Sixteen mL of scintillation cocktail was added to the gel slice solution with shaking. If the mixture was not clear, a small volume of concentrated HCl was added. The proportions of different M.W. fractions in the protein solutions were measured by counting ^{14}C activity in bands equivalent to protein size groups. Natural proteins extracted from sediment were also loaded on the same gel as a reference. The blanks of background gel slices were subtracted.

§7.2.4 *^{14}C Analysis of Rubisco from Sucrose Density Gradients*

One mL of the ^{14}C-labeled Rubisco solution extracted from sediments (SDS-2) was loaded on a sucrose density gradient (0 - 30 %). 35 μg of the original Rubisco solution (~ 2000 dpm) was added to 1 mL of the extraction solution, and heated in boiling water for 10 minutes. This denatured and dissociated the Rubisco into large and small subunits (Iwanij *et al.*, 1974). One mL of this solution was also loaded on a sucrose density gradient. After centrifuging at 39,000 rpm at 4 °C for 20 h, 1 mL increments of the protein-containing sucrose solution were pipetted into scintillation vials, and ^{14}C activity was measured. Addition of HCl was necessary for the most concentrated sucrose solutions (≥ 8 ml from top) to clarify the cocktail.

§7.2.5 *Natural Proteins in Sediments*

Extraction A cysteine molecule can react with another cysteine to form cystine, as in the following reaction:

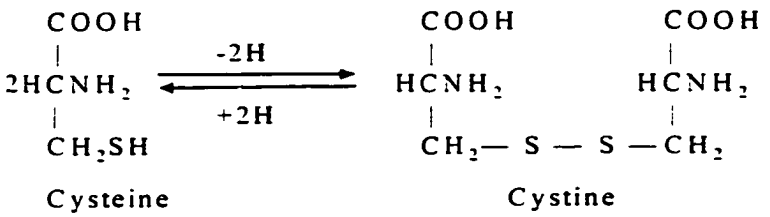

Although the disulfide bond is not as stable as the peptide linkage, it is more stable than non-covalent bonds. The formation of the sulfur bridge can occur within one protein or between two proteins, resulting in enlargement of protein size. The reaction in the reverse direction can be effected by a number of reducing reagents containing -SH (Cantarow and Schepartz, 1967). 2-mercaptoethanol and trichloroacetic acid (DTT) are used together in SDS extraction solutions to prevent the formation of sulfur bridges, and thereby to prevent the coagulation of proteins.

One g sediment from SB (6 cm) or RB (0 - 3 cm) was added to a pre-weighed glass vial. After centrifugation at 3,200 rpm for 5 minutes, the interstitial water was removed and weighed. 5 mL of extraction solution, which contained 5% SDS, 5% 2-mercaptoethanol, 0.1 M Tris buffer (pH 7.5) and 1 mM DTT was added. The sediment slurry was thoroughly mixed, and then was heated at 70°C for 24 h. The sediment and solution were centrifuged at 3,200 rpm for 10 min. The supernatant was saved for the protein concentration assay.

Natural proteins examined on an SDS-PAGE gel Natural proteins were extracted from 1 g of wet sediments by 250 μL SDS plus 2-mercaptoethanol extraction solution. The extraction mixture was heated at 70 °C for 24 h. The supernatant was separated after thorough mixing, and loaded on SDS-PAGE gel. To eliminate possible artifacts due to heating, the following comparison was carried out: 1) the extraction mixture was heated in boiling water for 30 min; or 2) wet sediments were frozen at -60 °C overnight, thawed at room temperature to break cell walls, and then extracted at 4°C for 2 h.

Generally, 12% SDS-PAGE gel can separate proteins > 14 kDa, but cannot separate proteins < 14 kDa (Bio-Rad). Natural proteins were loaded on both 15% and 20% SDS-PAGE gels. To obtain better resolution of small proteins, the 20% SDS-PAGE was modified according to the Bio-Rad mini-gel instructions and Christy *et al.* (1989). 1) The polyacrylamide concentration was increased to 20%; 2) the anode buffer contained Tris (0.025M), glycine (0.2M), SDS (0.1%) and sodium acetate (0.1M); and 3) the gel was developed at constant voltage (150V) for 45 minutes. SYPRO fluorescent orange stain

(from Bio-Rad) is ~ 100 times more sensitive than Coomassie Blue (from SIGMA) for detection proteins. Both the Coomassie Blue and SYPRO protein stains were used separately to stain 15% gels, and the 20% gel was stained using SYPRO. Molecular weight standards were from SIGMA and Bio-Rad, and both were used in one gel to double-check the protein sizes.

Protein concentration determination SDS has good solubilizing ability for proteins. But, it was necessary to remove SDS from the solution because of its interference in the protein concentration estimation by the Bradford method. Our method was modified from Pande and Murthy (1994). Briefly, 200 μL of the supernatant from the sediment extract was transferred to a 1.5 mL polypropylene centrifuge tube, and then 10 μL of 500 mM potassium phosphate (pH 7.5), 10 μL of 250 mM calcium chloride, and 1 mL of ethanol were added and thoroughly mixed. After the mixture was spun at 14,000 rpm for 1 minute, the supernatant was aspirated away. 100 μL of water and 1 mL of ethanol were added to the tube. The mixture was mixed, and then the supernatant removed after centrifugation. The precipitate was spun at 14,000 rpm for 10 seconds, and the last drop of solution was aspirated away. 100 μL Coomassie blue concentrate was added to the precipitate without mixing, and the tube was left undisturbed for 5 minutes; during this period the calcium phosphate-protein precipitate dissolved. 400 μL of Coomassie blue concentrate was added with gentle mixing, by inverting the tube twice. The absorbance was measured at 596 nm after 5 to 20 minutes of color development. Pore water was carried through the same procedure as a blank.

Using HPLC, THAA were measured in acid hydrolyzates after pre-column derivatization with *o*-phthaldialdehydehyde (OPA) and 2-mercaptoethanol (Jones *et al.*, 1981). 5 mL of 6 N HCl was added to 1 g wet SB or RB sediments, mixed, and heated at 110°C for 24 h. After centrifugation, the supernatant was neutralized using 6 N NaOH. 1 mL of borate buffer (pH 10.5, 25 mM), and 50 μL of OPA solution, containing 10 mg *o*-phthaldialdehyde, 10 μL 2-mercaptoethanol and 20 mg SDS in 1 mL methanol, were added

to 200 μL of sample solution. The sample was filtered through a 0.45 μm filter, and after reacting for 2 min, the sample was injected. Separation of amino acids was achieved in 25 min, using a gradient of sodium phosphate buffer (0.02 M, pH 6.5) and methanol (20 - 80%), at a flow rate of 1.5 mL/min. The difference between duplicate samples carried through the entire procedure was < 8%. The small blank was subtracted from sample concentrations.

Because 2-mercaptoethanol esterified in both acidic and alkaline aqueous solutions after heating and precipitated from solution, 5% SDS solution alone was used to extract protein, as described previously, for THAA measurement. 1 mL of the protein solution extracted by SDS was hydrolyzed in 1 mL 6N HCl at 110°C for 24 hours. After neutralization, SDS-THAA was measured using HPLC as above.

§7.3 Results

§7.3.1 Molecular Size Distribution of ^{14}C-Rubisco Extracted from Sediments

Table 7-1 shows that after 3 extractions, the percentage of ^{14}C activity in pore water and the extraction solutions tended to be greater in RB than SB sediments, especially in pre-adsorption experiments. The lowest ^{14}C activity was recovered after pre-adsorption on goethite and incubation in SB sediments.

Table 7-2 shows the molecular size distribution of ^{14}C activity after Rubisco decomposition in SB and RB sediments. In SB sediment extracts, about 63% of extracted ^{14}C is in the M.W. range of Rubisco subunits (10 - 60 kDa), while in SB pore water, about 49% of the activity was of the same molecular size as Rubisco, and 36% was from other dissolved materials which did not migrate on the gel. In RB sediments and pore water, there was no significant difference between 0 - 3 cm and 6 - 9 cm depths. The adsorbed ^{14}C was mostly from larger proteins (~ 60%, > 30 kDa), while dissolved ^{14}C was mostly from smaller proteins (~ 35%, < 10 kDa) and other substances which did not move under

electrophoresis (~36% in SB sediments and 22% in RB sediments).

Denatured Rubisco was found at different locations in the sucrose density gradient than the original Rubisco (Table 7-3). About 78% of the original Rubisco (550 kDa) was located at ≥ 9 mL from top, while about 81% of denatured Rubisco (55 kDa for the large subunit, and 15 kDa for the small subunit) was located at ≤ 8 mL from top. For non-preadsorbed Rubisco extracted from SB sediments, 86% was at ≤ 8 mL from top; for Rubisco pre-adsorbed on illite and goethite, the amounts at ≤ 8 mL were 73% and 88%, respectively. For non-preadsorbed Rubisco extracted from RB sediments, 79% was at ≤ 8 mL from top, and for that pre-adsorbed on goethite, 76% was. A portion of ^{14}C, about 10%, was precipitated by SDS and was located at the bottom of the tubes. The sucrose density gradient did not detect any difference between denatured Rubisco and ^{14}C-labeled proteins extracted from sediments after decomposition.

§7.3.2 *Molecular Size Distribution of Natural Sedimentary Proteins*

The protein concentrations in SB (6 cm) and RB (0-3 cm) sediments were 2.1 and 0.33 mg/g dry wt., respectively, according to the MB method. These account for about 4% and 6% of sedimentary TOC in SB and RB. For SDS-THAA, the concentrations were 3.8 mg/g for SB and 0.32 mg/g for RB, which account for about 7% and 6% of sedimentary TOC for SB and RB. THAA concentrations were 6.2 mg/g for SB and 0.57 mg/g for RB, which account for about 11% and 10% of sedimentary TOC (Table 7-4). Assuming that protein has a C/N ratio of 5 (mole/mole), N from proteins accounts for 8% of TN in SB sediment, and 12% for RB sediment.

SDS-extractable amino acids (THAA) in SB and RB show similar compositions (Figures 7-2 and 7-3). The most abundant amino acids in SB and RB sediments are Asp, Glu, Gly and Thr, and Ser, which accounted for about 80% of total sedimentary amino acids (Table 7-4). Both 15% and 20% SDS-PAGE gels show that most natural proteins were small (Figure 7-4). About 75 - 85% of the total proteins were < 12 kDa, and 15 - 25% of the proteins were > 100 kDa, and there was no protein detected between 12 and

100 kDa.

§ 7.4 Discussion

§7.4.1 *Decomposition of Proteins in Sediments*

Iron solid phases contribute a large specific surface area, and iron oxyhydroxides form strong complexes with organic substances having certain oxygen-containing functional groups, such as carboxylic acids (Stumm and Sulzberger, 1992). Also, the chemical form of reactive iron affects the surfaces available for organic matter adsorption. Fe redox cycling is known to affect the geochemistry of adsorbed substances such as phosphate (Stumm and Sulzberger, 1992). In sub-oxic and anoxic sediments, iron oxides can react as electron acceptors to reduce small monomers to CO_2 (Deming and Baross, 1993). Coupling of this process with OM oxidation occurs (Lovley, 1987).

In RB sediments, for non-preadsorbed decomposition, Rubisco was decomposed 1.1 times faster at 12 cm depth than at 6 cm depth. But for Rubisco pre-adsorbed on goethite, the decomposition rate at 12 cm was 3.8 times greater. Similarly, for GroEL pre-adsorbed on goethite, 1.3 times more was decomposed in 6 cm RB sediment than in surface sediment. This suggests that reduction of goethite caused protein desorption, making it more susceptible to decomposition. Microorganisms can readily reduce poorly crystalline Fe(III), but highly crystalline Fe(III), e. g., goethite, is generally not reducible (Phillips, *et al.*, 1993). Lovley and Phillips (1986b) found a strong correlation between the ability of Fe(III) reducers to reduce Fe(III) and the solubility of Fe(III) oxides in oxalate. Goethite generally cannot be extracted by oxalate. However, in the presence of catalytic quantities of Fe(II), it can be extracted, suggesting that goethite could be somewhat microbially-reducible in marine sediments, where Fe(II) is likely present.

Comparing the decomposition rates at 6 cm depth for both sites, non-preadsorbed Rubisco in SB sediment was decomposed 3.5 times more than in RB sediment after about 50 hours' incubation, for pre-adsorbed on illite, 3.6 times more; and for pre-adsorbed on goethite, 1.3 times more. The greater decomposition rates in SB sediments are consistent

with their greater organic content and higher rates of total OM oxidation. In both SB and RB sediments, pre-adsorption to clays generally decreased rates of protein decomposition to $^{14}CO_2$. However, the effect, compared to the decomposition rate of protein that was not preadsorbed, was small. This was probably because the SB and RB sediments rapidly and strongly adsorbed proteins, and any protective effect of adsorption existed in both types of experiments.

§7.4.2 *Protein Adsorption in Skan Bay and Resurrection Bay Sediments*

Clays and silts are thought to constitute most of the available surface for adsorption in continental margin sediments. Also, sedimentary organic matter could play an important role in the adsorption of amino acids, peptides, and aliphatic amines (Henrichs and Sugai, 1993; Wang and Lee, 1993; Luo, 1994). Data presented in Chapter 3 showed that pre-adsorption of charged poly-amino acids and proteins on minerals either enhanced or inhibited Rubisco adsorption substantially, reflecting the important role of adsorbate-adsorbate interactions in protein adsorption to sediments.

The apparent average adsorption partition coefficient of Rubisco on untreated SB sediments was 208 L/kg; for autoclaved sediments, it was 191 L/kg (Figure 5-2). The differences in adsorption partition coefficient between 0 - 3 cm and 6 - 9 cm depths, and between untreated and autoclaved RB sediments were small; all had a value of about 75 L/kg (Figure 6-2). SB sediments are organic-rich, containing 5 - 6% of TOC in surface sediments, which is about 10 times that in RB surface sediments. RB sediment consists of only about 2 - 3 % clay on a dry weight basis, primarily Fe-rich chlorites (Doyle, 1988). SB sediment contains < 6% clay, of which is 78% chlorites and 22% illite (Luo, 1994). In addition, data in Chapter 4 showed a tendency toward greater adsorption partition coefficients at lower particle concentrations. A series of adsorption experiments with constant Rubisco (15 μg) but varying sediment concentrations (3-6 cm, 0.25 - 1.25 g wet weight) were conducted. The results show that the adsorption partition coefficients were 55, 37, 25 and 17 L/kg at particle concentrations of 71, 135, 195 and 299 mg/mL,

respectively. For Rubisco adsorption to SB sediment (6 cm), they were 103, 96, 74, 53 L/kg at particle concentrations of 37, 51, 63 and 82 mg/mL, respectively. Because the pore water contents in RB and SB sediments were about 40% and 80%, the particle concentration in the adsorption experiments using RB sediments was about 2 times that for SB sediments. Therefore, the adsorption partition coefficients in SB and RB are the same at similar particle : solution ratios. This is surprising given the large differences in TOC, clay content, etc. One plausible explanation is that differences in adsorption behavior were not readily detected because the Rubisco solution contained a mixture of (mainly) strongly adsorbed Rubisco and weakly adsorbed, smaller proteins. The apparent partition coefficient measured here is essentially the ratio of Rubisco / weakly adsorbed proteins in the original solution, since (almost regardless of the properties of the adsorbent) nearly all of the Rubisco was adsorbed and almost none of the weakly adsorbed proteins were. This also accounts for similarities among adsorption isotherms of natural sediments, goethite, and clay minerals. Similar to Rubisco adsorption on pure minerals (Chapter 3), Rubisco was also resistant to desorption from both of the sediments, indicating that the partition coefficients of the strongly-adsorbed components of the solution were about the same as those for clay minerals.

Wang and Lee (1993) found that Lys adsorption to oxic sediment was much greater than that to anoxic sediments, which they attributed to enhanced adsorption by metal oxides. However, when Luo (1994) compared the adsorption of peptides in SB and RB sediments, she reported similar adsorption by these two sediments. Henrichs and Sugai (1993) and Sugai and Henrichs (in prep.) found that partition coefficients of amino acid adsorption to SB sediments were greater than those to RB sediments, although of the same order of magnitude. Also patterns of amino acid adsorption (basic » acidic > neutral) were similar at the two sites. Thus, the particle surface properties that govern adsorption of amino acids, peptides, and proteins do not seem to differ greatly between the two sediments, despite their obvious differences in other respects.

The difference between Rubisco adsorption on untreated and on autoclaved

sediments was significant, though small, in SB, while no difference was found for RB sediments. Autoclaving could change the apparent partition coefficient in several ways. Sugai and Henrichs (1992) found that autoclaving caused greatly increased amino acid concentrations in pore water, especially Glu, Gly and Ala, and decreased amino acid adsorption. Since the molecular size of Rubisco, and its adsorption partition coefficient, are much greater than those of amino acids and peptides, competitive adsorption is not a factor, but adsorbate-adsorbate attraction may be important. Desorption of charged and polar amino acids may result in less available binding sites for Rubisco. Alternatively, autoclaving could have caused structural change in sediment organic matter that slightly affected its sorptive properties. Luo (1993) also found that small peptide adsorption in autoclaved SB sediments was less than that in untreated sediments, but there was no difference in RB sediments, except for greater di-Glu adsorption in untreated sediments.

§7.4.3 *Extraction of ^{14}C-labeled Proteins from Sediments*

After adsorption and incubation for 48 h, ^{14}C-labeled Rubisco was extracted from sediments. The total % extracted results (Table 7-1) showed the order of ease of extraction: pre-adsorbed on a mineral in RB sediment > pre-adsorbed in SB sediment ≈ non-preadsorbed in both sediments (according to the sum of ^{14}C in SDS-1 and SDS-2).The total recovery of ^{14}C activity was: pre-adsorbed on a mineral in RB sediment > non-preadsorbed in RB sediment ≈ non-preadsorbed and pre-adsorbed on illite in SB sediment ≥ pre-adsorbed on goethite in SB sediment. This order was opposite to the decomposition rate (Chapters 5 and 6), except for pre-adsorbed Rubisco on goethite in 6 cm SB sediments, which had markedly slower decomposition. However, the overall pattern of incomplete recovery to extraction (about 70%) could be because adsorption on organic material-occupied surfaces makes a portion of the protein even more refractory than adsorption on organic-free mineral surfaces. Knicker and Hatcher (1997) found that encapsulation of labile proteins adsorbed on organic-rich sediments may make them refractory, as well as adsorption on minerals.

The extract solution (SDS-1) was subjected to SDS-PAGE. To make the solution ^{14}C activity high enough, only 250 μL of extraction solution was used to extract adsorbed Rubisco from 1 g wet sediment, which extracted the most easily removable portion. Therefore, less of the Rubisco (10 - 60 kDa, 57 - 67% of total added, Table 7-2) was extracted than from illite (~ 80% of total added, Table 3-7). Theoretically, the ratio between the large subunit (LS) and small subunit (SS) of Rubisco is 3.7. The ratio in the adsorbed fraction of Rubisco solution was 1.4 for 6 cm SB sediments, and 2.5 and 2.8 for 0 -3 and 6 - 9 cm RB sediments, respectively. The distribution of the ^{14}C activity in SDS-2 along a sucrose density gradient (Table 7-3) shows that adsorbed ^{14}C-labeled materials from SB have a greater portion of smaller proteins (2 - 3 mL from top), while those from RB have a greater portion of larger proteins (7 - 8 mL from top). Either the SS was preferentially extracted by SDS, especially from SB sediments, or there was less molecular size effect on adsorbed protein hydrolysis in RB sediments. In the pore water from decomposition experiments, the ratio of LS to SS was 6 for 6 cm SB, and 0.9 and 1 for 0 - 3 and 6 - 9 cm RB sediments. So, selective decomposition of small proteins may have occurred in SB pore water. In RB pore water, a lower proportion of larger proteins (> 60 kDa), and a smaller LS / SS ratio suggests that the LS has been hydrolyzed into smaller pieces. Also, there was less ^{14}C in the stacking gel of the SDS-PAGE of pore water from RB than SB, suggesting that more low molecular weight hydrolysis products were in SB pore water.

Rubisco and GroEL were adsorbed by minerals in their original forms (Chapter 3). Adsorbed Rubisco on SB and RB sediments was extracted after 48 h incubation then loaded on a sucrose density gradient. The results (Table 7-3) indicated that the adsorbed Rubisco was located at the same positions in the gradient as the original Rubisco denatured under the same conditions. This, in turn, is evidence that Rubisco was also mainly adsorbed in its original form by both SB and RB sediments.

§7.4.4 *Natural Proteins in Skan Bay and Resurrection Bay Sediments*

The major method currently used to estimate protein concentration in sediments is acid hydrolysis (e.g., Henrichs *et al.*, 1984), with the assumption that the total hydrolyzed amino acids are from proteins. The potential problem with this approach is that some amino acids from non-protein materials may be released, and thus lead to an overestimate of protein content. The method I developed for extracting protein without degradation has the potential problem of incomplete extraction, even though it has relatively high efficiency (~90%) for extracting adsorbed, radiolabeled Rubisco from both natural sediments and clay minerals.

Protein concentration determined by the MB method may be underestimated because 1) proteins precipitated by calcium phosphate may not be completely redissolved, to be stained by the dye reagent; and 2) some proteins, especially smaller ones, may have a different response to the dye reagent compared to the protein standard, BSA. However, the advantages of this new method are 1) quick and relatively efficient extraction of proteins from sediments, without serious degradation (but denaturation and dissociation occur); 2) the method of estimating protein concentration is simple, and eliminates the interference from soluble substances, such as humic substances and lipids (Pande and Murthy, 1994); and 3) the method greatly extends the usefulness of the Micro-Bradford procedure for low concentrations and complicated mixtures of sedimentary proteins.

The ratio of THAA/SDS-THAA was 1.6 for SB and 1.8 for RB. The excess of THAA relative to SDS-THAA could result from lysis and dissociation of living cells and greater degradation of detritus by the 6 N HCl. That is, some of the unextracted THAA may be refractory or insoluble proteins. Other non-protein substances may also contain THAA, e.g., humic acids and bacterial cell walls. The ratio of SDS-THAA/MB was 1.8 for SB and 0.97 for RB. The greater SDS-THAA/MB ratio for SB sediment may be related to its greater TOC and abundance of bacteria, since its TOC was about ten times

that of RB. So, about 30 - 50% of the sediment THAA was from proteins, and 60 - 100% of SDS-THAA was from proteins, based on the MB method. This is consistent with results of Mayer *et al.* (1986) and Pantoja and Lee (1998). But in all cases, the standardization of the method with BSA could lead to a systematic error, most likely an underestimate since most extractable sedimentary proteins are small. It is clear that much of the THAA, especially those extractable with SDS, are proteins.

Pantoja and Lee (1998) also compared the results of natural protein extraction using HCl hydrolysis and NaOH dissolution. The proteins, extracted by base, were separated by size by using various molecular weight cut-off membranes, available commercially incorporated into ultracentrifuge tubes. They found that larger proteins were selectively preserved in deeper sediments. The discrepancy between THAA removed by acid hydrolysis and base-extractable proteins tended to be larger in deeper sediments, and also depended on the sources and freshness of the proteins. A potential problem for their method is that the ultrafiltration membrane is designed to pass folded proteins, and the NaOH probably denatured them, leading to an overestimate of molecular size. Most adsorbed natural proteins, extracted by either acid or base or detergent, undergo partial hydrolysis, denaturation and dissociation. The unfolded proteins have long branch-like chains which may not pass through the "holes" in the filter if they are not in the right position. To investigate effects of denaturation on the performance of these ultrafilters, we used both 2% SDS plus 20% 2-mercaptoethanol and 5M guanidine-HCl to denature Rubisco (Iwanij *et al.*, 1974), and tried to use the 30 kDa cut-off membrane to separate its large subunit (LS, 55 kDa) and small subunit (SS, 15 kDa). Theoretically, 27% of the total added ^{14}C activity should pass through the filter (15 kDa / 55 kDa). Actually, after 30 minutes' centrifugation at 14,000 rpm, followed by twice diluting the upper solution with 2 times its original volume of 25 mM phosphate buffer (pH 7.2) and centrifugation at 14,000 rpm for 30 minutes, < 5% of the total added ^{14}C activity passed through the filter. Thus, we concluded that these ultrafilters would not provide reliable M.W. information.

Natural proteins in both SB (6 cm) and RB (0-12 cm) sediments extracted by using SDS plus 2-mercaptoethanol were predominantly small, with a molecular weight < 12 kDa, according to SDS-PAGE. Proteins extracted from both SB (6 cm) and RB (0-12 cm), were constituted of 15 - 25 % large proteins > 100kDa and 75 - 85% of small proteins < 12 kDa, with no detectable intermediate sized proteins. The apparently larger molecules may be coagulated proteins. Pantoja and Lee (1998) concluded that there is significant contribution of bacterial protein to sedimentary proteins. Typically, a cell membrane contains 40% lipid and 60% proteins (Orten and Neuhaus, 1970). Living cells in surface sediments may have been broken and the released proteins denatured by heating in the SDS solution. The denatured membrane proteins from living matter may flocculate when the pH is far from their pI, resulting in precipitation or coagulation after heating. Also, most membrane proteins are large and poorly soluble in aqueous solution. But, heating samples at 70°C for 24 h had little effect on the protein size distribution, except for slightly large proteins compared with mild extraction at 4°C, suggesting that the larger proteins were not an artifact of heating.

All depths analyzed from SB and RB sediments contained predominantly small proteins, indicating that most preserved proteins were small in both oxic and anoxic sediments. Conventionally, OM preserved in sediments is thought to be very high molecular weight, which renders it insoluble and relatively inaccessible to microbial attack. Such large molecules have been proposed to originate via condensation reactions and other diagenetic processes (Nissenbaum, 1974) or by selective preservation of refractory biopolymers (Tegelaar *et al.*, 1989). More recently, Mayer (1994b) proposed that preservation occurred because of physical protection within small "micropores" on clay mineral surfaces. Henrichs (1995) showed how multisite adsorption of macromolecules could lead to very strong adsorption with potential for preservation of OM on time scales of thousands of years.

I believe that my data provide strong evidence supporting the hypothesis that micropores, or similar small cavities, are preserving proteins in these sediments. Proteins

tend to adsorbed on solid surfaces via multi-site adsorption, especially at low particle concentrations or from much-diluted solutions (Chapter 4). Part of the adsorbed protein may be located within a "micropore" (Figure 7-5), but these are too small to completely accommodate larger proteins. For example, Mayer (1994b) has suggested that most clay mineral surface area is associated with pores < 10 nm in width. Metzler (1977) estimates the dimension of a 34 kDa protein to range from 100 × 0.5 nm (linear arrangement) to 5.4 × 2.7 nm (for an oblate spheroid). A domain consisting of 100 - 200 amino acid residues has an average diameter of 2.5 nm. For 100 amino acid residues, the length of unfolded protein is ~ 15 nm (Voet and Voet, 1995). Depending upon its conformation, it seems likely that only portions of such protein would be protected from enzymatic attack in a micropore. The exposed part could be "cut off" by proteolytic enzymes. Thus, eventually, most preserved proteins will be smaller ones.

Henrichs (1995) pointed out that large partition coefficients (K) would be necessary to the preservation of OM in coastal sediments by the mechanism of adsorption: K's on the order of 1000 or more would be required. She also discussed how multi-site adsorption of macromolecules can lead to such strong adsorption. Although the proteins and polypeptides found preserved in SB and RB sediments are small compared to many common proteins, they are sufficiently large to exhibit strong adsorption, consisting of up to 100 amino acid residues. Henrichs' (1995) calculations suggest that only 10 adsorption sites/molecule could lead to K's of 1000, given reasonable assumptions about adsorption strength at each adsorption site.

The THAA and SDS-THAA in both RB and SB sediments showed a similar distribution of amino acids, except for an order of magnitude difference in concentration. The most abundant amino acids in SB and RB sediments are Asp, Glu, Gly+Thr, Ser, which accounted for about 80% of total sedimentary amino acids (Table 7-4, Figures 7-2 and 7-3). This composition is similar to that found in most coastal sediments (Henrichs and Farrington, 1987; Burdige and Martens, 1988). The composition of THAA could reflect either source or adsorption behavior. For instance, Glu is the most abundant amino

acid in many plant and animal proteins (Orten and Neuhaus, 1970). Our previous work showed (Chapter 3) that negatively charged poly- Glu and Asp inhibited Rubisco adsorption, suggesting that carboxyl groups are involved in its adsorption. It is interesting that Gly is often the most abundant single amino acid in THAA, and is relatively in more abundant in sediment THAA than in most organisms (e. g., Henrichs and Farrington, 1987). Proteins are most flexible at glycine residues. It is reasonable that the most flexible (and glycine-rich) segments of proteins would be best able to accommodate to surfaces within micropores.

The fate of protein in marine sediments may be also associated with hydrolysis to small soluble organic substances, such as peptides and FAA, and their subsequent oxidation to CO_2. Glutamic acid and alanine are the predominant dissolved free amino acids (DFAA) in Skan Bay and most anoxic marine sediments (Henrichs and Farrington, 1987; Burdige and Martens, 1988; McDaniel, 1989; Burdige, 1991). DFAA are thought to be the product of hydrolysis of protein by fermentative bacteria (Reichardt, 1986; Mayer, 1989). Luo found that during decomposition, peptides in both pore water and sediment from SB were firstly hydrolyzed into FAA, and then oxidized to CO_2 by bacteria. Although the hydrolysis process is rapid, it may be a rate-limiting step for decomposition of small alanyl and glutamyl peptides in sediment. Again, the initial peptide hydrolysis was rapid, but this process was a rate-limiting step in the decomposition. Comparing the decomposition of peptides in SB and RB, no significant difference in peptide hydrolysis rates was found. Adsorption decreased peptide decomposition rates at both sites and may play a significant role in their longer-term preservation.

§ 7.5 Conclusions

1) The Rubisco decomposition rate was greater in SB sediments than in RB sediments. This is probably related to the greater organic content and OM oxidation rates in SB sediments.

2) Adsorption of Rubisco by organic-rich, anoxic SB sediment was nearly the same as adsorption by oxic, low-organic RB sediment.

3) Rubisco was adsorbed by sediments in its original form.

4) A greater proportion of smaller ^{14}C-labeled proteins in SB sediments than in RB sediments after decomposition indicated that larger proteins were being more rapidly hydrolyzed to smaller ones in SB sediments.

5) A new protein determination method showed that about 30 - 50% of THAA and 60 - 90% of SDS-extractable THAA were from proteins. The protein concentration in 6 cm SB sediments was 2.1 mg/g, and in surface RB sediments was 0.33 mg/g.

6) SDS-PAGE showed that the naturally-occurring proteins extracted from sediments by SDS were mainly < 12 kDa. This finding supports the hypothesis that proteins are preserved by adsorption in small cavities on particle surfaces.

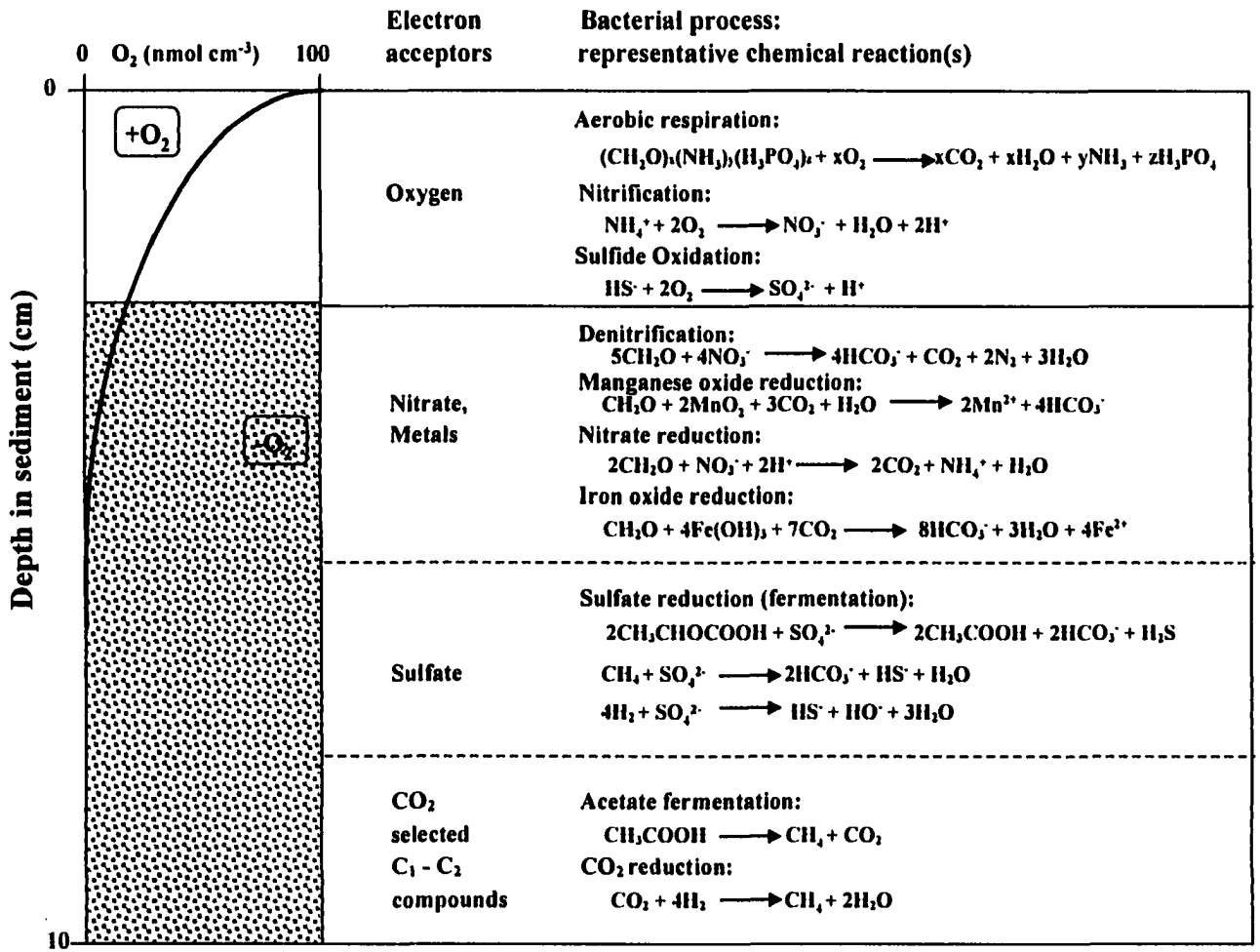

Figure 7-1. Idealized zones of organic carbon degradation, coupled to respiratory functions, by bacteria in sediments (from Deming and Baross, 1993)

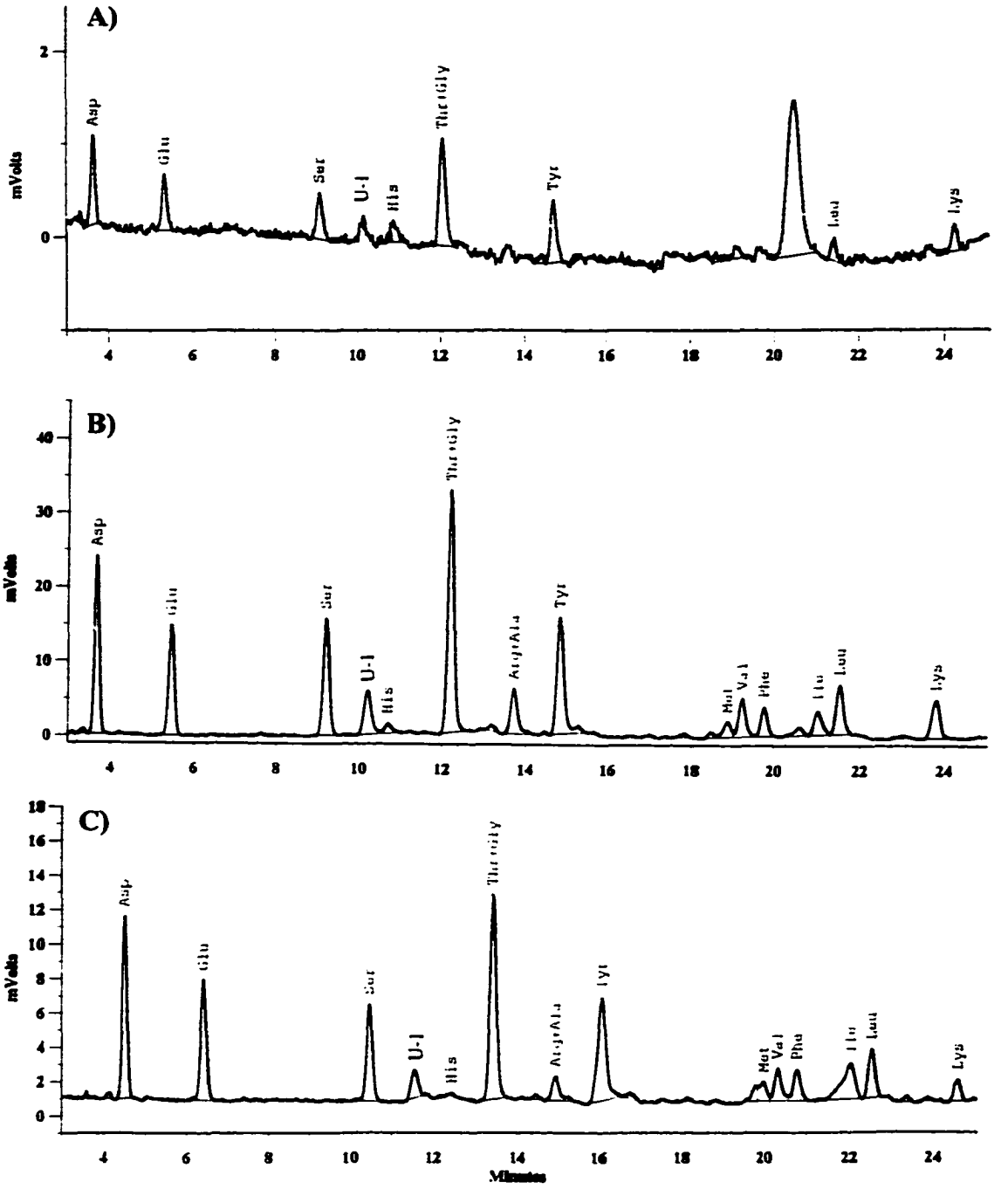

Figure 7-2. THAA in Skan Bay A) pore water; B) 6 cm sediment and C) 2.5% SDS extract solution.

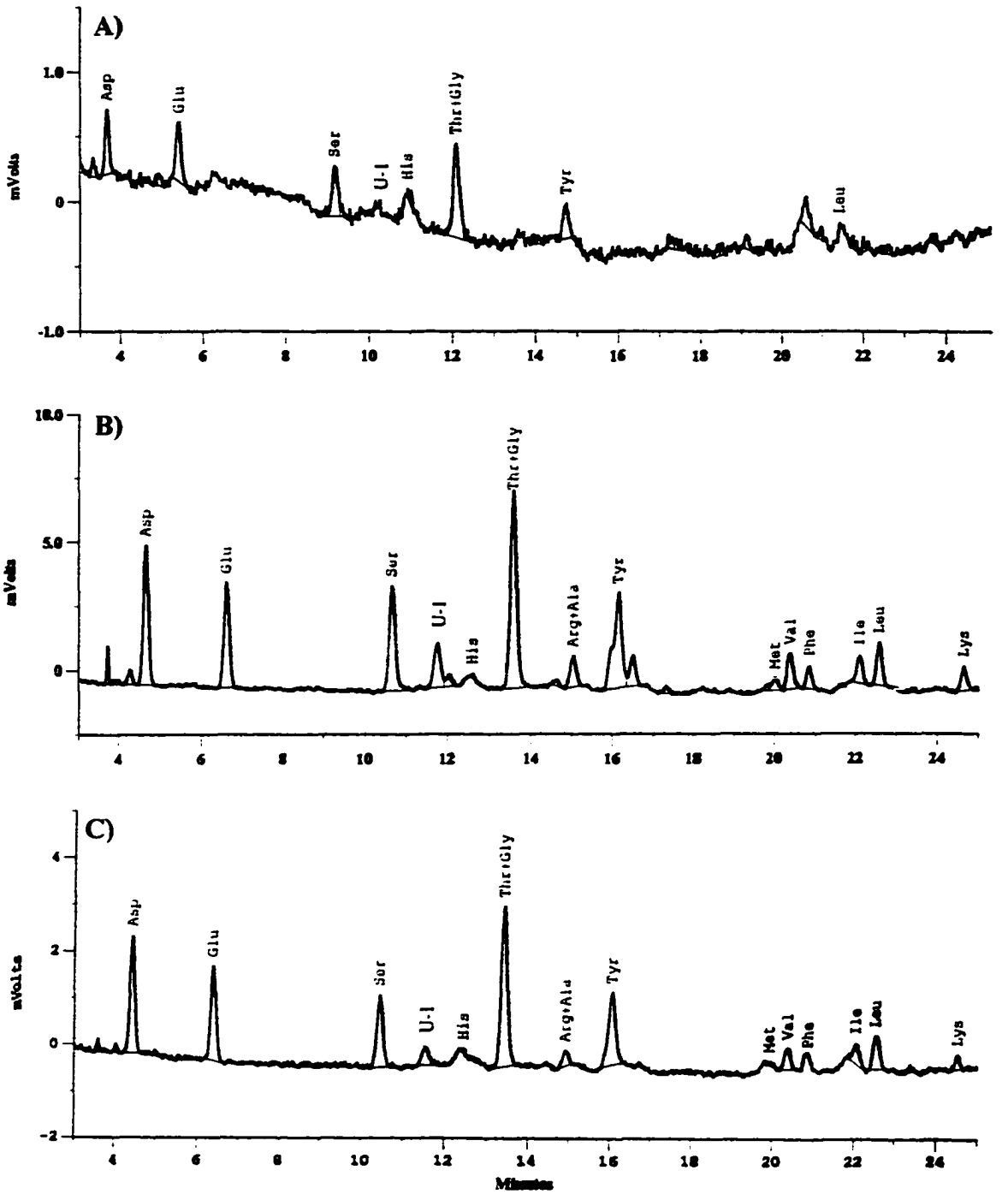

Figure 7-3. THAA in Resurrection Bay A) pore water; B) 6 cm sediment and C) 2.5% SDS extract solution.

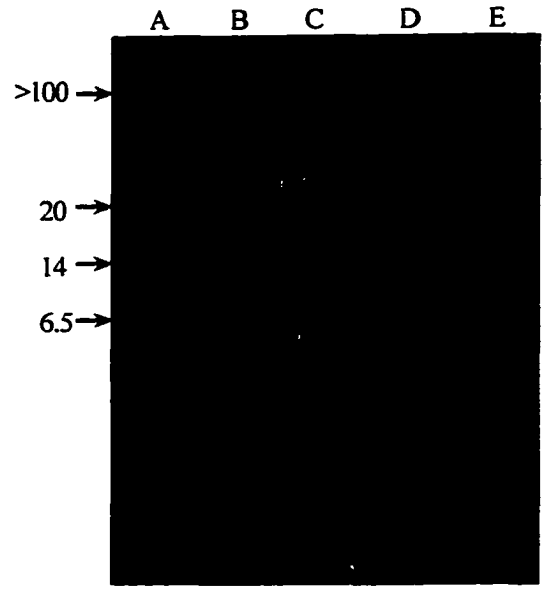

Figure 7-4. 20% SDS-PAGE of A) molecular weight standards (in kDa); sedimentary proteins from B) Skan Bay (6 cm) and C) to E) Resurrection Bay (0-3, 3-6 and 6-9 cm, respectively).

Table 7-1. Efficiency of extraction of adsorbed Rubisco from Skan Bay and Resurrection Bay sediments using 5% SDS plus 5% 2-mercaptoethanol.

Sediments	Rubisco[a]	Supernatant (%)[b]	SDS-1[c] (%)	SDS-2 (%)	SDS-3 (%)	Total (%)
SB (6 cm)	Non	5	12	36	19	72
	Ill	2	14	43	15	74
	Fe	< 1	13	43	10	67
RB (0-3 cm)	Non	11	14	36	15	76
	Ill	1	32	58	7	98
	Fe	1	26	64	4	95
RB (6-9 cm)	Non	13	13	36	15	77

a: abbreviations: Non: non-preadsorbed; Ill: pre-adsorbed on illite; Fe: pre-adsorbed on goethite.

b: % of total ^{14}C activity added.

c: 250 μL 5% SDS plus 5% 2-mercaptoethanol was used to extract adsorbed Rubisco from 1.0 g wet sediments in SDS-1; 5 mL were used in SDS-2 and SDS-3.

Table 7-2. ^{14}C activity distribution on SDS-PAGE gel after Rubisco decomposition in Skan Bay and Resurrection Bay sediments.

Adsorbed or Dissolved	Sediments	Location on gel	M.W. (kDa)	Relative composition (%)
adsorbed	SB, 6 cm	stacking		9
		separating	> 60	14
			30-60	37
			10-30	26
			< 10	13
Dissolved		stacking		36
		separating	> 60	6
			30-60	42
			10-30	7
			< 10	10
adsorbed	RB, 0-3 cm	stacking		12
		separating	> 60	12
			30-60	48
			10-30	19
			< 10	9
Dissolved		stacking		23
		separating	> 60	5
			30-60	18
			10-30	19
			< 10	36
adsorbed	RB, 6-9 cm	stacking		11
		separating	> 60	20
			30-60	42
			10-30	15
			< 10	12
dissolved		stacking		21
		separating	> 60	4
			30-60	21
			10-30	21
			< 10	34

Table 7-3. Sucrose density gradient distribution of adsorbed Rubisco extracted from Skan Bay (6 cm) and Resurrection Bay (0-3 cm) sediments using 5% SDS plus 5% 2-mercaptoethanol*.

Location (mL from top)	Original (%) [a]	Denatured (%)	SB Non(%)	SB Ill(%)	SB Fe(%)	RB Non(%)	RB Fe(%)
1	1.4	11	8	7	9	8	6
2	1.4	13	13	10	12	8	8
3	1.6	13	8	13	14	11	9
4	1.2	12	16	11	14	9	9
5	2.1	11	14	11	17	11	11
6	2.8	7	17	10	15	11	13
7	4.8	9	7	6	5	12	10
8	6.6	5	3	5	2	9	10
9	8.0	2	1	5	3	6	6
10	8.0	2	3	2	0	4	3
11	9.3	1	0	2	0	2	0
12	20.1	4	1	2	3	4	3
12-13	32.7	1	1	1	1	2	1
SDS [b]		9	8	15	5	3	10
Recovery [c]	91.1	98	88	86	99	93	90

*: abbreviations: Non: non-preadsorbed Rubisco; Ill: pre-adsorbed Rubisco on illite; Fe: pre-adsorbed Rubisco on goethite.
a: % of total ^{14}C activity measured in the sucrose gradient.
b: SDS precipitated from the sucrose density gradients.
c: % of total ^{14}C activity loaded on the sucrose gradient.

Table 7-4. Comparison of THAA in the pore water and sediments from Skan Bay (6 cm) and Resurrection Bay (0-3 cm).

	pore water (μg/mL)		SB (mg/g dry wt.)			RB (mg/g dry wt.)		
Amino acids	SB	RB	THAA	SDS-THAA	R*	THAA	SDS-THAA	R*
Asp	1.0	0.7	0.8	0.4	2.0	0.07	0.04	1.9
Glu	0.7	0.7	0.6	0.3	2.0	0.06	0.04	1.8
Ser	0.6	0.5	0.5	0.2	2.5	0.05	0.03	2.3
U-1#	0.3	0.2	1.4	0.3	4.7	0.14	0.05	2.8
His	0.4	0.2	0.2	0.03	6.7	0.01	0.03	0.5
Thr + Gly	0.7	0.6	0.6	0.2	3.0	0.05	0.04	1.1
Arg + Ala			0.3	0.1	4.3	0.02	0.01	2.2
Tyr#	0.7	0.3	0.6	1.8	0.3	0.06	0.02	2.4
Met			0.1	0.06	1.7	0.01	0.01	1
Val			0.2	0.07	2.9	0.02	0.01	2.9
Phe			0.2	0.1	2.0	0.02	0.01	1.9
Ile			0.1	0.1	1.0	0.02	0.01	1.6
Leu		0.03	0.3	0.1	3.0	0.02	0.01	2.2
Lys	0.7		0.3	0.1	3.0	0.02	0.01	3.3
Total	5.0	3.2	6.2	3.8	1.6	0.57	0.32	1.8

*: the ratio between THAA and SDS-THAA.

#: unknown, coeluted with Gln or Tyr. Gln could not be present in the hydrolyzed solution. It could be β-Ala.

Summary and Conclusions

The Copper River and streams draining the Bering and Malaspina Glaciers are the dominant sediment sources in the NE Gulf of Alaska and supply about 50% of the OM in these sediments. Annual TOC accumulation is 45 - 70 × 10^4 tons over the past century. Greater surface sedimentary TOC and TN were found in areas with larger Holocene sediment accumulations, except in the upper Copper River Delta sediments, and in glacially-derived sediments within and near the mouth of Icy Bay, and within Yakutat Bay and central Prince William Sound. Lighter carbon and nitrogen and greater C/N were associated with greater TOC and TN, indicating that the sediments with greater organic content had a larger terrigenous component.

The Great Alaskan Earthquake, Bering Glacier surge, the retreat of Malaspina Glacier and a climatic "Regime Shift" were recorded in some cores. However, most of the cores collected in the NE Gulf of Alaska showed little variation in OM content or sources with time. Further, within the sediment, diagenesis had only a modest effect on the isotopic composition of OM, and this appeared to occur mainly during the first few years after deposition. However, it is clear that decomposition, occurring either when the sediment particles were being transported to their ultimate deposition site or at the sediment-water interface, must have had a substantial impact on the quantity and isotopic composition of OM buried in the NE Gulf of Alaska. That is, fossil and terrigenous sources of OM dominated nearshore, but the offshore sediments contained predominantly marine-derived OM. Since the percent TOC of nearshore sediments was generally greater, and all of the sediment is lithogenic and presumably derived from the same continental sources, it appears that the fossil and terrigenous OM is destroyed in the sediments transported offshore, but preserved when buried nearshore. An alternate interpretation is that the finer-grained material carried offshore contained little or no OM to start with, compared to the generally coarser material found nearshore. But this is rather unlikely, given that many studies have shown that both terrigenous and marine-derived OM are mainly associated

with smaller particles (Keil *et al.*, 1994). Also, in the case of the physical rock weathering and lack of soil processing found in Icy Bay and Yakutat Bay, it seems unlikely that the OM content would vary systematically with particle size.

Henrichs (1995) proposed that desorption from particles as they are transported in water with low particle : solution ratios would tend to cause loss of OM due to desorption, while rapid burial in sediments, with high particle : solution ratios, would favor retention of OM. This could explain the patterns observed in the NE Gulf of Alaska. However, it remains to be conclusively demonstrated that adsorption can and does lead to OM preservation. And, if adsorption is a major process leading to preservation, it is unknown whether it is selective for certain types of OM, thus leading to a sedimentary record that does not necessarily quantitatively reflect the true sources. My studies of protein adsorption and decomposition begin to address these key questions.

Proteins were strongly adsorbed by illite, montmorillonite, and goethite. This process was rapid and reached steady state in < 1.5 hour. The partition coefficients for proteins were about 10^4 - 10^6 L/kg. These partition coefficients are large enough to be consistent with adsorptive preservation in sediments (Henrichs, 1995). Rubisco and GroEL were adsorbed on illite in their original forms. The activity remaining in the supernatant after adsorption was mostly smaller proteins, with partition coefficients of 10 - 10^2 L/kg, indicating a molecular size effect on adsorption. Pre-adsorption of negatively charged macromolecules inhibited Rubisco adsorption, indicating competition for the same binding sites, while positively charged macromolecules enhanced Rubisco adsorption. Both influences were greater when more poly-amino acid or protein was pre-adsorbed. These results indicate that the nature of the protein, the solid phase and any other adsorbed OM could all affect protein adsorption by sediments.

Rubisco was also adsorbed by SB and RB sediments in its original form. Because the sediments rapidly and strongly adsorbed proteins, their decomposition was slow regardless of whether the protein was adsorbed to a mineral. In both sediments, dissolved proteins were selectively decomposed relative to adsorbed proteins, indicating that

adsorption protects proteins from decomposition, at least on time scales of days to weeks. The Rubisco decomposition rate was greater in SB sediments than in RB sediments, consistent with the greater rate of TOC oxidation found in SB sediments (Henrichs and Doyle, 1986; Alperin *et al.*, 1992). SB Sediment anoxia did not inhibit protein decomposition. In 12 - 15 cm SB sediments, more Rubisco was decomposed than in 6 - 12 cm sediments, if the protein was adsorbed to goethite, suggesting that enhanced microbial activity or iron oxide dissolution due to Fe(III) reduction increased protein metabolism. In surface RB sediments, more Rubisco was decomposed than in deeper sediments, due to greater bacterial numbers near the sediment-water interface.

A new protein determination method showed that about 30 - 50% of the total hydrolyzed amino acids (THAA) and 60 - 90% of SDS-THAA (sodium dodecyl sulfate extracted THAA) were from proteins. The protein concentration in 6 cm SB sediments was 2.1 mg/g, and was it was 0.33 mg/g for surface RB sediments. SDS-PAGE showed that proteins extracted from both RB and SB sediments by SDS were mainly < 12 kDa. This finding supports the hypothesis that proteins are preserved by adsorption in small cavities on particle surfaces. The small size of most sedimentary proteins would then be explained by their fitting into the micropores. Larger proteins, or portions of proteins protruding from the cavities, would not be protected from decomposition on time scales of years.

However, there are still some unanswered questions. Nearly all naturally-occurring proteins are small, but is this true for other types of sedimentary OM, such as carbohydrates? I hypothesize that the small molecular sizes observed for proteins will be a general characteristic of labile biochemicals found in sediments. DNA would be an interesting material for a first test of this hypothesis, since dissolved DNA is rapidly decomposed by bacteria, and its molecular size is easily determined. Selective decomposition of proteins, and of organic nitrogen relative to carbon, has been found in many different marine sediments. The strength of adsorption and small molecular size may play an important role in OM preservation, but does not easily explain why strongly-adsorbed proteins are more labile than other OM (e.g., Henrichs *et al.*, 1984). The bulk of

sediment OM is not readily identifiable as major biochemicals such as carbohydrates, proteins, lignin, or nucleic acids. This uncharacterized material (often termed "humic material") tends to increase with time, and extent of decomposition. Some evidence indicates that it is of higher average molecular weight than preserved proteins, and it is not yet clear what the relative importance of adsorption, physical protection in micropores, and intrinsically refractory structure is in OM preservation. My results have helped to elucidate preservation mechanisms for an important fraction of sediment OM, but future work needs to examine whether processes important for proteins apply to all sediment OM.

References

Abeles, R. H., Frey, P. A. and Jencks, W. P., 1992, In: *Biochemistry*, Jones and Bartlett Publishers, **Ch. 7**, 173-210.

Ahmed, S. I. And Devol, A. H., 1995, Aerobic and anaerobic decomposition of organic matter in marine sediment: which is fastest?, *Limnol. Oceanogr.*, **40(8)**, 1430-1437.

Alperin, M. J., 1988, The carbon cycle in an anoxic marine sediment: concentrations, rates, isotope ratios, and diagenetic models, *Ph.D Thesis*, University of Alaska Fairbanks, **Ch. 2**, 14 - 68.

Alperin, M. J., Reeburgh, W. S. and Devol, A. H., 1992, Organic carbon remineralization and preservation in sediments of Skan Bay, Alaska. In: *Productivity, Accumulation and Preservation of Organic Matter in Recent and Ancient Sediments*, Whelan, J. K. and Farrington, J. W. (eds.), Columbia Univ. Press, New York, pp. 99-122.

Altabet, M. A. and Francois, R., 1994, Sedimentary nitrogen isotopic ratio as a recorder for surface ocean nitrate utilization, *Global Biogeochem. Cycles*, **8**(1), 103-116.

Andrade, J. D., 1985, Principles of Protein Adsorption, In: *Surface and Interfacial Aspects of Biomedical Polymers*, Andrade, J. D., (ed.), Plenum Press, New York and London, **2**, 1-80.

Arain, R., 1985, Carbon and mineral transport of Indus River 1982-1983, In: *Transport of Carbon and Minerals in Major World Rivers*, **part III**, Degens, E. T. *et al.*, (eds.), pp. 487-494.

Atlas, R. M. and Parks, L. C., 1993, *Handbook of Microbiological Media*, CRC Press, pp. 44-45.

Bada, J. L. and Mann, E. H., 1980, Amino acid diagenesis in DSDP cores: Kinetics and mechanisms of some reactions and their applications in geochronology and in paleotemperature and heat flow determinations, *Earth Sci. Rev.*, **16**, 21-57.

Benner, R., Maccubbin, A. E. and Hodson, R. E., 1984, Anaerobic biodegradation of the lignin and polysaccharide components of lignocellulose and synthetic lignin by

sediment microflora, *Appl. Environ. Microbiol.*, **47**, 998-1004.

Berner, R. A., 1980, In: *Early Diagenesis: A Theoretical Approach*, Princeton Univ. Press, Princeton, NJ, 241 pp.

Bigeleisen, J. and Wolfsberg, M., 1958, Theoretical and experimental aspects of isotope effects in chemical kinetics. *Adv. Chem. Phys.*, **1**, 15-76.

Biggs, D. C., Berkowitz, S. P., Altabet, M. A., Bidigare, R. R., De master, D. J., Dunber, R. B., Leventer, A., Macko, S. A., Nittrouer, C. A. and Ondrusek, M. E., 1988, A cooperative study of upper ocean particulate fluxes in the Weddell Sea, In: *Initial Reports of the Ocean Drilling Program Leg 113*, **part A**, Barker, P. F. *et al.* (eds.), College Station, TX pp. 77-85.

Biggs, D. C., Berkowitz, S. P., Altabet, M. A., Bidigare, R. R., De master, D. J., Macko, S. A., Ondrusek, M. E. and Noh, I., 1989, A cooperative study of upper ocean particulate fluxes in the Weddell Sea, In: *Initial Reports of the Ocean Drilling Program Leg 119*, **part A**, Larren, B. *et al.* (eds.), College Station, TX pp. 109-119.

Bochkareva, E. S., Lissin, N. M. and Girshovich, A. S., 1988, Transient association of newly synthesized unfolded proteins with the heat-shock GroEL protein, *Nature*, **336**, 254-257.

Bogdanov, K.,1963, Water circulation in the Gulf of Alaska and its seasonal variability (translated from Russian), *Deep Sea Res.*, **10**: 479-487.

Bolin, B. Crutzen, P. J. Vitousek, P. M., Woodmansee, R. G., Goldberg, E. D. and Cook, R. B., 1983, Interactions of biogeochemical cycles, In: *The Major Biogeochemical Cycles and Their Interactions*, Bolin, B. and Cook, R. B. (eds.), John Wiley & Sons, **Ch. 1**, pp. 1-39.

Bothner, J. L. and Horbett, T. A., 1986, Changes in adsorbed fibrinogen and albumin interactions with polymers indicated by decrease in detergent elutability, *J. Colloid Interface Sci.*, **111**, 363-377.

Bradford, M. M., 1976, A rapid and sensitive method for the quantitation of microgram

quantities of protein utilizing the principle of protein-dye binding, *Anal. Biochem.*, **72,** 248-254.

Broecker, W. S. and Peng, T.-H., 1982, In: *Tracers in the Sea*, Eldigio Press, New York.

Burbank D.C., 1974, Suspended sediment transport and deposition in Alaskan coastal waters. M. S. Thesis, *University of Alaska Fairbanks*, 222 pp.

Burdige, D. J., 1991, Microbial processes affecting alanine and glutamic acid in anoxic marine sediments, *FEMS Microb. Ecol.*, **85**, 211-232.

Burdige, D. J. and Martens, C. S., 1988, Biogeochemical cycling in an organic-rich marine basin: 10, the role of amino acids in sedimentary carbon and nitrogen cycling. *Geochim. Cosmochim. Acta*, **52**, 1571-1584.

Burdige, D. J. and Martens, C. S., 1990, Biogeochemical cycling in an organic-rich marine basin: 11, the sedimentary cycling of dissolved, free amino acids, *Geochim. Cosmochim. Acta*, **52**, 3033-3052.

Burns, R. G., 1978, Enzyme activity in soil: some theoretical and practical considerations, In: *Soil Enzymes*, Burn, R. G. (ed.), Academic Press, London, pp. 295-340.

Cadée, G. C., 1982, Organic carbon and phytoplankton in Zaire River, estuary and plume, In: *Transport of Carbon and Minerals in Major World Rivers*, **part I**, Degens, E. T. (ed.), pp. 429-431.

Cantarow, A. and Scheartz, B., 1967, Metabolism of proteins, In: *Biochemistry*, 4th edition, W. B. Saunders Company, **Ch. 21**, 539-605.

Carlson, P. R. and Molnia, B. F., 1977, Submarine faults and slides on the continental shelf, northern Gulf of Alaska, *Mar. Geotech.*, **2**, 275-290.

Carlson, P. R. and Molnia, B. F., 1978, Minisparker profiles and sedimentologic data from R/V Acona cruise (April 1976) in the Gulf of Alaska and Prince William Sound, U.S. Geological Survey Open-file Report 78-381. 2 sheets, 32 pp.

Carlson, P. R., Molnia, B. F., Kittelson, S. C. and Hampson Jr., J. C., 1977, Distribution of bottom sediments on the continental shelf, northern Gulf of Alaska. *U. S. Geol. Surv., Misc. Field Stud.*, Map MF-876. 2 sheets and 13 pp.

Carlson, P. R., Bruns, T. R., Molnia, B. F. and Schwab, W. C., 1982, Submarine valleys in the northeastern Gulf of Alaska: characteristics and probable origin, *Mar. Geo.*, **47**, 217-242.

Cauwet, G. and Martin, J. M., 1982, Organic carbon transported by French rivers. In: *Transport of Carbon and Minerals in Major World Rivers*, **part I**, Degens, E. T. (ed.), pp. 475-481.

Chandrasekhar, G. N., Tilly, K., Woolford, C., Hendrix, R. and Georgopoulos, C., 1986, Purification and properties of the groES morphogenetic protein of *Escherichia coli*, *J. Biol. Chem.*, **261**, 12414-12419.

Chen, Z. and Spreitzer, J., 1991, Proteolysis and transition-state-analogue binding of mutant forms of ribulose-1,5-bisphosphate carboxylase/oxygenase from *Chlamydomonas reinhardtii*, *Planta*, **183**, 597-603.

Christensen, D. and Blackburn, T. H., 1982, Turnover of ^{14}C-labeled acetate in marine sediments, *Mar. Biol.*, **71**, 113-119.

Christy, Jr., K. G., LaTart, D. B. and Osterhoudt, H. W., 1989, Modifications for SDS-PAGE of proteins, *Biotechniques*, 7(7), 692-693.

Clermont, M. G. and Rahire, M., 1986, Sequence, evolution and differential expression of the two genes encoding variant small subunits of ribulose bisphosphate carboxylase/oxygenase in *Chlamydomonas reinhardtii*, *J. Mol. Biol.*, **191**, 421-432.

Cline, J. D. and Kaplan, I. R., 1975, Isotopic fractionation of dissolved nitrate during denitrification in the eastern tropical North Pacific Ocean. *Mar. Chem.* **3**, 271-299.

Cloos, P., Calicis, B., Fripiat, J. J. and Makay, K., 1966, Adsorption of amino acids and peptides by montmorillonite, I. Chemical and X-ray diffraction studies, Proc. Int. Clay Conf., Jerusalem, *Clay Miner. Soc.*, **1**, 223-232.

Coale, K. H., Johnson, K. S., Fitzwater, S. E., Gordon, R. M., Tanner, S., Chavez, F. P., Ferioli, L., Sakamoto, C., Rogers, P., Millero, F., Steinberg, P., Nightingale, P.,

Copper, D., Cochlan, W. P. and Kudela, R., 1996, A massive phytoplankton bloom induced by an ecosystem-scale iron fertilization experiment in the Equatorial Pacific Ocean, *Nature*, **383**(6600), 495-501.

Coleman, M. L., Hedrick, D. B., Lovley, D. R., White, D. C. and Pye, K., 1993, Reduction of Fe (III) in sediments by sulphate-reducing bacteria, *Nature*, **361**, 436-438.

Committee on the Alaska earthquake, 1972, Tsunamis, In: *The Great Alaska Earthquake of 1964 - Oceanography and Coastal Engineering*, National Academy of Science, 31-248.

Committee on the Bering Sea Ecosystem, 1996, The Bering Sea ecosystem: geology, physics, chemistry, and biology of lower trophic levels, In: *The Bering Sea Ecosystem*, National Research Council, **Ch. 3**, 28-71.

Cowie, G. L. and Hedges, J. I., 1993, A comparison of organic matter sources, diagenesis and preservation in oxic and anoxic coastal sites, *Chem. Geol.*, **107**, 447-451.

Curiale, J. A., 1993, Oil to source rock correlation concepts and case studies, In: *Organic Geochemistry, Principles and Applications*, Engel, M. H. and Macko, S. A. (eds.), **Ch. 21**, 473-490.

de Leeuw, J. W. and Largeau, C., 1993, A review of macromolecular organic compounds that comprise living organisms and their role in kerogen, coal, and petroleum formation, In: *Organic Geochemistry, Principles and Applications*, Engel, M. H. and Macko, S. A. (eds.), Plenum Press, New York and London, **Ch. 2**, 23 - 72.

Delwiche, C. C. and Steyn, P. L., 1970, Nitrogen isotope fractionation in soils and microbial reactions, *Environ. Sci. Technol.* **4**, 929-935.

Deming, J. W. and Baross, J. A., 1993, The early diagenesis of organic matter: bacterial activity, In: *Organic Geochemistry, Principles and Applications*, Engel, M. H. and Macko, S. A., (eds), **Ch. 5**, 119-144.

Depetris, P. J. and Cascante, E., 1985, Carbon transport in the Paraná River, In: *Transport of Carbon and Minerals in Major World Rivers*, **part III,** Degens, E. T. *et al.*, (eds.), pp. 299-304.

Di Toro, D. M., Mahony, J. D., Kirchgraber, P. R., O'Byrne, A. L., Pasquale, L. R. and Piccirilli, D. C., 1986, Effects of nonreversibility, particle concentration, and ionic strength on heavy metal sorption, *Environ. Sci. Technol.*, **20**, 55-61

Doyle, A. P., 1988, Respiration and adsorption of alanine, glutamic acid, lysine and glucose in sediments from Resurrection Bay, Alaska. *M. S. Thesis*, University of Alaska Fairbanks.

Dyal, R. S. and Hendricks, S. B., 1950, Total surface of clays in polar liquids as a characteristic index, *Soil Sci.*, **69**, 421-43.

Ehrlich, H. L., 1978, Inorganic energy sources for chemolithotrophic and mixotrophic bacteria, *Geomicrobiol.*, **1**(1), 65-83.

Eisma, D., Cadée, G. C. and Laane, R., 1982, Supply of suspended matter and particulate and dissolved organic carbon from Rhine to the coastal North Sea, In: *Transport of Carbon and Minerals in Major World Rivers*, **part I**, Degens, E. T. (ed.), pp. 483-505.

Ellis, J., 1979, The most abundant protein in the world, *Trends Biochem. Sci.*, **4**, 241-244.

Emerson, S. E. and Hedges, J. I., 1988, Processes controlling the organic carbon content of open ocean sediments, *Paleoceanogr.*, **3**, 621-634.

Ensminger, L. E. and Gieseking, J. E., 1939, The adsorption of proteins by montmorillonite clay, *Soil Sci.*, **48**, 467-473.

Ertel, J. R. and Hedges, J. I., 1985, Sources of sedimentary humic substances: vascular plant debris, *Geochim. Cosmochim. Acta*, **49**, 2097-2107.

Feely, R. A., Baker, E. T., Schumacher, J. D., Massoth, G. J. and Landing, W. M., 1979, Processes affecting the distribution and transport of suspended matter in the northeastern Gulf of Alaska. *Deep -Sea Res.* **26**, 445-464.

Fenchel, T. and Blackburn, T. H., 1979, *Bacteria and Mineral Cycling*, Academic Press, London, p. 225.

Georgopoulos, C., 1992, The emergence of the chaperone machines, *Trends Biochem. Sci.*, **17**, 295-299.

Giordani, G., Bartoli, M., Cattadori, M. and Viaroli, P., 1996, Sulphide release from anoxic sediments in relation to iron availability and organic matter recalcitrance and its effects on inorganic phosphorus recycling, *Hydrobiologia*, **329**, 211-222.

Goodell, H. G., 1972, Carbon/nitrogen ratio, In: *Encyclopedia of Geochemistry and Environmental Science*, pp. 136-142.

Grim, R. E., 1968a, Ion exchange and sorption, In: *Clay Mineralogy*, McGraw-Hill Book Company, NY, 185-233.

Grim, R. E., 1968b, Clay mineral - organic reaction, In: *Clay Mineralogy*, McGraw-Hill Book Company, NY, 353-411.

Grinnel, F. and Feld, M. K., 1982, Fibronectin adsorption on hydrophilic and hydrophobic surfaces detected by antibody binding and analyzed during cell adhesion in serum-containing medium, *J. Biol. Chem.*, **257**, 4888-4893.

Gross, C. A., Straus, D. B., Erickson, J. W. and Yura, T., 1990, In: *Stress Proteins in Biology and Medicine*, Morimoto, *et al.* (eds.), Cold Spring Harbor Laboratory Press, pp. 166-190.

Hampton, M. A., Carlson, P. R. and Lee, H. J., 1987, In: *The Gulf of Alaska, Physical Environment and Biological Resources*, **Ch. 5**, 93-143.

Harrison, W. D., Echelmeyer, K. A., Chacho, E. F., Raymond, C. F. and Benedict, R. J., 1994, The 1987-88 surge of West Fork Glacier, Susitna Basin, Alaska, U. S. A., *J. Glaciology*, **40**(135), 241-254.

Hart, R. C., 1985, Aspects of the hydrogeochemistry of the Upper Orange River, In: *Transport of Carbon and Minerals in Major World Rivers*, **part III**, Degens, E. T. *et al.*, (eds.), pp. 435-442.

Hedges, J. I. and Keil, R. G., 1995, Sedimentary organic matter preservation: an assessment and speculative synthesis, *Mar. Chem.*, **49**, 81-115.

Hedges, J. I., Clark, W. A. and Cowie G. L., 1988a, Organic matter sources to the water column and surficial sediments of a marine bay, *Limnol. Oceanogr.*, **33**(5), 1116-1136.

Hedges, J. I., Clark, W. A. and Cowie G. L., 1988b, Fluxes and reactivities of organic matter in a coastal marine bay, *Limnol. Oceanogr.*, **33**(5), 1137-1152.

Heinrichs, T. A., Mayo, L. R., Trabant, D. C. and March, R. S., 1995, Observations of the surge-type Black Glacier, Alaska, during a quiescent period, 1970-92, *U. S. Geological Survey Open-File Report*, 94-512.

Hemmingsen, S. M., Woolford, C., van der Vies, S. M., Tilly, K., Dennis, D. T., Georgopoulos, C. P., Hendrix, R. W. and Ellis, R. J., 1988, Homologous plant and bacterial proteins chaperon oligomeric protein assembly, *Nature*, **333**, 330-334.

Hendricks, S. B., 1941, Base-exchange of the clay mineral montmorillonite for organic cations and dependence upon adsorption due to van der Waals forces, *J. Phys. Chem.*, **45**, 65-81.

Henrichs, S. M., 1993, Early diagenesis of organic matter : the dynamics (rates) of cycling of organic compounds, In: *Organic Geochemistry*, Engel, M. H. and Mack, S. A. (eds.), Plenum Press, New York, pp. 101-117.

Henrichs, S. M., 1995, Sedimentary organic matter preservation: an assessment and speculative synthesis - a comment, *Mar. Chem.*, **49**, 127-136.

Henrichs, S. M. and Doyle, A. P., 1986, Decomposition of ^{14}C-labeled organic substrates in marine sediments, *Limnol. Oceanogr.*, **31**, 765-778.

Henrichs, S. M., Farrington, J. W. and Lee, C., 1984, Pure upwelling region sediments near 15°S. 2. Dissolved free and total hydrolyzable amino acids, *Limnol. Oceanogr.*, **29**, 20-34.

Henrichs, S. M. and Farrington, J. W., 1987, Early diagenesis of amino acids and organic matter in two coastal marine sediments, *Geochim. Cosmochim. Acta*, **51**,1-15.

Henrichs, S. M., Reeburgh, W. S., 1987, Anaerobic mineralization of marine sediment organic matter: rates and the role of anaerobic processes in the oceanic carbon economy. *Geomicrobiol. J.* **5**, 191-237.

Henrichs, S. M. and Sugai, S. F., 1993, Adsorption of amino acids and glucose by sediments of Resurrection Bay, Alaska: functional group effects, *Geochim.*

Cosmochim. Acta, **57**, 823-835.

Hoering, T. and Ford, H. T., 1960, The isotope effect in the fixation of nitrogen by Azotobacter, *J. Am. Chem. Soc.*, **82**, 376-378.

Holeman, J. N., 1968, Sediment yield of major rivers of the world, *Water Resources Res.*, **4**, 737-747.

Hollerbach, A. and Dehmer, J., 1994, Diagenesis of organic matter, In: *Diagenesis, IV*, Wolf, K. H. and Chilinggarian, G. V. (ads), **Ch. 10**, 309-359.

Horovite, A., Bochkareva, E. S. and Girshovich, A. S., 1993, The N terminus of the molecular chaperonin GroEL is a crucial structural element for its assembly, *J. Biol. Chem.*, **268(14)**, 9957-9959.

Ishiwatari, R. and Uzaki, M., 1987, Diagenetic changes of lignin compounds in a more than 0.6 million-year-old lacustrine sediment (Lake Biwa, Japan), *Geochim. Cosmochim. Acta.*, **51**, 321-328.

Iwanij, V., Chua, N.-H. and Siekevitz, P., 1974, The purification and some properties of ribulose bisphosphate carboxylase and of its subunits from the green alga *Chlamydomonas reinhardtii*, *Biochim. Biophys. Acta*, **358**, 329-340.

Jacob, K. H., 1987, In: *The Gulf of Alaska - Physical Environment and Biological Resources*, **Ch. 6**, 145-184.

Jaeger, J. M., Nittrouer, C. A., Scott, N. D. and Milliman, J. D., 1998, Sediment accumulation along a glacially impacted mountainous coastline: north-east Gulf of Alaska, *Basin Res.*, **10**, 155-173.

Jensen, R. G. and Bahr, J. T. 1977, Ribulose 1,5-bisphosphate carboxylase-oxygenase, *Annu. Rev. Plant Physiol.* **28**, 379-400.

Jones, B. N., Pääbo, S. and Stein, S., 1981, Amino acid analysis and enzymatic sequence determination by an improved *o*-phthaldialdehyde precolumn labeling procedure, *J. Liquid Chromatogr.*, **4**, 565-586.

Kamb, B. C., 1987, Glacier surge mechanism based on linked cavity configuration of the basal water condition system, *J. Geophys. Res.*, **92**(B9), 9083-9100.

Kamb, B. C., Raymond, C. F., Harrison, W. D., Engelhardt, H., Echelmeyer, K. A., Humphrey, N., Brugman, M. M. and Pfeffer, T., 1985, Glacier surge mechanism: 1982-1983 surge of Variegated Glacier, Alaska, *Science*, **227** (4686), 469-479.

Kamireddi, M., Eisenstein, E. and Reddy, P., 1997, Stable expression and rapid purification of *Escherichia coli* GroEL and GroES chaperonins, *Protein Expression and Purification*, **11**, 47-52.

Keil, R. G. and Kirchman, D. L., 1993, Dissolved combined amino acids: chemical form and utilization by marine bacteria, *Limnol. Oceanogr.*, **38**(6), 1256-1270.

Keil, R. G., Montluçon, D. B., Prahl, F. G. and Hedges, J. I., 1994, Sorptive preservation of labile organic matter in marine sediments, *Nature*, **370**, 549-552.

Kim, J. and ZoBell, 1974, Occurrence and activities of cell-free enzymes in oceanic environments, In: *Effect of the Ocean Environment on Microbial Activities*, Colwell, R. R. and Morita, R. Y. (eds.), University Park, pp. 368-385.

Kirchman, D. L., Henry, D. L. and Dexter, S. C., 1989, Adsorption of proteins to surfaces in seawater, *Mar. Chem.*, **27**, 201-217.

Knicker, H. and Hatcher, P. G., 1997, Survival of protein in an organic-rich sediment: possible protection by encapsulation in organic matter, *Naturwissenchaften*, **84**, 231-234.

Kovalenko, O., Yifrach, O. and Horovitz, A., 1994, Residue lysine-34 in GroES modulates allosteric transition in GroEL, *Biochem.*, **33**(50), 14974-14978.

Kuchitsu, K., Tsuzuki, M., Miyachi, S., 1990, Polypeptide composition and enzyme activities of the pyrenoid and its regulation by CO_2 concentration in unicellular green algae, *Can. J. Bot.*, **69**, 1062-1069.

Ladd, J. N., 1978, Origin and range of enzyme in soil, In: *Soil Enzyme*, Burns, R. G. (ed.), Academic Press, London, pp. 51-96.

Lee, C., 1992, Controls on organic carbon preservation: the use of stratified water bodies to compare intrinsic rates of decomposition in oxic and anoxic systems, *Geochim. Cosmochim. Acta*, **56**, 3323-3335.

Leenheer, J., 1982, United States geological survey data information service, In: *Transport of Carbon and Minerals in Major World Rivers*, **part I**, Degens, E. T. (ed.), pp. 355-356.

Lehninger, A. L., Nelson, D. L. and Cox, M. M., 1993a, Amino acids and peptides, In: *Principles of biochemistry*, 2nd ed., Worth Publishers, NY, **Ch. 5**, 111-133.

Lehninger, A. L., Nelson, D. L. and Cox, M. M., 1993b, An introduction to proteins, In: *Principles of Biochemistry*, 2nd ed., Worth Publishers, NY, **Ch. 6**, 134-159.

Little, J. E., Sjogren, R. E. and Carson, G. R., 1979, Measurement of proteolysis in natural waters, *Appl. Environ. Microbiol.*, **37**, 900-908.

Lovley, D. R., 1987, Organic matter mineralization with the reduction of ferric iron: a review, *Microbiol. Rev.*, **5**(3-4), 375-400.

Lovley, D. R. and Phillips, E. J. P., 1986a, Organic matter mineralization with reducing ferric iron in anaerobic sediments, *Appl. Environ. Microbiol.*, **51**(4), 683-689.

Lovley, D. R. and Phillips, E. J. P., 1986b, Availability of ferric iron for microbial reduction in bottom sediments of the fresh-water tidal Potomac River, *Appl. Environ. Microbiol.*, **52**, 751-757.

Lovley, D. R., Phillips, E. J. P. and Lonergan, D. J., 1991, Enzymatic versus nonenzymatic mechanisms for Fe(III) reduction in aquatic sediments, *Environ. Sci. Technol.*, **25**, 1062-1067.

Ludwig, W., Amiotte-Suchet, P. and Probst, J., 1996, River discharge of carbon to the world's oceans: determining local inputs of alkalinity and of dissolved and particulate organic carbon, *C. R. Acad. Sci.*, **323**, 1007-1014.

Luo, H., 1994, Decomposition and adsorption of peptides in Alaskan coastal marine sediments, *Ph. D. Thesis*, University of Alaska Fairbanks.

Malloy, R. J. and Merrill, G. F., 1972, Vertical crustal movement on the sea floor, In: *The Great Alaska Earthquake of 1964, Vol. 6: Oceanography and Coastal Engineering*, National Research Council, National Academy of Science, Washington, D. C., pp. 252-265.

Marshman, N. A. and Marshall, K. C., 1981, Bacterial growth on proteins in the presence of clay mineral. *Soil Boil. Biochem.*, **13**, 127-134.

Martins, O., 1983, Transport of carbon in the Niger River, In: *Transport of Carbon and Minerals in Major World Rivers*, **part II**, Degens, E. T. *et al.*, (eds.), 435-449.

Masel, R. I., 1996, *Principles of Adsorption and Reaction on Solid Surfaces*, John Wiley & Sons, Inc., **Ch. 3**, 108-234.

Matthews, J. B. L. and Heimdal B. R.,1980, Pelagic productivity and food chains in fjord systems, In: *Fjord Oceanography*. Freeland, H. J. *et. al.* (ed.), Plenum Press, New York, NY. pp 377-398.

Mayer, L. M., 1993, Organic Matter at the sediment-water interface, In: *Organic geochemistry*, Engel, M. H. and Macko, S. A. (eds.), Plenum Press, New York & London, **Ch. 7**, 171-184.

Mayer, L. M., 1994a, Relationships between mineral surfaces and organic carbon concentrations in soils and sediments, *Chem. Geol.*, **114**, 347-363.

Mayer, L. M., 1994b, Surface area control of organic carbon accumulation in continental shelf sediments, *Geochim. Cosmochim. Acta*, **58(4)**, 1271-84.

Mayer, L. M. and Fink, L. K. Jr., 1980, Granulometric dependence of chromium accumulation in estuarine sediments in Maine, *Estuary, Coast. Mar. Sci.*, 11(5), 491-503.

Mayer, L. M., Schick, L. L. and Setchell, F. W., 1986, Measurement of protein in nearshore marine sediments, *Mar. Ecol. Prog. Ser.*, **30**, 159-165.

Mayer, L. M., Macko, S. A. and Cammen, L., 1988, Provenance, concentrations and nature of sedimentary organic nitrogen in the Gulf of Maine, *Mar. Chem.*, **25**, 291-304.

McDaniel, T. B., 1989, Biological availability of amino acids in marine sediments. *M. S. Thesis*, University of Alaska Fairbanks.

Metzler, D. E., 1977, In: *Biochemistry, the chemical reactions of living cells*, Academic Press.

Meybeck, M., 1982, Carbon, nitrogen, and phosphrous transport by world rivers, *Am. J.*

Sci., **282**, 401-450.

Meyer, P. A. and Ishiwatari, R., 1993, Lacustrine organic geochemistry - an overview of indicators of organic matter sources and diagenesis in lake sediments, *Org. Geochem.*, **20(7)**, 867-900.

Meyer-Reil, L.-A., 1991, Ecological aspects of enzymatic activity in marine sediments, In: *Microbial Enzymes in Aquatic Environments*, Ryszard, J. C. (ed.), Springer-Verlag, pp. 84-95.

Miller, D. J., 1953, Late Cenozoic marine glacial sediments and marine terraces of Middleton Island, Alaska, *J. Geol.*, **61**, 17-40.

Milliman, J. D. and Meade, R. H., 1983, World-wide delivery of river sediment to the oceans, *J. Geol.*, **91**, 1-21.

Milliman, J. D. and Syvitski, J. P. M., 1992, Geomorphic/tectonic control of sediment discharge to the ocean: the importance of small mountainous rivers, *J. Geol.*, **100**, 525-544.

Miyake, Y., Wada, E.,1967, The abundance ratio of $^{15}N/^{14}N$ in marine environment, *Rec. Oceanogr. Works Japan*, **9**, 37-53.

Molnia, B. F.,1977, Rapid shoreline erosion at Icy Bay, Alaska - a staging area for offshore petroleum development, *Proceedings of the Ninth Annual Offshore Technology Conference*, Houston, Texas, **3**, 115-126.

Molnia, B. F., 1979, Sedimentation in coastal embayments in the Northern Gulf of Alaska, *Proceedings, 11th Offshore Technology Conference*, **1**, 665-676.

Molnia, B. F., 1986, Glacial history of the northeastern Gulf of Alaska – a synthesis, In: *Glaciation in Alaska*, Hamilton, T. D. *et al.* (eds.), Alaska Geological Society, 219-235.

Molnia, B.,1989, Subarctic (Temperate) Glacial-Marine Sedimentation - the Northeastern Gulf of Alaska, In: *Glacial-Marine Sedimentation*, **Ch. IV**, 59-106.

Molnia, B. F. and Hein, J., 1982, Clay mineralogy of a glacially dominated subarctic continental shelf: northeastern Gulf of Alaska shelf, *J. Sediment Petrol.*, **52**, 515-

527.

Molnia, B. F., Post, A.,1995, Holocene history of Bering Glacier, Alaska: a prelude to the 1993-94 surge. *Physical Geography*, **16**(2), 87-117.

Mopper, K. and Degens, E. T., 1979, Organic carbon in the ocean: nature and cycling, In: *The Global Carbon Cycle*, Bolin, B. *et. al.* (eds.), John Wiley, New York, pp. 293-316.

Morrissey, B. W., 1977, Adsorption and conformation of proteins. *Ann. N. Y. Acad. Sci.*, **288**, 50-64.

Muller, P. J., 1977, C/N ratios in Pacific deep-sea sediments: effect of inorganic ammonium and organic nitrogen compounds sorbed by clays. *Geochim. Cosmochim. Acta.*, **41**, 765-776.

Munch, J. C. and Ottow, J. C. G., 1983, Reductive transformation mechanism of ferric oxides in hydromorphic soil. *Ecol. Bull.* (Stockholm), **35**, 383-394.

Murray, J. W., 1992,The oceans, In: *Global Biogeochemical Cycles*, Butcher, S. S. *et al.* (eds.), Academic Press, pp. 175-211.

Nemeth, A., Paolini, J. and Herrera, R.. 1982, Carbon transport in the Orinoco River: preliminary results, In: *Transport of Carbon and Minerals in Major World Rivers*, **part I**, Degens, E. T. (ed.), pp. 357-364.

Neudörfer, F. and Meyer-Reil, LA, 1997, A microbial biosensor for the microscale measurement of bioavailable organic carbon in oxic sediments, *Mar. Ecol. Prog. Ser.*, **147**, 295-300.

Newman, A. C. D. 1987, The interaction of water with clay mineral surfaces, In: *Chemistry of Clays and Clay Minerals*, Newman, A. C. D. (ed.), Longman Sci. & Tech., Mineralogical Society, **Ch. 5**, 237-274.

Newman, A. C. D. and Brown, G., 1969, Delayed exchange of potassium from some edges of mica flakes, *Nature, Lond.*, 223, 175-176.

Nissenbaum, A. 1974, The organic geochemistry of marine and terrestrial humic substances: Implications of carbon and nitrogen isotope studies, In: *Advances in*

Organic Geochemistry, 1973, Tissot, B. and Bienner, F. (eds.), Editions Technip, Paris, pp. 39-52.

North, B. B., 1975, Primary amines in California coastal waters: utilization by phytoplankton, *Limnol. Oceanogr*, **20**, 20-27.

O'Leary, M. H., 1988, Carbon isotopes in photosynthesis, *Bioscience*, **38**, 328-336.

Orten, J. M. and Neuhaus, O. W., 1970, Amino acids and proteins, In: *Biochemistry*, 8th ed., C. V. Mosby Company, Saint Louis, pp. 57-90.

Ostrom, N. E., Macko, S. A.,1992, Sources, cycling, and distribution of water column particulate and sedimentary organic matter in northern Newfoundland fjords and bays: a stable isotope study, In: *Organic Matter: Productivity, Accumulation, and Preservation in Recent and Ancient Sediments*, Columbia Univ. press, 55-81.

Pande, S. V. and Murthy, M. S. R., 1994, A modified micro-Bradford procedure for elimination of interference from sodium dodecyl sulfate, other detergents, and lipids, *Appl. Biochem.*, **220**, 424-426.

Pantoja, S. and Lee, C., 1998, The determination of concentration and molecular weight of protein in coastal marine sediments, *Limnol. Oceanogr.* (in press).

Park, R. B. and Pon, N. G. 1961, Correlation of structure with function in *Spinacea oleracea* Chloroplasts, *J. Mol. Biol.*, **3**, 1-10.

Parks, G. A., 1967, Aqueous surface chemistry of oxides and complex oxide minerals. Isoelectric point and zero point of charge. In: *Equilibrium Concepts in Natural Water System* (Symposium). *Advances in Agronomy* series 67. Am. Chem. Soc.

Parsons, T. R., Takahashi, M. and Hargrave, B., 1984, The primary formation of particulate material, In: *Biological Oceanographic Processes*, 3rd ed.., Pergamon Press, 61-118.

Perutz, M. F., 1978, Electrostatic effects in proteins, *Science*, **201**, 1187-1191.

Peters, K. E., Sweeney, R. E. and Kaplan, I. R., 1978, Correlation of carbon and nitrogen stable isotope ratios in sedimentary organic matter, *Limnol. Oceanogr.*, **23**(4), 598-604.

Pettine, M., La Noce, T., Pagnotta, R. and Puddu, A., 1985, Organic and trophic load of major Italian rivers, In: *Transport of Carbon and Minerals in Major World Rivers*, **part III,** Degens, E. T. *et al.*, (eds.), pp. 417-429.

Phillips, E. J. P., Lovley, D. R. and Roden, E. E., 1993, Composition of non-microbially reducible Fe(III) in aquatic sediments, *Appl. Environ. Microbiol.*, **59(8)**, 2727-2729.

Plafker, G. and Miller, D. J., 1958, Glacial features and surficial deposits of the Malaspina district, Alaska, *U. S. Geol. Survey Misc. Geo. Invest. Map* **I-271**, scale 1:125,000.

Plumley, F. J., Kirchman, D. L., Hodson, R. E., Schmidt, G. W., 1986, Ribulose bisphosphate carboxylase from three chlorophyll *c*-containing algae, *Plant Physiol.*, **80**, 685-691.

Pocklington, R., 1982, Carbon transport in major rivers: the St. Lawrence, Canada, In: *Transport of Carbon and Minerals in Major World Rivers*, **part I**, Degens, E. T. (ed.), pp. 347-353.

Porter, S. C., 1989, Late Holocene fluctuation of the fiord glacier system in Icy Bay, Alaska, U. S.A., *Arctic Alpine Res.* **21**(4), 364-379.

Price, N. B., 1976, Chemical diagenesis in sediments. In:*Chemical Oceanography*, Riley, J. P., Chester, R. (eds.), 2nd edition. London: Academic Press, **6**, 1-58.

Priest, F. G., 1984, In: *Extracellular enzymes*, Van Nostrand Reinhold (UK) Co. Ltd., Workingham.

Rau, G. H., 1994, Variations in sedimentary organic $\delta^{13}C$ as a proxy for past change in ocean and atmospheric CO_2 concentrations, In: *Carbon Cycling in the Glacial Ocean: Constraints on the Ocean's Role in Global Change*, Zahn, R. *et al.* (ed.), Springer-Verlag Berlin Heidelberg, 307-320.

Reeburgh, W. S., 1976, Methane consumption in Cariaco Trench water and sediments, *Earth Planet. Sci. Lett.*, **15**, 337-344.

Reeburgh, W. S., 1979, A major sink and flux control methane in marine sediments: anaerobic consumption, In: *The Dynamic Environment of the Ocean Floor*,

Fanning, K. and Manheimn F. T. eds.

Reeburgh, W. S., 1980, Anaerobic methane oxidation: rate depth distributions in Skan Bay sedments, *Earth Planet. Sci. Lett.*, **47**, 345-352.

Reeburgh, W. S., Kipphut, G., 1987, Chemical Distributions and Signals in the Gulf of Alaska, its Coastal Margins and Estuaries, In: *The Gulf of Alaska - Physical Environment and Biological Resources*, **Ch. 4**, 77-91.

Reed, R. K., Schumacher, J. D., and Wright, C., 1981, On Coastal Flow in the Northeast Gulf of Alaska near Yakutat, *Atmosphere-Ocean* , **19**, 47-53.

Reed, R. K. and Schumacher, J.D., 1987, Physical Oceanography, *The Gulf of Alaska, Physical Environment and Biological Resources,* **Ch. 3**, 57-75.

Reichardt, W., 1986, Enzymatic potential for decomposition of detritus biopolymers in sediments from Kiel Bay, *Ophelia*, **26**, 369-384.

Reimnitz, E.,1966, Late Quaternary history and sedimentation of the Copper River Delta and vicinity, Alaska. Ph.D. Dissertation, University of California, San Diego, CA. 160 pp.

Reimnitz, E., 1972, Effects in the Copper River Delta, In: *The Great Alaska Earthquake of 1964, Vol. 6: Oceanography and Coastal Engineering*, National Research Council, National Academy of Science, Washington, D. C., pp. 290-302.

Reimnitz, E. and Carlson, P. R., 1975, Circulation of nearshore surface water in the Gulf of Alaska. In: *Principal Sources and Dispersal Patterns of Suspended Particulate Matter in Nearshore Surface Water of the Northeast Pacific Ocean*, P. R. Carlson, T. J. Conomos, R. J. Janda and D. H. Peterson (ed.), Earth Resour. Technol. Satellite, final rep., Nat. Tech. Inf. Serv., E75-10266, pp. 10-25.

Richey, J. E., 1982, The Amazon River system: a biogeochemical model, In: *Transport of Carbon and Minerals in Major World Rivers,* **part I**, Degens, E. T. (ed.), pp. 365-378.

Roesler, K. R. and Ogren, W. L., 1990, Primary structure of *Chlamydomonas reinhardtii* ribulose 1,5-bisphosphate carboxylase/oxygenase activase and evidence for a single

polypeptide, *Plant Physiol.*, **94**, 1837-1841.

Romankevich, E. A., 1984, Organic carbon in late Quarternary sediments of seas and oceans, In: *Geochemistry of Organic Matter in the Ocean*, Spring-Verlag Berlin Heidelberg, **Ch. 4**, 105-160.

Rose, G. D., Geselowitz, A. R., Lesser, G. J., Lee, R. H. and Zehfus, M. H., 1985, Hydrophobicity of amino acid residues in globular proteins, *Science*, **229**, 834-838.

Rosenfeld, J. K., 1979, Amino acid diagenesis and adsorption in nearshore anoxic sediments, *Limnol. Oceanogr.*, **24**, 1014-1021.

Roush, J. J.,1996, The 1993-'94 surge of Bering Glacier, Alaska observed with satellite synthetic aperture radar, *M.S. Thesis*, University of Alaska Fairbanks, AK., 101pp.

Royer, T. C., 1975, Seasonal variations of waters in the northern Gulf of Alaska, *Deep Sea Res.*, **22**, 403-416.

Royer, T. C., 1979, On the effect of precipitation and runoff on coastal circulation in the Gulf of Alaska, *J. Phy. Oceanogr.*, **9**, 555-563.

Royer, T. C., 1981a, Baroclinic transport in the Gulf of Alaska. Part I. Seasonal variations of the Alaska Current. *J. Mar. Res.*, **39**, 239-250.

Royer, T. C. 1981b, Baroclinic transport in the Gulf of Alaska. Part II. A fresh water driven coastal current. *J. Mar. Res.*, **39**, 251-266.

Royer, T. C., 1982, Coastal fresh water discharge in the northeast Pacific. *J. Geophys. Res.* **87C**, 2017-2021.

Rullkötter, J., 1993, The thermal alteration of kerogen and the formation of oil, In: *Organic Geochemistry, Priciples and Applications*, Engel, M. H. and Macko, S. A. (eds.), Plenum Press, **Ch. 16**, 377-396.

Safiullah, S., Chowdhury, M. I., Mafizuddin, M., Ali, I. and Karim, M., 1985, Monitoring of the Padma (Ganges), the Jamuna (Brahmaputra) and the Baral in Bangladesh, In: *Transport of carbon and minerals in major world rivers*, **part III**, Degens, E. T. *et al.*, (eds.), 519-524.

Sambrotto, R. N., and Lorenzen C. J., 1987, Phytoplankton and Primary Production, In:

The Gulf of Alaska - Physical Environment and Biological Resources, 249-282.

Samuelsson, M.-O. And Kirchman, D. L., 1990, Degradation of adsorbed protein by attached bacteria in relationship to surface hydrophobicity, *Appl. Environ. Microbiol.*, **56**(12), 3643-3648.

Schulz, G. E. and Schirmer, R. H., 1979, In: *Principles of Protein Structure*, Springer-Verlag, New York.

Schwertmann, U. and Taylor, R. M., 1977, Iron oxide, In: *Minerals in Soil Environments*, Dixon, J. B. and Weed, S. B. (eds.), **Ch. 5**, Soil Sci. Soc. Am., Madison, Wisconsin.

Shaw, D. G., Alperin, M. J., Reeburgh, W. S., MaCintosh, D. L., 1984, Biogeochemistry of acetate in anoxic sediments of Skan Bay, Alaska. *Geochim. Cosmochim, Acta*, **48**, 1819-1825.

Shaw, D. G. and McIntosh, D. J., 1990, Acetate in recent anoxic sediments: direct and indirect measurements of concentration and turnover rates, *Estuar. Coastal Shelf Sci.*, **31**, 775-788.

Sims, S. R. and Holden, L. R., 1996, Insect bioassay for determining soil degradation of *Bacillus thuringiensis* subsp. *Kurstaki* CryIA(b) protein in corn tissue, *Environ. Entomol.*, **25**(3), 659-664.

Smith, S. V. and Hollibaugh, G. T., 1993, Coastal metabolism and the oceanic carbon balance, *Rev. Geophys.*, **31**, 75-89.

Soderquist, M. E. and Walton, A. G., 1980, Structural changes in proteins adsorbed on polymer surfaces, *J. Colloid Interface Sci.*, **75**, 386-392.

Spitzy, A. and Ittekkot, V., 1991, Dissolved and particulate organic matter in rivers, In; *Ocean Margin Processes in Global Change*, Mantoura, R. F. C., Martin, J. M. and Wollast R. (eds.), Wiley, New York, pp. 5-17.

Stumm, W. and Sulzberger, B., 1992, The cycling of iron in natural environments: considerations based on laboratory studies of heterogeneous redox processes. *Geochim. Cosmochim. Acta*, **56**, 3233-3257.

Suess, E., 1980, Particulate organic carbon flux in the oceans - surface productivity and oxygen utilization, *Nature*, **288**, 260-262.

Sugai, S. F. and Henrichs, S. M., 1992, Rates of amino acid decomposition in Resurrection Bay (Alaska) sediments, *Mar. Ecol. Prog. Ser.*, **88**, 129-141.

Sugai, S. F., Alperin, M. J. and Reeburgh, W. S., 1994, Episodic desorption and ^{137}Cs immobility in Skan Bay sdiments: a ten-year ^{210}Pb and ^{137}Cs time series, *Mar. Geol.*, **116,** 351-372.

Summons, R. E., 1993, biogeochemical cycles: a review of fundamental aspects of organic matter formation, preservation, and composition, In: *Organic Geochemistry,* Engel, M. H. and Macko, S. A. (eds.), Plenum Press, New York and London, **Ch. 1**, 3-21.

Taylor, R. M., 1987, Non-silicate oxides and hydroxides. In: Chemistry of clays and clay minerals, Newman, A. C. D. (ed.), Longman Sci. & Tech., Mineralogical Society, 129-201.

Tegelaar, E. W., de Leeuw, J. W., Derenne, S. and Largeau, C., 1989, A reappraisal of kerogen formation, *Geochim. Cosmochim. Acta*, **53**, 3103-3106.

Telang, S. A., Korchinski, M. and Hodgson, G. W., 1982, Abundances and transport of ions, nitrogen, and carbon in the Mackenzie River,In: *Transport of Carbon and Minerals in Major World Rivers*, **part I**, Degens, E. T. (ed.), pp. 333-346.

Tyson, R. V., 1995a, Bulk geochemical characterization and classification of organic matter: carbon:nitrogen ratios and lignin-derived phenols, In: *Sedimentary Organic Matter*, Chapman & Hall, **Ch. 22**, 383-394.

Tyson, R. V., 1995b, Bulk geochemical characterization and classification of organic matter: stable carbon isotopes ($\delta^{13}C$), In: *Sedimentary Organic Matter*, Chapman & Hall, **Ch. 23**, 395-416.

Van Olphen, H., 1977, In: *An Introduction to Clay Colloid Chemistry*, Wiley, New York, NY, 2nd ed., pp. 318.

Voet, D. and Voet J. G., 1995, Three-dimensional structures of proteins, In: *Biochemistry*, 2nd ed., John Wiley & Sons, Inc., **Ch. 7**, 141-190.

Voller, A., Bidwell, D. and Bartlett, A., 1980, In: *Manual of Clinical Immunology*, 2nd ed. (Rose, N. R. and Friedman, H. ed.), American Society for Microbiology, Washington, DC, 359-371.

Wada, E. and Hattori, 1991, In: *Nitrogen in the Sea : Forms, Abundances, and Rate Processes*, CRC press, **Ch. 7**, 141-176.

Wang, X., 1993, Biogeochemical study of aliphatic amines and amino acids in coastal marine sediments, *Ph.D. Thesis*, State Univ. of New York at Stony Brook.

Wang, X. and Lee, C., 1993, Adsorption and desorption of aliphatic amines, amino acids and acetate by clay minerals and marine sediments, *Mar. Chem.*, **44**, 1-23.

Welschmeyer, N. A., Strom, S., Goericke, R., Di Tullio, G., Belvin, M. and Petersen, W., 1993, Primary production in the subarctic Pacific Ocean: project SUPER, *Prog. Oceanogr.*, **32**, 101-135.

Westrich, J. T. and Berner, R. A., 1984, The role of sedimentary organic matter in bacterial sulfate reduction; the G-model tested, *Limnol. Oceanogr.*, **29**, 236-247.

White, A., Handler, P. and Smith, E. L., 1968a, In: *Principles of Biochemistry*, 4th ed., McGraw-Hill Book Company, **Ch. 8**, 166-180.

White, A., Handler, P. and Smith, E. L., 1968b, In: *Principles of Biochemistry*, 4th ed., McGraw-Hill Book Company, **Ch. 4**, 57-86.

Williams, P. J. leB., 1995, Evidence for the seasonal accumulation of carbon-rich dissolved organic material, its scale in comparison with changes in particulate, material and the consequential effect on net C/N assimilation ratios, *Mar. Chem.*, **51**, 17-29.

Wu, J., Calvert, S. E. and Wong, C. S., 1997, Nitrogen isotope variations in the northeast Pacific: relationships to nitrate utilization and trophic structure, *Deep Sea Res.*, **44**(2), 287-314.

Xiong, Q. and Royer, T. C., 1984, Coastal Temperature and Salinity in the Northern Gulf of Alaska, 1970-1983, *J. Geophys. Res.*, **89**, 8061-8068.

Yang, R. C. A., Dove, M., Seligy, V. L., Lemieux, C., Turmel, M. and Narang, S. A.,

1986, Complete nucleotide sequence and mRNA-mapping of the large subunit gene of ribulose-1,5,-bisphosphate carboxylase/oxygenase (Rubisco) from *Chlamydomonas moewussi*, *Gene*, **50**, 259-270.

Appendix I. Minimal Medium for Growth of Algae.

Trizma Base	7.26 g
H_2O	2.85 L
1 M Phosphate Buffer, pH 7.0	3 mL
Trace Metals	3 mL
B Solution	150 mL
Conc. HCl	4.6 mL

1 M Potassium Phosphate Buffer, pH 7.0

K_2HPO_4	106 g
KH_2PO_4	53 g
H_2O	1 L

Trace Metals

1) Dissolve in order, one at a time, in 550 ml deionized H_2O:

1. $ZnSO_4 \cdot 7\ H_2O$	22.0 g
2. H_3BO_3	11.4 g
3. $MnCl_2 \cdot 4H_2O$	5.1 g
4. $FeSO_4 \cdot 7H_2O$	5.0 g
5. $CoCl_2 \cdot 6H_2O$	1.6 g
6. $CuSO_4 \cdot 5H_2O$	1.6 g
7. $(NH_4)_6Mo_7O_{24}$	1.1 g

2) Dissolve 50 g of EDTA (free acid) in 250 ml deionized H_2O by adjusting to pH 7.0 with KOH.

3) Warm metal solution with mixing to 70 °C

4) Add EDTA solution

5) Adjust to pH 6.5 - 6.8

6) Dilute to 1 L

7) Age for a few weeks until purple

8) Filter out brown precipitate

B Solution

NH_4Cl	16 g
$CaCl_2 \cdot 2H_2O$	2 g
$MgSO_4 \cdot 7H_2O$	4 g
H_2O	2 L

Appendix II. Culture Medium for Growth of *E. coli*

Composition per liter (5×):

K_2HPO_4	52.5 g
KH_2PO_4	22.5 g
$(NH_4)_2SO_4$	5.0 g
Sodium citrate·$2H_2O$	2.5 g
Carbon source solution	10.0 mL
$MgSO_4 \cdot 7H_2O$ solution	1.0 mL

pH 7.0 ± 0.2 at 25 °C

Carbon source solution:

composition per 100 mL : 20.0 g

Preparation of carbon source solution : Add glucose and ^{14}C labeled glucose to distilled water and bring the volume to 100.0 mL. Mix throughly. Sterilize by filtration.

$MgSO_4 \cdot 7H_2O$ solution:

composition per 100 mL : 24.7 g

Preparation of $MgSO_4 \cdot 7H_2O$ solution : Add $MgSO_4 \cdot 7H_2O$ to distilled water and bring volume to 100.0 mL. Mix thoroughly. Sterilize by filtration.

Preparation of Medium:

Add components, except carbon source solution and $MgSO_4 \cdot 7H_2O$ solution, to distilled water and bring volume to 1.0 L. Mix thoroughly. Gently heat and bring to a boil. Autoclave for 30 min. Cool to 45 ~ 50 °C. Aseptically dilute 200.0 mL of 5× stock solution with 789.0 mL of sterile distilled water for use (1×). Aseptically add 10.0 mL of sterile $MgSO_4 \cdot 7H_2O$ solution. Mix throughly. Aseptically distribute into sterile flasks.

Appendix III. Sedimentary Organic Matter in the Northeastern Gulf of ALaska.

Table A-1. Surface sedimentary organic matter content in the northeastern Gulf of Alaska (0 - 2 cm).

Station	Long.	Lat.	TN(%)	$\delta^{15}N$(‰)	TOC(%)	$\delta^{13}C$(‰)	C/N
101	-147.104	59.806	0.054	5.36	0.530	-23.49	9.8
102	-146.964	60.212	0.022	4.25	0.281	-23.19	12.8
103	-147.206	60.076	0.040	4.74	0.411	-23.63	10.3
104	-146.941	60.080	0.049	4.83	0.486	-23.54	9.9
105	-145.656	60.141	0.040	4.40	0.410	-23.83	10.3
106	-145.523	60.176	0.029	4.17	0.310	-24.00	10.9
107	-145.571	60.056	0.052	4.76	0.538	-23.57	10.3
108	-144.966	59.705	0.032	4.06	0.423	-24.55	13.2
109	-145.127	59.663	0.036	3.94	0.447	-24.58	12.4
110	-144.999	59.572	0.044	4.09	0.460	-23.60	10.5
111	-143.708	59.944	0.045	1.82	0.619	-24.81	13.8
113	-143.566	59.961	0.047	1.64	0.604	-24.60	12.9
114	-143.442	59.765	0.046	3.87	0.480	-23.49	10.4
115	-143.286	59.808	0.040	3.72	0.368	-22.81	9.2
117	-141.336	60.020	0.038	2.28	0.426	-24.24	11.2
118	-141.507	59.943	0.032	2.78	0.325	-23.71	10.2
119	-142.354	59.588	0.051	5.06	0.484	-21.77	9.5
120	-142.338	59.592	0.063	4.87	0.539	-21.81	8.6
121	-142.156	59.664	0.044	4.09	0.418	-23.43	9.5

(continued)

Table A-1. (continued)

Station	Long.	Lat.	TN(%)	$\delta^{15}N$(‰)	TOC(%)	$\delta^{13}C$(‰)	C/N
122	-141.966	59.748	0.043	3.95	0.388	-23.28	9.0
123	-141.841	59.800	0.021	3.27	0.230	-23.66	11.0
124	-141.333	59.523	0.031	4.71	0.305	-23.09	9.8
125	-141.213	59.469	0.076	5.63	0.555	-21.72	7.3
126	-140.770	59.486	0.081	5.78	0.635	-21.74	7.8
127	-139.560	60.007	0.006	12.0	0.126	-21.83	21.0
128	-139.655	59.908	0.010	7.20	0.158	-22.01	15.8
129	-139.802	59.634	0.043	4.28	0.389	-22.55	9.0
130	-139.051	59.102	0.014	6.44	0.150	-21.37	10.7
131	-139.137	59.148	0.019	5.90	0.170	-22.09	8.9
132	-139.101	59.210	0.002	36.8	0.050	-21.23	25.0
146	-141.261	59.368	0.081	5.93	0.627	-21.15	7.7
147	-140.359	59.497	0.071	5.13	0.569	-21.05	8.0
148	-140.396	59.497	0.089	5.55	0.693	-20.64	7.8
149	-138.961	58.795	0.100	5.52	0.711	-21.13	7.1
150	-138.665	59.049	0.035	5.43	0.311	-20.89	8.9
151	-141.663	59.711	0.036	3.63	0.368	-23.42	10.2
152	-141.884	59.801	0.030	3.69	0.302	-23.26	10.1
153	-142.221	59.904	0.030	3.31	0.326	-23.64	10.9
154	-146.515	60.614	0.049	4.98	0.446	-21.89	9.1
155	-146.793	60.566	0.044	4.40	0.429	-22.85	9.7
156	-146.884	60.449	0.039	4.55	0.389	-22.65	10.0
200	-146.408	60.561	0.031	5.05	0.323	-21.62	10.4
201	-146.884	60.452	0.025	4.99	0.292	-22.28	11.7
202	-146.853	60.514	0.038	5.41	0.374	-22.34	9.8

(continued)

Table A-1. (continued)

Station	Long.	Lat.	TN(%)	$\delta^{15}N$(‰)	TOC(%)	$\delta^{13}C$(‰)	C/N
203	-147.043	60.767	0.047	5.56	0.437	-22.37	9.3
204	-146.995	60.811	0.039	4.72	0.386	-22.43	9.9
205	-146.584	60.176	0.049	4.64	0.419	-22.53	8.6
206	-146.607	60.177	0.029	4.52	0.348	-22.22	12.0
210	-138.865	58.934	0.092	5.75	0.715	-20.27	7.8
212	-140.000	59.000	0.029	3.62	0.347	-24.07	12.0
213	-141.407	59.678	0.017	4.57	0.235	-23.49	13.8
214	-141.493	59.612	0.027	4.65	0.326	-23.60	12.1
215	-141.581	59.517	0.032	5.04	0.354	-23.36	11.1
216	-141.665	59.459	0.044	5.61	0.416	-22.71	9.5
217	-141.750	59.400	0.052	5.65	0.432	-22.00	8.3
219	-142.844	59.786	0.053	5.43	0.488	-22.68	9.2
220	-142.842	59.870	0.043	4.83	0.431	-22.81	10.0
221	-142.839	59.978	0.038	4.31	0.401	-23.34	10.6
222	-142.812	60.053	0.025	3.60	0.376	-24.15	15.0
225	-141.513	59.948	0.015	5.84	0.229	-24.09	15.3
226	-142.498	59.942	0.037	5.57	0.399	-23.30	10.8
227	-143.183	60.020	0.020	5.04	0.311	-23.76	15.6
228	-143.497	60.023	0.031	1.98	0.306	-25.93	9.9
229	-143.677	60.001	0.036	0.64	0.360	-25.62	10.0
230	-144.020	59.859	0.027	4.36	0.391	-24.11	14.5
231	-144.254	59.777	0.037	5.01	0.423	-23.48	11.4
232	-144.580	59.671	0.042	4.33	0.461	-23.53	11.0
233	-145.003	59.815	0.035	3.70	0.446	-24.04	12.7

(continued)

Table A-1. (continued)

Station	Long.	Lat.	TN(%)	$\delta^{15}N$(‰)	TOC(%)	$\delta^{13}C$(‰)	C/N
234	-144.738	59.968	0.056	3.62	0.623	-24.58	11.1
235	-144.558	60.068	0.089	4.40	0.941	-24.01	10.6
236	-145.159	60.124	0.025	4.47	0.289	-24.32	11.6
239	-145.909	60.211	0.062	4.20	0.579	-23.42	9.3
240	-146.091	60.164	0.085	4.60	0.755	-23.24	8.9
241	-146.250	60.236	0.038	2.86	0.432	-23.64	11.4
243	-147.190	59.684	0.068	4.36	0.620	-23.24	9.1

(Continued)

Table A-2. Total organic matter burial flux in the northeastern Gulf of Alaska.

Station	Long.	Lat.	Flux (g m^{-2} yr^{-1})
101	-147.104	59.806	15.9
102	-146.964	60.212	73.1
103	-147.206	60.076	53.4
104	-146.941	60.080	24.3
105	-145.656	60.141	73.8
106	-145.523	60.176	62.0
107	-145.571	60.056	37.6
108	-144.966	59.705	63.4
109	-145.127	59.663	84.9
110	-144.999	59.572	27.6
111	-143.708	59.944	68.1
114	-143.442	59.765	4.80
119	-142.354	59.588	4.84
120	-142.338	59.592	5.39
121	-142.156	59.664	16.7
122	-141.966	59.748	19.4
123	-141.841	59.800	9.2
124	-141.333	59.523	3.1
125	-141.213	59.469	5.6
130	-139.051	59.102	0.8
131	-139.137	59.148	1.7
132	-139.101	59.210	0.5
146	-141.261	59.368	6.3
147	-140.359	59.497	17.1

(continued)

Table A-2. (continued)

Station	Long.	Lat.	Flux (g m^{-2} yr^{-1})
148	-140.396	59.497	13.9
149	-138.961	58.795	14.2
150	-138.665	59.049	3.1
151	-141.663	59.711	18.4
152	-141.884	59.801	15.1
153	-142.221	59.904	3.3
156	-146.884	60.449	81.7
200	-146.408	60.561	19.4
201	-146.884	60.452	32.1
202	-146.853	60.514	56.1
203	-147.043	60.767	4.4
204	-146.995	60.811	15.4
205	-146.584	60.176	41.9
206	-146.607	60.177	34.8
210	-138.865	58.934	14.3
212	-140.000	59.000	34.7
213	-141.407	59.678	2.4
214	-141.493	59.612	22.8
215	-141.581	59.517	14.2
216	-141.665	59.459	8.3
217	-141.750	59.400	4.3
219	-142.844	59.786	14.6
220	-142.842	59.870	12.9

(continued)

Table A-2. (continued)

Station	Long.	Lat.	Flux (g m^{-2} yr^{-1})
221	-142.839	59.978	32.1
222	-142.812	60.053	48.9
226	-142.498	59.942	8.0
227	-143.183	60.020	12.4
228	-143.497	60.023	30.6
229	-143.677	60.001	36.0
230	-144.020	59.859	15.6
231	-144.254	59.777	8.5
232	-144.580	59.671	4.6
233	-145.003	59.815	89.2
234	-144.738	59.968	124.6
235	-144.558	60.068	75.3
236	-145.159	60.124	57.8
239	-145.909	60.211	104.2
240	-146.091	60.164	60.4
241	-146.250	60.236	86.4

(continued)

Table A-3. Subsurface sedimentary organic matter content in the northeastern Gulf of Alaska.

Station	Depth (cm)	TN (%)	$\delta^{15}N$ (‰)	TOC (%)	$\delta^{13}C$ (‰)
101	0	0.056	5.72	0.537	-23.38
	1	0.053	4.99	0.523	-23.59
	2	0.046	4.19	0.442	-23.09
	3	0.046	3.86	0.475	-23.31
	4	0.044	3.50	0.449	-23.12
	5	0.046	4.37	0.446	-22.72
	6	0.052	4.46	0.492	-23.20
	7	0.045	3.90	0.455	-23.26
	8	0.044	3.85	0.433	-23.34
	9	0.055	4.77	0.571	-23.61
	11	0.048	4.55	0.503	-23.41
	13	0.045	4.68	0.500	-23.36
	15	0.045	4.58	0.510	-23.55
	17	0.045	4.03	0.504	-23.45
	19	0.042	4.25	0.495	-23.48
	24	0.040	3.92	0.497	-23.57
	29	0.042	4.12	0.522	-23.55
	34	0.042	4.03	0.514	-23.48
	39	0.040	4.68	0.458	-23.83
	44	0.041	4.20	0.491	-23.62
	49	0.041	3.70	0.495	-23.64
	69	0.039	3.81	0.502	-23.68

(continued)

Table A-3. (Continued)

Station	Depth (cm)	TN (%)	$\delta^{15}N$ (‰)	TOC (%)	$\delta^{13}C$ (‰)
	89	0.037	4.23	0.489	-23.89
	119	0.039	3.59	0.485	-23.57
	159	0.037	4.25	0.496	-23.83
	199	0.039	3.42	0.492	-23.62
	239	0.039	4.10	0.431	-23.48
	279	0.044	3.17	0.525	-23.51
105	0	0.042	4.56	0.417	-23.89
	1	0.038	4.23	0.403	-23.77
	2	0.035	3.56	0.346	-23.00
	3	0.034	3.02	0.337	-22.87
	5	0.029	3.99	0.382	-23.05
	7	0.042	3.71	0.396	-22.90
	9	0.042	3.40	0.414	-23.06
	14	0.033	4.00	0.314	-22.97
	20	0.021	2.42	0.274	-22.48
	50	0.025	2.32	0.276	-23.28
	100	0.037	1.79	0.362	-23.11
	150	0.037	2.16	0.360	-23.25
	200	0.037	3.37	0.372	-23.18
106	0	0.032	5.22	0.323	-24.04
	1	0.026	3.12	0.297	-23.95
	2	0.022	4.02	0.304	-23.46
	3	0.022	3.19	0.297	-23.37

(continued)

Table A-3. (continued)

Station	Depth (cm)	TN (%)	$\delta^{15}N$ (‰)	TOC (%)	$\delta^{13}C$ (‰)
	5	0.018	3.03	0.246	-22.76
	7	0.017	2.81	0.242	-23.27
	9	0.020	2.79	0.296	-22.45
	14	0.025	2.31	0.322	-22.98
	20	0.022	2.43	0.328	-21.80
	50	0.026	2.54	0.373	-23.09
	100	0.023	2.38	0.325	-22.37
	150	0.029	2.13	0.350	-23.64
	200	0.028	1.43	0.357	-23.53
109	0	0.035	4.14	0.446	-24.53
	1	0.037	3.74	0.448	-24.63
	2	0.035	2.25	0.458	-24.75
	3	0.033	2.38	0.465	-24.46
	5	0.031	2.93	0.455	-24.22
	7	0.030	2.99	0.458	-24.26
	9	0.031	2.76	0.448	-24.29
	14	0.029	2.81	0.430	-24.27
	20	0.030	3.26	0.435	-24.37
	100	0.033	4.19	0.475	-24.59
	150	0.035	2.76	0.473	-24.38
	200	0.032	2.75	0.489	-24.48
111	0	0.046	2.41	0.651	-24.89
	1	0.043	1.22	0.587	-24.73

(continued)

Table A-3. (continued)

Station	Depth (cm)	TN (%)	$\delta^{15}N$ (‰)	TOC (%)	$\delta^{13}C$ (‰)
	2	0.043	1.35	0.655	-25.20
	3	0.041	1.26	0.655	-25.21
	5	0.046	1.59	0.707	-25.07
	7	0.052	0.97	0.807	-24.88
	9	0.046	1.95	0.534	-23.95
	14	0.035	3.56	0.436	-23.80
	20	0.033	2.76	0.421	-23.79
	50	0.032	3.34	0.359	-24.83
	100	0.038	2.40	0.409	-25.10
	150	0.040	2.60	0.511	-25.59
	200	0.035	2.23	0.375	-25.05
117	0	0.040	3.56	0.390	-23.78
	1	0.035	0.91	0.462	-24.70
	2	0.032	2.45	0.315	-24.51
	3	0.035	2.13	0.370	-24.25
	5	0.028	1.89	0.371	-24.63
	7	0.026	4.36	0.316	-24.69
	9	0.030	2.19	0.337	-24.82
	14	0.031	1.46	0.374	-24.25
	20	0.027	1.95	0.359	-24.24
	50	0.031	0.59	0.433	-23.66
	100	0.023	1.42	0.288	-24.32
	150	0.025	2.36	0.260	-24.00
	200	0.027	1.51	0.338	-23.87

(continued)

Table A-3. (continued)

Station	Depth (cm)	TN(%)	$\delta^{15}N$ (‰)	TOC (%)	$\delta^{13}C$ (‰)
119	0	0.049	4.86	0.465	-21.87
	1	0.053	5.25	0.502	-21.67
	2	0.056	3.97	0.440	-20.70
	3	0.054	3.91	0.464	-21.43
	5	0.045	4.21	0.426	-21.44
	7	0.033	4.56	0.334	-22.10
	9	0.033	5.60	0.372	-21.12
	14	0.026	5.23	0.308	-20.66
	20	0.023	6.26	0.319	-19.55
122	0	0.044	3.52	0.377	-23.25
	1	0.041	4.37	0.399	-23.29
	2	0.031	4.89	0.344	-23.05
	3	0.024	5.41	0.306	-22.89
	5	0.030	4.91	0.365	-22.93
	7	0.030	4.18	0.354	-23.06
	9	0.026	4.81	0.325	-23.15
	14	0.026	4.58	0.332	-23.08
	20	0.027	5.46	0.325	-23.34
	50	0.026	3.85	0.327	-23.41
	100	0.025	3.34	0.381	-24.24
	150	0.028	2.54	0.406	-24.20
126	0	0.083	6.00	0.638	-21.83
	1	0.078	5.56	0.631	-21.65

(continued)

Table A-3. (continued)

Station	Depth (cm)	TN (%)	$\delta^{15}N$ (‰)	TOC (%)	$\delta^{13}C$ (‰)
	2	0.075	5.57	0.641	-21.21
	3	0.077	5.78	0.655	-21.47
	5	0.071	5.30	0.614	-21.35
	7	0.062	5.80	0.578	-20.83
	9	0.072	5.18	0.694	-21.27
	14	0.078	5.32	0.661	-20.56
	20	0.076	5.53	0.682	-20.08
	50	0.063	5.35	0.566	-20.37
	100	0.069	4.74	0.614	-20.28
	150	0.059	4.53	0.522	-20.73
128	0	0.011	7.48	0.164	-22.10
	1	0.009	5.68	0.152	-21.91
	2	0.009	3.13	0.148	-21.60
	3	0.009	2.85	0.144	-22.41
	5	0.017	3.33	0.225	-22.65
	7	0.021	2.84	0.251	-23.67
	9	0.019	2.69	0.239	-23.64
	50	0.024	2.23	0.293	-24.27
	100	0.017	2.04	0.248	-23.76
147	0	0.070	5.12	0.561	-21.11
	1	0.072	5.13	0.577	-20.99
	2	0.065	5.15	0.470	-21.90
	3	0.065	5.79	0.490	-20.82

(continued)

Table A-3. (continued)

Station	Depth (cm)	TN (%)	$\delta^{15}N$ (‰)	TOC (%)	$\delta^{13}C$ (‰)
	5	0.050	5.43	0.395	-19.63
	7	0.050	6.23	0.405	-18.97
	9	0.050	8.51	0.470	-18.45
	14	0.045	7.38	0.390	-20.29
	50	0.020	10.87	0.215	-21.75
	100	0.020	5.92	0.180	-20.28
	150	0.020	3.45	0.250	-19.60
	200	0.020	2.56	0.260	-20.48
148	0	0.087	5.80	0.689	-20.54
	1	0.090	5.29	0.696	-20.74
	2	0.104	5.84	0.833	-22.28
	3	0.098	5.81	0.803	-22.01
	5	0.089	5.25	0.735	-21.91
	7	0.085	5.38	0.702	-21.81
	9	0.081	5.43	0.635	-21.74
	14	0.067	5.12	0.563	-21.68
	20	0.040	4.12	0.357	-21.85
149	0	0.098	5.67	0.671	-21.17
	1	0.102	5.36	0.750	-21.09
	2	0.102	5.93	0.804	-21.00
	3	0.094	5.54	0.677	-20.84
	5	0.096	5.72	0.743	-21.00
	7	0.085	5.30	0.633	-20.96

(continued)

Table A-3. (continued)

Station	Depth (cm)	TN (%)	$\delta^{15}N$ (‰)	TOC (%)	$\delta^{13}C$ (‰)
	9	0.079	5.60	0.569	-21.04
	14	0.065	4.89	0.455	-20.73
	20	0.043	5.66	0.355	-20.32
	50	0.027	5.39	0.258	-20.10
	100	0.047	4.04	0.363	-19.88
	150	0.039	5.30	0.335	-19.51
150	0	0.031	5.24	0.295	-20.53
	1	0.039	5.61	0.327	-21.25
	2	0.043	5.42	0.360	-21.42
	3	0.042	5.13	0.348	-20.18
	5	0.044	4.88	0.353	-20.81
	7	0.042	5.27	0.357	-20.04
	9	0.033	4.87	0.285	-20.70
	14	0.029	4.71	0.245	-20.00
	20	0.027	2.99	0.265	-20.94
152	0	0.032	3.70	0.306	-22.97
	1	0.028	3.68	0.297	-23.55
	2	0.028	5.22	0.299	-23.19
	3	0.030	5.52	0.270	-23.42
	5	0.022	4.80	0.294	-23.37
	7	0.020	5.29	0.240	-23.26
	9	0.023	1.34	0.232	-23.14
	14	0.017	3.68	0.199	-23.42
	20	0.020	2.84	0.210	-24.47

(continued)

Table A-3. (continued)

Station	Depth (cm)	TN (%)	$\delta^{15}N$ (‰)	TOC (%)	$\delta^{13}C$ (‰)
	50	0.020	0.60	0.200	-24.34
	100	0.020	-1.94	0.230	-26.50
	150	0.020	-1.05	0.200	-25.38
153	0	0.033	3.12	0.362	-23.74
	1	0.026	3.50	0.290	-23.54
	3	0.022	3.08	0.328	-23.38
	5	0.018	3.43	0.288	-23.55
	7	0.018	2.79	0.290	-23.59
	9	0.019	3.20	0.296	-23.77
	14	0.022	1.57	0.356	-23.84
	20	0.020	3.15	0.423	-24.21
	50	0.017	2.05	0.301	-24.39
	100	0.021	2.01	0.388	-24.62
	150	0.019	1.83	0.373	-24.57
156	0	0.042	4.62	0.415	-22.65
	1	0.035	4.47	0.361	-22.64
	2	0.029	4.49	0.327	-22.64
	3	0.031	4.36	0.348	-22.46
	5	0.026	4.08	0.301	-22.42
	7	0.026	4.74	0.314	-22.27
	9	0.025	4.11	0.303	-22.41
	14	0.024	3.92	0.305	-22.27
	20	0.026	4.33	0.316	-22.61
	50	0.024	4.50	0.304	-22.43

(continued)

Table A-3. (continued)

Station	Depth (cm)	TN (%)	$\delta^{15}N$ (‰)	TOC (%)	$\delta^{13}C$ (‰)
	100	0.025	4.41	0.304	-22.78
	150	0.026	3.33	0.328	-23.20
	200	0.024	3.64	0.302	-22.72
158	0	0.029	3.09	0.290	-22.99
	1	0.024	3.18	0.303	-23.02
	2	0.026	4.53	0.312	-22.77
	3	0.022	3.85	0.315	-22.04
	5	0.019	4.45	0.277	-22.18
	7	0.019	3.19	0.270	-22.23
	9	0.020	3.53	0.286	-22.32
	14	0.022	3.36	0.333	-21.60
	20	0.025	3.87	0.313	-22.62
201	0	0.029	5.29	0.321	-22.42
	1	0.020	4.68	0.263	-22.13
	2	0.026	2.50	0.320	-23.78
	3	0.031	4.10	0.347	-23.73
	4	0.032	3.53	0.351	-23.66
	6	0.030	3.82	0.330	-24.02
	8	0.029	3.74	0.319	-23.99
	10	0.030	3.26	0.319	-24.10
	12	0.029	3.48	0.323	-24.08
	15	0.033	4.18	0.352	-24.09
205	1	0.044	4.20	0.405	-22.42
	2	0.047	5.19	0.437	-23.15

(continued)

Table A-3. (continued)

Station	Depth (cm)	TN (%)	$\delta^{15}N$ (‰)	TOC (%)	$\delta^{13}C$ (‰)
	3	0.039	4.93	0.423	-23.55
	4	0.040	5.30	0.409	-23.40
	6	0.038	4.22	0.401	-23.29
	8	0.039	4.88	0.399	-23.27
	10	0.035	4.68	0.367	-23.36
	12	0.042	4.05	0.411	-23.50
	14	0.043	3.93	0.423	-23.42
	16	0.042	3.61	0.410	-23.59
	20	0.042	4.32	0.407	-23.79
	25	0.041	3.66	0.407	-23.92
	30	0.042	2.64	0.407	-23.82
	35	0.039	4.01	0.382	-23.82
	40	0.041	3.49	0.391	-23.89
	50	0.040	3.27	0.403	-23.71
	75	0.035	2.53	0.355	-24.07
	100	0.032	2.82	0.332	-23.99
	125	0.029	3.09	0.291	-24.11
	150	0.029	2.39	0.249	-23.82
	175	0.026	1.94	0.222	-23.63
224	0	0.027	4.59	0.511	-24.57
	10	0.035	2.58	0.502	-26.02
	20	0.033	2.83	0.487	-25.95
	30	0.041	2.96	0.603	-25.76
	40	0.037	2.14	0.696	-25.50

(continued)

Table A-3. (continued)

Station	Depth (cm)	TN (%)	$\delta^{15}N$ (‰)	TOC (%)	$\delta^{13}C$ (‰)
	50	0.033	1.04	0.468	-25.70
	75	0.048	0.99	0.892	-25.77
	125	0.056	1.17	0.286	-25.63
227	0	0.020	5.04	0.311	-23.76
	1	0.026	3.31	0.333	-24.51
	2	0.031	3.85	0.423	-24.24
	4	0.029	3.69	0.441	-24.16
	6	0.030	3.13	0.393	-23.98
	10	0.032	3.04	0.431	-24.09
	14	0.028	2.76	0.367	-24.53
	19	0.038	1.75	0.640	-25.16
	25	0.036	1.05	0.555	-25.31
228	0	0.031	3.43	0.306	-25.93
	2	0.040	3.58	0.440	-25.27
	4	0.050	2.90	0.490	-24.94
	7	0.050	4.85	0.530	-24.22
	10	0.046	0.07	0.550	-24.70
	14	0.029	-0.63	0.354	-24.14
	19	0.012	-2.96	0.151	-23.57
229	0	0.034	0.65	0.325	-25.67
	1	0.038	0.62	0.395	-25.58
	2	0.051	2.11	0.580	-25.19
	4	0.042	2.43	0.540	-24.97

(continued)

Table A-3. (continued)

Station	Depth (cm)	TN (%)	$\delta^{15}N$ (‰)	TOC (%)	$\delta^{13}C$ (‰)
	6	0.053	1.69	0.745	-25.26
	8	0.061	1.23	0.862	-25.39
	10	0.051	1.70	0.786	-25.44
	14	0.071	2.81	1.015	-25.56
	19	0.065	-0.18	0.941	-25.57
	24	0.050	0.78	0.727	-25.50
	30	0.053	0.52	0.756	-25.51
231	0	0.040	4.89	0.444	-23.50
	1	0.034	5.12	0.402	-23.45
	2	0.037	3.39	0.423	-24.26
	4	0.033	3.00	0.396	-24.29
	6	0.037	2.93	0.437	-24.30
	8	0.035	2.82	0.402	-24.40
	10	0.034	3.22	0.405	-24.45
	14	0.033	3.57	0.412	-24.68
	19	0.029	1.66	0.427	-24.77
	25	0.021	1.01	0.338	-24.96
235	0	0.085	4.77	0.928	-24.11
	1	0.093	4.02	0.954	-23.90
	2	0.073	4.50	0.805	-23.57
	4	0.066	4.83	0.745	-23.28
	6	0.077	3.45	0.869	-24.90

(continued)

Table A-3. (continued)

Station	Depth (cm)	TN (%)	$\delta^{15}N$ (‰)	TOC (%)	$\delta^{13}C$ (‰)
	8	0.057	2.52	0.695	-24.24
	10	0.073	1.89	0.898	-25.44
	14	0.061	2.42	0.686	-24.35
	19	0.061	2.85	0.750	-24.94
	25	0.064	2.15	0.835	-24.50
	30	0.050	-1.15	0.666	-24.55
	40	0.054	-1.11	0.682	-24.60
	50	0.053	-0.21	0.624	-24.45
	60	0.056	0.49	0.708	-24.28
	75	0.055	3.50	0.605	-24.36
	100	0.061	2.35	0.774	-24.53
	125	0.051	4.71	0.723	-24.73
	150	0.049	2.93	0.705	-24.68
	175	0.056	-0.04	0.796	-24.64
	200	0.052	0.03	0.807	-24.69
	225	0.056	2.42	0.849	-24.80
236	0	0.025	4.47	0.289	-24.32
	4	0.024	4.47	0.277	-24.21
	7	0.028	3.35	0.307	-23.80
	9	0.031	2.14	0.362	-23.85
	17	0.026	3.24	0.303	-23.71
	28	0.023	1.89	0.273	-23.64
	38	0.031	3.90	0.332	-23.85

(continued)

Table A-3. (continued)

Station	Depth (cm)	TN (%)	$\delta^{15}N$ (‰)	TOC (%)	$\delta^{13}C$ (‰)
	48	0.036	3.04	0.424	-23.90
	78	0.033	2.13	0.438	-24.38
	104	0.022	3.35	0.323	-23.66
	128	0.030	2.67	0.389	-24.09
	150	0.033	1.77	0.452	-24.32
239	0	0.059	4.16	0.555	-23.35
	1	0.065	4.04	0.603	-23.48
	2	0.046	4.83	0.440	-24.43
	4	0.041	5.06	0.431	-24.13
	6	0.040	4.40	0.414	-24.27
	8	0.042	4.07	0.433	-24.09
	10	0.043	4.03	0.449	-24.11
	14	0.039	4.48	0.403	-24.14
	19	0.035	3.76	0.393	-24.57
	24	0.041	5.18	0.423	-24.36
	25	0.043	3.81	0.438	-23.96
	30	0.041	4.00	0.425	-24.33
	40	0.044	3.62	0.454	-24.44
	50	0.033	2.26	0.366	-24.58
	75	0.039	2.51	0.464	-24.20
	100	0.040	2.95	0.424	-24.82
	125	0.042	3.52	0.470	-24.83
	150	0.031	2.47	0.330	-25.01
	175	0.028	3.39	0.283	-24.90

(continued)

Table A-3. (continued)

Station	Depth (cm)	TN (%)	$\delta^{15}N$ (‰)	TOC (%)	$\delta^{13}C$ (‰)
	200	0.044	4.31	0.460	-24.85
241	0	0.040	2.68	0.444	-23.76
	1	0.036	3.04	0.420	-23.52
	2	0.029	2.84	0.329	-23.95
	4	0.028	3.98	0.321	-23.82
	6	0.027	3.29	0.318	-24.00
	8	0.027	4.19	0.296	-24.14
	10	0.028	3.20	0.329	-24.16
	14	0.026	2.43	0.310	-23.97
	19	0.022	3.12	0.282	-24.10
	25	0.027	1.93	0.347	-23.96
	30	0.027	2.21	0.339	-24.03
	40	0.026	2.73	0.364	-24.51
	50	0.025	2.83	0.332	-24.00
	75	0.028	2.86	0.332	-23.94
	100	0.028	1.88	0.344	-24.25
	150	0.030	2.09	0.374	-24.12
	175	0.029	2.01	0.379	-24.60
	200	0.029	1.50	0.361	-24.56
	225	0.026	1.18	0.332	-24.42
	250	0.031	2.38	0.402	-24.46

(continued)

Table A-4. Protein decomposition in Skan Bay sediments.

Experiment*	Time (hr)	$^{14}CO_2$ concentration (% of total added)	^{14}C concentration in IW (% of total added)
Ru-Ill-6cm-A	0.8	0.7	1.2
	4.8	1.4	1.0
	21.5	3.4	0.5
	45.0	4.0	0.4
	75.0	6.9	0.3
Ru-Sup-6cm	0.8	1.8	31.0
	5.6	7.2	15.0
	22.0	14.0	11.2
	45.7	19.2	2.5
	74.6	28.5	2.5
Non-Ill-6cm	0.3	1.1	10.8
	25.8	6.5	3.6
	51.0	6.7	1.6
Ru-Ill-6cm-B	0.3	1.0	3.6
	25.2	4.5	1.8
	49.8	6.4	1.5
Ru-Fe-6cm	0.5	1.4	2.6
	25.2	2.7	1.5
	51.8	2.8	1.2
Non-Ru-12cm	0.5	2.3	11.1
	26.3	8.4	8.3
	50.4	14.1	4.8
Ru-Ill-12cm	0.3	1.2	3.9
	26.0	2.3	3.0
	50.1	3.5	2.5
Ru-Fe-12cm	0.3	3.3	2.1
	26.0	7.6	1.9
	50.5	10.0	1.5

(continued)

Table A-5. Protein decomposition in Resurrection Bay sediments.

Experiment*	Time (hr)	$^{14}CO_2$ concentration (% of total added)	^{14}C concentration in IW (% of total added)
Non-Ru-6cm	0.7	0.5	3.9
	10.6	1.5	2.9
	26.0	2.1	2.2
	46.5	2.1	2.0
Ru-Fe-6cm	1.0	0.7	1.8
	11.1	1.1	1.3
	26.7	1.6	0.8
	46.9	1.8	0.3
Ru-Ill-6cm	1.5	0.4	1.2
	11.7	1.0	0.7
	27.2	2.0	0.5
	48.0	1.9	0.1
Ru-Mon-6cm	2.0	0.3	0.4
	12.2	1.4	0.3
	27.7	1.6	0.2
	48.4	1.7	0.2
Non-Ru-0cm	0.7	0.2	3.7
	10.8	1.3	2.9
	21.3	1.5	2.5
	45.1	2.2	0.7
Ru-Fe-0cm	1.1	0.1	0.9
	11.4	0.7	0.5
	25.9	0.8	0.4
	47.4	1.2	0.3
Ru-Ill-0cm	0.7	0.2	1.1
	11.9	0.8	1.0

(continued)

Table A-5. (continued)

Experiment*	Time (hr)	$^{14}CO_2$ concentration (% of total added)	^{14}C concentration in IW (% of total added)
	26.4	0.9	0.7
	48.0	1.6	0.3
Ru-Mon-0cm	1.1	0.2	1.6
	12.3	1.2	1.1
	26.9	1.3	1.0
	48.6	1.7	0.9
Non-Ru-6cm-Long	0.8	0.4	4.0
	12.4	1.4	2.2
	23.0	2.4	1.9
	79.2	2.8	1.2
	171.8	4.6	4.9
	1050.8	10.2	2.2
Ru-Ill-6cm-Long	1.0	0.4	2.7
	13.2	1.6	0.9
	23.4	2.2	0.8
	79.6	2.3	0.5
	172.0	4.8	3.9
	1051.6	9.6	1.2
Ru-Sup-6cm-Long	1.3	4.4	66.6
	13.6	7.9	22.9
	23.8	8.0	12.8
	80.0	8.9	10.7
	173.3	22.4	27.7
	1052.1	59.4	4.7
Non-EL-6cm-A	0.6	2.0	2.9

(continued)

Table A-5. (continued)

Experiment*	Time (hr)	$^{14}CO_2$ concentration (% of total added)	^{14}C concentration in IW (% of total added)
	9.7	2.5	1.3
	24.4	2.4	0.8
	49.4	2.5	0.8
EL-Fe-6cm	1.3	1.6	1.8
	10 1	2.5	1.6
	24.8	2.9	1.1
	49.8	3.0	0.7
EL-Ill-6cm-A	0.6	1.9	1.6
	10.6	2.1	1.5
	25.3	2.2	1.1
	50.5	2.3	0.6
EL-Mon-6cm	1.0	1.7	4.8
	11.1	1.9	2.1
	25.8	1.9	0.8
	50.9	1.9	0.6
Non-EL-0cm	0.9	0.2	0.8
	15.6	0.8	0.7
	28.0	1.2	0.5
	47.2	1.8	0.3
EL-Fe-0cm	1.3	0.1	1.1
	16.0	0.4	0.7
	28.5	0.5	0.6
	47.7	0.7	0.3
EL-Ill-0cm	0.7	0.2	1.4
	16.4	1.1	0.8
	28.9	1.4	0.7

(continued)

Table A-5. (continued)

Experiment*	Time (hr)	$^{14}CO_2$ concentration (% of total added)	^{14}C concentration in IW (% of total added)
	48.3	2.1	0.7
EL-Mon-0cm	1.4	0.3	1.6
	16.8	0.6	1.5
	29.4	0.9	1.1
	48.8	2.2	0.7
Non-EL-6cm-B	1.0	0.8	2.0
	26.0	1.4	1.0
	54.9	2.2	0.4
EL-Ill-6cm-B	1.5	0.3	0.4
	26.6	0.7	0.3
	55.4	1.1	0.2
EL-Sup-6cm	1.1	4.1	11.7
	27.0	7.0	6.9
	55.8	7.5	2.9
Non-ES-6cm	0.6	2.4	4.1
	10.4	4.8	1.7
	23.3	5.2	1.6
	50.7	5.5	1.0
ES-Fe-6cm	1.0	3.5	6.9
	10.9	4.1	3.8
	23.9	5.1	3.3
	52.0	5.6	2.3
ES-Ill-6cm	0.7	1.9	3.3
	11.3	3.2	1.1
	24.4	3.3	1.0
	52.6	3.8	0.9

(continued)

Table A-5. (continued)

Experiment*	Time (hr)	$^{14}CO_2$ concentration (% of total added)	^{14}C concentration in IW (% of total added)
ES-Mon-6cm	1.1	0.4	3.4
	11.7	3.3	3.0
	24.8	3.7	2.8
	53.2	5.1	1.7

* abbreviations: Non: no preadsorption; Ru: Rubisco; EL: GroEL; ES: GroES; Fe: pre-adsorption on goethite; Ill: pre-adsorption on illite; Mon: pre-adsorption on montmorillonite; Sup: weakly adsorbed proteins from the supernatant after Rubisco or GroEL adsorption.

IMAGE EVALUATION TEST TARGET (QA-3)

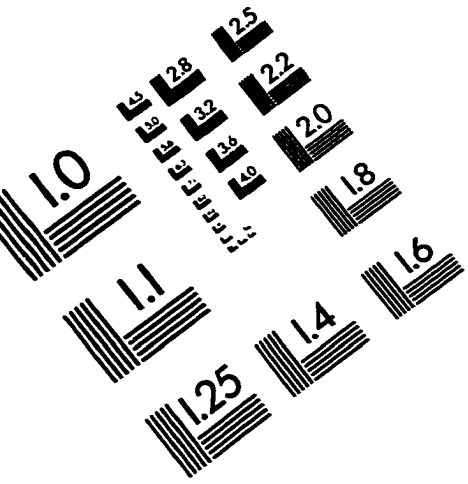

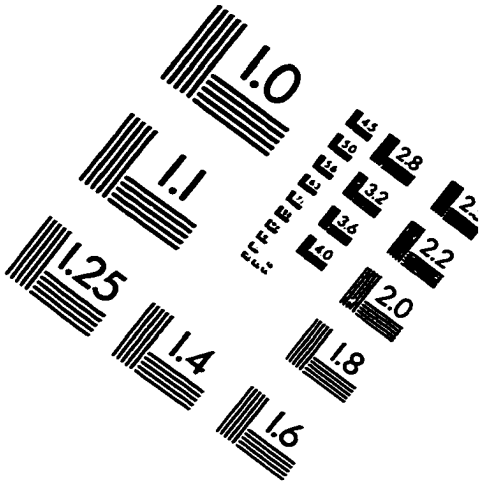

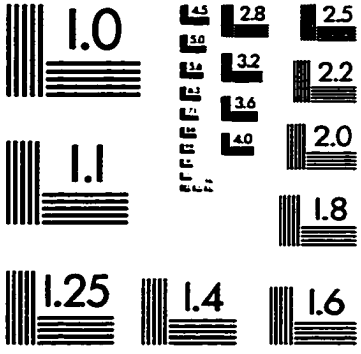

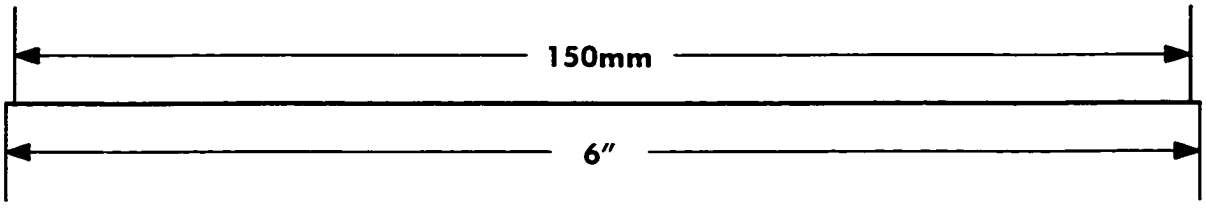

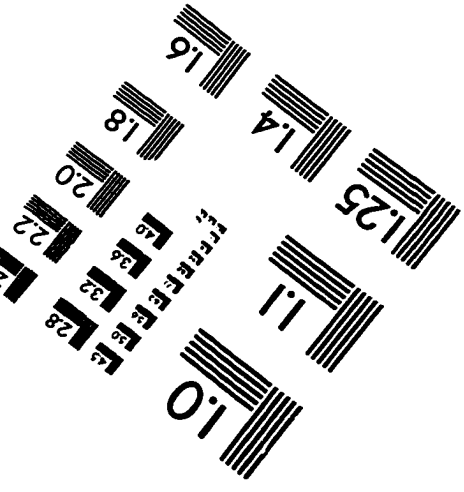

APPLIED IMAGE . Inc
1653 East Main Street
Rochester, NY 14609 USA
Phone: 716/482-0300
Fax: 716/288-5989